Collagen and Elastin based Tissue Engineered Vascular Grafts

AUTHOR(S)

Alan J. Ryan

CITATION

Ryan, Alan J. (2016): Collagen and Elastin based Tissue Engineered Vascular Grafts. Royal College of Surgeons in Ireland. Thesis. https://doi.org/10.25419/rcsi.10809272.v1

DOI

10.25419/rcsi.10809272.v1

URL

https://repository.rcsi.com/articles/thesis/Collagen_and_Elastin_based_Tissue_Engineered_Vascular_Grafts/10809272/1

Collagen and Elastin based Tissue Engineered Vascular Grafts

Alan James Ryan

PhD **2016**

Collagen and Elastin based Tissue Engineered Vascular Grafts

Submitted to the National University of Ireland in fulfilment of the requirements for the degree of

Doctor in Philosophy

Royal College of Surgeons in Ireland

April 2016

Alan J. Ryan, B.Eng, M.Sc.

Department of Anatomy, Royal College of Surgeons in Ireland, Dublin.

Supervisor

Prof. Fergal J. O'Brien

Declaration

I declare that this thesis, which I submit to RCSI for examination in consideration of the award of a higher degree of Doctor of Philosophy, is my own personal effort. Where any of the content presented is the result of input or data from a related collaborative research programme this is duly acknowledged in the text such that it is possible to ascertain how much of the work is my own. I have not already obtained a degree in RCSI or elsewhere on the basis of this work. Furthermore, I took reasonable care to ensure that the work is original, and, to the best of my knowledge, does not breach copyright law, and has not been taken from other sources except where such work has been cited and acknowledged within the text.

Signed _____

Student Number **11129581**

Date **11-04-16**

Abstract

Cardiovascular disease is the leading cause of death worldwide, accounting for 29% of all global deaths and is set to rise to 23 million deaths a year by 2030 (World Health Organisation, 2012). Arterial bypassing, both peripheral and coronary, is usually performed with autologously harvested vessels. However, the quantity available is often very limited as well as the vessels of elderly patients often suffering from thrombus, aneurysm formation or arthrosclerosis in high pressure arterial sites. The shortcomings of autografts has led to a substantial amount of research being directed towards tissue engineered vascular grafts (TEVGs) (Kakisis et al., 2005). Currently available artificial grafts for small diameter vasculature (<6 mm) suffer from poor patency rates due to thrombosis, aneurysm formation, and a compliance mismatch, which often stems from the inherent properties of synthetic polymers.

The primary goal of the research presented in this thesis was to develop a small diameter tissue engineered vascular graft (TEVG) using the natural polymers collagen and elastin, coupled with dynamic mechanical conditioning. In this context, the aim was to develop a collagen-elastin composite scaffold with optimised intrinsic physiochemical characteristics which displayed the capacity to support smooth muscle cells *in vitro* while also displaying suitable viscoelastic properties. Subsequent investigation focused on emulating the anatomical architecture of native vessels using this novel collagen-elastin composite, and examining *in vitro* maturation through dynamic conditioning in a custom designed pulsatile bioreactor.

In the study presented in Chapter 2 of this thesis, elastin addition to a porous collagen scaffold was shown to play a major role in altering its biological and mechanical response. The addition of elastin improved the viscoelastic characteristics with a higher degree of cyclical strain recovery and creep resistance, which indicates the biomaterial may possess sufficient recoil to be utilised for long-term cyclical distension with reduced aneurysm risk. Additionally, the gene expression and proliferation data suggested that the presence of elastin resulted in a more contractile smooth muscle cell (SMC) phenotype, in the absence of any exogenous stimulation. This biomaterial

platform was deemed to possess great potential for cardiovascular tissue engineering and was amenable to multiple fabrication methods.

In Chapter 3, this biomimetic collagen-elastin composite was subsequently fabricated into a physiologically relevant bilayered tubular architecture. The bilayered scaffold consisted of a porous outer layer with an optimised microarchitecture to support SMCs, while the inner layer consisted of a dense film designed to increase the overall scaffold mechanical properties and present a suitable surface for future endothelial seeding. The properties of the dense luminal lining were shown to be highly controllable via crosslinking, which enabled the modification of the mechanical properties, degradation resistance, and inflammatory profile. These bilayered tubular scaffolds were ultimately considered highly suitable for further investigation as a TEVG.

In Chapter 4, a novel pulsatile flow bioreactor system was developed which was capable of recreating the complex haemodynamic environment *in vitro*. The system was capable of applying physiological fluid shear stresses, cyclical strain and pulsatile pressure to mounted constructs. The flexible design allowed the mounting of variable diameter constructs and was designed to be utilised to examine the effect of mechanical stimulation on the *in vitro* maturation of the bilayered tubular collagen-elastin TEVGs described.

In the final chapter (Chapter 5), the effect of TEVG architecture, crosslinking, and dynamic conditioning on the maturation of the grafts was examined in the custom pulsatile bioreactor from Chapter 4. Specifically, bilayered scaffolds coupled with EDAC crosslinking displayed far greater mechanical properties than single layered scaffolds and DHT crosslinking respectively. Furthermore, the application of dynamic conditioning resulted in further increases in the TEVG mechanical properties as a result of increased cell density, improved collagen circumferential alignment, and an apparent increase in vessel wall density.

Collectively, this study has led to the development of a composite bilayered tubular scaffold with optimised intrinsic physiochemical characteristics to support smooth muscle cells *in vitro* while subsequently displaying suitable viscoelastic properties for sustained dynamic conditioning in a custom designed pulsatile bioreactor.

Table of Contents

Acknowledgements

Firstly, I wish to extend my sincere gratitude to my supervisor Professor Fergal O'Brien for taking me on as a student and guiding my research over the past few years. I have learned an invaluable amount from you during my time in RCSI and your enthusiasm, support and scientific knowledge contributed immensely to my research. I am particularly grateful for the unwavering support you have shown for me and for the time and care that you put into reviewing this thesis, I'm sure you enjoyed it almost as much as me!

To everyone in the Tissue Engineering Research Group and in the various labs around RCSI, thank you for the help and support. In no particular order; Tanya, Andrew, Paula, David, Ryan, Christina, Orlaith, Joanne, Janice, Tati, Peter, Irene, Rukmani, Will, Laura, Tommy, Tijna, Conor, Emily, Greg, Sara, Kai, Alan H, Adolfo, Caroline H, Emmet, Amro, Amos, Nicola, John Glesson and Johnny. P.s Damn you Rosie!

Thanks to the fellow bioengineers in Trinity who I often went to bug about all things mechanical, including Clive, Eimear & Bruce. Special thanks to Gill for showing me Picosirius red staining when I was up against the clock, and to Simon Carroll for all things hydroxyproline! Thanks to my fellow cardiovascular engineers Steve Sheridan and Claire Brougham, great to have somebody else to moan to! Speaking of moaning, how could I forget Hugo and the other band of people who I probably drank more tea with than is healthy, thanks Cian, Erica, Rob.

Garry I'll even give you the start of this paragraph, thanks for letting me ask you annoying questions constantly, thanks for your poker face which constantly confuses me, and thanks for the science/career chats over coffees. You've helped me more than you know.

For existential, extracurricular and extraneous assistance I would like to thank all my friends for keeping me sane and realising there's more to life

than science! A special thanks to Simon and Brendan for the constant slagging, I'm constantly entertained by the two of you.

Deborah Sheedy, thank you for always being there for me. We met when I first started the PhD so you've struggled through the whole thing with me from the start! Thanks for putting up with my weird sleeping hours during the thesis write up, it's done! To Lorna and Emily, for being the best siblings anyone could deserve.

Finally, I would like to thank my parents, Cyril and Una, for their unwavering support in all my endeavours and their understanding, endless patience, and encouragement when it was most required. I hope I can repay you some day.

Publications, Prizes and Presentations

Journal publications

Ryan, A.J., O'Brien, F.J., 2015. Insoluble elastin reduces collagen scaffold stiffness, improves viscoelastic properties, and induces a contractile phenotype in smooth muscle cells. Biomaterials 73, 296–307.

Sheridan, W.S., Ryan, A.J., Duffy, G.P., O'Brien, F.J., Murphy, B.P., 2014. An experimental investigation of the effect of mechanical and biochemical stimuli on cell migration within a decellularized vascular construct. Ann. Biomed. Eng. 42, 2029–38.

Ryan, A.J., Gleeson, J.P., Matsiko, A., Thompson, E.M., O'Brien, F.J., 2014. Effect of different hydroxyapatite incorporation methods on the structural and biological properties of porous collagen scaffolds for bone repair. J. Anat.

Prizes

Winner of the 2014 IET Postgraduate Scholarship for an Outstanding Researcher Awarded the 2014 IET postgraduate scholarship (£10,000) for an Outstanding Researcher.
Joint-winner of the inaugural SurgaColl Technologies Award in Regenerative Medicine for an Early Career Investigator The Anatomical Society Summer Meeting: Form and Function in Regenerative Medicine (October 2013)
Awarded 1st place overall in oral presentation in the regenerative medicine category Young Life Scientists Ireland conference (March 2014)
Awarded 1st place for student oral presentation Human Disease Mapping Conference (January 2014)
Finalist Engineering Ireland Biomedical Engineering Research Medal 20th Annual Conference of the Bioengineering Section of the Royal Academy of Medicine (January 2014)
Finalist Engineering Ireland Biomedical Engineering Research Medal 21h Annual Conference of the Bioengineering Section of the Royal Academy of Medicine (January 2015)
Awarded Engineers Ireland Student Research Bursary Bioengineering in Ireland 20th Annual conference (January 2014)
Awarded 1st place for oral presentation TCBE Winter Symposium (2013)

AMBER Research Day 2nd Place Oral (2013)
National Finalist SFI Thesis in Three Competition (2013)
Award 1st place for overall poster at TERMIS-EU 2014 TERMIS-EU Genoa (June 2014)

Conference abstracts

Ryan A.J. and O'Brien F.J. (2015). Elastin Reduces Collagen Scaffold Stiffness, Improves Viscoelastic Properties, and Induces a Contractile Smooth Muscle Cell Phenotype in a Multi-layered Vascular Graft *4th Tissue Engineering and Regenerative Medicine International Society World Congress*, Boston, USA. Kaplan, D. L and Marra, K.G (Eds.). 156.
Ryan A.J., O'Brien F.J. (2014). A Novel Viscoelastic Collagen-Elastin Bilayered Tubular Scaffold for Vascular Graft Tissue Engineering In: *Abstracts from The World Congress of Biomechanics*, Boston, USA.
Ryan A.J., O'Brien F.J. (2014). A Biomimetic Tissue Engineered Vascular Graft fabricated from Collagen and Elastin. In: *Abstracts from the Tissue Engineering and Regenerative Medicine International Society European Union*, Genoa, Italy: 35 Abstract published in *Journal of Tissue Engineering and Regenerative Medicine* 8 (Suppl. 1): 393.
Ryan, A.J., O'Brien, F.J. (2014) Vascular Tissue Engineering Utilising a Novel Collagen-Elastin Bilayered Tubular Scaffold. *Proceedings of the 20th Annual Conference of the Section of Bioengineering of the Royal Academy of Medicine in Ireland,* M. Walsh, D. Hoey, E. deBarra (Eds.), Limerick, Ireland: 7.
Ryan, A.J., O'Brien, F.J. (2014) Tissue Engineered Blood Vessels Using the Natural Polymers Collagen and Elastin In: *Abstracts from Human Disease Mapping,* C.Whelan, A. Mitrugno (Eds.), Dublin, Ireland: OP24, 37.
Ryan, A.J., O'Brien, F.J. (2014) Generating Viable Tissue Engineered Vascular Grafts from Natural Polymers In: Abstracts from Young Life Scientists Ireland Conference. L. Dyke, T. McGivern (Eds.) Dublin, Ireland: OP5C, 24.
Ryan, A.J., O'Brien, F.J. (2013) Development of a Bilayered Tubular Collagen-Elastin Scaffold for Vascular Tissue Engineering In: *Abstracts from the Anatomical Society Summer Meeting: Form and Function in Regenerative Medicine,* Dublin, Ireland. Abstract published in *Journal of Anatomy* 224 (2): 228-249. Volume 224, 2014.
Ryan, A.J.; O'Brien, F.J. (2013) Application of Viscoelastic Bilayered Tubular Collagen-Elastin Scaffolds for Vascular Tissue Engineering. In: Abstracts from the Tissue Engineering and Regenerative Medicine International Society European Union, Istanbul, Turkey: 350.
Ryan, A. and O'Brien, F.J. (2012) Development of a collagen-elastin scaffold for vascular tissue engineering *Proceedings of the 19th Annual Conference of the Section of Bioengineering of the Royal Academy of Medicine in Ireland,* D. Kelly and C. Buckley (Eds.), Enfield, Ireland: 138.

Ryan, A.; Gaynor, A. and O'Brien, F.J. (2011) Design and evaluation of a novel collagen-based tissue engineered vascular graft. Proceedings of the 18th Annual Conference of the Section of Bioengineering of the Royal Academy of Medicine in Ireland, F. Buchanan (Ed.), Belfast, Ireland.

List of figures

Nomenclature

°C	Degrees Celsius
α-SMA	Alpha smooth muscle actin
ANOVA	Analysis of variance
bFGF	Basic fibroblast growth factor
CaCl2	Calcium chloride
cDNA	Complimentary deoxyribonucleic acid
CVD	Cardiovascular disease
CE	Collagen elastin
CoII	Collagen
CE	Colagen-elastin
DAPI	4', 6- diaminido-2-phenylindole
dH2O	Deionised water
DHT	Dehydrothermal
DMEM	Dulbecco's modified eagles medium
DNA	Deoxyribonucleic acid
EC	Endothelial cell
ECM	Extracellular matrix
EDAC	1-Ethyl-3-(3-dimethylaminopropyl) carbodiimide
EDTA	Ethylenediaminetetraacetic acid
ELISA	Enzyme-linked immunosorbent assay
ELN	Elastin gene
ePTFE	Expanded polytetrafluoroethylene
FBS	Foetal bovine serum
FDA	Food and drug administration
FGF	Fibroblast growth factor
g	Gram
GAG	Glycosaminoglycan
H & E	Haemotoxylin & eosin
HCl	Hydrochloric acid
HEPES	4-(2-hydroxyethyl)-1-piperazineethanesulfonic acid
HGF	*Hepatocyte growth factor*
hMSC	Human mesenchymal stem cell
hr	Hour
HRP	Horseradish peroxidase
ITS	Insulin-Transferrrin-Selenium
MMP	Matrix metalloproteinase
Mrna	Messenger ribonucleic acid
MSC	Mesenchymal stem cell

MTGase	Microbial transglutaminase
NaHCO3	Sodium bicarbonate
NHS	N-hydroxysuccinimide
Non-XL	Non-crosslinked
PBMC	Peripheral blood mononuclear cell
PBS	Phosphate bufferedsaline
PCI	Percutaneous coronary intervention
PDGF-BB	Platelet derived growth factor BB
PET	Polyethylene terephthalate
PGA	Polyglycolic acid
PGS	*Poly(glycerol sebacate)*
PLGA	Poly(lactic-co-glycolic acid)
PTFE	Polytetrafluoroethylene
RNA	Ribonucleic acid
RT-PCR	Reverse transcription polymerase chain reaction
SEM	Scanning electron microscopy
SIS	Small intestinal submucosa
SMC	Smooth muscle cell
SM-MHC	Smooth muscle myosin – heavy chain
TEVG	Tissue engineered vascular graft
TGF-β1	Transforming growth factor beta 1
TNBS	2,4,6-Trinitrobenzenesulfonic acid
TNF-α	Tumour necrosis factor alpha
TRIS-HCL	Tris-hydrochloride
UTS	Ultimate tensile strength
UV	Ultraviolet
VEGF	Vascular endothelial growth factor
VEGF-R2	Vascular endothelial growth factor receptor 2

Chapter 1: Introduction and literature review

1.1 Introduction

Cardiovascular disease is the leading cause of death worldwide, accounting for 631,636 deaths in the US alone in 2006 and 17.3 million deaths worldwide. This represents 29% of all global deaths and is set to rise to 23 million deaths a year by 2030. The number of non-institutionalised adults with diagnosed vascular disease is estimated at 26.6 million which represents 12% of the US population. It is calculated that this disease cost the American economy $475.3 billion in the year 2009 (Centre for Disease Control, 2013; World Health Organisation, 2012). The primary causes of vascular disease are atherosclerosis, aneurysm formation, and inflammatory stenosis. Atherosclerosis is the most common cause of vascular disease and is characterised by a raised focal plaque. The plaque consists of a lipid core covered in smooth muscle cells, extracellular matrix, and a fibrous cap. As the plaque grows in size it restricts blood flow and may eventually fully block the vessel and require an arterial bypass.

Arterial bypassing is usually performed with autologously harvested vessels, which are still considered the “gold standard”. As autografts are patient derived there is a limited quantity available and the donor vessels are often suboptimal, with the saphenous vein grafts often suffering from thrombus, aneurysm formation, or atherosclerosis in high pressure arterial sites. Allografts have also previously been used; however, they have the added risks of tissue rejection and disease transmission and consequently are no longer used clinically. Artificial vascular grafts, therefore, are seen as the “holy grail” of vascular surgery resulting in an extensive quantity of research into the area (Kakisis et al., 2005).

Vascular grafts constructed from synthetic materials, such as polytetrafluoroethylene (PTFE) and Dacron®, have displayed impressive long-term success in the replacement of large diameter vessels (> 6 mm). This success, however, has not being replicated with small diameter grafts (< 6 mm) where there is no synthetic graft available with suitable long-term patency rates due to high thrombosis rates and a compliance mismatch.

Additionally, these synthetic grafts do not have the ability to grow and remodel presenting a particular disadvantage for paediatric patients. Thus, recent research has focused on developing suitable vascular grafts using tissue engineering (Fig. 1.1).

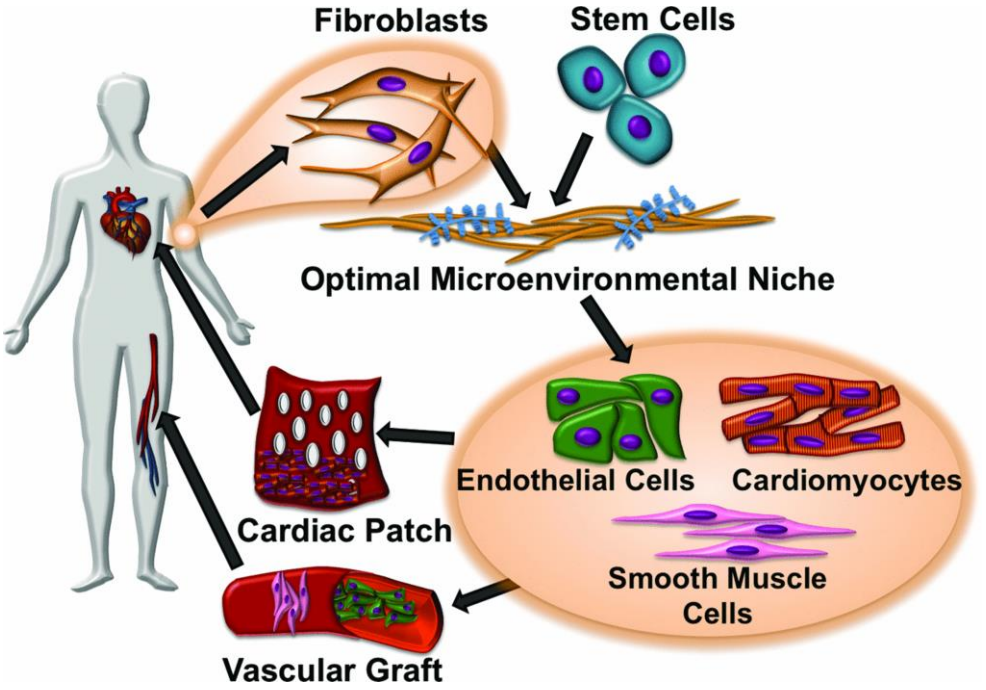

Figure 1.1 Overview of differentiation for cardiovascular tissue engineering

Due to the difficulty in extracting native cardiovascular cells (i.e. smooth muscle cells) many approaches to cardiovascular tissue engineering focus on generating an optimal microenvironment niche to promote differentiation down a cardiovascular lineage (Nakayama et al., 2014). Ultimately, both approaches require cells, scaffolds, and appropriate signals.

Tissue engineering can be defined as a triad of scaffolds, cells, and signals which function synergistically to enable new functional tissue growth either *in vitro* or *in vivo* (Langer and Vacanti, 1993). For cardiovascular tissue engineering, it is possible to utilise precursor stem cells which may be differentiated towards a cardiovascular lineage (Fig. 1.1) using a suitable microenvironment. However, the difficulty in promoting differentiation and maintaining the correct phenotype has led to the widespread use of terminally differentiated cells as a more practical option.

Natural biodegradable polymers, such as collagen, were the basis of some of the first scaffolds for vascular tissue engineering (Hirai et al., 1994;

L'Heureux et al., 1993; Weinberg and Bell, 1986). Collagen is an excellent choice as the biomaterial for a tissue engineered vascular graft due to its inherently excellent biological performance, biodegradability and high concentration in native vasculature. These initial studies utilised cells embedded into tubular collagen gels, yet required the use of a Dacron® mesh to provide structural support. However, in the last 20 years, significant advances in collagen fabrication techniques has brought about increased interest in utilising collagen as the basis for tissue engineered vascular grafts. In native vessels elastin serves to dampen pulsatile flow of blood by its efficient storage of elastic-strain energy. Thus, the addition of elastin to a collagen-based scaffold might provide a more natural viscoelastic response and, in combination with the high tensile strength of collagen, may provide compliance closer to native vessels than currently available grafts. Compliance mismatch has frequently been cited as a major reason for the poor patency of prosthetic grafts (Gershon et al., 1992). Elastin also serves an important role in controlling smooth muscle cell (SMC) proliferation and thus stabilises the arterial structure (Li et al., 1998a).

Tissue engineered vascular grafts, hereafter referred to as TEVGs, have challenging mechanical constraints to meet, including high strength coupled with high elasticity, a difficult balance to achieve. Applying appropriate dynamic mechanical conditioning through pulsatile bioreactors has been shown to aid in this endeavour immensely (Engbers-Buijtenhuijs et al., 2006; Hahn et al., 2007; Syedain et al., 2011a). However, the highly specialised nature of these systems means that custom designed bioreactors remain the mainstay of the field. Therefore, the focus of this thesis is the generation of a small diameter TEVG using a combination of native SMCs, natural polymers, and *in vitro* maturation using a custom designed bioreactor.

1.2 Blood vessels

Blood vessels function to carry blood to and from the heart, tissues, and organs of the body. They form a complex system of arteries, veins and capillaries which vary in size, shape, ultrastructural organisation, mechanical properties, biochemical and cellular content. Arteries are thick walled highly elastic vessels whose primary function is to carry high pressure oxygenated blood to organs and tissues where they branch into smaller arterioles and capillaries (Ratcliffe, 2000). Disruption of this system can lead to localised tissue damage or ultimately death, and so the blood supply must remain undisturbed at all times.

1.2.1 Arterial wall composition

The large and medium arteries consist of three distinct circumferentially aligned layers with each layer possessing a distinct cellular and protein composition. Each of these layers has a specific role in maintaining normal vascular form and function. These three layers, the tunica intima (inner layer), tunica media (middle layer) and tunica adventitia (outer layer), vary in thickness and composition depending on anatomical location (Fig. 1.2).

The tunica intima is located on the luminal aspect of vessels and consists of a monolayer of endothelial cells adhered to a thin basal lamina composed of collagen type IV, fibronectin, and proteoglycans (Ratcliffe, 2000). The endothelial monolayer provides a non-thrombogenic interface for blood and controls the diffusion of molecules through the vascular wall. A fenestrated elastin dominated layer, the internal elastic lamina, separates the tunica intima from the tunica media (Patel et al., 2006). The tunica media consists of circumferentially arranged laminae of contractile smooth muscle cells (SMCs) and fenestrated elastin and collagen sheets (O'Connell et al., 2008). The number of laminae of SMCs and extracellular matrix (primarily elastin) is variable depending on location in the vascular tree, and represents a developmental adaption to the stresses of that particular location. The numbers of lamellar units in an artery wall has been shown to be proportional to the wall stress, and so high pressure arterial sites, such as in the

abdominal aorta, may have up to 40 lamellar units while low pressure venous sites may contain only one unit (Li et al., 1998b).

The external elastic lamina separates the tunica media from the tunica adventitia (Patel et al., 2006). The adventitia is the outer layer of an artery that helps anchor vessels to the surrounding tissue and provides some structural support. It is a collagen rich layer containing mainly fibroblasts and, in larger vessels, the tunica adventitia may be innervated and contain its own capillary network, termed the *vasa vasorum* (Pugsley and Tabrizchi, 2000).

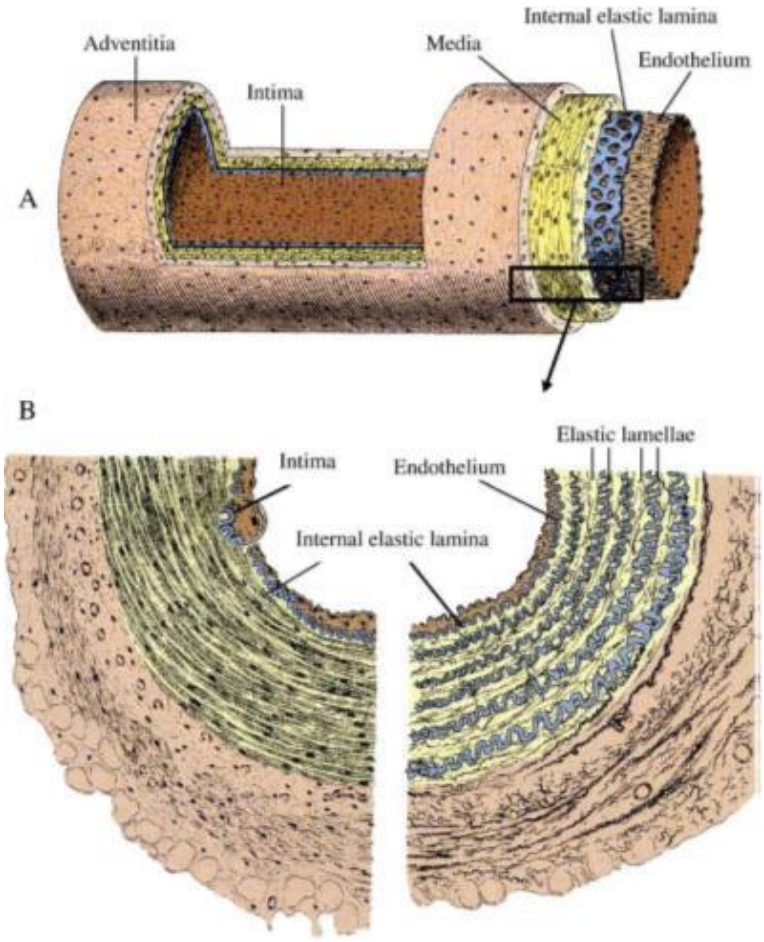

Figure 1.2 Arterial wall structure

(A) The structure of the arterial wall is shown with each of the 3 layers identified. (B) The lamellar structure of a muscular artery (left) and elastic artery (right) is shown (Patel et al., 2006). The medial layer lamellae exist in a crimped state when unloaded, which contributes to the non-linear mechanical response of the vessel.

1.2.2 Haemodynamic forces

The haemodynamic forces which arteries are exposed to leads to unique mechanical properties that are difficult to recapitulate. The vascular network is naturally pre-stressed in the longitudinal (or axial) direction and during surgery this is easily demonstrable where cut vessels retract. However, the physiological reasoning for this axial pre-stretch has been shown to be highly adapted to maintain an even force longitudinally over the physiological range of vascular pressure (60mmHg to 160mmHg) (Dye et al., 2007). Thus, as arteries experience systolic (~120mmHg) and diastolic (~80mmHg) pressure changes, the force longitudinally remains relatively constant (Humphrey et al., 2009). Blood pressure also induces stress in a radial direction and circumferentially (Fig. 1.3). The circumferential stress in the artery wall is one of the primary stresses in arteries and the extracellular matrix (ECM) of the medial layer is arranged circumferentially to deal with this stress, including a circumferential orientation of the embedded smooth muscle cells (Spronck et al., 2014).

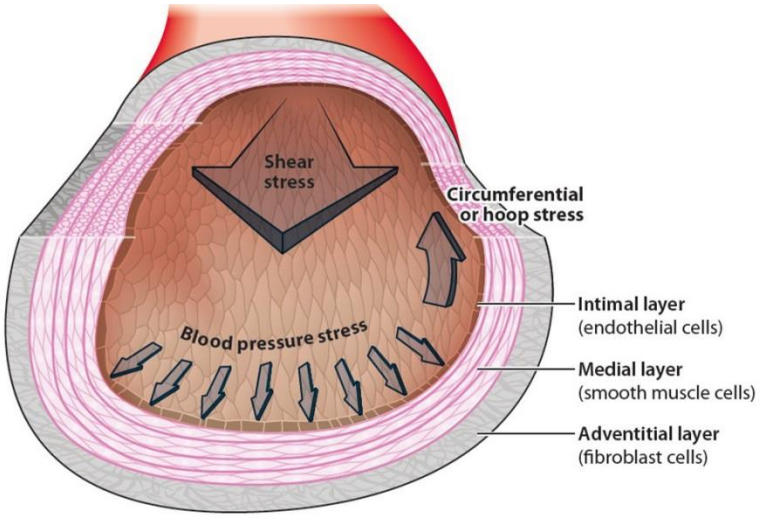

Figure 1.1 Haemodynamic forces acting on the arterial wall

Arteries experience radial, circumferential, and wall shear stress due to the pressurised pulsatile flow of blood. An axial pre-stress is also present natively in all vessels and contributes to normal function (Tarbell et al., 2014).

The fluid flow through the artery causes a shear stress to act on the endothelial cells (ECs) lining the vessel. This shear stress has been shown to be an important mechanotransduction pathway (the conversion of

mechanical stresses to biochemical responses) of biomechanical stimuli to ECs (Davies, 2009). Variations in mean wall shear stress results in ECs altering their morphology, and also regulates gene and protein expression, in addition to nitric oxide production (Corson et al., 1996). Long terms changes in mean wall shear stress can result in changes in vascular diameter and may even induce adaptive wall remodelling (Mattsson et al., 1997). This effect may be negative however, as low walls shear stress is a known contributing factors to the generation of diseases such as atherosclerosis (Davies, 2009; Passerini et al., 2004).

1.2.3 Artery mechanical properties

The effect of each major component of arteries on the mechanical properties of the tissue has been examined extensively. Popular methods of doing so include a selective digestion of either the collagen or elastin fibres followed by tensile testing. Proteoglycans contribute mainly to the compressibility of the tissue. The complex arrangement of collagen (type I and III), elastin, and proteoglycans results in the viscoelastic response of arteries to loads (O'Connell et al., 2008). The arterial system is highly elastic due to the high ratio of elastin to collagen and, as such, expands to accommodate increases in blood pressure. The aorta serves to dampen and smooth the pulsatile output of the left ventricle, thus reducing the pulse pressure. This ability of a blood vessel to expand and contract passively with changes in pressure is referred to as vessel compliance. Vessel compliance is defined as the change in volume of a vessel over the change in pressure. The compliant phase of vessels is where the load is primarily carried by the elastin fibres and collagen fibres are still crimped (Humphrey, 2013). As strain increases collagen fibres begin to be recruited and stiffness increases (Fig. 1.4). Aortic compliance is therefore a very important characteristic as, along with stroke volume, it determines pulse pressure.

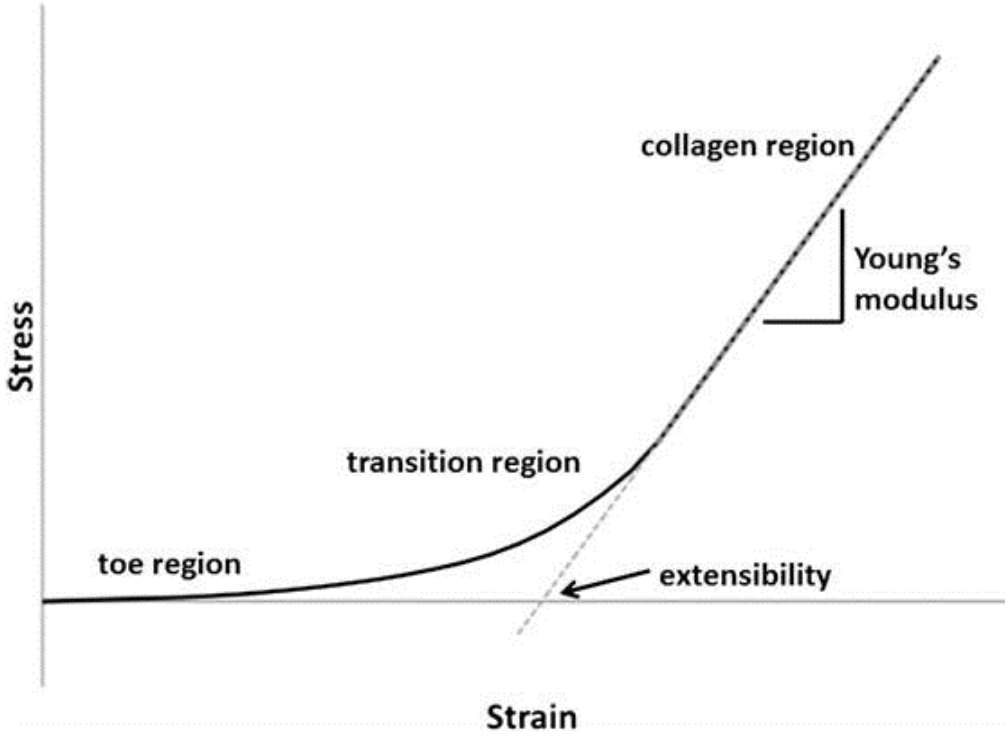

Figure 1.4 Stress-strain response of arterial tissue

Representative stress-strain curve for tensile testing of arterial tissue with a compliant toe region and as strain increases collagen fibres begin to be recruited and thus, stiffness increases (Connell et al., 2012).

The degree of elasticity of an artery changes depending on the proximity to the heart with compliance being highest close to the heart and steadily decreases as one moves away. The elasticity is determined by the structure and composition of the arterial wall while the stiffness is partially controlled by the regulatory function of the endothelial lining of the vessel (Holzapfel et al., 2000). This ability to control stiffness allows the arterial system to accommodate the large changes in cardiac output experienced during daily living. In the long term, arteries can adapt to changes in physiological conditions by changing their structural composition, such as changing the thickness of the medial layer (Pugsley and Tabrizchi, 2000).

1.2.4 Cardiovascular diseases

Cardiovascular disease (CVD) is the leading cause of death worldwide, accounting for 610,000 deaths in the US alone in 2013 and 17.5 million deaths worldwide (Centre for Disease Control, 2013; World Health

Organisation, 2012). This represents 31% of all global deaths and is set to rise to 23 million deaths a year by 2030. The number of non-institutionalised adults with diagnosed cardiovascular disease is estimated at 26.6 million which represents 12% of the US population (Yang et al., 2015). It is calculated that this disease cost the American economy $320.1 billion in the year 2011 (Mozaffarian et al., 2014). The morbidity rate of CVD continues to rise worldwide due to the prevalence in society of risk factors such as obesity, lack of exercise, diabetes, unhealthy diets, stress, and smoking. However, our ability to combat CVD has improved with advanced treatment modalities resulting in reduced mortality of the disease (O'Flaherty et al., 2013).

Within CVD, many of the disorders are characterised by a narrowing or blockage of the vasculature leading to reduced blood flow and tissue damage. The primary causes of vascular disease are atherosclerosis, aneurysm formation, and inflammatory stenosis. A coronary artery aneurysm is defined as a localised and permanent dilation of a coronary artery by more than 1.5 times of its normal diameter. The incidence of coronary aneurysms has been reported to be between 1.5 - 5% (Syed and Lesch, 1997). Although the incidence is low, if left untreated, the aneurysm may rupture leading to a systemic inflammatory response and a high mortality rate (Pahlavan and Niroomand, 2006). Atherosclerosis has been shown be the cause of 50% of coronary aneurysms (Syed and Lesch, 1997). Moreover, atherosclerosis is the most common cause of vascular disease and is characterised by a raised focal plaque (Fig. 1.5). The plaque consists of a lipid core covered in smooth muscle cells, extracellular matrix and a fibrous cap. As the plaque grows in size it restricts blood flow and may eventually fully block the vessel and require an arterial bypass. Additionally, the atherosclerotic plaque results in a loss of local vessel elasticity and potential calcification of the arterial walls.

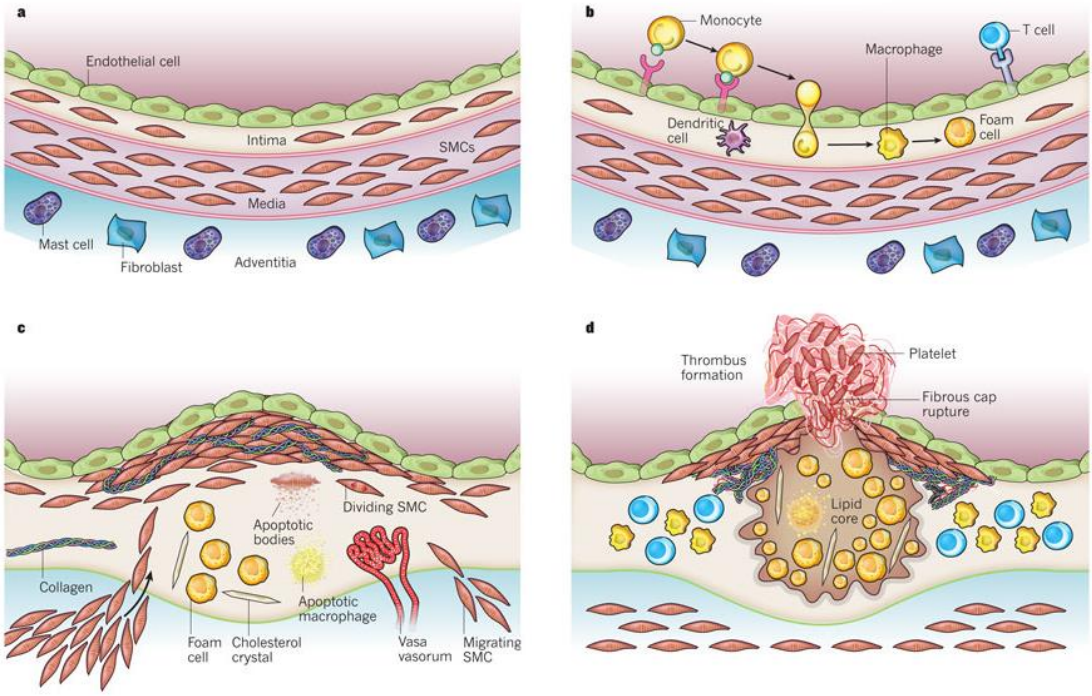

Figure 1.5 Development of atherosclerotic lesions

Healthy vessel wall (A) is infiltrated by macrophages (B) which begin forming foam cells and begin the degenerative cascade (C) which results in an atherosclerotic lesion (D) (Libby et al., 2011).

1.2.5 Traditional treatments

Treatment for diseased and damaged vessels is usually angioplasty, stenting, or bypass grafting. The SYNTAX trial, a large randomised controlled trial of 1800 patients with coronary artery disease, compared coronary artery bypass grafting versus percutaneous coronary intervention (PCI) using drug-eluting stents. Results from the study indicate that coronary artery bypass grafting remains the standard of care for patients with multi-vessel or left coronary artery disease due to a lower incidence of major adverse cardiac and cerebrovascular events versus PCI after both 3 years and 5 years post-surgery (Kappetein et al., 2011; Mohr et al., 2013). Vascular grafting, therefore, remains the gold standard of care for the leading cause of death worldwide.

Arterial bypassing, both peripheral and coronary, is usually performed with autologously harvested vessels. In clinical practice, autologous vascular grafts (autografts) are considered the current “gold standard”. Autografts are

vessels, usually the saphenous vein or internal thoracic artery, which are taken from non-essential sites on the patient's body and re-implanted where needed. However, the quantity available is often very limited as well as the saphenous vein of elderly patients often suffering from thrombus, aneurysm formation or arthrosclerosis in high pressure arterial sites. Additionally, the secondary surgery site also results in an increased infection risk. Allografts have also previously been used however they have the added risks of tissue rejection and disease transmission and consequently are no longer used clinically. The shortcomings of autografts and allografts have led to a substantial amount of research being directed towards artificial vascular grafts (Kakisis et al., 2005).

Vascular grafts constructed from synthetic materials such as expanded polytetrafluoroethylene (ePTFE) and polyethylene terephthalate (PET), commonly known by the trade name Dacron®, have displayed impressive long-term success in the replacement of large diameter vessels (> 6 mm). This success, however, has not being replicated with small diameter grafts (< 6 mm) where there is no synthetic graft available with suitable long-term patency rates. High thrombosis rates and compliance mismatch are frequently cited as the causes of the poor patency rates. Additionally, these synthetic grafts do not have the ability to grow and remodel presenting a particular disadvantage for paediatric patients. Thus, recent research has focused on developing suitable vascular grafts using tissue engineering. Tissue engineering offers the potential of replacing a patient's damaged or diseased vessels with tissue engineered vessels which aim to function well haemodynamically, have the ability to remodel and repair in response to injury or altered conditions, and possess the long-term durability and growth potential of native vasculature.

1.3 Tissue Engineering

The emerging field of tissue engineering holds much promise for vascular tissue repair. The term “tissue engineering” can be defined as “an interdisciplinary field that applies the principles of engineering and the life sciences toward the development of biological substitutes that restore, maintain, or improve tissue function” (Langer and Vacanti, 1993). While the tissue engineering field may be relatively new, the idea dates as far back as circa. 800BC when skin grafting was first described by Sushrata in his work “Sushruta Samhita” (Ang, 2005). Gasparo Tagliacozzi (1546-1599), widely hailed as the founding father of plastic surgery, arguably also laid the foundation for the goals of tissue engineering with his widely quoted statement “We restore, repair and make whole, those parts....which nature have given but which fortune has taken away”.

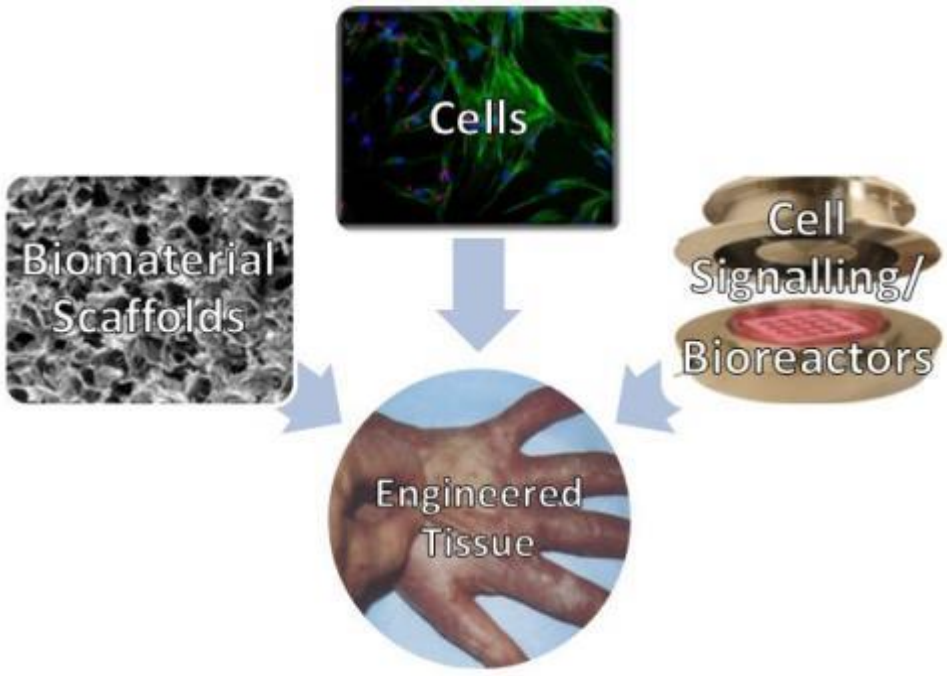

Figure 1.6 Tissue engineering triad

Tissue engineering requires the development of suitable biomaterial scaffolds to act as a platform to seed cells and apply appropriate signalling (Images adapted from (Al-Munajjed and O’Brien, 2009; Cartmell et al., 2002; Dantzer and Braye, 2001; Thorpe et al., 2010)*.*

Practically speaking, tissue engineering can be defined as a triad of scaffolds, cells, and signals which function synergistically to enable new functional tissue growth either *in vitro* or *in vivo* (Fig. 1.6). This thesis focused

on the development of a tissue engineered vascular graft (TEVG), which involved the development of a novel scaffold platform (Chapter 2), suitable architecture (Chapter 3), and *in vitro* maturation in a custom designed bioreactor to apply physiologically relevant biomechanical signals (Chapters 4/5) Consequently, the requirements for each of these facets will be examined in further detail.

1.4 Cells

Cells are a vital component of the tissue engineering triad as they are involved in remodelling and secretion of the extracellular matrix (ECM) which forms the structural framework for tissue. It is required that the cell source be viable, easily extractable, and possess the functional characteristics necessary for a vascular cell. The optimal cell type for vascular tissue engineering has yet to be elucidated. Cell sources may be extracted from the same intended patient (autologous), transplanted from another human (allogeneic), or sourced from a different species (xenogeneic). The field of tissue engineering of vascular grafts generally focuses on replicating the medial layer of native vessels as this layer is responsible for much of the vessels mechanical strength and vasoactivity. For vascular tissue engineering of the medial layer, the field has generally focused on utilising allogeneic smooth muscle cells (SMCs), autologous fibroblasts, or autologous mesenchymal stem cells (MSCs).

1.4.1 Endothelial cells

Vascular endothelial cells (ECs) form the luminal lining of blood vessels where they are crucially involved in maintaining vessel patency. The EC interface between blood and the vessel wall achieves this antithrombotic effect primarily by i) minimising plasma protein attachment to the vessel wall, ii) production of nitric oxide (NO) and prostacyclin which regulates platelet adhesion/activation, iii) inhibition of the blood coagulation cascade though heparan sulfate, and iv) production of the protease tissue plasminogen activator which breaks down thrombus by converting plasminogen to plasmin (Fig. 1.7) (Li and Henry, 2011). Indeed, this has been shown multiple times

where TEVGs with an EC lining maintain an open patent lumen while unlined TEVGs quickly became occluded (Deutsch et al., 1999; Seifalian et al., 2002; Shindo et al., 1987).

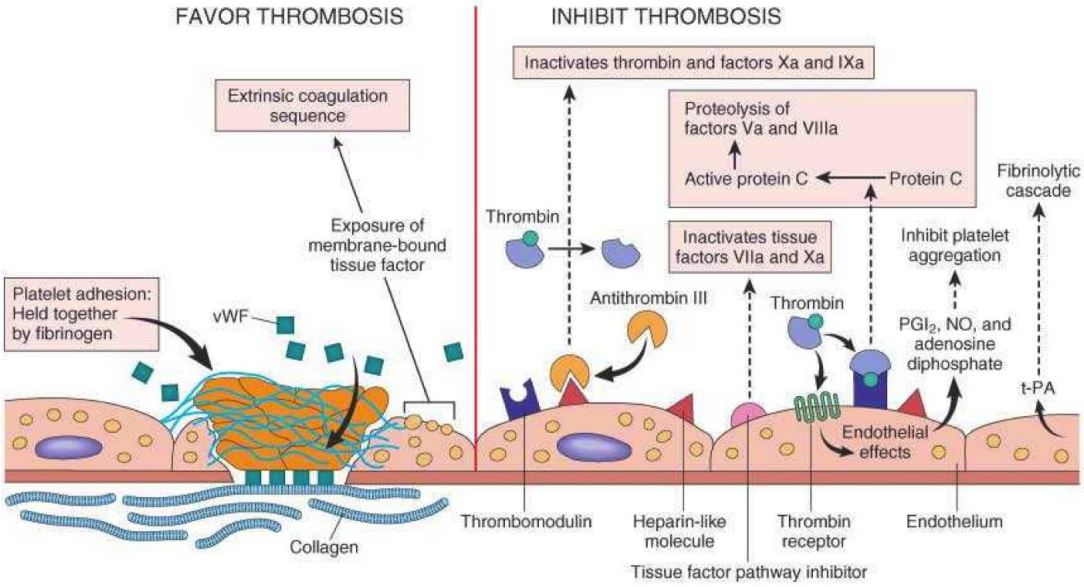

Figure 1.7 Anticoagulant properties of normal endothelium.

Disrupted/activated endothelium favours thrombosis (left) while normal endothelium (right) inhibits thrombosis (Kumar et al., 2014).

Endothelial cells also crosstalk with SMCs and reduce the risk of intimal hyperplasia by reducing SMC proliferation (Nackman et al., 1998; Tsai et al., 2009). In the generation of a TEVG the effect of ECs is rather complicated with co-cultures of ECs and SMCs resulting in reduced ECM production versus SMC culture alone (Bulick et al., 2009), an undesirable characteristic for generating a TEVG. As a result, the most appropriate approach when maturing TEVGs has been found to mature the vessel with SMCs/fibroblasts and to culture ECs immediately pre-implantation to provide a suitable non-thrombogenic lining (Quint et al., 2011). Additionally, ECs are partially responsible for vascular tone by releasing vasoconstrictors (e.g. endothelin) and vasodilators (e.g. NO, prostacyclin) which act on SMCs, and thus are necessary to generate a vasoactive vessel (Lüscher, 1990).

While the role of ECs has clearly been highlighted, the optimal method of creating and maintaining a confluent endothelium has yet to be determined. Initial research in the area focused on *in vitro* seeding of ECs on TEVGs,

however issues with EC sloughing, where the lining becomes disrupted due to high shear stress from trauma during implantation, has resulted in the field examining other approaches (Johnson et al., 2000; Meinhart et al., 2005; Rosenman et al., 1985). One of the most promising approaches involves the *in situ* recruitment of circulating endothelial progenitor cells (EPCs) (Shi et al., 1998) or the encouragement of native EC migration through the anastomosis sites (Zhang et al., 2004). Endothelial progenitor cells are a small circulating population of mononuclear cells which may differentiate towards an endothelial cell lineage (Asahara, 1997; Peichev et al., 2000). EPCs exhibit a number of cell markers including CD133+, CD34+, and vascular endothelial growth factor receptor-2 (VEGFR2). Therefore, it has been shown to be possible to coat TEVGs with these specific antibodies to encourage homing of native EPC (Rotmans et al., 2005).

Coatings with less specificity for a single cell type have also being examined, such as TEVGs functionalised with fibronectin-derived RGD peptide (Zheng et al., 2012), and laminin-derived YIGSR peptide (Jun and West, 2005). While this approach greatly simplifies the fabrication process, it does require the initial lumen surface to be non-thrombogenic during the time is takes for the circulating EPCs/native ECs to coat the TEVG lumen. Consequently, recent research has sought to alleviate this problem by releasing anticoagulants such as heparin (Conklin et al., 2002; Yao et al., 2014), antiplatelet adhesion molecules such as nitric oxide (Taite et al., 2008; Zhao et al., 2013), or creating surfaces which are inherently non-thrombogenic, such as elastin coated surfaces (de Torre et al., 2015; Simionescu et al., 2006; Waterhouse et al., 2011).

1.4.2 Mesenchymal stem cells

Mesenchymal stem cells (MSCs) have been extensively investigated as an alternative cell source for vascular tissue engineering due to the difficulty in isolating autologous smooth muscle cells. MSCs are multipotent progenitor cells capable of differentiating towards a number of different lineages under appropriate conditions, including smooth muscle and endothelial cells (Gong and Niklason, 2011; Kim et al., 2005; Wingate et al., 2012). Additionally,

MSCs are more easily accessible, from a clinical perspective, as well as exhibiting a higher proliferation capacity than SMCs (Gong and Niklason, 2011; McKee et al., 2003). Their role in a regenerative capacity is further enhanced by the immunomodulatory role they exhibit (Aggarwal and Pittenger, 2005).

The ability of MSCs to differentiate towards a SMC lineage has been examined through a defined multitude of mechanochemical conditions (Gong and Niklason, 2008). Differentiation factors commonly utilised for SMC differentiation include transforming growth factor-β1 (TGF-β1) (Zhang et al., 2009), numerous members of the platelet derived growth factor family (PDGF-BB, PDGF-CC), ascorbic acid, basic fibroblast growth factor (bFGF), hepatocyte growth factor (HGF) and vascular endothelial growth factor (VEGF).

In addition to soluble growth factors, environmental factors such as extracellular matrix proteins (Lozito et al., 2009) and mechanical forces (Kobayashi et al., 2004) have also been shown to play an important role in the differentiation towards SMCs (Gong and Niklason, 2011). Furthermore, ECM matrix stiffness, architecture and composition have each been shown to be involved in directing MSC differentiation (Engler et al., 2006; Wingate et al., 2012). Despite the wide range of growth factors and the various combinations examined in the literature, a robust protocol for the controlled differentiation of MSCs towards either synthetic or contractile SMC has not been established. Many of the published data pertaining to differentiation of MSCs towards a SMC lineage fail to report the expression of late stage SMC markers such as smooth muscle-myosin heavy chain (Wingate et al., 2012; Zhang et al., 2009).

Very little research into the effect of the natural protein elastin on MSC or SMC differentiation has been published. Gong and Niklason have previously shown that MSCs seeded on elastin coated substrates resulted in a significant increase in calponin gene expression versus uncoated surfaces although alpha-SMA and cell proliferation levels were not significantly different (Gong and Niklason, 2008). Additionally, Park (Park et al., 2004)

have shown that MSCs seeded on elastin-coated membranes expressed higher levels of alpha-actin protein than on collagen-coated membranes when subjected to equiaxial strain. While it is clear that MSCs present great potential for vascular tissue engineering, the lack of reproducibility between donors and lack of a robust differentiation protocol has led many researchers to revert to utilising allogeneic smooth muscle cells.

1.4.3 Smooth muscle cells (SMCs)

Vascular smooth muscle cells (SMCs) are primarily responsible for the ability of the human body to actively alter the diameter of vasculature through contraction which leads to precise control over the volume and pressure of blood delivered to the tissues of the body. These mature, contractile smooth muscle cells exhibit a particularly low level of migration, proliferation, and extracellular matrix (ECM) production. However, mature SMCs display extraordinary plasticity over the course of their life and may switch phenotype in response to local environment changes (Rensen et al., 2007). These local environment changes may result in SMCs changing from a contractile phenotype to a more synthetic phenotype (Fig. 1.8). Synthetic SMCs display drastically increased cell migration, proliferation, and ECM production and this phenotype is generally observed during vessel wall remodelling. Vessel wall remodelling may be required following vascular injury or in response to altered physiological conditions such as pregnancy or exercise (Yoshida and Owens, 2005).

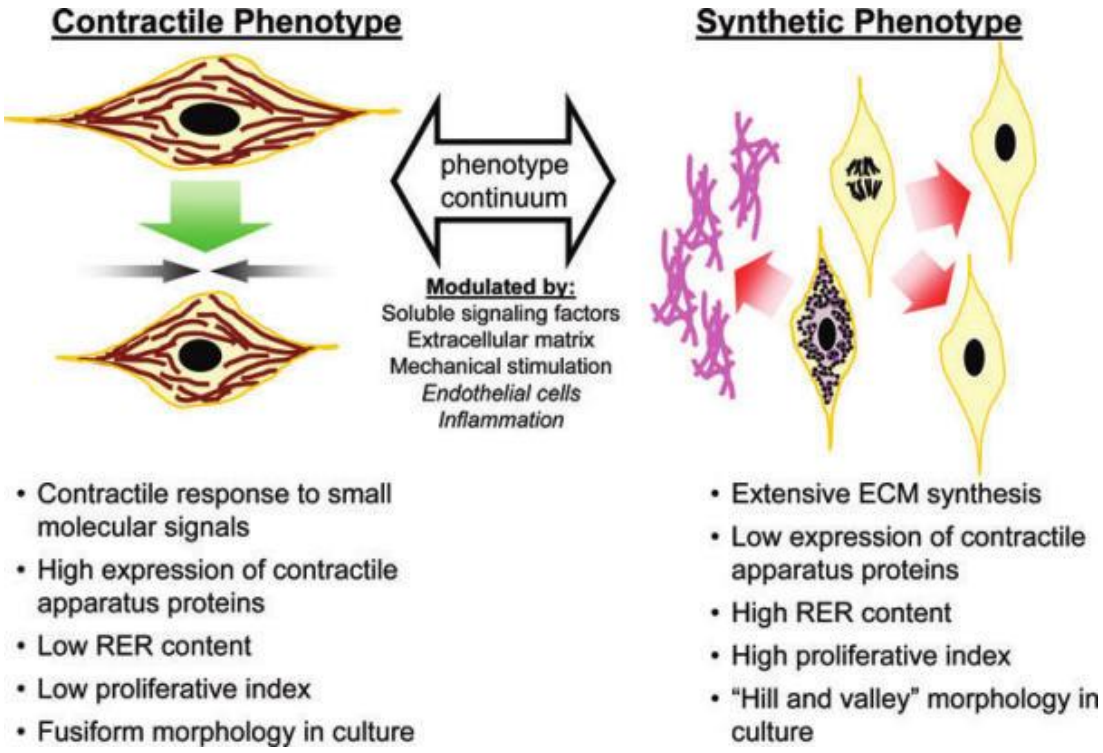

Figure 1.8 Smooth muscle cell phenotypic plasticity

SMCs can display a phenotypic continuum from contractile (left) to synthetic (right). Contractile SMCs are present in native vessels and display a spindle-like morphology and respond to vascular agonists. Synthetic SMCs are present in pathological vessel conditions, display a fibroblast-like morphology, and proliferate rapidly while producing large amount of ECM (Beamish et al., 2010).

For the purposes of vascular tissue engineering, smooth muscle cells are a vitally important component of a bioengineered vessel as they function to synthesise important structural ECM components such as elastin, collagen I, and collagen III. The ability to control the phenotype of SMCs may be very advantageous as it could allow *in vitro* maturation of vascular grafts through inducing high ECM producing synthetic smooth muscle cells followed by a switch to a contractile phenotype to produce vessels which would contract and relax in response to vascular agonists. It is this latter function of SMCs, contractility, which has arguably been the most difficult function to replicate *in vitro*. Mature SMCs express a number of protein monomers, such as α-SMA, calponin, and smooth muscle-myosin heavy chain, which form force generating myofilaments. These contractile protein monomers are commonly utilised as markers of SMC differentiation (Gong and Niklason, 2008). However, SMCs quickly revert to a synthetic phenotype upon expansion *in*

vitro and so alternative methods need to be investigated to control this phenotypic switch. However, cell behaviour is also dictated by the substrate upon which they are cultured upon, whether that be a 2D surface, or more preferably, a 3D scaffold.

1.5 Scaffolds

The primary requirement of a tissue engineered scaffold is to help guide the growth of 3D functional tissue *in vivo*. The scaffold can be considered analogous to the natural extracellular matrix produced by cells through providing structural support, adhesion sites, facilitating movement, regulating a cell's behaviour, and assisting cell-to-cell recognition. The requirements for a tissue engineered scaffold are numerous and are often application specific (Gleeson and O'Brien, 2011). Some of the key factors examined in this project are:

1. Biocompatibility
2. Biodegradability
3. Bulk Mechanical Properties
4. Pore Size and Pore Size Distribution
5. Porosity, Pore Interconnectivity and Permeability

1. Biocompatibility

Historically, biocompatibility has been defined as "the ability of a material to perform with an appropriate host response in a specific situation" (Williams, 1987). This definition is very broad as it must encompass the very diverse applications to which biomaterials are utilised. For tissue engineering scaffolds, a more appropriate definition of biocompatibility has been proposed (Williams, 2008):

ñThe biocompatibility of a scaffold or matrix for a tissue engineering product refers to the ability to perform as a substrate that will support the appropriate cellular activity, including the facilitation of molecular and mechanical signalling systems, in order to optimise tissue regeneration, without eliciting any undesirable local or systemic responses in the eventual hostò

Further to the definition of biocompatibility above, the degradation products of a scaffold biomaterial must also be biocompatible. This requirement is especially important when considering synthetic polymers such as polyglycolic acid (PGA). PGA has previously been used to create successful scaffolds for vascular tissue engineering although the material's hydrolysis products have been implicated to be involved in the dedifferentiation of SMCs (Gong and Niklason, 2011; Niklason et al., 2001). Additionally, the hydrolysis products can lead to a lowering of local pH levels and a resulting inflammatory response (Athanasiou et al., 1996).

2. Biodegradability

Biodegradability refers to materials which can be broken down in the physiological environment via biological agents or environmental conditions such as temperature or pH. Biodegradable materials are very suitable for applications that only require temporary implant presence. At a mechanical level it is desirable for a gradual stress transfer and thus a slow degradation rate. This gradual stress transfer minimises the problems associated with rigid vascular grafts such as failure at the anastomosis site due to a compliance mismatch.

At the biological level, it is desirable for the degradation level to match the rate of new tissue growth which generally necessitates a faster degradation rate. A considerable challenge in tissue engineering scaffolds is modifying the degradation rate of biomaterials to strike a balance between these two factors; mechanical and biological. A major advantage of biodegradable materials is that they do not require an additional surgical procedure for implant removal as well as circumventing the potential toxicity and safety problems associated with long term implants. Biodegradability is linked inextricably to biocompatibility as the degradation products must also be biocompatible (Bouten et al., 2011).

3. Bulk mechanical properties

The required bulk mechanical properties of a scaffold can vary enormously depending on the application. All tissue engineered scaffolds should have

adequate integrity to withstand surgical handling and subsequent implantation. There is contention and contradictory evidence in the literature as to the most suitable approach for vascular tissue engineering. The focus of a significant amount of research is towards scaffolds which strive to maximise the burst pressure of the scaffolds with compliance and biological suitability often relegated due to this (Girton et al., 2000; Hoerstrup et al., 2001; Isenberg et al., 2006). Numerous researchers have reported suitable burst pressures although this was associated with a compliance mismatch (L'Heureux et al., 1998; Niklason et al., 1999). The compliance of native vessels is primarily influenced by the high concentration of elastin within the vessel walls and the relative alignment of the other ECM components. Possible reasons for the association of compliance mismatch and graft failure may be failure at the anastomosis site due to high strain, turbulent flow resulting in a change in endothelial cell biochemistry and unnatural stress resulting in intimal hyperplasia(Salacinski et al., 2001a, 2001b; Sarkar et al., 2007; Tai et al., 2000).Thus, the most appropriate approach would seem to find a suitable compromise between burst pressure strength and other important mechanical properties, such as compliance.

4. Substrate stiffness

Substrate stiffness plays a critical role in the biological response of cells to a scaffold as it has been shown to influence cell migration and development, proliferation and morphology (Discher et al., 2005). It has previously shown that mesenchymal stem cells (MSCs) are extremely sensitive to substrate stiffness and they specify their lineage and phenotype partially based on this. They have shown that a comparatively soft substrate resulted in neurogenic differentiation, a moderately stiff substrate resulted in a myogenic differentiation, and a highly stiff matrix results in osteogenic differentiation (Engler et al., 2006). Harley (Harley et al., 2007) has investigated the difference between the bulk mechanical properties of Coll-GAG scaffolds and the stiffness of the substrate which seeded cells would experience. It was found that the individual strut modulus (~5MPa) was in the order of 2.5×10^3 times higher than the bulk modulus of the scaffold (~200Pa). This large disparity is a property inherent of highly porous scaffolds. A substrate

stiffness of 11-15kPa has previously been shown to result in myogenic differentiation of MSCs and so this can be used during the biomaterial design stage to help produce a scaffold with suitable substrate stiffness for vascular tissue engineering (Engler et al., 2006; Wingate et al., 2012).

4. Pore size and pore size distribution

The control of the distribution of pores and pore size in a scaffold is imperative to the biological performance of the scaffold and should be unique to the particular application it is required for *in vivo.* Pore size may be used to preferentially exclude or promote in-growth of certain cell types. This data may then be utilised in the design of a multi-layered vascular scaffold to reduce the risk of neointimal hyperplasia of SMCs. Previous research has shown that pore size can have a significant effect on cell attachment, proliferation and migration with collagen based scaffolds (Murphy et al., 2010; O'Brien et al., 2005). The optimal pore size for SMCs and MSCs for vascular engineering has been reported as being in the range of 75μm to 120μm (Kang et al., 1999; Ross and Tranquillo, 2003). An average pore size of between 10μm and 45 μm has been shown to be ideal for fibrovascular infiltration and endothelialisation of the luminal aspect of grafts (He and Matsuda, 2002; Zhang et al., 2004).

Previous *in vivo* results have shown that a mean pore size of >100 μm results in an increased rate of tissue in-growth and vascularisation (Cao et al., 2006; Mikos et al., 1993; Oh et al., 2007). However, for vascular tissue engineering the permeability of a scaffold is a very important factor to consider, with large pore sizes leading to an increase in permeability and potentially leakage of a vascular graft. While it is important to prevent leakage from scaffolds with large pore sizes, reducing pore sizes below approximately 50 um would likely result in an inability of cells to infiltrate to any great depth into the scaffold and potentially result in core necrosis due to a lack of nutrient transfer and vascularisation. Therefore, a compromise must be sought between a suitable pore size for cellular attachment and infiltration, and an appropriate permeability which will not result in graft leakage.

5. Porosity, pore interconnectivity, and permeability

A central requirement for tissue engineered scaffolds is that they must possess sufficient mass transport and mechanical function to stimulate tissue repair. Mechanical function and mass transport are both inextricably linked to the porosity, pore interconnectivity, and permeability of the scaffold. Porosity can be defined as the percentage of void space in a solid (Leon, 1998). It has been suggested by multiple researchers that a scaffold should possess a porosity of 90% or greater for effective tissue repair (Gleeson and O'Brien, 2011; Harley et al., 2006; Rezwan et al., 2006). *In vivo* studies have shown that a high porosity results in an increase in vascularisation and tissue in-growth versus low porosity scaffolds (Karageorgiou and Kaplan, 2005). In addition to a high void fraction, or porosity, an open-cell pore geometry will result in highly interconnected pores that allows for enhanced angiogenesis due to increased cell distribution and migration.

1.5.1 Biomaterial composition

Tissue engineered scaffolds can be fabricated from a wide range of biomaterial classes. The scope of this project involves the use of the natural biodegradable polymers collagen and elastin and so subsequent chapters will focus solely on these pertinent materials and suitable crosslinking methods to increase their structural stability.

Collagen

The natural polymer collagen is the most abundant structural protein in the body with 28 genetically distinct types identified to date (Veit et al., 2006). It is found in high concentrations in connective tissues such as skin, ligaments, tendons, and the cardiovascular system. It is composed of polypeptide chains of amino acids arranged in a right handed triple helical structure (Fig. 1.9A). All collagen utilised within this project is collagen type I, which is the primary structural collagen present in native vasculature.

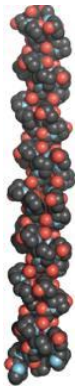

A

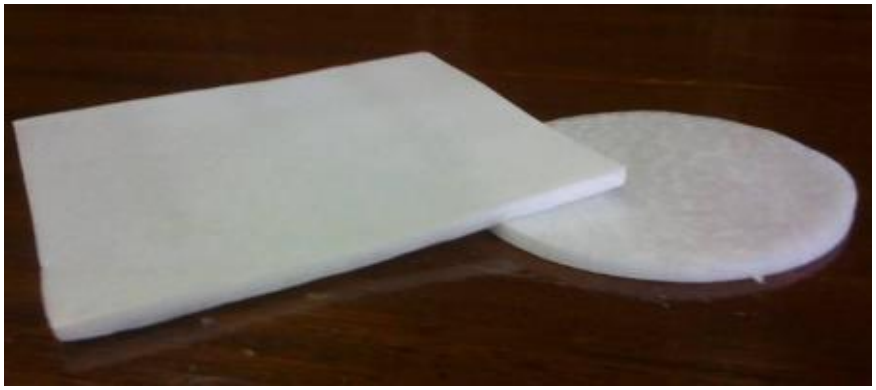

B

Figure 1.9 Collagen for tissue engineering

(A) Overview of collagen triple helix structure (Shoulders and Raines, 2009)*.*
(B) Freeze-Dried collagen-GAG scaffolds.

Collagen isolated for tissue engineering purposes is generally of a bovine, porcine or murine origin. Collagen often suffers a loss of structural integrity during the isolation process and is an inherently heterogeneous protein. Its heterogeneity can cause it to denature easily, even at body temperature (Leikina *e t* ., 2001), however it usually occurs several degrees above normal body temperature. This denaturation process, where collagen breaks down from its naturally occurring quaternary structure into a random chain configuration, is a very important consideration when selecting a suitable scaffold fabrication process and crosslinking method(Miles and Bailey, 2001). Freeze-drying, or lyophilisation, is a suitable technique which has been extensively used by the laboratory at RCSI to fabricate highly porous collagen based scaffolds (Fig. 1.9 & 1.10) (O'Brien et al., 2004).

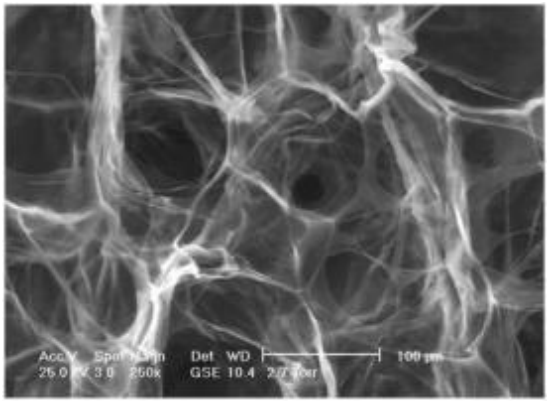

Figure 1.10 Scanning electron micrograph of porous collagen structure

SEM of the open porous nature of a Collagen-Glycosaminoglycan scaffold (O'Brien et al., 2004)

With reference to the aforementioned ideal tissue engineered scaffold requirements, collagen exhibits excellent biocompatibility and biodegradability. As a collagen matrix forms part of the natural vascular growth, healing, and remodelling processes, it is ideally suited as a scaffold material for a vascular graft. The major disadvantage associated with collagen scaffolds is the inherently low stiffness and strength which it imparts when it is not in a highly organised structure. However, this can be improved significantly through physical and chemical crosslinking methods which can also be used to control the degradation rate (Koh and Atala, 2004).

Elastin

Elastin is an extracellular matrix protein responsible for the elastic properties of many tissues. It is present in high concentration in native vasculature and can form up to half of the total protein content in highly elastic vessels. It is a highly insoluble hydrophobic protein usually present in arteries as a large covalently crosslinked network arranged in wavy concentric layers. In native vasculature elastin serves to act as a recoil component and prevents aneurysm formation via its efficient strain-energy storage. From a mechanical viewpoint, it has previously been reported that at 35% strain in native arteries, a minimum of 48% of the arterial load is carried by elastin (Lammers et al., 2009). Additionally, elastin has been shown to control the proliferation of smooth muscle cells and may have a role in the prevention of intimal hyperplasia (Li et al., 1998a, 1998b).

Elastin is an extremely durable protein and as such, it has an extremely low turnover rate *in vivo* (Shapiro et al., 1991). Consequently there exists a significant challenge in stimulating cells to synthesize this essential protein either *in vitro* or *in vivo* (Long and Tranquillo, 2003). Due to a difficult purification process, the use of elastin for the fabrication of tissue engineering scaffolds has only emerged in the last decade. The high extensibility and resilience of this protein, coupled with its low stiffness, may allow it to provide improved mechanical properties for tissue engineered vascular grafts. Thus, the addition of elastin to a collagen-based scaffold is expected to provide a more natural viscoelastic response and, in

combination with the high tensile strength of collagen, may provide compliance closer to native vessels than currently available grafts (Gershon et al., 1992).

1.6 Tissue engineered vascular grafts (TEVGs)

While a number of standard scaffold requirements must be appeased to generate 3D functional tissue, the highly optimised nature of native tissue results in a large number of specific requirements for a successful tissue engineered vascular graft (TEVG). All TEVGs should have adequate integrity to withstand surgical handling, suitable suture retention strength, and sufficient burst pressure and compliance to ensure it can withstand the challenging haemodynamic environment. In addition to the mechanical considerations for a vascular graft, it is also a necessary requirement for a graft to enable an appropriate healing response. This requires that the graft is not susceptible to neointimal hyperplasia, inflammation, or fibrous encapsulation. Neointimal hyperplasia can be defined as a migration and proliferation of SMCs to the intima where they form a proteoglycan rich matrix which may occlude the vessel or give rise to an atherosclerotic lesion (Cizek et al.). Furthermore, a TEVG must be non-thrombogenic, infection resistant, and be vasoactive in order to integrate as a functional tissue with the cardiovascular system. The specific requirements of a TEVG and the related scaffold characteristics are listed in Table 1-1, below.

In order to satisfy these requirements, a number of different approaches have been investigated, with altered biomaterial classes, architectures, fabrication technologies, and approaches to tissue maturation. In terms of biomaterials utilised for TEVGs, there are four main classes, namely:

- Decellularized tissue
- Synthetic biodegradable polymers
- Cell-sheet engineering
- Natural biodegradable polymers

Table 0-1 Key requirements for a tissue engineered vascular graft.

TEVG Specific Requirements	Related Scaffold Characteristics
1. Adequate integrity to withstand surgical handling, suitable suture retention strength and flexibility.	¶ Bulk Mechanical Properties
2. Leak resistance but permeability sufficient to allow diffusion of nutrients necessary for tissue growth and maturation.	¶ Pore Size and Pore Size Distribution ¶ Porosity, Pore Interconnectivity and Permeability
3. Suitable mechanical properties such as burst strength, compliance and the ability to withstand long-term cyclical strain.	¶ Bulk Mechanical Properties
4. Appropriate healing response i.e. no neointimal hyperplasia, inflammation, or fibrous encapsulation.	¶ Biocompatibility ¶ Biodegradability
5. Grafts must be non-thrombogenic, biocompatible and infection resistant.	¶ Biocompatibility
6. Active physiological properties such as vasoconstriction and dilation.	¶ Biocompatibility ¶ Mechanical properties
7. Resist aneurysm formation due to creep. If a recoil element, such as elastin, is not present in a vessel then permanent dilation of the vessel may occur (aneurysm).	¶ Biocompatibility ¶ Biodegradability ¶ Bulk Mechanical Properties
8. Easy to manufacture, sterilize, and store, as well as be economical and available in a variety of sizes.	N/A

1.6.1 Decellularized TEVGs

Decellularized TEVGs are produced by removing the cellular and antigenic components from xenografts or allografts to leave behind the intact native ECM (Fig. 1.11). Decellularization may be achieved with numerous methods encompassing physical, chemical, or enzymatic methods (Crapo et al., 2011). The choice of decellularization method is informed by the tissue density, organisation, architecture, and retainment of biological properties.

Physical methods such as pressure, agitation, or abrasion can be utilised for large tissues but invariable tissue damage occurs due to the high forces applied to the tissue. Alternative methods such as detergents, hyper/hypotonic solutions, or gentle enzymatic treatments often result in less tissue damage and the improved removal of antigens (Conklin et al., 2002; Yang et al., 2010). While the primary aim of decellularization is the removal of potential antigens, it is imperative that the mechanical properties are retained and so extensive optimisation of the process must be completed to balance the effects of decellularization and loss of structural integrity (Sheridan et al., 2012).

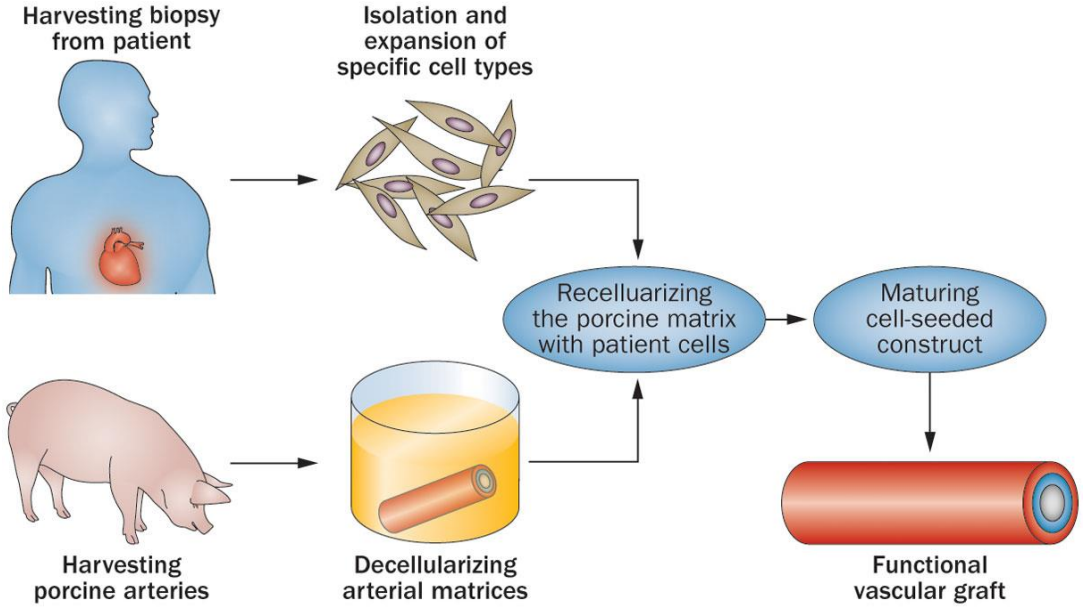

Figure 1.11 Decellularized TEVG fabrication

Native arteries are harvested from a viable animal source, and decellularized using chemical, mechanical, or enzymatic methods. Autologous cells may be sourced from the patient, expanded, and seeded upon the decellularized matrix to create a TEVG (Seifu et al., 2013).

The origin of the tissues may be vascular or non-vascular, such as carotid arteries or small intestinal submucosa (SIS) respectively. Utilising native arteries has been shown to have a number of advantages including possessing the native ECM composition and architecture as well as excellent mechanical properties. Commercially available grafts, such as bovine carotid based Artegraft® and bovine mesenteric vein based ProCol®, have been available clinically for up to 45 years yet widespread adoption has not been realised. This is primarily due to the limited advantages which these grafts

offered clinically over cheaper synthetic grafts in long-term trials (Brems et al., 1986; Guidoin et al., 1989; VanderWerf et al., 1975). Failure of these grafts was determined to primarily be due to thrombosis or aneurysm formation which could stem from the lack of cell infiltration observed in the grafts.

While decellularized TEVGs retain their native ECM structure, poor cell infiltration due to the highly dense tissue inhibits any significant cell migration (Berardinelli, 2006; Chemla and Morsy, 2009). This lack of cellularity within the TEVGs results in degrading mechanical properties over time *in vivo* and ultimately contributes significantly to graft failure. Novel seeding techniques have been developed to attempt to overcome this problem, such as magnetic nanoparticle guided cell-seeding (Shimizu et al., 2007), creating longitudinal seeding channels (Sheridan et al., 2014a), or a combination of biochemical and biophysical stimulation to encourage cell migration (Sheridan et al., 2014b). Furthermore, adverse immunogenic responses are often still encountered due to remaining antigens within the decellularized TEVGs (Allaire et al., 1997). While it is clear that there are a number of advantages to utilising decellularized TEVG, progress with these grafts has been marred by the time consuming decellularization process, issues with vessel sourcing, poor cell infiltration, and lack of control over the final vessel geometry. Bioengineers have thus sought to create custom TEVGs using advanced fabrication techniques and a variety of synthetic and natural polymers.

1.6.2 Synthetic biodegradable polymer TEVGs

Synthetic biodegradable polymers, such as polyglycolic acid (PGA), are commonly used as a basis for TEVGs. The premise behind utilising biodegradable synthetic polymers is that the polymers would exhibit sufficient strength to withstand implantation in high pressure arterial sites while also slowly being degraded and replaced by functional vascular tissue. Consequently, these polymers are often formed as copolymers to control the degradation rate and mechanical properties of the resulting scaffolds.

One of the first viable TEVGs was reported by Shinoka and colleagues who utilised a polyglactin/polyglycolic acid tubular mesh seeded with autologous myofibroblasts and implanted in an ovine pulmonary artery (Shinoka et al., 1998). While this initial study was a TEVG of diameter 15mm, it did serve as a proof of concept study and the field of vascular tissue engineering greatly expanded after. One of the first groups to report success with small diameter (< 6mm) TEVGs was Niklason and colleagues who utilised a SMC seeded polyglycolic acid based mesh to generate mechanically impressive grafts after 8 weeks of bioreactor conditioning (Niklason et al., 1999). These grafts have displayed promising results in a porcine carotid artery model where they remained patent for 30 days (Quint et al., 2011), and also as an arteriovenous shunt in baboons (Dahl et al., 2011). Following successful trials of these grafts this technology has recently progressed towards the clinic through spin-out company Humacyte Inc. (Dahl et al., 2011). The first human clinical trials of this technology began in mid-2013 where the tissue engineered graft was implanted as an arteriovenous graft for haemodialysis access in order to test *in vivo* efficacy and safety. It should be noted, however, that the TEVGs were decellularized to remove the seeded cells prior to human trials due to the allogeneic cell source (Dahl et al., 2011; Quint et al., 2012).

While these trials are extremely encouraging there are yet doubts over the technology as many synthetic based vascular grafts have exhibited poor long term patency rates due to issues such as compliance mismatch, thrombosis, rejection, intimal hyperplasia, calcification, and infection. Additionally, biodegradable synthetic polymers, such as PGA, have been shown to dedifferentiate SMCs due to their hydrolysis products (Gong and Niklason, 2011; Niklason et al., 2001). Furthermore, PGA degrades into glycolic acid, which can be removed via the Krebs cycle or excreted by the kidneys unchanged, however the high concentrations released can lead to a lowering of local pH levels and a resulting inflammatory response (Athanasiou et al., 1996). Endothelialisation of the luminal aspect of these grafts has previously been utilised to reduce thrombogenicity with a good success rate (Gao et al., 2008). The patency of these grafts can additionally be improved via

passivation of biologics such as heparin (Dimitrievska et al., 2015), growth factors, or antibiotics (Thomas, 2003). Despite the advances in synthetic biodegradable scaffolds, many of the grafts can have a limited potential for remodelling as well as a lack of vasoactivity.

Cell-free approaches utilising synthetic polymers have recently come to the fore due to impressive *in vivo* results (Allen et al., 2014; Matsumura et al., 2013; Wu et al., 2012). Cell-free approaches require tightly controlled degradation characteristics to enable tissue growth rate at the same rate as polymer degradation. Wang and colleagues have developed a fast degrading polymer, poly (glycerol sebacate) (PGS), which displays impressive mechanical properties and is resorbed within 60-90 days *in vivo* (Wang et al., 2002). Additionally, as PGS is an elastomer it allows the efficient transfer of mechanical stimulation to seeded SMCs which migrate into the porous walls, resulting in high levels of elastin formation *in vitro* (Gao et al., 2008; Lee et al., 2011). Adapting this polymer for use as a cell-free TEVG *in vivo* has displayed impressive results in a rat abdominal aorta model and rapidly remodelled to resemble native arteries after 3 months (Wu et al., 2012). Furthermore, at 1 year these grafts became innervated, exhibited substantial elastin expression, and displayed good patency rates of 80% (Allen et al., 2014). Due to the rapid degradation rate, it remains to be seen whether the tissue regenerative rate of the patient cohort requiring a TEVG is capable of matching the rate of polymer degradation.

1.6.3 Self-assembled TEVGs

A completely autologous technique to fabricate vascular grafts via self-assembly, sometimes termed cell-sheet engineering, relies on stimulating cells to produce high levels of extracellular matrix proteins followed by assembly around a support mandrel and *in vitro* maturation of the construct (Fig. 1.12a). The autologous cells are generally fibroblasts isolated from skin biopsies which are cultured for up to 6 weeks to produce a sheet of cell embedded in extracellular matrix. This cell-sheet is detached from the cell

culture substrate and rolled around a mandrel and cultured for up to 10 weeks until the layers fuse into a homogenous tissue.

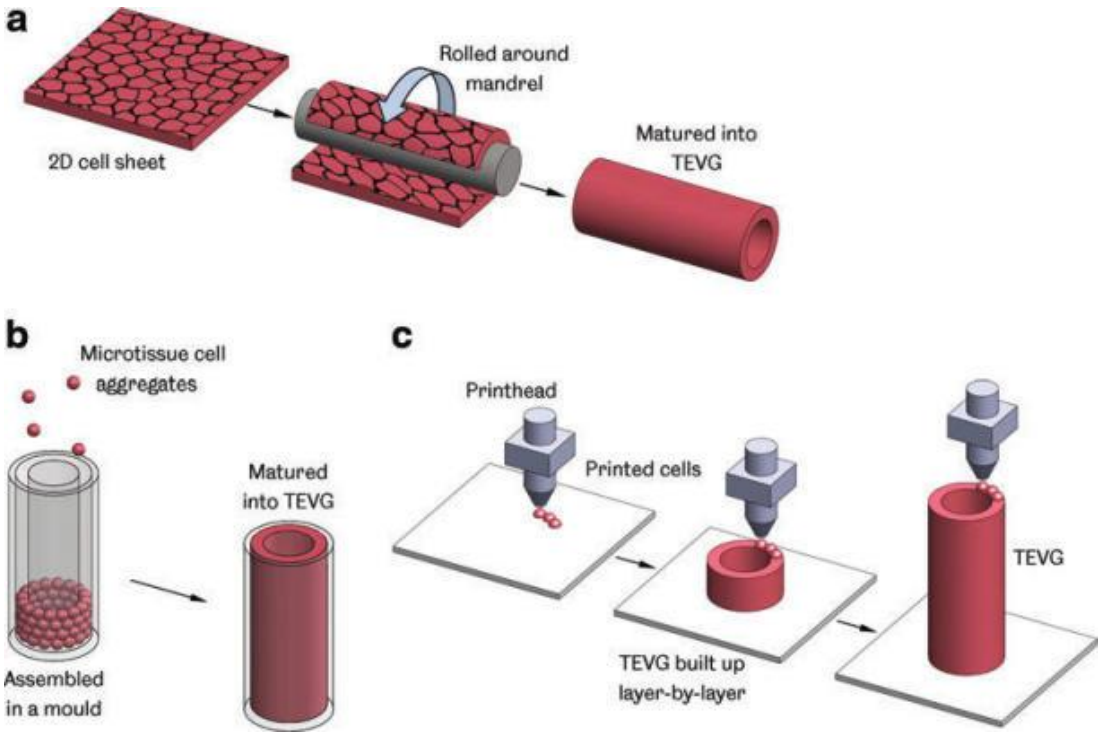

Figure 1.12 Self-assembled TEVG fabrication

Cell-sheet engineering (a) involves culturing to produce high levels of ECM and wrapping this cell-sheet around a mandrel for maturation. An alternative method involves creating cell aggregates and forming them into tubular shapes using custom molds (b) or 3D printing around degradable supports (c) (Pashneh-Tala et al., 2015).

Utilising this technique, L'Heureux and colleagues (L'Heureux et al., 1998) have shown that the TEVGs display burst pressures similar to native vessels and vascular reactivity, such as a response to vascular agonists (L'Heureux et al., 2001). Results using this strategy have, thus far, been very promising and have produced moderately successful clinical trials as arteriovenous (AV) shunts in human patients through the spin-out company Cytograft Tissue Engineering, Inc (Wystrychowski et al., 2014). However, due to the method in which these TEVGs are produced, they require very long culture times (~24 weeks) as well as the high cost associated with long term culture (L'Heureux et al., 2007). Additionally, the tissue formed is primarily composed of collagen with negligible quantities of elastin observed leading to vessels with a compliance of 2% - 3.1% per 100 mmHg (Wystrychowski et

al., 2014), a significant mismatch from native vessels which display values generally ranging from 8% -11.5% per 100 mmHg for human muscular arteries (Konig et al., 2009; Tai et al., 2000). In an effort to counteract a number of these issues they have moved towards using banked cells (allogenic) due to cost and manufacturing considerations. Furthermore, they have expanded the technology to create ECM threads which may be utilised to produce woven grafts, which has been patented (L'Heureux and McAllister, 2010) yet scientific details remain unpublished (Peck et al., 2011).

An alternative method of producing self-assembled TEVGs is to create cell pellets or aggregates which are arranged in a tubular shape using a mold and allowed to fuse during culture to produce a tubular structure (Fig. 1.12b). This approach enables precise control over the final architecture by utilising a mold machined to the exact dimensions required, although extended culture to ensure fusion is required (Gwyther et al., 2011). While this approach does allow control of relative cell positioning and density, the cell numbers required (>100 million per 1cm construct) limited its potential for clinical application (Kelm et al., 2010). While the use of a mold allows easy repeatability and a structure upon which to mature the delicate tissue, a layer-by-layer assembly approach using 3D printing would seem to offer far greater flexibility (Fig. 1.12c). Previous research has shown the ability to print a custom a tubular structure from multicellular spheroids within a 3D printed agarose support structure (Norotte et al., 2009). The flexibility of the approach allows the potential generation of complex architectures such as bifurcations, tortuous vessels, or vessels with varying diameters along its length. Furthermore, the ability to control the spatial organisation of cells allows the ability to replicate complex cell organisations, such as in native vasculature (Guillotin and Guillemot, 2011). Utilising this technique has resulted in vessels with burst pressures of up to 773 mm Hg, although once again, the high required cell numbers limit the clinical applicability of this technique (Marga et al., 2012)

1.6.4 Natural biodegradable polymer TEVGs

Natural biodegradable polymers, such as collagen and fibrin, were the basis of some of the first tissue engineered vascular grafts (Hirai et al., 1994; L'Heureux et al., 1993; C. . Weinberg and Bell, 1986). For the purpose of vascular tissue engineering, collagen is an excellent choice as the basis of a tissue engineered scaffold due to its inherently excellent biological performance, biodegradability and high concentration is native vasculature. Each of these early collagen grafts were formed from cells seeded in a collagen gel. However, this method produced scaffolds with poor mechanical properties due to the disorganised nature of the collagen which was randomly orientated. These early collagen-based grafts displayed very low burst pressures of 90 mmHg and thus each of the grafts required the use of a Dacron® mesh to provide structural support (Hirai et al., 1994)

Despite the limitations associated with these early grafts, significant advances in collagen fabrication techniques over the last 20 years have enhanced the potential for development of successful collagen-based tissue engineered vascular grafts. Fabrication methods such as magnetic alignment of the collagen, coupled with the use support mandrels to control the direction of scaffold compaction, can greatly influence the maturation of collagen-based TEVGs (Barocas et al., 1998). The use of dynamic mechanical conditioning through bioreactor technologies has also been shown to improve ECM deposition, orientation, and ultimately improve the strength of the TEVGs (Schutte et al., 2010; Seliktar et al., 2000). Further research into improved biofabrication methods and maturation strategies are needed to create collagen-based vascular grafts capable of being utilised effectively in the arterial system.

While collagen does represent the primary structural protein in arteries (along with elastin), greater success in fabricating TEVGs has been reported using alternative natural polymers such as chitosan, silk fibroin, or fibrin. Chitosan has previously been utilised to form TEVGs where a combination of industrial knitting, thermally induced phase separation, and a high wall

density led to burst pressures up to 4300 mm Hg, although compliance was unreported (Zhang et al., 2006). While the strength of these TEVGs was impressive, the low wall porosity was not suitable for efficient cell migration. A chitosan based TEVG with a higher wall density resulted in similar mechanical properties to collagen-based TEVGs (Zhu et al., 2009). Due to the improved biological properties of collagen, and no clear mechanical advantage to utilising chitosan, recent research has focused on more mechanically robust polymers.

Silk fibroin, a protein generally extracted from the silkworm *Bombyx Mori*, exhibits extraordinary toughness, a slow degradation rate, and is amenable to a large variety of fabrication methods allowing potentially precise control over the final TEVG properties (Kundu et al., 2013). Biologically, electrospun silk fibroin has been shown to be highly suitable for vascular cell culture where SMCs and ECs remained viable and maintained a native phenotype (Zhang et al., 2008). Unfortunately, silk fibroin exhibits a very high stiffness (Lovett et al., 2008) which results in a low compliance value for TEVGs (Marelli et al., 2010). Nevertheless, *in vivo* testing in a rat model revealed a patency rate of 85% at 1 year, although histologically the very slow degradation rate resulted in large proportions of silk remaining in the vessel walls (Enomoto et al., 2010).

Fibrin has arguably been the most successful natural polymer employed thus far for TEVGs. A major advantage of fibrin is that it can be extracted from a patient's blood, and if combined with patient extracted cells, may be able to provide a totally autologously sourced TEVG. As fibrin is a gel formed from the polymerisation of fibrinogen by thrombin, it can be easily molded to recreate complex architectures such as heart valves (Flanagan et al., 2007; Jockenhoevel et al., 2001). Numerous investigations to improve the mechanical strength of fibrin based TEVGs have been reported, including varying biochemical stimulation (Grouf et al., 2007), optimisation of protease inhibitors such as aprotinin (Jockenhoevel, 2001), altered cell density (Yao et al., 2005), or fusing concentric layers of tissue (Huynh and Tranquillo, 2010). Burst pressures of up to 600 mm Hg have been reported using a

combination of these culture techniques (Huynh and Tranquillo, 2010). Furthermore, *in vivo* results in a low pressure ovine jugular vein model revealed good patency and extensive remodelling (Swartz et al., 2005). The relatively high burst pressure of fibrin TEVGS when compared to collagen gels primarily stems from the enhanced contraction, and consequently enhanced density, observed during extended culture (Grassl et al., 2003). By applying mechanical conditioning for up to 9 weeks in a bioreactor, the burst pressure of these TEVGs can reach up to approximately 1500 mm Hg although suture retention strength was below the values necessary for surgical implantation (Syedain et al., 2011b).

It is clear that no single natural polymer presents the ideal properties to satisfy all the requirements for a TEVG. A hybrid of synthetic and natural polymers provides an interesting approach to this problem by leveraging the advantages of each polymer class, while minimising the adverse properties. By incorporating a polylactide-based mesh as a backbone, the group of Jockenhoevel have shown the ability to improve the mechanical properties of fibrin-based TEVGs at a shorter timepoint of 21 days (Tschoeke et al., 2008). Further success of this approach was demonstrated by implanting these hybrid TEVGs in ovine carotid arteries, where good patency was observed up to 6 months (Koch et al., 2010). However, the ideal TEVG would be biomimetic and be fabricated solely from the natural components found in the native tissue.

1.6.5 Elastin in TEVGs

Elastin has been utilised in many forms for both cardiac and vascular specific tissue engineering applications. While decellularized TEVGs have intact native elastin, minimal production of elastin has been observed in all other TEVG types. *In vivo* elastin matrix assembly is a complex and tightly regulated process which involves the secretion of tropoelastin, cell surface aggregation coordinated by fibulins, partial crosslinking through lysyl oxidase, further aggregation, excretion and localisation to extracellular microfibrils (mainly composed of fibulins), followed by coalescence and

further crosslinking with lysyl oxidase (Wagenseil and Mecham, 2007). While the secretion of tropoelastin is regulated by a single gene (ELN), it is the complex spatial and temporal process to form the insoluble proteins which has inhibited the field from replicating the required conditions (Csiszar, 2001).

From a tissue engineering perspective, the deposition of insoluble elastin has been shown to be influenced by numerous factors including scaffold degradation rate, stiffness, topography, and growth factor supplementation (Pashneh-Tala et al., 2015). An initial requirement for elastin production has been shown to be a 3D culture environment as 2D culture interferes with elastogenesis by SMCs (Lin et al., 2011). The stiffness of this environment has also been shown to be crucial, with a low compressive modulus (50-80 kPa) resulting in significantly enhanced elastin expression versus high modulus scaffolds (3 MPa) (Crapo and Wang, 2010). Furthermore, elastogenesis is also sensitive to the biochemistry of the scaffold (Kim et al., 1999b), with fibrin providing a distinct advantage over other natural polymers (Koch et al., 2010; Long and Tranquillo, 2003), although this may be enhanced partially by fibrins fast degradation rate which is also involved in regulating elastogenesis (Wu et al., 2012) . In addition to scaffold properties, biochemical cues such as culture supplementation with transforming growth factor-β1 (TGF-β1) and hyaluronan oligomers are also specifically implicated in this process (Kothapalli and Ramamurthi, 2009a) as is mechanical straining (Kim et al., 1999a). It is clear that great strides in understanding elastogenesis have been made in the last decade, however a lack of control over the spatial and temporal expression *in vitro* has resulted in this approach not yet achieving its potential for tissue engineering. A more practical approach has therefore been taken in the field to circumvent this issue by utilising elastin, and elastin derived molecules, directly in the biofabrication step of TEVGs rather than attempting to induce cells to secrete it.

An alternative approach is to use the soluble precursor of elastin, tropoelastin, or soluble hydrolysed elastin which both retain many interesting

characteristics for tissue engineering purposes. Buttafoco and colleagues have shown the ability to electrospin soluble hydrolysed elastin with collagen to produce TEVGs matching native vessel composition (Buttafoco et al., 2006b). Improved mechanical properties could be obtained by electrospinning the hydrolysed elastin with synthetic polymers such as poly(lactic-co glycolic acid) PLGA (Han et al., 2011; Stitzel et al., 2006). Furthermore, by altering the quantity of elastin the TEVG compliance can also be tailored (Sell et al., 2006). Electrospinning onto rotating mandrel allows the ability to easily create tubular structures ideal for use as a TEVG, including the ability to create multi-layered TEVGs (McClure et al., 2012). However, the biological effects of these soluble elastin forms are markedly different from the insoluble parent protein This is primarily due to altered binding sites available, although interestingly tropoelastin generally facilitates improved cell binding and spreading versus hydrolysed elastin (Bax et al., 2009; Broekelmann et al., 2008). SMC response to native insoluble elastin has been shown to result in reduced proliferation and a contractile morphology while tropoelastin has the opposite effect and results in a proliferative synthetic morphology (Satyajit K. Karnik et al., 2003; Mochizuki et al., 2002). It is clear that while soluble elastin forms may be amenable to fabrication processes such as electrospinning, the native biological response is altered and thus insoluble elastin remains the optimal form for generating a TEVG.

Mature elastin's very large size, insolubility, and high hydrophobicity, limit the manipulation of the material and therefore limits its use due to its incompatibility with many biofabrication techniques. Freezedrying is one such technique which is suitable for insoluble proteins, such as elastin, while retaining both biological activity and native molecular structure. Chapter 2 of this thesis focused on the utilisation of elastin as a composite with collagen via freeze-drying, with the ultimate aim of creating a biomimetic TEVG.

1.7 Maturation of TEVGs

As detailed in Section 1.1, tissue engineering requires an appropriate scaffold, cell source, and the application of signals to encourage tissue maturation. These signals may be biochemical or mechanical in nature and often must be tailed for the specific tissue of interest.

1.7.1 Biochemical signals

L'Heureux produced the first completely biological TEVG with sufficient mechanical properties for implantation. A key factor in this achievement was the utilisation of a high concentration of ascorbic acid, a cofactor for collagen synthesis, to induce SMCs to produce enhanced quantities of ECM (L'Heureux et al., 1998). The ability to biochemically alter cellular response is a very useful tool for tissue engineering where the protein composition and ultimately the mechanical properties of the engineered tissue can be tailored independently of scaffold chemistry or microarchitecture. Ascorbic acid supplementation has been shown to result in improved SMC proliferation, ECM deposition, and consequently enhanced the mechanical properties of hyaluronic acid based TEVGs (Arrigoni et al., 2006). However, ascorbic acid also modulates the expression profile of the proteins deposited, with elastin production severely impeded concomitant with increased production of collagens I and III (Davidson et al., 1997). Coupled with the effect of ascorbic acid on proliferation, it has also been shown to cause reduced calponin expression, indicating a switch to a synthetic SMC phenotype (Gong and Niklason, 2008). A similar pro-synthetic phenotype effect has been reported with platelet derived growth factor-BB (PDGF-BB), basic fibroblast growth factor (bFGF), and hepatocyte growth factor (HGF) (Gong and Niklason, 2008; Kurane et al., 2007; Sheridan et al., 2014b).

The addition of transforming growth factor-beta1 (TGF-β1) during culture of fibrin based TEVGs has been shown to increase collagen production 4-fold and ultimate strength and modulus 10-fold (Grassl et al., 2003). Insulin was found to have a synergistic effect and further increased these properties. However, TGF-β1 has also been shown to reduce cell numbers versus

controls, while enhancing expression of the contractile markers α-SMA (Grouf et al., 2007) and calponin (Gong and Niklason, 2008). Thus, it can be concluded that TGF-β1 has a pro-contractile phenotype effect.

An alternative method for increasing the mechanical stability of TEVGs involves inhibiting proteolytic activity and thus inhibiting scaffold degradation. Completely biological TEVGs created from fibrin commonly utilise inhibitors of fibrin degradation e.g. aprotinin or tranexamic acid to maintain mechanical stability while the embedded cells proliferate and produce more stable ECM (Cholewinski et al., 2009; Swartz et al., 2005). Lysyl oxidase, the extracellular enzyme responsible for crosslinking the soluble pre-cursors of collagen and elastin into the insoluble fibrils, has also been investigated to improve the mechanical properties of tissue engineered constructs (Elbjeirami et al., 2003; Makris et al., 2014). Importantly, lysyl oxidase has also been shown to enhance SMC synthesis of elastin while cell phenotype and matrix metalloproteinase (MMP) production were unaltered (Kothapalli and Ramamurthi, 2009b). Rather than relying on cell-mediated ECM production or inhibition of proteolytic activity, crosslinking of the base scaffold or TEVG prior to cell seeding may offer a more practical approach to improving the mechanical properties and degradation rate of TEVGs.

1.7.2 Crosslinking of scaffolds

Crosslinks are chemical bonds formed between polymer chains in order to alter a polymer's physical properties. Natural polymers, such as collagen and elastin, contain amino acid residues that may form large networks of crosslinked fibres via a wide range of biophysical or chemical crosslinking methods. One effect of crosslinking collagen or elastin fibres to each other is increased structural stability which can result in stronger and stiffer scaffolds. Additionally, crosslinking can serve to control the degradation rate of collagen/elastin scaffolds *in vitro* and *in vivo.* Degradation of natural proteins *in vivo* is caused by cleavage of peptide bonds by collagenase enzymes. In this thesis, several crosslinking methods were utilised in order to tailor the mechanical properties and degradation rate of a novel scaffold for vascular

tissue engineering. The crosslinking methods of interest in this thesis include both physical (dehydrothermal, riboflavin/UV) and chemical (glutaraldehyde, (-ethyl-3-(3-dimethyl aminopropyl) carbodiimide, microbial transglutaminase) crosslinking mechanisms.

Dehydrothermal (DHT) crosslinking

It has previously been shown by our research group that dehydrothermal (DHT) treatment is an effective crosslinking method and sterilisation technique for collagen based scaffolds (Haugh et al., 2009). As the residual (bound) moisture is evaporated, the amino acids in the collagen molecules are altered and they bind to neighbouring free amino acid groups, this is referred to as crosslinking. In collagen, the application of temperature greater than $90^{o}C$ results in condensation reactions between the carboxyl groups of aspirate or glutamate residues and amino acids of lysine or hydroxylysine. These crosslinks stabilise the matrix and thus alter its mechanical properties. A potential disadvantage of this method is that it may denature part of the collagen and so a suitable compromise must be reached between the level of crosslinking and the resulting denaturation.

EDAC Crosslinking

EDAC (1-ethyl-3-(3-dimethyl aminopropyl) carbodiimide) is a chemical crosslinking agent which forms “zero length” crosslinks of approximately 1nm between adjacent collagen molecules. EDAC forms isopeptide bonds between the carboxyl and amino groups of multiple residues. The by-product of the crosslinking reaction is soluble urea which can be easily washed away. The advantages of using this chemical crosslinker is that the small bond size does not alter the microstructure whereas other chemical crosslinking, such as the use of glutaraldehyde, may form long polymer chains as well as having a potential cytotoxic effect (Hey et al., 1990; Powell and Boyce, 2006).

Glutaraldehyde crosslinking

Glutaraldehyde has been widely used as a crosslinking agent for bioprosthetics and tissue engineered scaffolds. Glutaraldehyde forms

crosslinks between aldehyde groups and the e-amine groups of lysine or hydroxylysine residues in collagen. It has, however, been shown to be cytotoxic by inducing apoptosis in cells (Gough et al., 2002; Hey et al., 1990). Additionally, glutaraldehyde has been shown to cause increased calcification of collagen based scaffolds versus uncrosslinked and EDAC crosslinked controls (Golomb et al., 1987; Jorge-Herrero et al., 1999; Olde Damink et al., 1996). Despite its drawbacks, it has been included in this study due to its widespread use so that it may be used as a comparison for the other crosslinking methods.

Riboflavin/Ultraviolot crosslinking

Riboflavin/ultraviolet (UV) crosslinking is a photochemical crosslinking treatment which relies on riboflavin as a photosensitiser. The application of ultraviolet light causes free radicals to be formed on tyrosine and phenylalanine which can form crosslinks. Riboflavin is added to act as a photosensitiser to ultraviolet light which helps release an increase quantity of free radicals and thus may speed up the reaction (Fig. 1.13). Riboflavin has been shown to be a biocompatible and non-toxic photosensitiser although high levels of riboflavin/UV crosslinking may cause cytotoxic effects due to high levels of free radicals. As free radicals display a very short half-life, only cells seeded onto scaffolds prior to crosslinking would be affected (Ibusuki et al., 2007; Mi et al., 2011; Tirella et al., 2012).

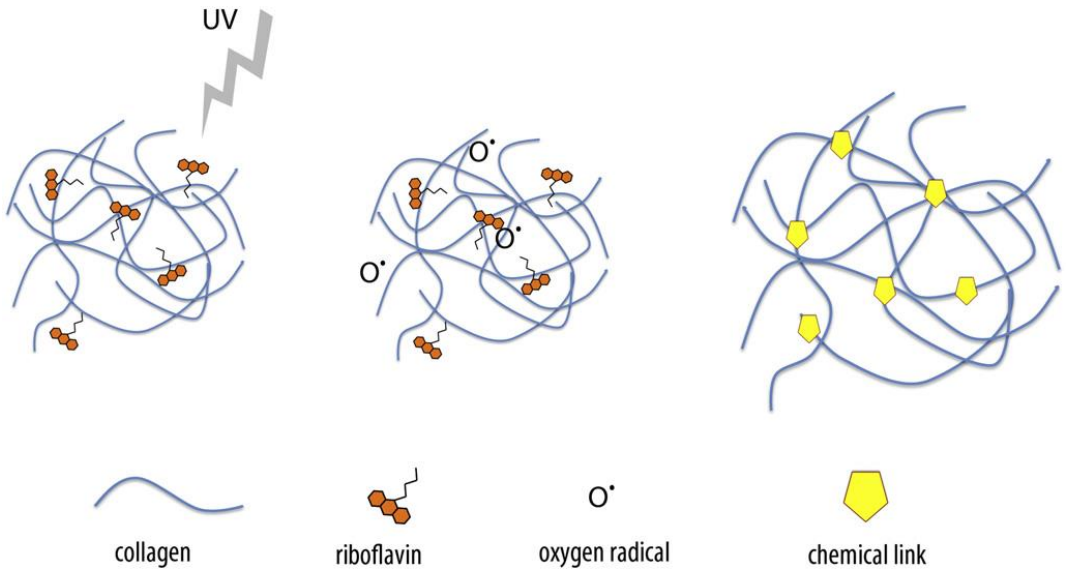

Figure 1.13 Method of riboflavin assisted UV crosslinking

Ultraviolet light strikes the riboflavin molecules which results in the generation of free oxygen radicals and consequently crosslinks (Tirella et al., 2012)

Microbial transglutaminase crosslinking

Discovered by the Japanese company Ajinomoto Corporation Inc., microbial transglutaminase (mTGase) is a calcium-independent enzyme derived from the bacteria *Streptomyces mobaraensis.* Microbial transglutaminase catalyses the reaction of the isopeptide bond ε-(γ-glutamyl)lysine between lysine and glutamine residues in collagen. As a crosslinking method it is of particular interest for tissue engineering applications as it does not alter the triple helical structure of collagen or affect its banding period. Furthermore, it has previously been shown to enhance cell attachment, spreading, proliferation, and stimulate angiogenesis (Chau et al., 2005; Garcia et al., 2008). Additionally, mTGase has been shown to increase collagenase resistance and improve mechanical properties of collagen scaffolds (Chen et al., 2005).

1.7.3 Dynamic mechanical conditioning through bioreactors

Native vascular tissue consists of three distinct circumferentially aligned layers with each layer possessing a distinct cellular and protein composition.

This composite structure leads to a complex multifactorial biomechanical environment. Consequently, this has led to the development of a number of alternative methods for the culture of tubular vascular constructs which can be generally categorised as endothelium biomechanical simulators (Moore et al., 1994; Zhao et al., 1995), medial layer biomechanical simulators (Huang and Niklason, 2011), or complete physiological mimicking biomechanical simulators (Tschoeke et al., 2009). In native tissue, medial and adventitial cells primarily experience cyclical hoop stress and strain imparted by the cardiovascular haemodynamics. These cells sense and respond to changes in these biomechanical signals during pathological conditions, such as atherosclerosis, where altered hoop strains and stresses are imparted. Thus, medial layer simulating bioreactors generally focus on the response of medial layer cells, such as SMCs, to physiological or pathological levels of cyclical strain. Medial layer simulating bioreactors, such the systems described by Seliktar (Seliktar et al., 2000), and Isenberg and Tranquillo (Isenberg and Tranquillo, 2003), indirectly apply the cyclical distension required for hoop stress and strain via inflating compliant tubes hydraulically or pneumatically (Fig. 1.14).

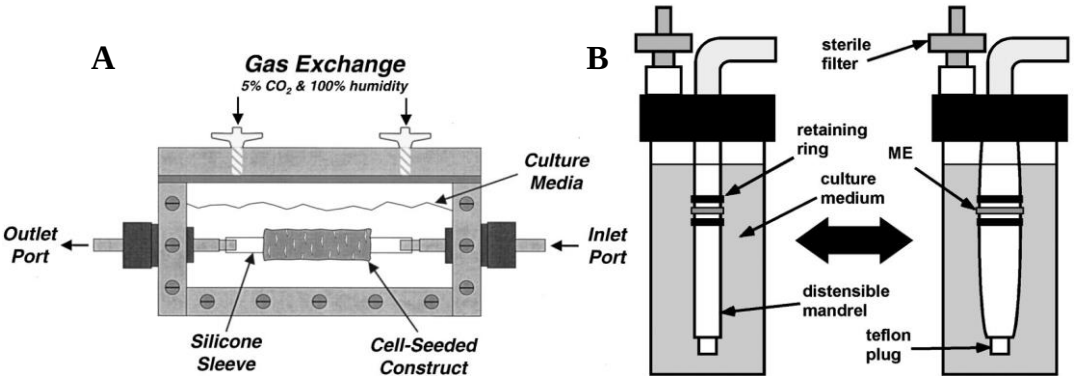

Figure 1.14 Medial layer simulating bioreactor designs

(A) Cyclical distension of the silicone sleeve via pulsatile fluid flow imparts physiologically relevant hoop stress and strain to the cell-seeded construct (Seliktar et al., 2000)*. (B) Distension of the mandrel is achieved by a pneumatic system* (Isenberg and Tranquillo, 2003)

Endothelium biomechanical simulators focus on studying the effects of biomechanical cues, such as fluid shear stress, on endothelial cells.

Endothelium biomechanical simulating bioreactors such as the systems described by Moore (Moore et al., 1994) and Ziegler (Zhao et al., 1995) , apply fluid shear stress via peristaltic pumps which provide a pulsatile fluid flow through rigid tubes onto which endothelial cells are seeded. While it has been well documented that vascular cells respond to a number of different mechanical cues independently, their normal cell physiology is, in part, regulated by the wide variety of forces they are subjected to *in vivo* including cyclical strain, shear stress, and hydrodynamic pressure. Although medial and endothelium simulating bioreactors have merit in understanding the isolated effects of certain biomechanical forces on vascular cells, it is often the synergistic effects of these forces which elicits the normal physiological response *in vitro* (Zhao et al., 1995). Thus, recent research has begun to focus on the application of complete physiological simulators in order to provide a biomimetic environment for graft maturation *in vitro.*

The complex physiological biomechanics of the human circulatory system are often best emulated through a reproduction of the haemodynamics via pulsatile flow systems. The cyclical waveform of the pressure, fluid flow, and strain experienced by vessels *in vivo* can be reproduced in a number of different ways. Some of the previously used methods to apply this cyclical waveform include compressed air driven pulse duplicators (Hoerstrup *et al.,* 2001), peristaltic pumps (Tschoeke *et al.,* 2009), syringe pumps (Syedain *et al*., 2011), or a combination of pumps (Conklin *et al.,* 2000). Peristaltic pumps offer the simplest method to produce an intraluminal pulsatile flow which can closely mimic the flow and pressure profile of the native vasculature. The pulsatile flow of fluid causes shear stress to be imparted to the luminal aspect of mounted grafts while the pressure profile of the flow causes cyclic distension which imparts cyclical strain to medial layer cells. There is contention and contradictory evidence in the literature as to the most suitable bioreactor culture conditions for the maturation of a tissue engineered blood vessel. A significant portion of early work focused on applying physiological conditions such 5%-10% cyclic strain, 120/80 mmHg pressure, and 10 dyne/cm^2 shear stress (Conklin et al., 2000). Applying dynamic physiological conditions resulted in increasing the rate of tissue

maturation versus statically cultured vessels. However, researchers are now reporting improved tissue maturation by imparting foetal or pathological-like biomechanical conditions over physiological conditions. Conditions such as foetal pulse rates (Solan et al., 2009, 2003) and incremental cyclical strains (Syedain *et al.,* 2008) have led to increased collagen deposition and subsequently improved mechanical properties. Consequently, further research into the application of suitable biomechanical cues to developing vascular grafts is needed in order to fully elucidate the ideal culture conditions and ideal bioreactor system to impart those conditions. Consequently, Chapters 4 and 5 of this thesis will examine these areas.

1.8 Thesis Objectives/Aims

The primary goal of the research presented in this thesis was to develop a small diameter tissue engineered vascular graft using the natural polymers collagen and elastin, coupled with dynamic mechanical conditioning. To achieve this, we sought to develop tubular collagen-elastin scaffolds with optimised intrinsic physiochemical characteristics which displayed the capacity to support smooth muscle cells *in vitro* while subsequently displaying suitable viscoelastic properties capable of sustained biomechanical conditioning in a custom designed pulsatile bioreactor.
To accomplish this, the specific objectives of the thesis were as follows:

1) Develop a collagen-elastin composite scaffold with potential application for vascular tissue engineering and examine the influence of elastin addition on the resultant scaffold microstructure, mechanical properties, and *in vitro* response to smooth muscle cells (Chapter 2).

2) Develop a biofabrication strategy to produce a multi-layered collagen-elastin tubular scaffold with a physiologically relevant tubular architecture. Further control over the physiochemical properties of these tubular scaffolds was examined through a multitude of crosslinking techniques (Chapter 3).

3) To design, develop, and validate a versatile pulsatile bioreactor for dynamic conditioning of small diameter vascular grafts including the multi-layered collagen-elastin tubular scaffold developed in the previous chapter (Chapter 4).

4) Examine the effect of vessel architecture, crosslinking, and dynamic conditioning in the custom pulsatile bioreactor from Chapter 4, on the maturation of collagen-elastin based tissue engineered vascular grafts (Chapter 5).

<u>Chapter 2:</u> Effect of elastin incorporation on the microstructure, mechanical properties, and biological response of collagen scaffolds for cardiovascular tissue engineering

2.1 Introduction

A major challenge in cardiovascular tissue engineering is the design and fabrication of biomaterials with suitable biological instructive cues to guide cell behaviour, while additionally supporting the challenging haemodynamic mechanical environment once implanted in vivo (Annabi et al., 2013; Quint et al., 2011). These instructive cues are chemical, physical, and mechanical in nature and play a major role in governing cellular adhesion, migration, proliferation, and differentiation, while encouraging synthesis of appropriate proteins/glycosaminoglycans (Cameron et al., 2014; Nakayama et al., 2014). Cells natively receive a large quantity of these cues through interaction with the extracellular matrix (ECM) and so a biomimetic approach to biomaterial design has a number of innate advantages. Natural-based materials, such as collagen and fibrin, are thus ideal candidates to construct biomaterial scaffolds from as they can form part of an adaptive tissue which is mechanically and biologically responsive to the haemodynamic environment (Grassl et al., 2003; Huynh and Tranquillo, 2010). The ubiquitous nature of collagen in the body and comparatively good mechanical properties in comparison to other natural polymers has thus led to its widespread use for cardiovascular tissue engineering as a cardiac cell delivery patch (Roche et al., 2014) and vascular graft among others(Kumar et al., 2013; Schutte et al., 2010).

Despite numerous advances in biofabrication methods for natural polymers, these collagen-based scaffolds often do not meet the mechanical requirements for the dynamic cardiovascular environment. Often this stems from the propensity of collagen-alone to creep over time, a process which would lead to aneurysm formation *in vivo* if utilised as a vascular graft (Dunphy et al., 2014; Seliktar et al., 2000; Singh et al., 2015). In order to address some of the mechanical limitations of natural polymers such as collagen, composites have been developed in order to improve the strength of the scaffolds while also retaining biological activity (Heydarkhan-Hagvall et al., 2008; Tillman et al., 2009; Tschoeke et al., 2009; Wise et al., 2011). Natural polymers, such as collagen and fibrin, have been combined with

synthetic polymers, such as polylactic acid and polyethylene terephthalate, in order to further enhance the mechanical properties of the vessels (Burrows et al., 2012; Koch et al., 2010). While the strength of vascular grafts can be improved via the incorporation of synthetic polymers, this also generally reduces the compliance of the scaffolds as the synthetic polymers are relatively stiff. Consequently, despite some advances in the area, many of these grafts suffer from a compliance mismatch in comparison to a native vessel (Tiwari et al., 2002). Additionally, biodegradable synthetic polymers, such as PGA, have been shown to dedifferentiate SMCs due to their hydrolysis products (Gong and Niklason, 2011; Niklason et al., 2001) which may also lead to a lowering of local pH levels and a resulting inflammatory response (Athanasiou et al., 1996). Consequently, recent research has begun to focus on creating composites of purely natural polymers to engineer a regenerative niche which can guide cell behaviour and ultimately promote tissue regeneration.

In native vasculature, elastin serves to dampen the pulsatile flow of blood by its efficient storage of elastic-strain energy. From a tissue engineering perspective, the high extensibility and resilience of this protein, coupled with its low stiffness, may allow it to closer match the mechanical properties of native cardiovascular tissue. In particular, the addition of elastin to vascular scaffolds has been shown to alter the mechanical response of scaffolds through increasing compliance and reducing thrombogenicity (Wise et al., 2011). In addition, elastin has been attributed with activating pathways which govern the proliferation and differentiation of vascular cells. Specifically, elastin has been found to stimulate gene expression of the SMC markers α-SMA and calponin *in vitro* for MSCs seeded on elastin coated substrates (Gong and Niklason, 2008; Park et al., 2004). Elastin can bind to the 67kDa elastin/laminin binding protein which has been shown to be involved in mechanotransduction (Spofford and Chilian, 2003), ECM assembly (Li *et al*., 1998), cell chemotaxis and proliferation (Mochizuki et al., 2002). It is clear that emulation of native tissue composition by elastin incorporation would therefore address many of the biological and mechanical issues seen in this field. However, there is a dearth of research on native elastin in tissue

engineering due to the proteins large size and insolubility which makes it incompatible with many biofabrication techniques. Previous studies utilizing elastin have primarily focused on initial incorporation methods and characterisation (Buttafoco et al., 2006b; Grover et al., 2012) the effects of elastin *in vivo*(Daamen et al., 2008, 2005). Thus, the effects of native elastin on biomaterial properties have yet to be fully elucidated for cardiovascular tissue engineering.

In this study, we hypothesised that the presence of elastin in a porous collagen scaffold would markedly alter the mechanical and biological response and, from a cardiovascular tissue engineering perspective, that its incorporation would produce a more natural viscoelastic response while inducing a more contractile SMC phenotype. The aim of the study was thus to elucidate the influence of elastin addition on the microstructural and mechanical properties of collagen scaffolds and to examine the biological response of smooth muscle cells when seeded on the composite scaffolds. Specifically, after elastin incorporation, we investigated the resultant scaffold microarchitecture via scanning electron microscopy and used histological techniques to quantify pore architecture and elastin distribution. Mechanical properties were investigated via compression and uniaxial tensile testing while viscoelastic response was assessed by examining creep and cyclical strain recovery analysis. Subsequently, we assessed the effect of elastin addition on SMC phenotypic modulation towards a synthetic or contractile phenotype by assessing cell proliferation and gene expression.

2.2 Materials and Methods

2.2.1 Scaffold fabrication

Fabrication of collagen-elastin scaffolds

To fabricate Collagen-Elastin (CE) scaffolds, a freeze-drying process was used. Firstly, it was necessary to prepare a co-suspension of collagen and elastin in an aqueous acetic acid solution as per Fig 2.1. This collagen-elastin suspension was produced by mixing 0.5% w/v of fibrillar Type I bovine collagen (Integra Life Sciences, Plainsboro, NJ) and elastin from bovine neck ligament (Sigma-Aldrich, Germany) in 0.05M acetic acid. Elastin was blended into the collagen and acetic acid suspension in one of three different concentrations: 1:0.1 collagen:elastin ratio (CE10), 1:0.35 collagen:elastin ratio (CE35) and 1:1 collagen:elastin ratio (CE100) - which corresponds to the ratios found in dry native skin, lung and arterial tissues respectively. The suspension was then added to a mixing vessel, cooled to 4^{o}C, where it was blended using an overhead blender (Ultra Turrax T18, IKA Works Inc., Wilmington, NC) at a speed of 15000rpm to homogenise the suspension, A desiccator was used to degas the high viscosity suspension and it was then placed in a stainless steel pan and freeze-dried at a cooling rate of 0.9 ^{o}C/minute to a final freezing temperature of -40^{o}C (Advantage EL, Vir-Tis Co., Gardiner NY). This freeze-drying profile has been previously optimised by O'Brien *et al.* (2004) to develop collagen-based scaffolds with a homogeneous pore structure.

Following freeze-drying the scaffolds were dehydrothermally (DHT) crosslinked as per Haugh *et al*. (2009). Briefly, the scaffolds were subjected to a DHT treatment of 105^{o}C for 24 hours at 0.05 bar in a vacuum oven (Vacucell 22, MMM, Germany). This crosslinking method also sterilises the scaffolds for use in cell culture.

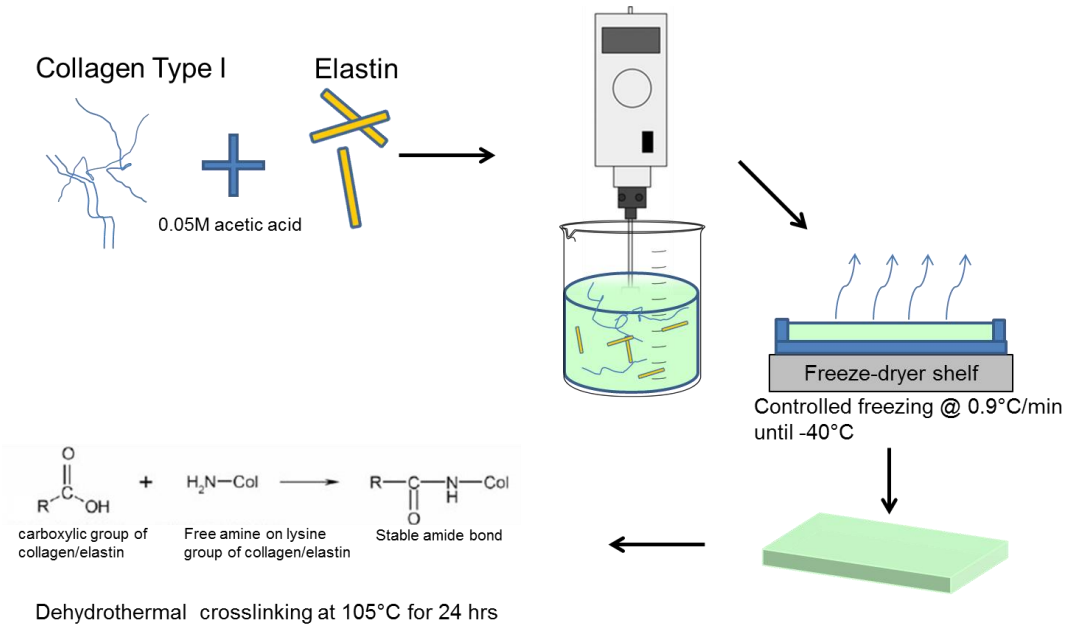

Figure 2.1 Fabrication of collagen- elastin composite scaffolds

Collagen and elastin were blended together to form a co-suspension in acetic acid before controlled freeze-drying was used to produce an open porous scaffold network. Carboyxlic groups were then covalently crosslinked to the free amine groups to form stable amide bonds via dehydrothermal treatment.

2.2.2. Scaffold microstructural characterisation

Assessment of elastin distribution in the CE scaffolds

Histological analysis was performed to evaluate the spatial distribution of elastin within the freeze-dried scaffolds. Scaffold samples were placed in a solution of 10% formalin for 30 minutes followed by embedding in paraffin by an automatic tissue processor (ASP300, Leica, Germany). The samples were sectioned at 10μm using a microtome (Leica RM 2255, Leica, Germany) and mounted on glass histology slides followed by deparaffinization in xylene. The slides were then stained with a modified Verhoeff-van Gieson staining procedure adapted from the manufacturer's instructions (Sigma-Aldrich, Dublin, Ireland) and coverslips were applied with DPX mountant. The mounted sections were imaged on a microscope (Nikon Eclipse 90i, Nikon, Japan) and digital images were recorded at 10x

magnification using the attached control unit connected to a PC and imaging software (Nikon DS Camera control unit, Nikon, Japan with NIS Elements Basic Research V3.06, Nikon Instruments Europe, The Netherland).

<u>Effect of elastin addition on scaffold mean pore size, porosity, and pore architecture</u>

The scaffold mean pore size was determined using a polymer resin embedding technique as previously described (O'Brien et al., 2004). Samples were embedded in a JB-4 glycomethacrylate (Polysciences, Germany) resin according to the manufacturers protocol and serially sectioned at 10µm using a microtome (Leica RM 2255, Leica, Germany). Sections were stained with toluidine blue and digital images were acquired before quantification by a pore typography analyser script previously written for MATLAB® (MathWorks Inc, MA, USA) (Haugh et al., 2010). The software thresholds the images, identifies pore boundaries, and the mean pore size was calculated from best fit ellipses inside each pore. A minimum of 200 pores were analysed for each scaffold variant and samples were selected from multiple batches in order to account for the inherent batch variability in pore sizes.

Additionally, scanning electron micrographs were acquired at 5kV and a magnification of 350x to further examine the pore architecture.

The porosity of scaffolds was calculated using the density of the scaffolds ($\rho_{scaffold}$) in relation to the theoretical dry solid composite as per Equation (1), below. The solid composite scaffold density was calculated using the mass of collagen and elastin used and their relative densities, ρ_{solid} =1.3 g/cm^3 for both proteins(Hoffmann et al., 2003; Yannas and Burke, 1980). The density of the scaffolds was calculated by measuring their volume and mass using a digital Vernier callipers (Krunstoffwerke, Radionics, Dublin, Ireland) and digital scale respectively (Mettler Toledo MX5, Mason Technology, Dublin, Accuracy ±0.01mg).

ΰ έ ὶ έ ίΡΩ ὼ ώρ ” ὼ ρ π π (1)

2.2.3. Scaffold mechanical characterisation

Effect of elastin addition on scaffold compressive and tensile properties

Uniaxial tensile testing of the scaffolds was performed using a uniaxial tensile testing machine (Z050, Zwick/Roell, Ulm, Germany) with a 5N load cell (Haugh et al., 2009). Samples for testing were freeze-dried in a custom dog-bone mold as per ASTM Standard D638, type V (American Society for Testing and Materials International). The scaffolds were pre-hydrated in PBS (Sigma-Aldrich, Germany) for 1 hour prior to transfer to the testing rig in order to test the hydrated response of the scaffolds as per in vivo conditions. A tensile preload of 0.01N was applied followed by testing at a rate of 5mm/minute until failure. The tensile modulus was determined at low strain (2-5%) and high strain (20-25%).

Unconfined compression testing of the scaffolds was performed using cylindrical samples punched out of sheets. Compressive testing was performed at a rate of 10%/minute up to a maximum strain of 10%. The compressive modulus was defined as the slope of the stress strain curve between 2% and 5% which avoids the less stiff toe region below 2% strain and the densification region at levels higher than 5%. To account for the effect of scaffold density on the resulting mechanical properties the specific compressive modulus and specific tensile modulus was determined by dividing the modulus by the scaffold density ($\frac{\text{modulus}}{\text{density}}$).

Effect of elastin addition on scaffold creep and cyclical strain recovery.

The above analysis revealed that CE100 scaffolds were optimal for further testing due to the good distribution of elastin and low standard error on the mechanical and microstructural analysis, indicating a homogenous scaffold. Tensile creep testing and cyclical strain recovery analysis were then performed in order to elucidate the viscoelastic response of the scaffolds. All tests were performed using a uniaxial tensile testing machine (Z050, Zwick/Roell, Ulm, Germany) with a 5N load cell. Samples for testing were fabricated and prepared as per the uniaxial tensile testing. Creep testing was

performed for 10 minutes at a loading level equivalent to 33% of the ultimate tensile strength of each sample (Berglund et al., 2005). A tensile preload of 0.01N was first applied followed by three preconditioning cycles to 5% strain at a strain rate of 5mm/minute. Creep data was analysed with Burger's four-parameter constitutive model (Eqn. 2), with the schematic shown in Fig. 2.6. The model consists of a Maxwell unit (spring and dashpot in series) and Voigt unit (spring and dashpot in parallel) in series and can be described by the following equation:

$$\varepsilon(t) = \frac{\sigma_0}{E_1} + \frac{\sigma_0}{\eta_1}t + \frac{\sigma_0}{E_2}\left(1 - e^{-\frac{E_2}{\eta_2}t}\right) \qquad (2)$$

Where the strain (ε) at a given time (t) was modelled utilising the applied stress (σ_0) by utilising the generalised reduced gradient algorithm to match the experimental and model curves by minimising the sum of the square error between the two curves. The four variants in the nonlinear model represent elastic parameters (E_1 and E_2) and viscous parameters (η_1 and η_2).

Cyclical strain recovery was performed by applying a preload of 0.01N followed by 25 cycles at 5mm/min to 10% strain. The degree of strain recovery after 25 cycles was determined using the following equation (3) where ε_L is the applied strain and ε_N is the strain after N cycles (Lendlein et al., 2001):

$$R_f = \frac{\varepsilon_L - \varepsilon_N}{\varepsilon_L} \qquad (3)$$

2.2.4. Analysis of the biological response

Cell Culture and scaffold seeding

The biological performance of the CE scaffolds was assessed using a human smooth muscle cell line with collagen-only scaffolds fabricated at the same temperature and crosslinking levels acting as controls. CE100 scaffolds were determined to be the optimal scaffolds for this *in vitro* testing due to the good distribution of elastin and homogenous architecture and mechanical

properties. The human smooth muscle cell (hSMCs) line was purchased from ATCC (CRL-1999) having been previous extracted from the aorta of an 11-month old female Caucasian. Cells were cultured using the recommended complete growth media and subculturing procedures as per the manufacturer's instructions.

Scaffolds of diameter 8mm and height 3.5mm were hydrated in PBS for 30 minutes prior to cell seeding. Scaffolds were seeded at a density of 2.0x 10^5 per sample with cells seeded using a previously optimised technique (Murphy *et al.,* 2010). Cell seeded scaffolds were cultured for up to 14 days in complete growth media consisting of Ham's F-12K (ATCC 30-2004, LGC Standards, Middlesex, UK) supplemented with 10% foetal bovine serum, 2% penicillin/streptomycin (Sigma-Aldrich, Arklow, Ireland), 50 µg/mL ascorbic acid (Sigma-Aldrich, Arklow, Ireland), 16ul/ml 1x ITS (Insulin, Transferrin, Selinium) (BD Biosciences, Oxford, UK), 10 mM HEPES, 10mM TES, 0.03 mg/ml endothelial cell growth supplement (Sigma-Aldrich, Arklow, Ireland). Media was changed every 3 days.

Effect of elastin addition on cell density and cell-mediated scaffold contraction

Cell number was quantified via an Invitrogen Quant-iT™ PicoGreen dsDNA kit (Biosciences, Dublin, Ireland). Four scaffolds per group (n=3) at each of the time points (4, 7 and 14 days) were homogenised in 1 mL of 0.2M carbonate buffer with 1% triton to lyse cells using a hand-held homogeniser (Finemech, Portola Valley, CA, USA) equipped with a T6 homogenising shaft attachment (Finemech). Cell number was then quantified as per Singer (Singer et al., 1997)using a Picogreen dsDNA assay kit which fluorescently labels double-stranded DNA. The samples were prepared in triplicate and the fluorescence was read at an emission of 520 nm after excitation at 480 nm using a fluorescence spectrophotometer (Wallac Victor2™ 1420 multilabel counter, Perkin Elmer Life Sciences, Waltham, MA, USA). Sample fluorescence was compared to a standard curve to determine cell number.

Scaffold contraction was measured at each timepoint using Vernier callipers (Krunstoffwerke, Radionics, Dublin, Ireland) and graphed as percentage

contraction versus day 0. This data can be utilised for cellular solids modelling and also give an indication of cell-mediated contraction forces.

Effect of elastin addition on gene expression

The relative RNA levels for genes of interest were measured by reverse transcription followed by quantitative real-time polymerase chain reaction. Total RNA was isolated utilising a Qiagen RNeasy mini kit and DNase set (Qiagen, Crawley, Uk) as previously described (Duffy et al., 2011). RNA concentration and purity was determined via a spectrophotometer (NanoDrop Technologies, Inc., Rockland, DE). Total RNA (200ng) was reversed transcribed to cDNA using a QuantiTect Reverse Transcription kit (Qiagen) and a thermal cycler (Mastercycler Personal, Eppendorf, UK), as per the manufacturer's instructions. A QuantiTect SYBR Green PCR kit was utilised with a 7500 Real-Time PCR System (Applied Biosystems, UK) in order to perform real time polymerase chain reactions in duplicate for each sample. Predesigned and validated human QuantiTect primer assays (Qiagen) were utilised for the mRNAs of interest, namely; collagen type 1 (Coll 1), alpha-smooth muscle actin (αSMA), Calponin 1 (Calponin), and smooth muscle-myosin heavy chain 11 (SM-MHC). These target genes were chosen as they represent early stage (αSMA), mid-stage (calponin) and late stage (SM-MHC) SMC markers as well as ECM production (Coll 1). Gene expression results were normalised to the reference gene, 18S, using the ς٩ ڈ ڀ ۃmethod.

Statistical analysis

Statistical analysis was conducted using one-way or two-way ANOVA followed by the Holm-Sidak post hoc test for pairwise comparisons using Sigmaplot Version 11.2 (Systat Software Inc., USA). A P-value of 0.05 or less was considered statistically significant ($p \leq 0.05$). The strength and direction of linear relationships between material parameters was determined using the Pearson product moment correlation coefficient (r), while the coefficient of determination (r^2) was utilised to indicate the degree of linear

association between factors. A strong positive correlation is considered to exist if the r is between 0.7 and 1 (Taylor, 1990).

2.3 Results

2.3.1 Effect of elastin addition on collagen scaffold microarchitecture

Histological analysis was used to determine the spatial distribution of elastin within the scaffold matrix and to determine whether the method of elastin incorporation was appropriate (Fig. 2.2A). Some minor clumping of elastin was observed at lower concentrations (CE10 & CE35) but elastin was found to be homogenously distributed at higher concentrations, as observed in the CE100 scaffolds (Fig. 2.2A). SEM analysis revealed that elastin was primarily observed to be encapsulated by the collagen (Fig. 2.2B); although at higher magnification some single elastin fibres are visible and thus available for cell binding (Fig. 2.2C). The SEM analysis also shows the highly interconnected pore architecture and porous nature of the scaffolds.

Analysis of the scaffold porosity indicated that there was a strong linear decrease (Pearson Correlation Coefficient, r =-0.97) in the porosity of the scaffolds (Fig. 2.2E) with increasing elastin concentration. A significant reduction ($p < 0.001$) in percentage porosity was found between the CE100 scaffolds versus all other scaffolds. Additionally, there is a significant decrease ($p < 0.05$) between the collagen-only and CE10 scaffolds. The reduction in porosity may be explained by the increased overall protein concentration with the addition of elastin, although the absolute difference in porosity is <0.5%. However, all scaffolds exhibited mean porosities above 98.8%, far greater than the porosity of ≥ 90% that is desired for effective tissue repair (Zeltinger et al., 2001; Gleeson and O'Brien, 2011).

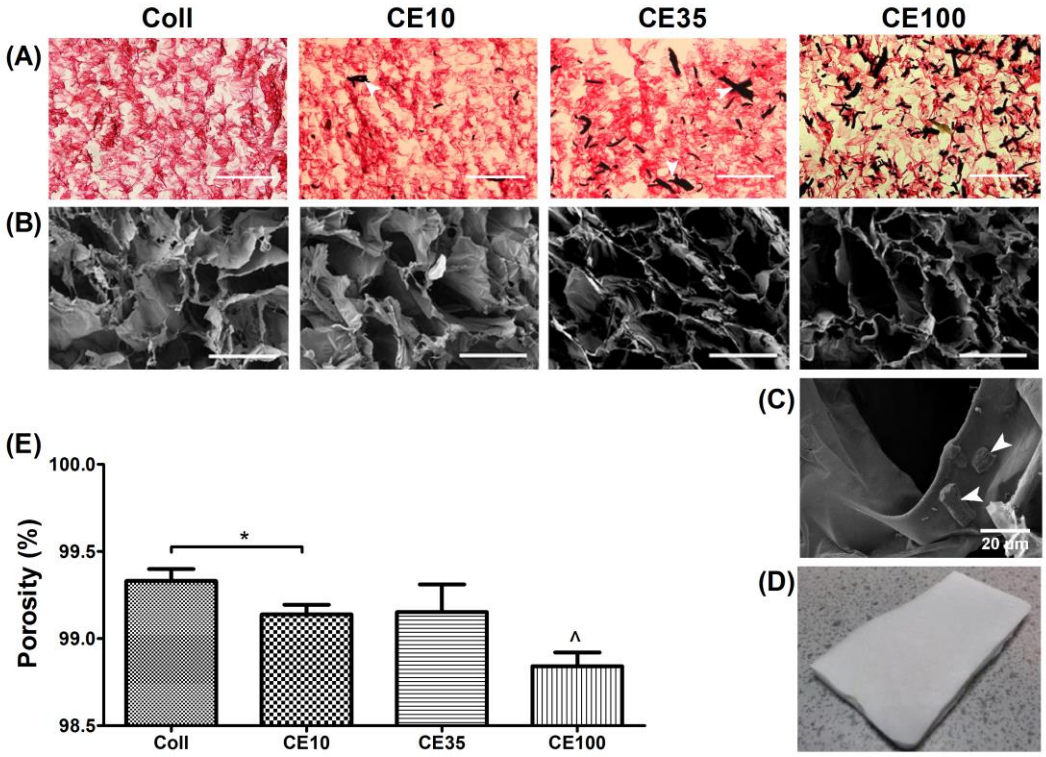

Figure 2.2 Effect of elastin addition on scaffold microarchitecture

Modified Verhoeff-van Gieson staining was performed on paraffin embedded scaffolds to determine the distribution of collagen (red) and elastin (black) in collagen scaffolds and CE scaffolds (A). SEM images (B) of the scaffolds showing the excellent pore interconnectivity, homogenous pore structure and porous nature. Individual elastin fibres are visible at higher magnification and are partially encapsulated by collagen (C). Macroscopically all scaffold variants produced homogenous scaffold sheets (D) with very high porosities (E). (*) denotes p<0.05 versus indicated group or (^) versus all other groups. Scale bar = 200 microns

The addition of elastin did not significantly affect the pore size (Fig. 2.3) of the scaffolds at higher concentrations (CE35 & CE100) but did reduce the pore size at low concentrations (CE10) versus the other elastin containing scaffolds ($p<0.05$) (Fig. 2.3). A mean pore size (± standard deviation) of 87.7 ± 4.6 µm, 84.8± 2.3 µm, 96.1± 6.0 µm and 93.5± 2.9 µm was found for the collagen-only, CE10, CE35, and CE100 scaffolds respectively (Fig. 2.3B). All scaffolds had mean pore sizes within the optimal range of 60µm-150µm proposed for MSCs and SMCs (Jeong et al., 2005; Lee et al., 2008; Zeltinger et al., 2001).

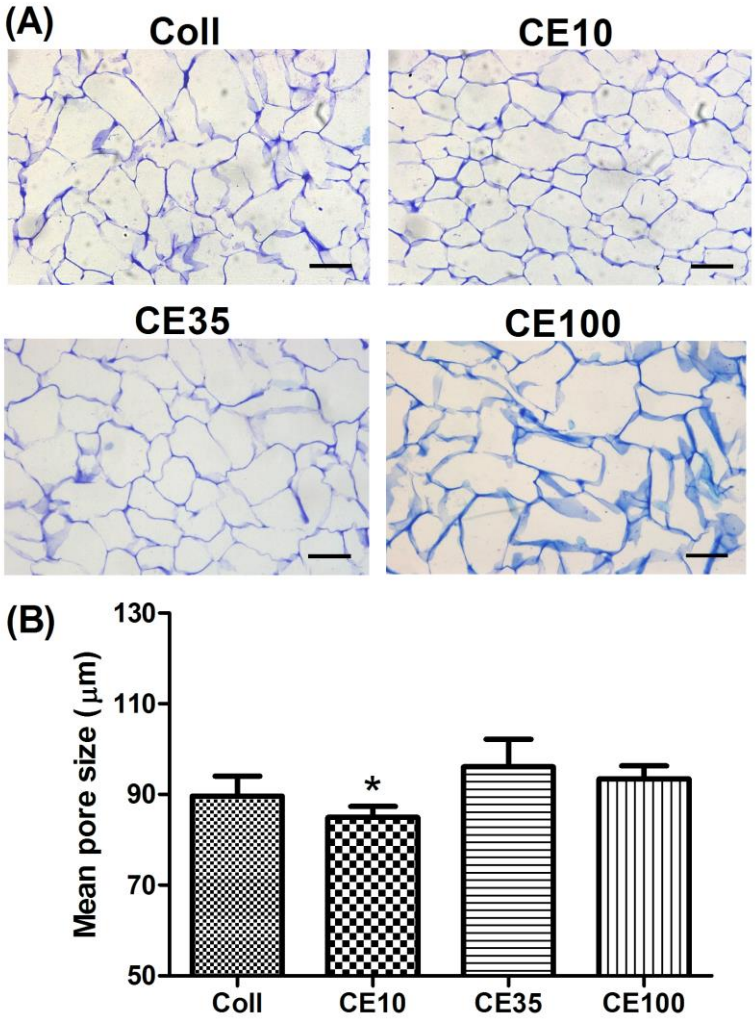

Figure 2.3 Effect of elastin addition on scaffold pore size

Micrographs of polymer embedded sections reveal minimal changes to pore architecture with the addition of elastin (A). Mean pore size was measured as the average of the major and minor diameter of a best-fit ellipse to each pore (B). The addition of elastin resulted in a negligible change in mean pore size for all scaffolds, although CE10 scaffolds exhibited a statistically significant reduction in pore size versus the CE35 and CE100 scaffolds ($p<0.05$). (*) denotes $p<0.05$ statistical significant difference in comparison to CE35 & CE100. Scale bar = 200 microns

2.3.2 Effect of elastin addition on collagen scaffold mechanical properties

Elastin addition resulted in a decrease in scaffold compressive modulus versus collagen controls ($p<0.05$) (Fig. 2.4A). A compressive modulus (± standard deviation) of 0.32±0.04 kPa, 0.26±0.03 kPa, 0.26±0.05 kPa and 0.25±0.03 kPa was found for the collagen-only, CE10, CE35, and CE100 scaffolds respectively. Scaffold specific compressive modulus ($\frac{\text{compressive modulus}}{\text{density}}$) was calculated to account for differences in scaffold density due to the addition of elastin, with a strong decreasing linear trend observed ($r = -0.9$). Collagen scaffolds had a significantly higher specific compressive modulus than all elastin containing scaffolds ($p<0.05$) while the CE100 scaffolds had a significantly lower specific compressive modulus than all other groups ($p<0.05$). Additionally, scaffold tensile properties were also examined with representative stress-strain curves shown in Fig. 2.5A. While no significant difference was observed in the uniaxial tensile properties (Fig. 2.5B), when density was again accounted for it was found that elastin resulted in a concentration dependant decrease in scaffold specific tensile modulus which further corroborates the results obtained via compressive testing. These results indicate that elastin results in a reduction in scaffold stiffness in a concentration dependent manner.

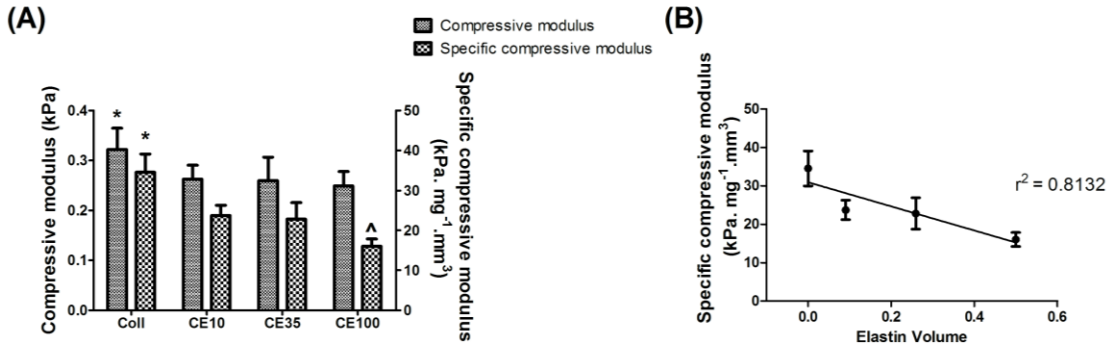

Figure 2.4 Effect of elastin addition on scaffold compressive properties.

Elastin addition reduced the compressive moduli of all scaffolds versus the collagen control ($p<0.05$) (A). When scaffold density is accounted for via the scaffold specific compressive modulus (modulus divided by density) a strong decreasing linear trend is found ($r = -0.9$) with a coefficient of determination (r^2) of 0.81 (B). This indicates that elastin addition results in reduced scaffold

stiffness in a concentration dependant manner. (*) indicates p<0.05 versus CE10, CE35, and CE100 groups. (^) denotes p<0.05 versus Coll, CE10, and CE35.

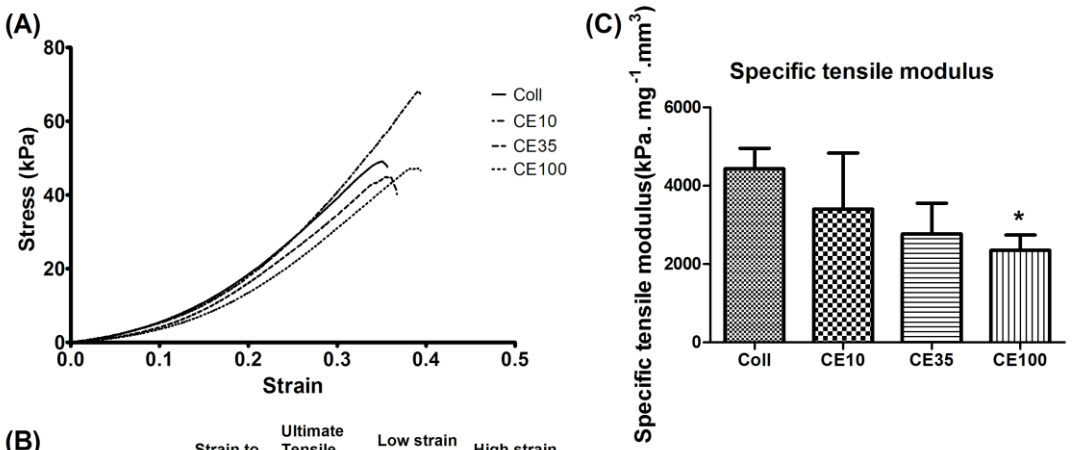

(B)

	Strain to failure (%)	Ultimate Tensile Strength (kPa)	Low strain modulus (2-5%)	High strain modulus (20-25%)
Coll Control	42.9 ± 8.2	72.2 ± 21.6	41.3 ± 4.8	189.5 ± 20.9
CE10	41.0 ± 8.3	53.7 ± 24.8	37.7 ± 15.8	161.9 ± 70.4
CE35	40.1 ± 5.8	44.9 ± 16.4	31.5 ± 8.9	155.1 ± 30.5
CE100	35.6 ± 4.2	50.8 ± 10.9	36.6 ± 6.0	199.8 ± 30.5

Figure 2.5 Effect of elastin addition on scaffold tensile properties.

Representative stress-strain curves of uniaxial tensile tested scaffolds (A) and relevant mechanical properties (B). No significant difference in strain to failure, ultimate tensile strength, low strain modulus, or high strain modulus was observed with the addition of elastin (p>0.05). When scaffold density is accounted for a decreasing linear trend of specific tensile modulus (C) is observed with increasing elastin concentrations, with CE100 scaffolds having significantly lower moduli than the collagen controls (p<0.05), and a coefficient of correlation (r^2) of 0.851. (*) indicates p<0.05 difference to collagen controls.

While compressive and tensile testing allowed analysis of many important material mechanical properties they do not allow analysis of the viscoelastic properties, the time-dependent mechanical characteristics important for the long term success of a tissue engineered vascular construct. Creep (Fig. 2.6A) and cyclical strain recovery (Fig. 2.6B) tests were therefore performed to determine the viscoelastic characteristics of the scaffolds. It was found that elastin addition resulted in improved creep resistance as determined by the total induced strain and the viscoelastic model fitting parameters (Fig. 2.6). Specifically, elastin incorporation resulted in a 3.5-fold decrease (p<0.05) in induced strain caused by creep (CE100: 13.8 ± 3.6%, Coll: 48.24

± 7.1%). The early creep response is modelled by the instantaneous strain level parameter, γ_0, which was increased by 2.6-fold ($p<0.05$) with the addition of elastin, indicating a reduced instantaneous strain level. Elastin also resulted in a 2.7-fold and 4.3-fold increase in the transition region parameters τ_2 and τ_3 respectively, indicating that elastin results in a lower strain magnitude and a shorter duration in the transition region. Furthermore, an 8.7-fold increase in τ_0, the parameter which governs long term viscoelastic behaviour, indicates an increased resistance to long term deformation/creep. The large increase in τ_0 due to elastin may indicate long term strain rates reaching values close to zero.

Additionally, elastin addition resulted in a significant increase in the percentage cyclic strain recovery (Fig. 2.6B) versus collagen scaffolds ($p<0.05$). The presence of elastin caused scaffolds to recover 82.8% of the applied strain while collagen scaffolds recovered to 13.1% of the applied strain following 25 cycles to 10% strain. The cyclical strain regime applied was a dynamic test of scaffold viscoelastic properties by applying stepwise strain inputs to simulate pulsing vasculature.

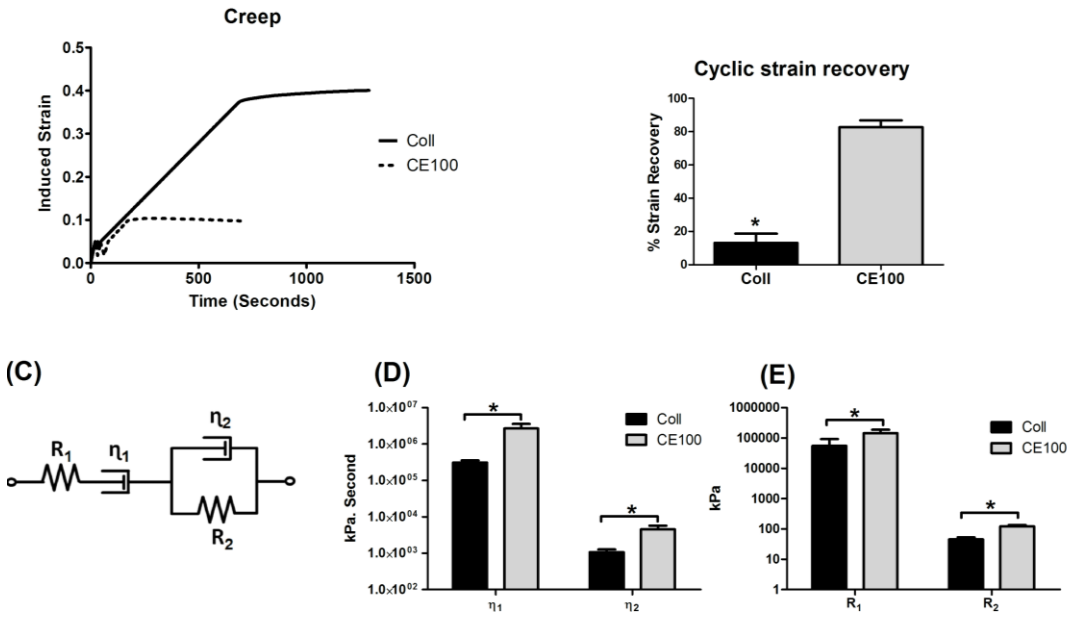

Figure 2.6 Effect of elastin addition on collagen scaffold creep response and cyclical strain recovery.

Elastin addition was found to significantly affect the creep response and cyclical strain recovery of collagen scaffolds. Collagen-only scaffolds exhibited an induced strain of 48.24 ± 7.1% while CE100 scaffolds exhibited a significantly lower (p<0.05) induced strain of 13.8 ± 3.6% (A). Elastin addition significantly improved (p<0.05) the cyclical strain recovery of the scaffolds (B). Burgerôs four parameter constituti creep data to determine the (D) viscous parameters (–ₒ and –.) and (E) elastic parameters (ˈYₒ and ˈY.). Elastin resulted in higher moduli values for ˈYₒ and ˈY., which indicates a lower instantaneous strain level and a lower overall strain magnitude respectively. Furthermore, elastin caused a significant increase in –ₒand –., indicating an increased resistance to long term deformation/creep and a shorter duration in the transition region.
(*) indicates p<0.05

2.3.4 Effect of elastin addition on *in vitro* response

Having determined the effects of elastin addition on collagen scaffold microarchitectural and mechanical properties we next sought to determine its effect on cellular response. From the above analysis, the CE100 scaffold was determined to be the optimal scaffold and so was utilised for all *in vitro* experiments.

DNA content was quantified on each scaffold at timepoints up to 14 days to determine smooth muscle cell proliferation. Elastin addition resulted in a 2.2-fold increase in initial cell attachment in the CE100 scaffolds (43.6% ± 11.1%) versus the collagen controls (20.2% ± 1.8%). However, when examining cellular proliferation the collagen-only scaffolds displayed significantly higher levels of proliferation at days 7 and 14 than the CE100 scaffolds ($p < 0.05$, Fig. 2.7A). The increased proliferation on the collagen-only scaffolds resulted in comparable cell numbers between the groups by day 14 ($p > 0.05$). Consequently, while elastin resulted in higher initial cell numbers, cell proliferation was inhibited over the 14 days, indicative of the cells becoming quiescent wh0ich is a hallmark of the contractile SMC phenotype (Rensen et al., 2007. Elastin addition also caused an increased resistance to cell-mediated contraction by day 14 ($p<0.05$) (Fig. 2.7B). Coll scaffolds retained 35.8% of the original area at day 14 while CE100 scaffolds retained 44.1% of their original area.

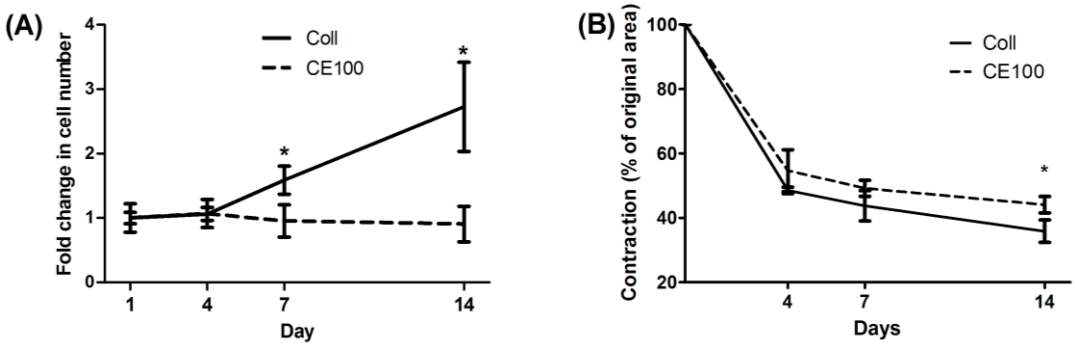

Figure 2.7 Effect of elastin addition on smooth muscle cell proliferation and cell-mediated scaffold contraction.

Elastin addition was found to significantly increase initial cell attachment (43.6%±11.1%) versus the collagen controls (20.2%±1.8%) (data not shown). However, the Coll scaffolds exhibited increased proliferation over the 14 days with significantly higher proliferation at days 7 and 14 ($p<0.05$). Elastin addition resulted in increased resistance to cell-mediated contraction by day 14 ($p<0.05$). Coll scaffolds contracted to 35.8 ± 3.5% of the original scaffold area by day 14 while CE100 scaffolds contracted to 44.1 ± 2.5% of the area at day 0. (*) denotes $p<0.05$ statistical significant difference in comparison to collagen.

Real-time RT-PCR analysis (Fig. 2.8) shows that, overall, elastin addition results in an earlier and more sustained expression of the mid and late stage contractile smooth muscle cell markers, calponin and smooth muscle myosin heavy chain (SM-MHC) respectively. It is evident that the mid/late stage SMC markers appear to be expressed much earlier in the presence of elastin than in the collagen controls (Figs.2.8 C, D). In particular, stable expression of calponin and SM-MHC was found in the presence of elastin as early as day 4. Additionally, elastin addition resulted in increased Coll I gene expression at day 4 although comparable expression levels were observed between the scaffold groups at all other timepoints (Fig. 2.8A). The level of α-SMA expression, an early SMC marker, was found to significantly increase over time in both groups and the presence of elastin resulted in a 3.1-fold higher expression at day 14 than the collagen control scaffolds (Fig. 2.8B).

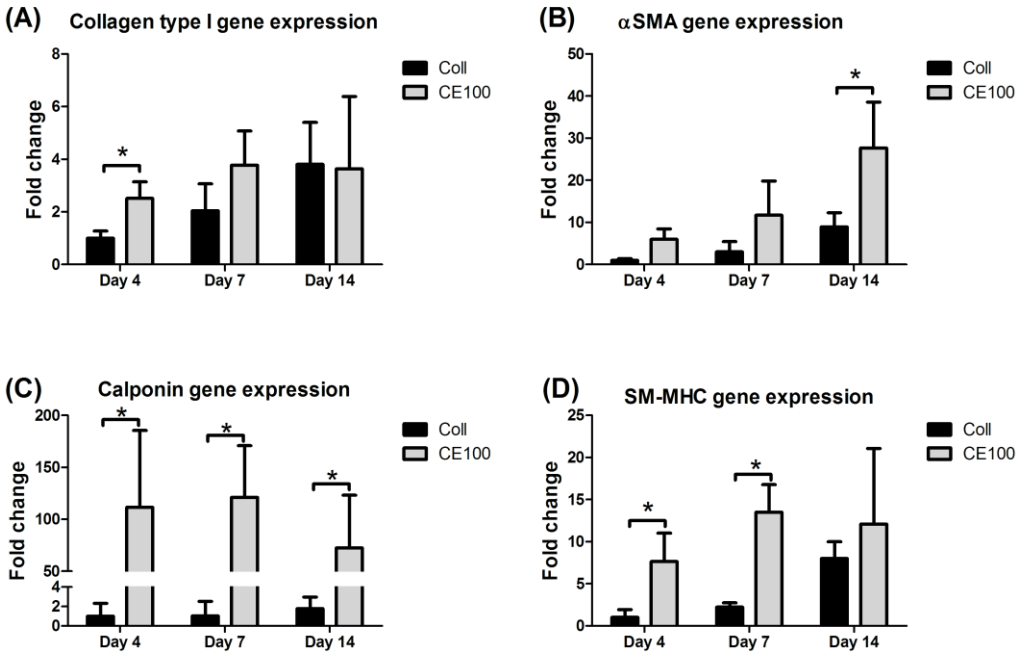

Figure 2.8 Effect of elastin addition on SMC gene expression.

The effect of elastin addition on SMC gene expression of Coll I (A), ŭSMA (B), Calponin (C), and SM-MHC (D) at timepoints up to 14 days. While elastin addition resulted in a significant increase in Col1 gene expression at day 4 the results are comparable at days 7 and 14 (A). The early stage SMC marker Ŭ-SMA was expressed at similar levels at days 4 and 7 but increased expression was observed on CE100 scaffolds by day 14. Elastin addition also resulted in significantly higher gene expression of the mid/late stage contractile SMC markers, calponin and SM-MHC at timepoints 4 and 7 days. By day 14 similar expression levels of SM-MHC were found in both groups but Calponin expression remained significantly higher in the CE100

scaffolds. Gene expression was normalised to the housekeeping gene 18S and expressed as fold change versus cell seeded collagen scaffolds at day 0. (*) denote p<0.05.

2.4 Discussion

The overall goal of this study was to investigate the effects of elastin addition on collagen scaffold microstructure, mechanical properties, and subsequently the response to seeded smooth muscle cells (SMC) *in vitro.* The results demonstrate that elastin addition resulted in minimal changes to scaffold pore architecture with both scaffold porosity and pore size still within the ideal ranges for tissue engineering applications. Mechanically, elastin decreased the scaffold compressive and tensile specific moduli in a concentration dependant manner (Figs. 2.4 & 2.5). More importantly from a cardiovascular perspective, the viscoelastic properties were significantly improved with elastin addition (Fig. 2.6). A 6-fold increase in cyclical strain recovery and 3.5-fold decrease in induced creep strain was found. Thus, elastin reduces the collagen scaffolds stiffness but also provides viscoelastic properties more representative of native cardiovascular tissue. Furthermore, elastin was found to result in the modulation of SMC phenotype towards a contractile state which was determined via reduced proliferation (Fig. 2.7A) and significantly enhanced expression of early (α-SMA) (Fig. 2.8B), mid (calponin) (Fig. 2.8C), and late stage (SM-MHC) contractile proteins (Fig. 2.8D). Taken together, the ability of elastin to alter the mechanical and biological response of collagen scaffolds has led to the development of a biomimetic biomaterial highly suitable for cardiovascular tissue engineering.

For cardiovascular biomaterial design, elastin is an ideal protein to examine as a composite with collagen due to its important mechanical and biological role *in vivo*. However, the structural-functional relationship of native elastin is difficult to ascertain due to the protein's large size and insolubility and thus many studies have focused on elastin-based peptides (Lim et al., 2008), hydrolysed elastin (Leach et al., 2005), or its soluble precursor, tropoelastin (Mithieux et al., 2004). While this provides us with increasing knowledge of

the molecular basis for elastin's mechanical and biological effects, the use of the native insoluble protein fibres provides numerous advantages for tissue engineering. Utilising peptides of native ECM molecules which contain cell binding motifs has attracted much research, especially those based on fibronectin (RGD), laminin (YIGSR), and elastin (VGVAPG) (de Mel et al., 2008). However, the bioactivity of peptides is significantly altered from the derived protein with the selectivity, affinity, activity, and proteolytic sensitivity changed (Martino et al., 2009). Thus, individual peptides can never recapitulate the multi-faceted effects or intricacies of their parent ECM proteins, in addition to usually lacking the fibrillar structure of native proteins and consequently having reduced mechanical properties.

We have successfully created composite scaffolds of collagen and elastin and found that, morphologically, elastin was homogenously distributed at higher concentrations (CE100), with the elastic fibres primarily encapsulated in the collagen struts (Fig. 2.2 A,B,C). Elastin addition caused a decrease in scaffold porosity in a concentration dependant manner from 99.3% to 98.8%, although the porosity is still within the suggested ideal range for effective tissue repair (Rezwan et al., 2006). Buttafoco has have previously reported a porosity of 90% for collagen-elastin freeze-dried scaffolds(Buttafoco et al., 2006a); however, the scaffolds were constructed from a starting suspension of twice the protein concentration used in the current study and so they are not directly comparable. Due to the elastic fibres being encapsulated by the collagen struts there were only minor variations in the scaffold mean pore size (84.8μm-96.1μm) and pore architecture was unaffected (Fig. 2.3). This mean pore size range has previously been reported to result in effective cell migration, proliferation (Lee et al., 2008) and ECM production (Ross and Tranquillo, 2003) while facilitating sufficient nutrient exchange for SMCs/MSCs. Previous *in vivo* results have shown that a mean pore size of >100 μm results in an increased rate of tissue in-growth and vascularisation (Cao et al., 2006; Mikos et al., 1993; Oh et al., 2007). However, for vascular tissue engineering the scaffold permeability is a very important factor to consider with large pore sizes leading to an increase in bulk fluid permeability and potentially leakage of a vascular graft. This poses a

challenge in specifying an ideal pore size as an average pore size of less than approximately 50 μm would likely result in core necrosis due to a lack of nutrient transfer and vascularisation. A suitable balance in pore size and vascular leakage can be achieved by maturing scaffolds *in vitro* as the cells contract the scaffold and produce new matrix, both leading to a reduction in the permeability of the scaffold.

Extensive examination of the mechanical properties of the scaffolds was carried out including analysis of the compressive, tensile, and viscoelastic characteristics (Figs. 2.4-2.6). Elastin addition was found to reduce the compressive modulus of the scaffolds, with a maximum decrease of 22% observed in the CE100 scaffolds versus the collagen controls ($p<0.05$). Interestingly, the uniaxial tensile properties were unaltered with elastin addition. However, when density differences in the scaffolds are accounted for, via calculation of the specific modulus ($\frac{\text{modulus}}{\text{density}}$), we found a strong decreasing linear correlation with scaffold specific compressive modulus and specific tensile modulus ($r^2 = 0.81$). This indicates that elastin addition reduces the stiffness of collagen scaffolds in a concentration dependant manner. Moreover, when the viscoelastic characteristics were examined it was found that elastin significantly improved the creep characteristics and cyclical strain recovery of collagen scaffolds. A four parameter viscoelastic model was utilised to determine the creep parameters from the experimental data (Fig. 2.6C). The mathematical model accurately represented the experimental data with a coefficient of determination (r^2) ranging from 0.9-0.98 for all tests. Elastin seems to confer an ability to resist long term creep in scaffolds, as determined via the 3.5-fold decrease in induced strain ($p<0.05$) and a 8.7-fold increase in τ_o, indicative of increased resistance to long term deformation/creep. Further increases in the parameters which govern the instantaneous strain ($\dot{\gamma}_o$), transition region duration (τ_r), and strain magnitude (γ) support the importance of elastin as a load bearing cardiovascular protein which is imperative to store elastic-strain energy and prevent creep of cardiovascular tissue. This was further tested dynamically

with cyclical straining where elastin resulted in a 6-fold increase in recovery strain versus collagen alone.

Similar levels of creep as the collagen control analysed in this study have previously been reported for collagen gels (Berglund et al., 2005). Native arteries exhibit significant resistance to creep while being cyclically strained for approximately 2.5 billion cycles over a person lifetime. This remarkable creep resistance has been attributed primarily to the presence of elastin with can be demonstrated through elastase-induced degradation which results in aneurysm formation *in vivo* (Anidjar et al., 1990; Halpern et al., 1994). Indeed, multiple reports of tissue engineered vessels with an absence of elastin in their structure have exhibited graft dilation via creep *in vivo* (Niklason *et al*., 2001; L'Heureux *et al*., 2007). Additionally, the ability to tailor the stiffness of a scaffold with elastin in a concentration dependant manner is a powerful tool to tailor the cell microenvironment to reduce the risk of unwanted calcification found in a number of cardiovascular tissue engineered scaffolds (de Valence et al., 2012; Tedder et al., 2009). Overall, these results suggest that elastin addition causes a more native-like viscoelastic response which may be capable of sufficient elastic recoil and creep resistance for the cardiovascular environment.

Contrary to expectations, the stiffer collagen scaffolds contracted more than the collagen-elastin scaffolds (Fig. 2.7). Using this volumetric contraction data we can calculate that the final density of the scaffolds increases to ~200mg/cm^3 for both scaffold types which may indicate an upper limit to the contraction based on final protein density. As the struts in the scaffolds collapse due to cell-mediated contraction a densification regime is entered and the stress would sharply rise, thus inhibiting further cell–mediated contraction. Interestingly, we can also use this data to calculate the changes in scaffold elastic modulus during contraction via cellular solids modelling(Caliari and Harley, 2014; Ryan et al., 2014) with the collage-elastin scaffold modulus closely matching native heart tissue at ~33kPa and the collagen scaffold calculated to reach ~150kPa, more similar to a fibrotic scar or bone (Berry et al., 2006; Bhana et al., 2010). However, it should be

noted that the local stiffness of the scaffold struts is expected to be higher than this bulk stiffness, although the cells will experience large gradients due to the differing stiffnesses of collagen (~5MPa) and elastin (~0.5MPa) (Nowatzki and Tirrell, 2004). In terms of the stiffness of native blood vessels, low strain artery moduli have previously been reported to range from 700kPa for porcine carotid arteries (Sheridan et al., 2012) to 16.7kPa for human coronary arteries (Kural et al., 2012). Thus, the scaffolds described are within the normal stiffness range for whole arteries. However, the tunica media generally displays a significantly lower modulus than other artery layers, in the range of 1.3kPa for human coronary arteries (Holzapfel et al., 2005) and 190kPa for human carotid arteries (Khamdaeng et al., 2012). Thus, the scaffolds described would be highly suitable for use as a media layer equivalent rather than a whole artery.

Subsequent SMC proliferation and gene expression analysis revealed that the addition of elastin significantly affected both parameters ($p<0.05$), indicating phenotype modulation due to ECM interaction (Figs. 2.7 & 2.8). The ability to control SMC phenotype is an important characteristic for cardiovascular tissue engineering due to the extraordinary plasticity these mature cells display in response to local environment changes (Rensen et al., 2007). These local environmental changes may result in SMCs changing from a quiescent-like contractile phenotype to a more synthetic phenotype. Synthetic SMCs display drastically increased cell migration, proliferation and ECM production and this phenotype is generally observed during vessel wall injury or pathological conditions (Yoshida and Owens, 2005). Our results indicate that seeded SMCs revert to a synthetic phenotype when cultured on collagen-only scaffolds, as determined via the enhanced cell proliferation (1.5-fold) and lower expression of multiple contractile proteins, including α-SMA, calponin, and SM-MHC (Figs. 2.7 & 2.8). This corresponds well to the work of Yamamoto (Yamamoto et al., 1993) and Stegemann and Nerem (Stegemann and Nerem, 2003) who have previously shown that collagen type I stimulates proliferation but simultaneously results in the reduction of the contractile protein α-SMA.

Notably, with the addition of elastin, the SMCs became quiescent (proliferation was inhibited over the 14 days), while the contractile proteins α-SMA, calponin, and SM-MHC were all significantly upregulated at multiple timepoints ($p<0.05$). Thus, elastin addition results in a phenotypic switch to a more contractile SMC phenotype.

Elastin has previously been identified as an important regulator of SMC phenotype where the soluble elastin peptides present in diseased arteries can modulate SMCs towards a proliferative synthetic phenotype (Mochizuki et al., 2002). However the specific effects of the whole insoluble protein are markedly different to the soluble peptides where elastin is known to have an anti-proliferative effect and thus is critical in maintaining the native contractile phenotype. Numerous mechanisms as to why this occurs have been reported including the insoluble elastin sequestering growth factors otherwise involved in SMC proliferation (Urbán et al., 2002) and direct anti-mitotic signalling through the protein itself (Li et al., 1998). The direct signalling has been reported to occur through G-protein coupled receptors, the 67-kDa elastin binding protein, and a variety of integrins (Bax et al., 2009; Lee et al., 2014). This corresponds well to previous work that has suggested that elastin is involved in maintaining a contractile phenotype both *in vitro* (Gong and Niklason, 2008; Yamamoto et al., 1993)and *in vivo* (Satyajit K Karnik et al., 2003). Conflicting results on the effects of elastin on SMCs in 3D scaffolds have also been reported with SMCs showcasing synthetic phenotype hallmarks, such as proliferation and migration, on a number of elastin containing scaffolds (Boland et al., 2004; Buttafoco et al., 2006a). However, we believe we have demonstrated the first conclusive evidence that elastin can be utilised to direct SMC phenotype in a 3D environment for tissue engineering purposes. It was hypothesised that elastin addition may have resulted in the downregulation of Coll I gene expression due to the phenotype modulation, but no significant difference was observed after day 4 (Fig. 2.8). It is clear that complex cell-ECM signalling is occurring in the scaffolds due to the scaffold composition, mechanical properties, and architecture. However, the collagen-elastin scaffolds described here would seem to emulate many of the desirable characteristics for cardiovascular

tissue engineering and represents a promising biomaterial platform for further investigation.

2.5 Conclusion

In this study, we have shown that elastin addition to a porous collagen scaffold can play a major role in altering its biological and mechanical response. With the addition of elastin we observed a higher degree of cyclical strain recovery and creep resistance which indicates the biomaterial may possess sufficient recoil to be utilised for long-term cyclical distension for cardiovascular tissue engineering. While scaffold remodelling will occur once the scaffolds are cell seeded, the environment presented by the collagen-elastin composite scaffolds closer mimics the native mechanical response and protein composition of arterial tissue and may lead to improved formation of arterial tissue. Additionally, the presence of elastin resulted in a more contractile-like SMC phenotype which is necessary for vasoactivity and inhibition of intimal hyperplasia *in vivo*. This biomimetic biomaterial is amenable to multiple fabrication methods and represents a versatile biomaterial platform which is capable of being applied for numerous tissues including skin, elastic cartilage, lung tissue engineering, or as a cardiac patch for cell delivery.

Chapter 3: Development of bilayered tubular collagen-elastin scaffolds for vascular tissue engineering

3.1 Introduction

Tissues are 3D self-assembled constructs developed to serve very precise needs based on their location. The organisation of the cells and ECM components in a tissue ultimately dictates the tissues potential function and is highly adapted to deal with any mechanical loads which it will encounter (Stella et al., 2010). This hierarchical structuring from the nanostructure to the macrostructure is a tightly regulated and complex process which has proven elusive to recreate fully *in vitro* (Fratzl and Weinkamer, 2007). Thus, bioengineers have resorted to developing biofabrication tools and techniques in order to aid in recreating tissues *ex vivo*. The ideal tissue engineered vascular graft (TEVG) would thus mimic native tissue microenvironment and structure, and be composed of a multi-layered lamellar structure (Fig. 3.1).

The biofabrication technique selected ultimately dictates the possible end architectural constraints. Multiple techniques now exist to generate structures with control over the nano/microstructure and with the capability to generate large, anatomically correct scaffolds with a suitable macrostructure. However, many of these techniques are limited to either synthetic polymers capable of withstanding the elevated temperatures required for 3D printing techniques (e.g fused deposition modelling) or require specialist photosensitive materials (e.g. stereolithography, two-photon polymerisation). Freezedrying, as a technique, is amenable to a broad range of materials and is highly suitable for thermosensitive natural polymers which may denature

under elevated temperature conditions. However, freezedrying is often seen as limited in the scope of microstructural and macrostructural manipulation possible. Previous work has shown that although the microstructure can be manipulated, it is influenced by the composition (Ryan et al., 2014) as well as the specific freeze-drying conditions, such as freezing rate (O'Brien et al., 2004) and final freezing temperature (Haugh et al., 2009). Therefore, optimisation of microstructure may be achieved by altering these parameters. Hierarchical structured scaffolds can be fabricated through a combination of techniques to leverage the advantages of each while minimising the disadvantages. So far, this thesis has demonstrated that generating three dimensional porous scaffolds from collagen and elastin (Chapter 2) elicits a number of distinct advantages as a template for tissue regeneration. Utilising this data we next sought to further optimise this biomaterial by structuring it hierarchically. Specifically, we sought to create a physiologically relevant bilayered tubular architecture through generation of a porous outer layer (analogous to the tunica media) and a dense film inner layer (analogous to the tunica intima).

Traditional tissue engineered vascular grafts are created as a single homogenous layer in a tubular structure. Some of the earliest work utilising natural polymers for this application were in the form of easy to fabricate collagen gels. Indeed, a number of researchers have investigated SMC-seeded collagen type I gels which were compacted by the seeded cells over time to produce vascular grafts (L'Heureux et al., 1993; Seliktar et al., 2003a). However, due to the low polymer density and disorganised matrix formed, these grafts did not possess the required mechanical properties for the challenging haemodynamic environment (Barocas et al., 1998; Hirai et al., 1994). Consequently, the field progressed to incorporate synthetic polymer meshes within the natural polymers in order to improve the overall graft mechanical properties (Tillman et al., 2009; Tschoeke et al., 2008). However, despite the limitations associated with these early grafts, significant advances in natural polymer fabrication techniques over the last 20 years have enhanced the potential for development of a successful collagen-based tissue engineered vascular grafts. The hierarchical

structuring of natural polymers, like collagen, can be achieved by altering the protein concentration between the layers to leverage the effect of density on mechanical properties (Caliari et al., 2011; Kumar et al., 2013). The integration of a dense luminal layer would further match the native architecture, would potentially increase mechanical properties, and provide a suitable surface for endothelialisation. While it is clear that emulation of natural vessel architecture and polymer composition has distinct advantages, the optimal combination of biomaterial and architecture for vascular tissue engineering applications has yet to be elucidated.

In addition to their inherently excellent biological properties, natural polymers offer the ability to easily modify their mechanical properties and degradation rates through crosslinking. Crosslinking, as a technique, offers the powerful ability of being able to tune a material's properties independently of the density or microstructure by creating covalent bonds between nearby collagen molecules. Thus, a hierarchically structured scaffold can be further fine-tuned to match the desired mechanical properties. While the native collagen crosslinking pathway occurs through the enzyme lysyl oxidase *in vivo*, the harsh extraction procedures used to process collagen for medical device applications result in the degradation of these bonds. Thus, exogenous methods based upon physical, chemical, or alternative enzymatic methods are often utilised (Koh and Atala, 2004; Tierney et al., 2013). These exogenous crosslinks are capable of causing vastly improved mechanical properties but also result in cytotoxicity and/or unwanted cellular responses such as calcification. Crosslinking also can be used to tailor the degradation rate of the biomaterial where a slow degradation rate allows a gradual stress transfer to occur and is favourable from a mechanical viewpoint. However, biologically the most favourable outcome would be for the degradation rate to match the rate of new tissue growth which generally necessitates a faster degradation rate. The ideal solution involves striking a balance between the mechanical and biological suitability of the degradation rate for effective tissue repair. Interestingly, crosslinking has also being implicated as being involved in host-biomaterial interactions by modifying the immunogenic response (McDade et al., 2013).

3.1.1 Objectives

The overall objective of this chapter was to develop bilayered tubular scaffolds with controllable properties for use as a tissue engineered vascular graft. This chapter focused on optimising the architecture of the previously optimised biomaterial composition from Chapter 2. In line with these objectives, the specific aims of this study were:

- Study 1: Develop the optimal biofabrication method to produce porous collagen-elastin tubular scaffolds using a custom designed mold and varying the freezing rate to control microstructure.

- Study 2: Develop dense protein films with controllable mechanical properties and degradation rates through varied crosslinking procedures. Additionally, the effect of crosslinking on the inflammation response of macrophages was also examined *in vitro*.

- Study 3: Develop bilayered tubular scaffolds by selecting the optimal methods from studies 1 and 2 above. The microstructure was further optimised through altering the freezing direction (horizontal v vertical) and mold materials during fabrication. Preliminary *in vitro* culture focused on examining tubular scaffold seeding and compaction on a custom constrainment rig during static culture.

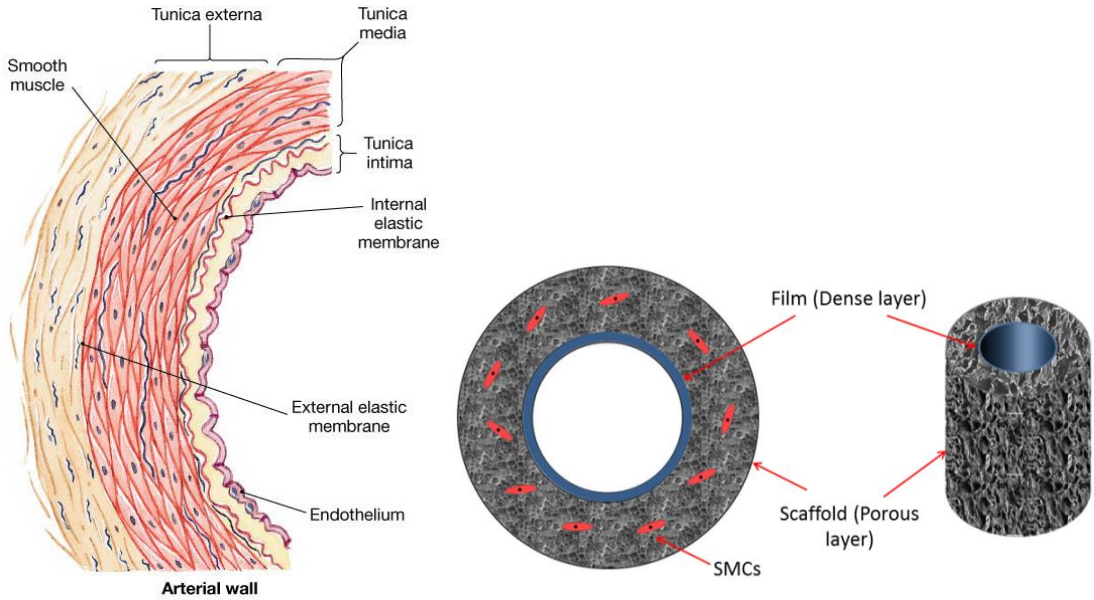

Figure 3.1 Graphical abstract of the chapter aims

The initial study focused on developing tubular porous scaffolds using the optimal composition from Chapter 2. Hierarchically structuring to mimic native architecture (left) was providing by a dense film layer (intima mimic) on the luminal aspect and a porous outer layer (media mimic) to form a bilayered tubular scaffold (right). Control over the mechanical properties, degradation rate, and inflammation response was examined via crosslinking. Validation of cells seeding and static culture effects were also performed.

3.2 Materials and Methods

3.2.1 Study 1: Development of tubular scaffolds

In order to be able to produce tubular scaffolds via freezedrying a custom designed mold was machined in Trinity College Dublin mechanical engineering workshop. Preliminary experiments focused on examining a number of alternative mandrel materials, altered outer mold diameters, and altered freezing cycles in order to achieve a reliable fabrication process. A collagen-elastin suspension (CE100) was created as per Section 2.2.1. The suspension was then pipetted into the mold (Fig. 3.2), which had an outer diameter of 11mm and an inner diameter of 5mm, and freeze-dried as per Section 2.2.1. Due to shrinkage of the scaffold during the freezedrying process the final wall thickness was approximately 2.5mm. This thickness was selected based upon the contraction data obtained in Section 2.3.4, where it was calculated that an initial wall thickness of 2.5mm would contract to <1mm after 14 days culture.

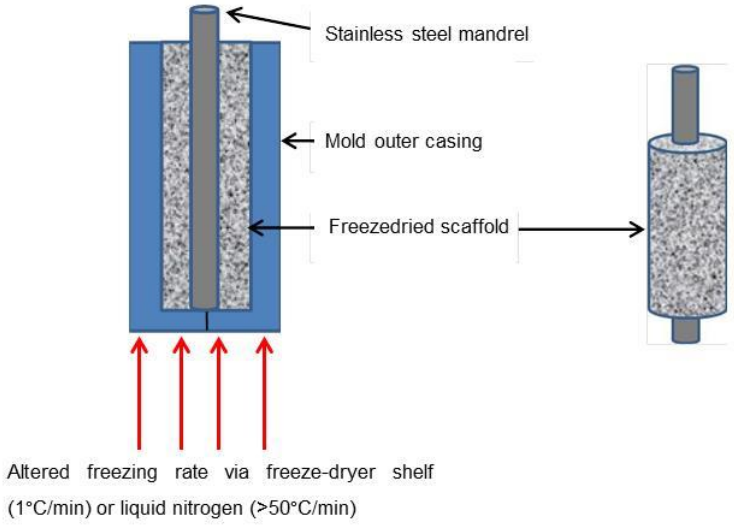

Figure 3.2 Cross-section schematic of the mold used for producing tubular scaffolds.

The interstitial space between the mold outer casing and the mandrel is filled with the collagen-elastin suspension and freezedried. The mold casing and mandrel are both stainless steel to ensure they transfer heat efficiently to result in a homogenous freezing profile. Once freezedried the mold is easily disassembled and the tubular scaffold can be removed from the mandrel.

To enable the production of multiple tubular scaffolds per freezedrying cycle the mold was designed with eight cavities. Additionally the external diameter of the mold cavities ranged from 9 mm to 12 mm to allow controllable variation in the wall thickness of the tubular scaffold walls (Fig. 3.3). The mandrel size could also be altered although for the scope of this project it was maintained as 5 mm.

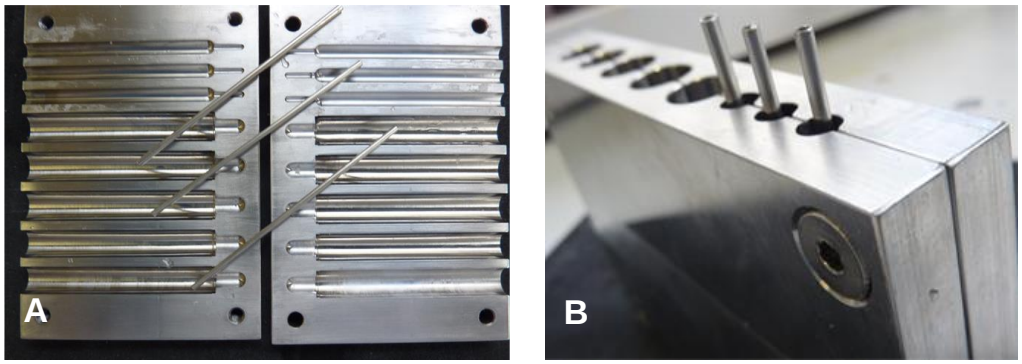

Figure 3.3 Custom designed mold for tubular scaffold fabrication.

(A) The custom designed mold consists of two machined stainless steel plates which are held together via hex head screws (B) A 5mm diameter mandrel fits down the mold cavity to create an interstitial space where the protein suspension can be freezedried to form tubular scaffolds.

3.2.1.1 Effect of freezing rate on tubular scaffold microarchitecture

Two distinct freezing rates were examined to determine the optimal microarchitecture capable of supporting the growth of smooth muscle cells. The optimal pore size should be large enough to facilitate effective cell migration to within the scaffold structure. Samples were frozen via controlled freezing on the freeze-drier shelf at 1°C/min, or via liquid nitrogen immersion which would produce a freezing rate of >50°C/min. All samples were then transferred to the freeze-dryer and dried using a previously optimised drying profile (O'Brien et al., 2004). Microstructural analysis was performed via SEM as per Section 2.2.2.

3.2.2 Study 2: Protein film development with controllable mechanical properties, degradation rates, and inflammation response

The design for the bilayered tubular scaffolds required a dense, non-porous protein mat or film which could be incorporated as a luminal layer. The native tunica intima is primarily composed of a dense elastin rich layer (internal elastic lamina) along with collagens and proteoglycans, and so the protein blend from Chapter 2 (CE100) was deemed highly suitable for this application. A solvent casting technique was selected and preliminary work examined the relationship between volume and the resulting film thickness. Briefly, Collagen-Elastin (CE100) protein suspensions were fabricated using the same procedure as Section 2.2.1. Following degassing the suspension was transferred to a polytetrafluoroethylene (PTFE) plate with a square stainless steel mold clamped over the edges of the PTFE plate (Fig. 3.4). The optimal volume was determined to be 1ml of protein suspension per 288 mm^2. Controlled dehydration of the solvent was achieved under a fume hood for 24 hours to achieve formation of a protein film. PTFE was chosen as the dehydration substrate as it possesses excellent non-stick properties in addition to a very low coefficient of friction and being highly hydrophobic. This allowed for easy removal of the dehydrated films. As per Section 2.2.2, films were examined under SEM and also embedded in JB-4

glycomethacrylate, sectioned, stained with toloudine blue, and imaged to determine an accurate value of film thickness.

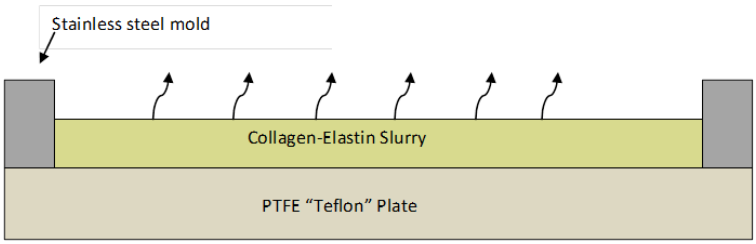

Figure 3.4 Film dehydration setup.

CE100 films were prepared by dehydrating the protein suspension on a PTFE plate for 24 hours under controlled conditions until water content was negligible.

3.2.2.1 Crosslinking to control film physiochemical properties

Following fabrication of the films a number of crosslinking treatments were examined in order to provide control over the resulting mechanical properties. As the films will bear the majority of the mechanical load due to the far greater density, the crosslinking technique used will ultimately determine the mechanical response of the final bilayered scaffold. An additional advantage of crosslinking is that it generally increases the resistance to degradation *in vivo*. This is an important characteristic as ideally we wish to match the rate of degradation to the rate of new tissue formation. The panel of crosslinking treatments ranged from physical treatments (dehydrothermal), chemical (carbodiimide based crosslinker, glutaraldehyde), combination physical/chemical (riboflavin + UV), and enzymatic (microbial transglutaminase).

<u>Dehydrothermal (DHT) Crosslinking</u>

Following dehydration the films were dehydrothermally (DHT) crosslinked as per Haugh et al. (2009). Briefly, the films were subjected to a DHT treatment of 105°C for 24 hours at 0.05 bar in a vacuum oven (Vacucell 22, MMM, Germany).

EDAC Crosslinking

Films were prepared for crosslinking by the chemical crosslinker EDAC (1-ethyl-3-(3-dimethyl aminopropyl) carbodiimide) by hydrating in phosphate buffered saline for 1 hour (PBS, Sigma-Aldrich, Germany). The EDAC/NHS solution was at a concentration of 3 mM EDAC per gram of collagen with the addition of the catalyst N-Hydroxysuccinimide (NHS) at a concentration of 2.5 mM per mol EDAC as found optimal for scaffold stiffness by Haugh et al. (2011). Films were immersed for 2 hours in the EDAC/NHS solution followed by washes in PBS to remove any residual EDAC and the urea by-product of the reaction.

Glutaraldehyde Crosslinking

Films were prepared for crosslinking by hydrating in phosphate buffered saline for 1 hour followed by immersion for 2 hours in a 0.2% glutaraldehyde/PBS solution at room temperature. Following crosslinking, the films were washed in PBS three times to remove any residual glutaraldehyde followed by a final wash in distilled water (Charulatha and Rajaram, 2003, 1997).

Riboflavin/UV Crosslinking

Films were prepared for crosslinking by hydrating in phosphate buffered saline for 1 hour. Following hydration the films were immersed in a 0.1 % wt/vol (2.657 mM) solution of Riboflavin 5′-phosphate sodium salt hydrate (Sigma-Aldrich, Dublin, Ireland) in PBS and crosslinked via exposure to ultraviolet light (Fig. 3.4) at a wavelength of 365nm for 120 minutes with a 4 watt lamp (UVGL-25, UVP Ltd, Upland, California, USA). The lamp intensity was 750 μW/cm² at 3" (76.2mm) from the films. This corresponds to 0.045 joules/minute and a total energy exposure of 5.4 joules/ cm² for the crosslinked films after 120 minutes. Following crosslinking, the films were washed in PBS three times to remove any residual riboflavin.

Microbial Transglutaminase (mTGase) Crosslinking

Microbial transglutaminase (Activa WM) was a kind gift from Ajinomoto Co. Inc, Japan. The product, Activa WM, contains the enzyme microbial

transglutaminase combined with maltodextrin. The maltodextrin was not expected to have any effect on the collagen or elastin in the films and its excellent solubility means that it could be easily washed off the films once crosslinking was complete (Schloegl et al., 2012). The quantity of microbial transglutaminase to use for crosslinking was optimised in a separate study (results not shown). The optimal concentration of the enzyme containing powder was 10mg per mg of collagen. The enzyme was dissolved in PBS and the films were incubated for 12 hours at 37°C. Following crosslinking, the films were washed in PBS three times to remove any residual maltodextrin and enzyme.

3.2.2.2 Quantification of film crosslinking efficiency

Quantification of the film crosslinking efficiency was determined via analysis of the reaction of free primary amines with 2,4,6-trinitrobenzene sulfonic acid (TNBS), which yields a yellow coloured product which is read colormetrically. As these primary amines are consumed in the crosslinking reactions, the relative level of crosslinking can be determined by comparing the number of free amines in the uncrosslinked samples to the amines in the crosslinked samples.

Briefly, each protein film sample of weight 5mg was added to a screw-top vial containing 500µl of 4% w/v NaHCO3 (pH8.5) and 500µl of 0.5% w/v TNBS (Sigma-Aldrich, Dublin, Ireland). Sampled were reacted for 2 hours at 37°C before the addition of 1ml of 6M HCl and allowed to solubilise at 60°C for a further 2 hours. Samples were diluted with 2mls of dH20 and allowed to cool before absorption at 345nm was read using a spectrometer (Wallac Victor2™ 1420 multilabel counter, Perkin Elmer Life Sciences, Waltham, MA, USA)). A standard curve was generated using the amino acid L-arginine.

3.2.2.3 Effect of crosslinking on film enzymatic degradation resistance

Film degradation properties were assessed using bacterial collagenase from Clostridium histolyticum (C7926 Sigma Blend Type F, Sigma-Aldrich, Dublin,

Ireland). Films were cut into evenly sized pieces (~15mg in weight) and hydrated for 1 hour at 37°C in a buffer containing 0.1 M Tris-HCL and 0.05 M CaCl2 at pH 7.4. Using this buffer, collagenase solutions were formulated and added to the hydrated films to give a final activity of 25 units/ml. The films were incubated for a further 2 hours at 37°C before the degradation reaction was stopped by placing the samples in an ice bath and adding 0.25 M EDTA (pH 9) at a ratio of 1:6 EDTA:buffer. Samples were centrifuged at 12,000 rpm for 10 minutes and the supernatant was removed. Distilled water was added to the sample followed by vortexing and re-centrifugation. Washing was repeated 3 times with distilled water and then 3 times with ethanol. Samples were air dried followed by a gravimetric assessment of the samples to determine the percentage of protein remaining. The optimal degradation time of 2 hours was assessed experimentally (results not shown). The optimal degradation time was determined as the time at which partial degradation had occurred for all groups yet below complete degradation. This allowed an accurate representation of the relative differences between crosslinking treatments.

3.2.2.4 Effect of crosslinking on film mechanical properties

Tensile testing of the films was performed using a uniaxial tensile testing machine (Z050, Zwick/Roell, Ulm, Germany) with a 5N load cell. Samples for testing were cut from the sheet using a razor blade and a dog-bone mold as per ASTM Standard D638, type V (American Society for Testing and Materials International). Samples were then tested as per Section 2.1.6.

3.2.2.5 Effect of crosslinking on film inflammatory response

Following determination of the optimal crosslinking treatments from a mechanical and degradation perspective, the inflammatory response of the three best treatments was determined using primary human monocytes/macrophages to determine any potential negative inflammatory potential. The effect of crosslinking on film inflammatory response was

assessed via assaying the release of the inflammatory cytokine TNFα from primary human macrophages seeded on the crosslinked films. Under approved licence from the RCSI Ethics Committee human blood from 3 donors was extracted into syringes containing 3.8% w/v tri-sodium citrate (0.129M) as an anticoagulant. Ficoll-Paque Plus density gradient centrifugation was utilised to isolate the peripheral blood mononuclear cells (PBMC) fraction which includes monocytes, T cells, NK cells, B cells, dendritic cells and basophils. Briefly, the sodium citrate buffered blood was diluted 1:1 with PBS before careful addition of the blood/PBS mixture into Ficoll-Paque Plus (Fisher-Scientific Ltd, Dublin, Ireland) at a ratio of 2:1. Following centrifugation at 300rcfs with no brake the white blood cell ring fraction was extracted carefully before further centrifugation. Any residual red blood cells were lysed using 5mls of Red Cell Lysis Buffer (Miltenyl Biotec) and the isolated PBMCs are resuspended in RPMI-1640 medium (Sigma-Aldrich, Dublin) and counted using a haemocytometer.

The PBMC fraction contain numerous cell types and so to isolate monocytes a positive selection procedure was applied using magnetic separation to antibody bound superparamagnetic microbeads. CD14 was selected as a suitable marker for monocytes. Briefly, 20µl of CD14 microbeads were added per 10^7 cells in the PBMC fraction and incubated for 15 minutes at 4°C to allow binding. Magnetic separation of the CD14 positive cells was then achieved using MACS LS columns (Miltenyi Biotec Ltd, Surrey, UK) and the MACS separator as per the manufacturer's instructions.

Monocyte seeding and culture

CE100 films were fixed within CellCrown™ cell culture inserts (Scaffdex Oy, Tampere, Finland) to maintain an even strain on the films and prevent undulations and consequent uneven cell dispersion. The purified human monocytes were seeded at a density of 3×10^5 cells per cm^2 of the CE100 films. Monocytes were cultured for up to 2 days in RPMI-1640 supplemented with 10% foetal bovine serum (FBS, Biosera, East Sussex, UK) and 2% penicillin-streptomycin (Sigma-Aldrich, Dublin, Ireland). The differentiation of the monocytes towards an inflammatory macrophage phenotype (M1

phenotype) was then assessed by TNFα release using an enzyme linked immunosorbent assay (ELISA).

Tumour necrosis factor α (TNFα) release and assessment using enzyme linked immunosorbent assay (ELISA)

The cytokine TNFα was selected as a suitable marker of inflammatory response from primary human macrophages. A human TNFα DuoSet ELISA assay (R&D systems, Abington, UK) was used as per the manufacturer's instructions to quantify the levels of TNFα released by the CD14+ monocytes. This assay uses a mouse anti-human TNFα capture antibody, a biotinylated goat anti-human TNFα detection antibody, and a recombinant human TNFα protein as standard. Horseradish peroxidase (HRP)-tetramethylbenzidine substrate solution was used for colorimetric detection.

3.2.3 Study 3: Development of bilayered tubular scaffolds a porous outer layer and dense film layer

In order to mimic the multi-layered structure of native arteries we combined the porous tubular scaffold and dense film, developed above, to create a physiologically relevant bilayered tubular architecture (Fig. 3.5). This biomimicry endows a large number of advantages with the porous layer offering a highly suitable environment for SMCs, while the dense film layer provides increased mechanical integrity and a suitable smooth surface for future endothelialisation.

The dense CE100 films were hydrated in 0.5M acetic acid for 90 minutes followed by wrapping around the stainless steel mandrel to form a 2-ply tube. The 2-ply tube was then air-dried under a fume hood to ensure fusion of the layers. The CE100 film-coated mandrels were then placed into the tubular scaffold fabrication mold with the interstitial space filled with CE100 suspension. The suspension and film coated mandrel were maintained in contact for 30 minutes prior to freezedrying to allow the films surface to hydrate and partially solubilise due to the acetic acid present in the suspension. This process resulted in fusion between the film and resulting porous scaffold (Fig. 3.5).

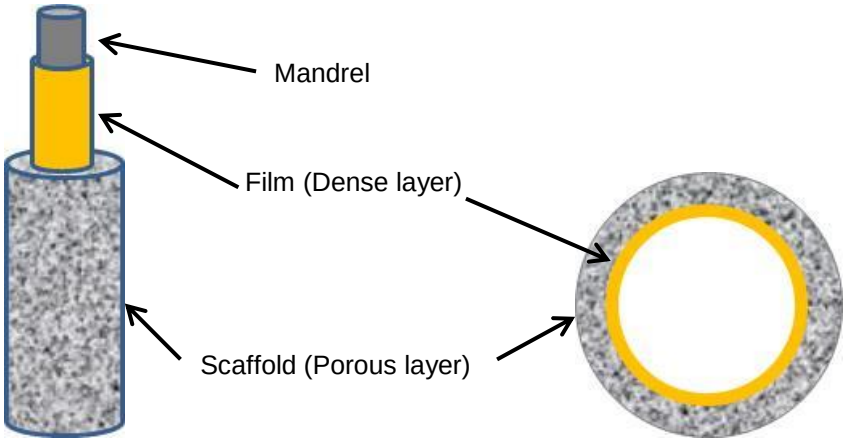

Figure 3.5 Bilayered tubular scaffold schematic

The architecture of the bilayered tubular scaffolds is shown with the film coated mandrel and porous outer scaffold.

3.2.3.1 Effect of freezing direction and mandrel material on scaffold microarchitecture

Combining the porous layer and dense film layer to create a bilayered scaffold was hypothesised to alter the resulting microarchitecture of the outer porous layer due to changes in freezing dynamics. Consequently, consideration was shown to this by re-examining the microarchitecture after combining the two layers. The incorporation of the dense inner film layer was found to alter the direction of travel of the freezing front by inhibiting heat transfer from the inner mandrel and thus forced the freezing front to primarily travel radially towards the lumen.

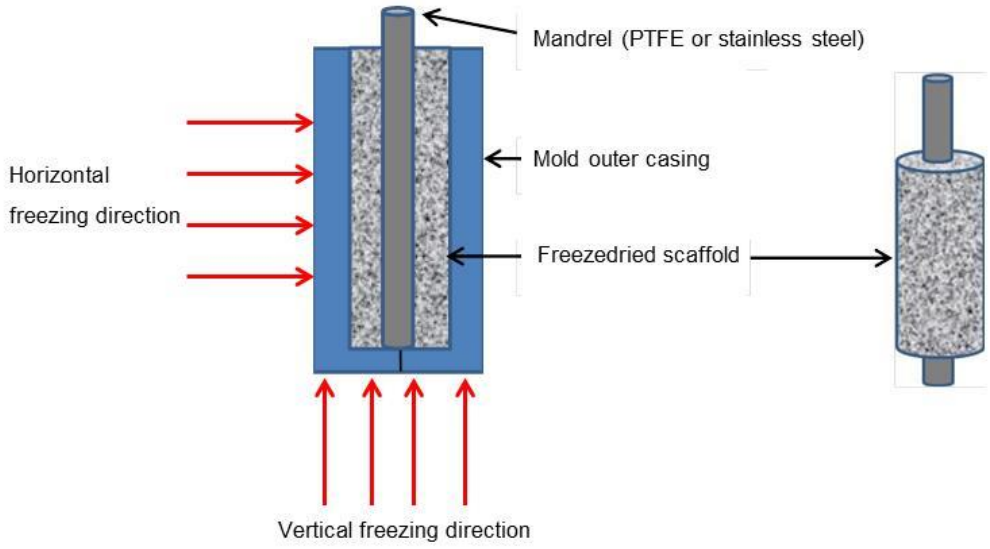

Figure 3.6 Freezing direction and altered mandrel material to control bilayered scaffold microarchitecture

Freezing direction was altered from the vertical or horizontal direction to control the resulting scaffold microarchitecture as shown. The mandrel was also altered from stainless steel to PTFE to either act as an efficient conductor of heat or to act as an insulator, which consequently alters the freezing front path.

In order to address this issue, control over the direction of the freezing fronts and consequently the resulting scaffold microarchitecture was possible as the mold was designed to enable alterations of the freezing direction (horizontal v vertical) and/or the mandrel materials (heat conductors v insulators). Freezing direction was altered from the vertical direction to the horizontal direction as shown in Figure 3.6. Viton® O-Rings (McMaster-Carr, Atlanta, USA) were secured over the top of the mandrel to ensure that it stayed centred and to prevent leakage of the protein suspension when placed in the horizontal direction. Prior to the drying step the O-rings were removed and all samples placed upright to ensure adequate sublimation during the freeze-dryer cycle.

3.2.3.2 Cell seeding, static culture, and compaction

Initial validation of cell seeding and compaction of the vascular grafts was determined using hSMCs as per Section 2.2.4. Constrained static culture was performed using a custom designed culture rig (Fig. 3.7). Constrained

static culture has previously been shown to result in superior circumferential ECM alignment due to compaction being permitted solely in the longitudinal direction (Barocas et al., 1998; Cummings et al., 2003). Tubular scaffolds of length 30mm were loaded onto the custom holder, placed in a 6-well plate, hydrated in media for 30 minutes, and then partially dried in a sterile flow hood. SMCs were resuspended at a concentration of 4 x 10^6 cells per ml. Cells were pipetted along the length of the scaffold in volumes of 50µl. Scaffolds were then rotated 90° and the process was repeated until the outer porous section of the scaffold has been seeded with a total of 3 x 10^6 cells. Scaffolds were transferred to the incubator and cells were allowed to attach for 30 minutes prior to the addition of 3mls of media per well. Histological analysis was performed after 21 days culture. Samples were fixed in 10% formalin for 20 minutes prior to tissue processing and paraffin embedding. Samples were section at 10µm, deparaffinised, and stained with Haematoxylin and Eosin (H&E) and DAPI (4', 6- diaminido-2-phenylindole) to fluorescently label cell nuclei.

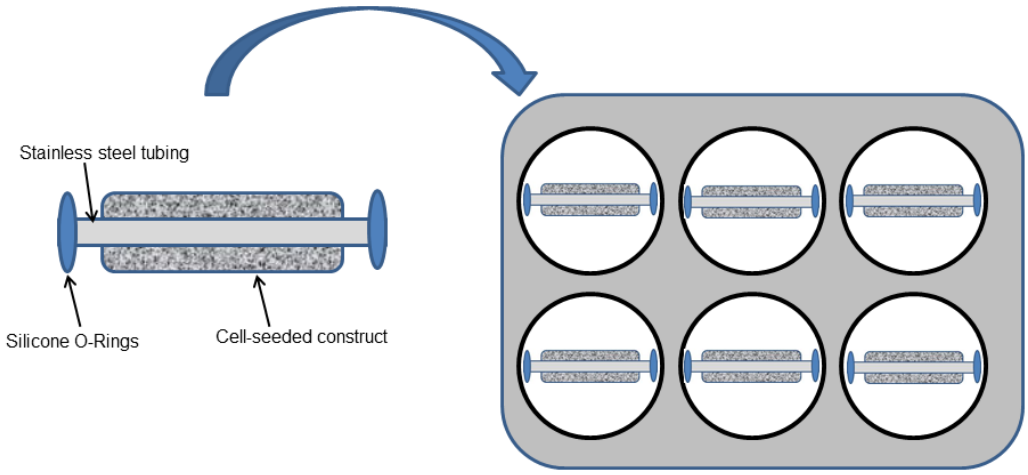

Figure 3.7 Static culture constrainment rig

Static culture of the tubular scaffolds was performed in a custom holder which permitted contraction in the longitudinal direction but not in the circumferential direction. The holder was designed to fit within a standard 6-well plate and could accommodate scaffolds up to 30mm in length.

Statistical analysis

Statistical analysis was conducted using one-way or two-way ANOVA followed by the Holm-Sidak post hoc test for pairwise comparisons using Sigmaplot Version 11.2 (Systat Software Inc., USA). A p-value of 0.05 or less was considered statistically significant ($p \leq 0.05$). The strength and direction of linear relationships between material parameters was determined using the Pearson product moment correlation coefficient (r), while the coefficient of determination (r^2) was utilised to indicate the degree of linear association between factors. A strong positive correlation is considered to exist if the r is between 0.7 and 1 (Taylor, 1990). Error bars indicate standard deviation unless otherwise states.

3.3 Results

3.3.1 Study 1: Development of tubular scaffolds

Tubular collagen-elastin scaffolds were successfully fabricated via the custom designed mold. The macrostructure of the freezedried tubular scaffolds was comparable to the scaffolds produced in flat trays (Chapter 2). The scaffolds retained very high porosity and minimal defects were observed in the structures macroscopically. The fabrication process proved to be highly repeatable and reliable wall thicknesses were achieved. The tubular scaffolds displayed excellent pore interconnectivity and a homogenous pore structure. The custom mold allowed the fabrication of tubular scaffolds of lengths up to 65mm and variable wall thicknesses. Further control over the pore structure was examined by altering the freezing rate.

3.3.1.1 Effect of freezing rate on tubular scaffold microarchitecture

Freezing rate control offers the ability to alter the dynamics of ice crystal nucleation and growth, and consequently affects the final scaffold pore size. The molds were designed and manufactured to enable flash freezing (>50°C/min) via liquid nitrogen (Fig 3.8 A-D) or slow and controlled freezing (1 °C/min) via the freeze-dryer shelf (Fig 3.8 E-H). Flash freezing resulted in pores averaging 16.2μm ± 4.9μm while controlled freezing resulted in significantly larger pores of average 105.6μm ± 36.0μm ($p<0.001$).

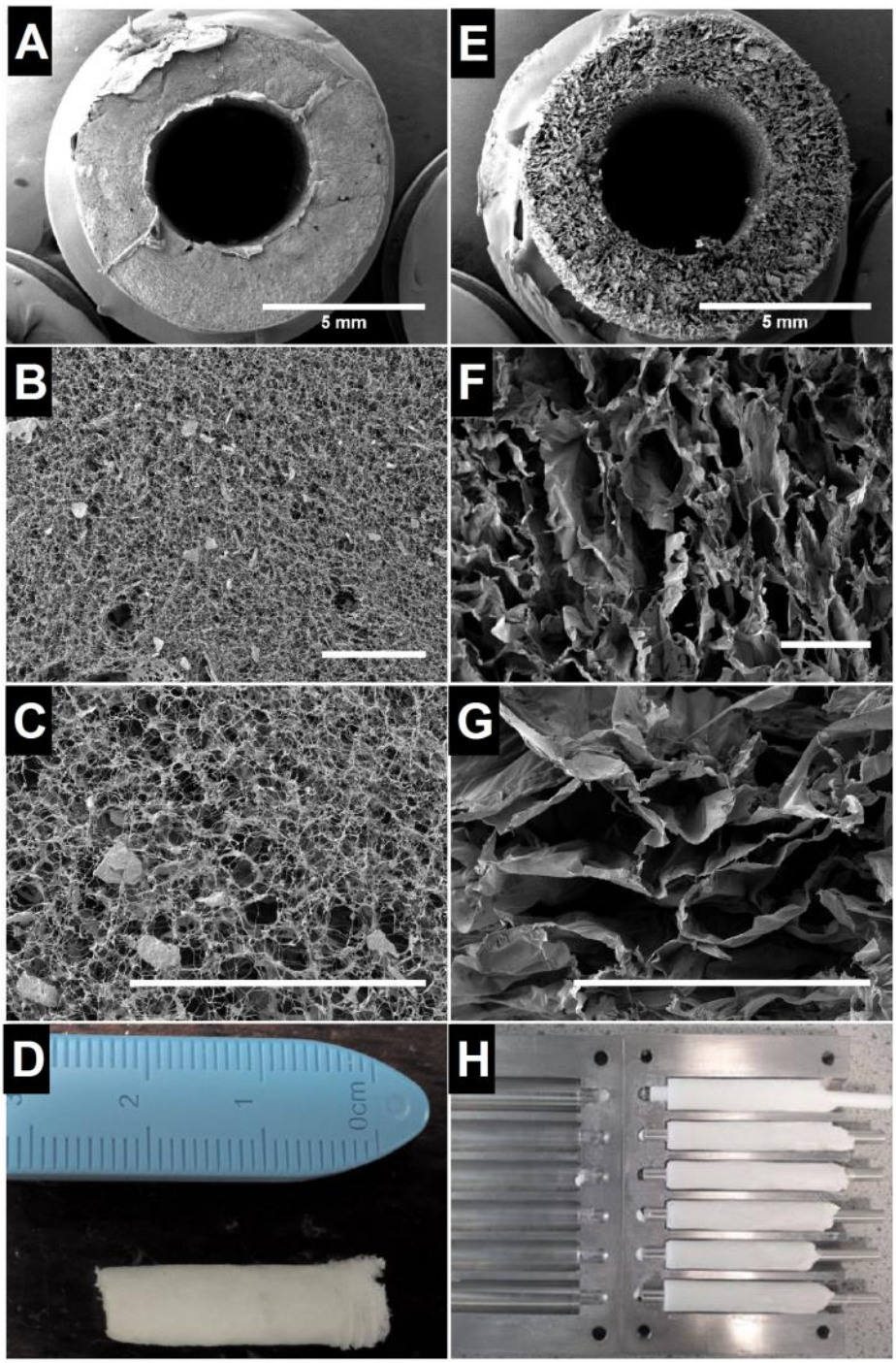

Figure 3.8 Effect of flash freezing or controlled freezing on tubular scaffold microarchitecture

(A-D) Flash freezing the collagen-elastin suspension using liquid nitrogen resulted in a microarchitecture with very small pores (~20εm). Controlled freezing (E-H) at a freezing rate of 1°C/min resulted in an open porous network with relatively large pores (~100εm.) Scale bar 200εm unless otherwise stated.

3.3.2 Study 2: Protein film development with controllable mechanical properties, degradation rates, and inflammation response

In order to create bilayered tubular scaffolds we first examined methods to generate a dense protein film. As the dense film was designed to bear the majority of the mechanical load of the final scaffold, we therefore also investigated the effect of crosslinking to control the mechanical properties, degradation rates, and inflammation response.

3.3.2.1 Fabrication of dense, non-porous protein films

Dense protein films of collagen-elastin were successfully fabricated as shown macroscopically in Fig. 3.9 A (below). The surface (Fig. 3.9 B, D) lacks pores and offered a more suitable surface for endothelial cell monolayer formation than freezedried porous scaffolds. The addition of elastin significantly affected the topography of the films with elastin addition producing films with a rougher surface (Fig. 3.9 B) than the collagen controls (Fig. 3.9 C). The film thickness was determined to be 49.2μm ± 8.5μm (Fig. 3.9 E) with a lamellar fibrous structure which is discernable from the polymer embedded section image (Fig. 3.9 E)

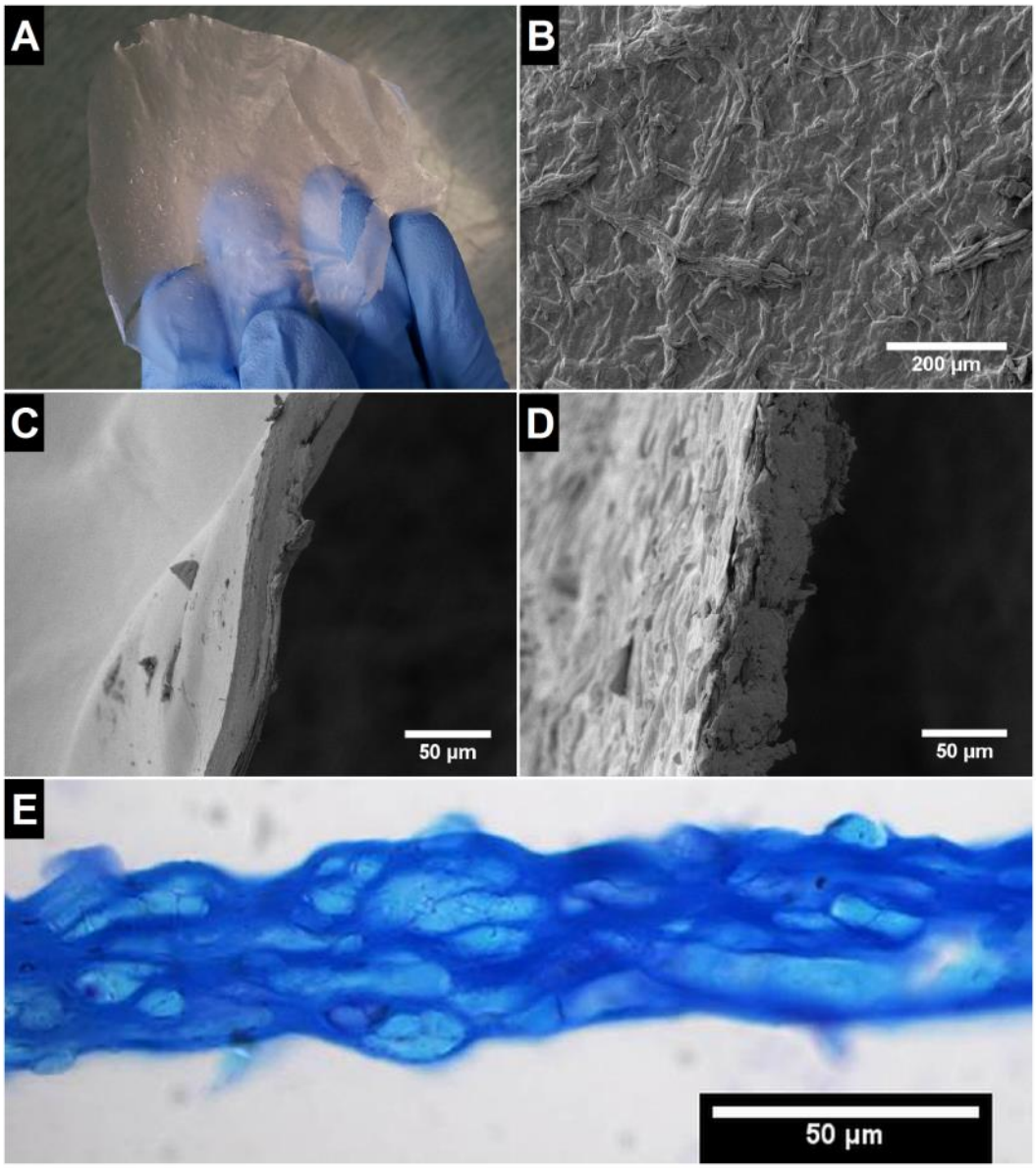

Figure 3.9 Fabrication of dense, non-porous CE100 films.

Macroscopic image of CE100 film (A) and SEM images of a Coll (C) and CE100 (B,D) films. Elastin addition resulted in a rougher topography as observed by the cross-section images of a Coll film (C) and CE100 films (B,D). Sectioned films revealed a lamellar fibrous structure with a mean thickness of 49.2εm ± 8.5εm.

3.3.2.2 Quantification of film crosslinking density

The relative efficiency of each of the crosslinking methods was determining by assessing the amine group content prior to and post crosslinking via TNBS assays. EDAC crosslinking (1.64-fold ± 0.97 fold), and glutaraldehyde (2.99-fold ± 0.65-fold) crosslinking resulted in significantly higher crosslink density than the Non-XL controls ($p<0.01$). DHT (1.05-fold ± 0.05 fold),

Riboflavin/UV (1.23-fold ± 0.14 fold) and mTGase (1.13-fold ± 0.22 fold) also displayed increased crosslink density although this was non-significant versus the Non-XL controls ($p>0.05$). Additionally, EDAC and glutaraldehyde displayed a higher degree of crosslinking than all other crosslinking groups ($p<0.05$).

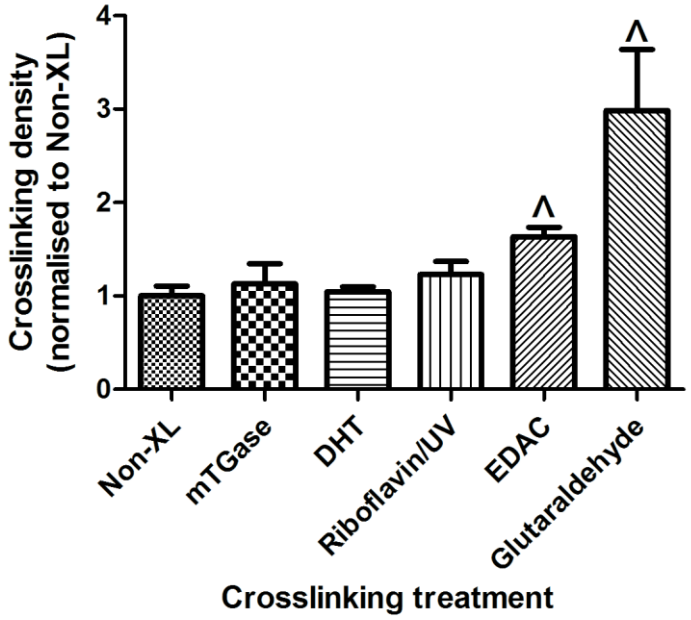

Figure 3.10 Characterisation of degree of crosslinking efficiency

Crosslinking had a significant effect on crosslinking density ($p<0.0001$, 1-way ANOVA). EDAC and glutaraldehyde crosslinking resulted in a significantly higher degree of crosslinking than the Non-XL controls ($p<0.01$). EDAC and glutaraldehyde crosslinking density was also significantly higher than all other groups ($p<0.05$). ^ indicates $p<0.05$ versus all other groups.

3.3.2.3 Effect of crosslinking on film enzymatic degradation resistance

Estimation of the *in vivo* degradation rate was achieved by examining the resistance to collagenase *in vitro*. Crosslinking was found to significantly affect enzymatic degradation resistance ($p<0.05$, 1-way ANOVA). The chemical crosslinkers EDAC and glutaraldehyde resulted in films with the highest degradation resistance, with remaining masses of 89.9% ± 3.45% and 91.0% ± 0.8% respectively, significantly higher than all other groups ($p<0.05$). Physical crosslinking with DHT (68.5% ± 12.9%) resulted in films with significantly higher degradation resistance ($p<0.05$) than riboflavin/UV

(34.2% ± 15.3%). Meanwhile the enzymatic crosslinker mTGase (45.8% ± 3.5%) displayed a similar result to the Non-XL controls (45.7% ± 10.3%).

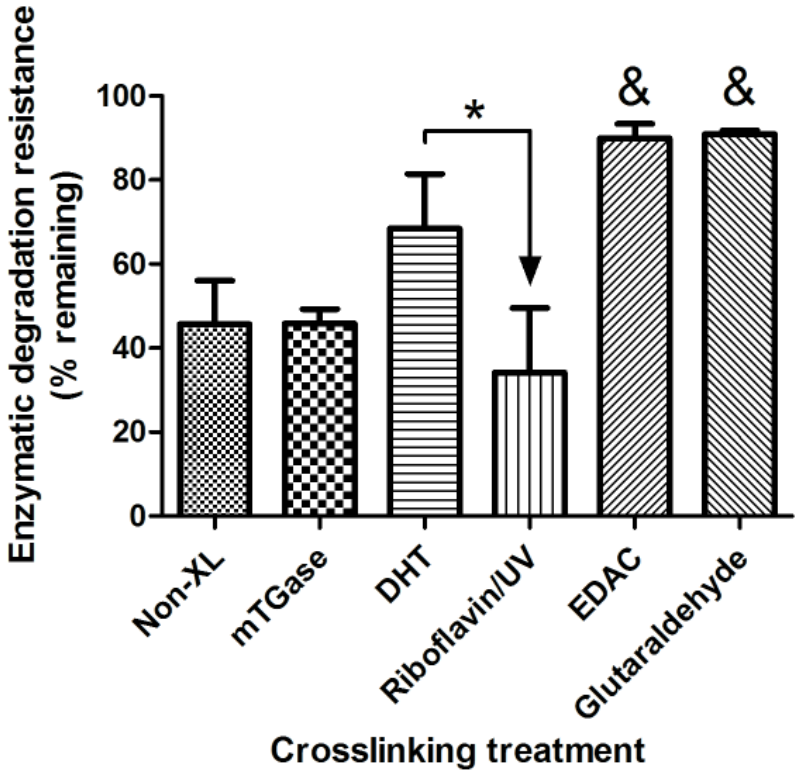

Figure 3.11 Effect of crosslinking on enzymatic degradation resistance

*Crosslinking resulted in a significant effect on enzymatic degradation resistance of CE100 films as determined via 1-way ANOVA ($p<0.05$). Both EDAC and Glutaraldehyde crosslinking resulted in a significant resistance to enzymatic degradation by collagenases, with both of these treatments significantly higher than all other groups ($p<0.05$). Additionally, DHT treatment was found to be significantly more resistant to degradation versus Riboflavin/UV. * indicates $p<0.05$ as indicated. & indicates $p<0.05$ versus Non-XL, mTGase, DHT, Riboflavin/UV, Glutaraldehyde*

3.3.2.4 Effect of crosslinking on film mechanical properties

Crosslinking was found to be a highly effective method to modulate the mechanical properties of the films (Fig. 3.12 A), having Crosslinking a significant effect on the film tensile modulus, failure strain, and ultimate tensile strength (1-way ANOVA, $p<0.05$). Tensile moduli ranged from 0.58 MPa ± 0.11 MPa for the uncrosslinking films (Non-XL) to 39.14 MPa ± 5.67 MPa for the glutaraldehyde crosslinked films, a 67.7-fold increase ($p<0.05$). Furthermore, the tensile modulus could be altered between these values with

a 2.2-fold increase with mTGase, 6.26-fold with DHT, 8.8-fold with riboflavin/UV, and 23.52-fold with EDAC. However, a negative linear correlation (r=0.74) was found between the film tensile modulus and the resulting failure strain, with EDAC and glutaraldehyde displaying significantly lower failure strain than all other groups ($p<0.05$). DHT and riboflavin/UV crosslinking also resulted in reduced failure strain in comparison to the Non-XL controls ($p<0.05$). Failure strain ranged from 44.38 % ± 4.05 % in the Non-XL films to 5.11 % ± 0.50 % for the glutaraldehyde crosslinking films.

Crosslinking also caused a significant change in the ultimate tensile strength (UTS) of the films (1-way ANOVA, $p<0.05$). Riboflavin/UV crosslinking resulted in a 4.2-fold increase ($p<0.05$) in ultimate tensile stress (2.87 MPa ± 1.21 MPa) versus the Non-XL group (0.68 MPa ± 0.21 MPa). No further significant differences in UTS were found for mTGase (2.60 MPa ± 0.99 MPa), DHT (1.12 MPa ± 0.14 MPa), EDAC (1.06 MPa ± 0.55 MPa), or glutaraldehyde (2.18 MPa ± 0.83 MPa). No correlation between UTS and tensile modulus or failure strain was found.

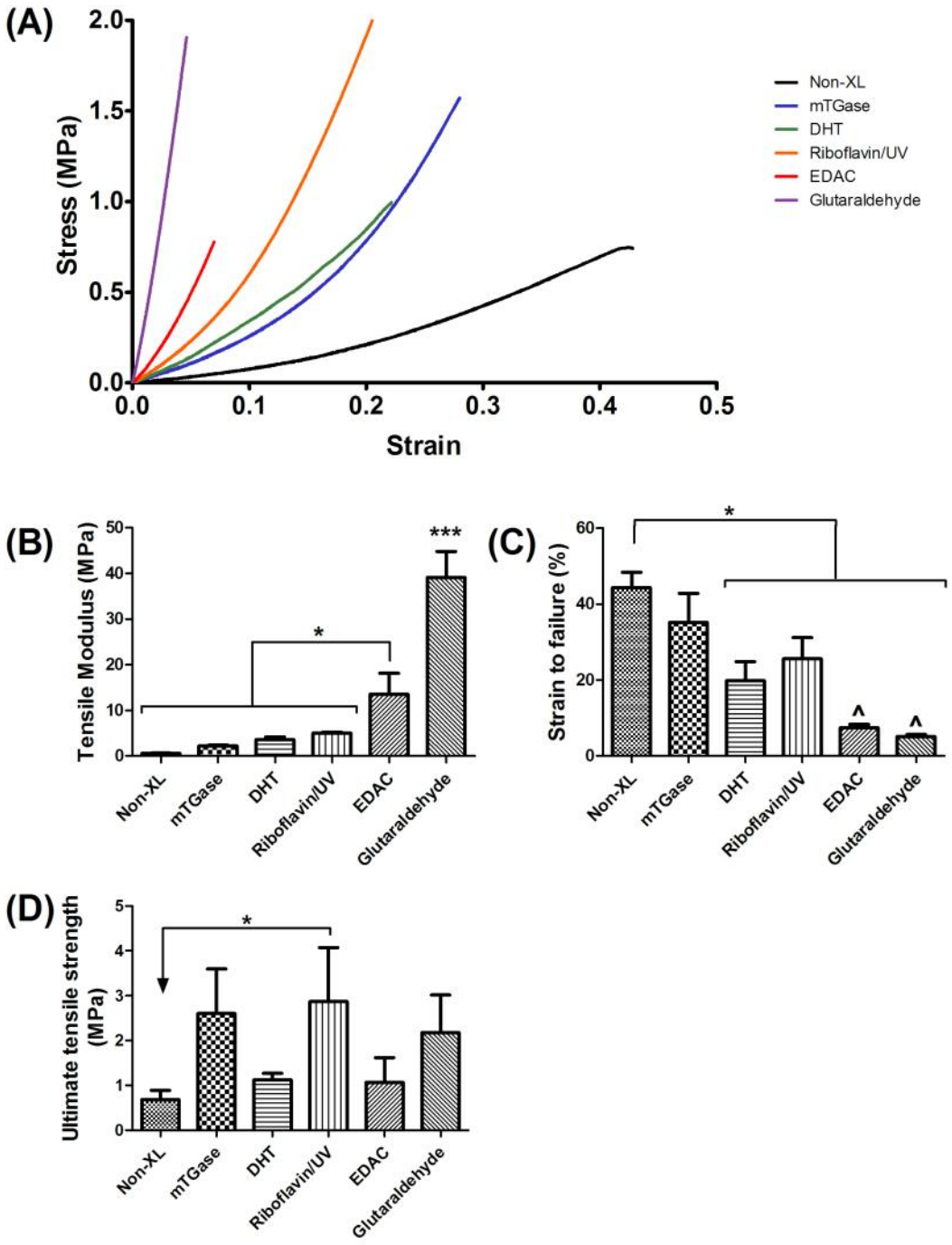

Figure 3.12 Effect of crosslinking on film mechanical properties

*(A) Representative stress-strain curves show the ability to significantly modulate the mechanical response of the CE100 films due to crosslinking. EDAC and glutaraldehyde resulted in significantly higher ($p<0.05$) tensile moduli (B) than all other groups although an inverse relationship with the failure strain (C) was observed ($R^2=0.55$) with EDAC and glutaraldehyde displaying significantly lower failure strains than all other groups ($p<0.05$). Riboflavin/UV had a significantly higher ultimate tensile stress (D) than the non-XL control group ($p<0.05$). * indicates $p<0.05$ as indicated. *** indicates $p<0.05$ versus all other groups.*

Following the assessment of the crosslinking efficiency, enzymatic degradation resistance, and mechanical properties, 3 crosslinking treatments were selected for further examination. EDAC treatment was selected on the basis of excellent crosslinking density, excellent degradation resistance, and high tensile modulus but at the expense of low failure strain & UTS. Riboflavin/UV was also selected on the basic of good crosslinking density, poor degradation resistance, moderate tensile modulus, and excellent failure strain & UTS. DHT was the final crosslinking treatment selected as it provided properties intermediate of that of EDAC and riboflavin/UV.

3.3.2.5 Effect of film crosslinking on film inflammatory response

Assessment of the effect of film crosslinking on the inflammatory response of the films was determined via TNFα release from primary human macrophages. Crosslinking had a significant effect on TNFα release at day 1 ($p<0.001$) (Fig 3.13A) but no effect was observed at day 3 ($p>0.05$) (Fig. 3.13B). Riboflavin/UV crosslinking resulted in the highest inflammatory response at both timepoints, with a 57% increase at day 1 versus Non-XL control ($p<0.05$), although this reduced to a 4.8% increase by day 3. Crosslinking by DHT treatment resulted in a decrease of 15% and 7.6% at days 1 and 3 respectively ($p>0.05$). EDAC crosslinking resulted in the lowest inflammatory response with a 40.3% decrease at day 1 and a 72.5% decrease at day 3 ($p>0.05$). An interesting caveat to note is that the Non-XL CE100 films displayed an increase in TNFα release versus the Non-XL Coll controls, with a 67% increase and 305% increase at days 1 and 3 respectively. However, EDAC crosslinking CE100 films seems to ameliorate this pro-inflammatory response of elastin, with the EDAC crosslinked CE100 films resulting in 16% lower TNFα release than the Non-XL Coll films at day 3.

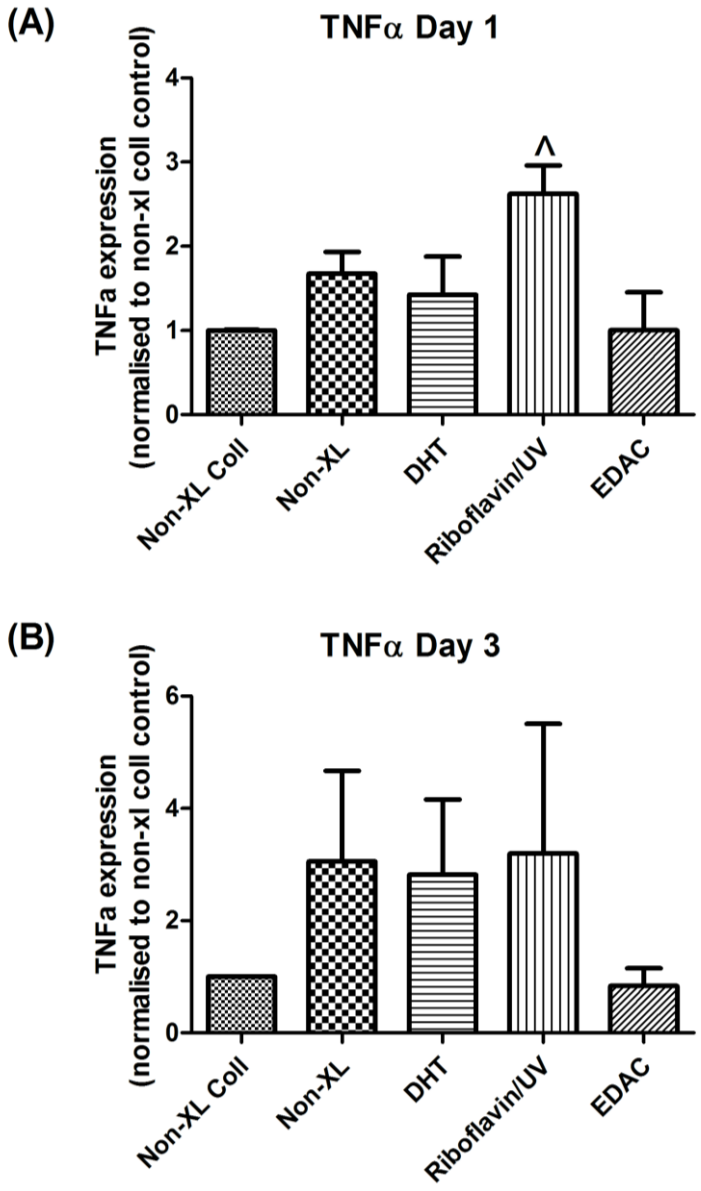

Figure 3.13 Effect of crosslinking on primary macrophage polarisation

Crosslinking of CE100 films was found to have a significant effect (p<0.001) on the expression of the inflammatory cytokine TNFŬ a t d a y 1 (A) , difference was observed at day 3 (B). Riboflavin/UV crosslinking resulted in the highest inflammatory response at day 1 (p<0.05) and day 3 (p>0.05). EDAC crosslinking resulted in the lowest inflammatory response at both timepoints. ^ indicates p<0.05 versus all other groups.

3.3.3 Study 3: Development of bilayered tubular scaffolds with a porous outer layer and dense film layer

Having developed biofabrication methods to generate both tubular porous scaffolds and dense films with controllable properties, we next sought to create a physiologically relevant architecture by incorporate both of these

methods to create bilayered tubular scaffolds. Initial research indicated that the incorporation of the film on the luminal aspect altered the freezing dynamics and resulted in variable microstructures. Consequently, we examined the effect of freezing direction and mandrel material in order to counteract the effect the film layer was having on ice crystal nucleation.

3.3.3.1 Effect of freezing direction on resulting microstructure of bilayered scaffolds

Utilising temperature probes to track the freeze-dryer shelf temperature and mold temperature revealed a temperature gradient was developing when freezing in the vertical direction. This temperature gradient was further exacerbated when a PTFE mandrel was used and resulted in a radial architecture (Fig. 3.14 A, B). By freeze-drying with the mold in the horizontal direction the thermal gradient was greatly reduced which resulted in a more homogenous structure (Fig. 3.14 C, D).

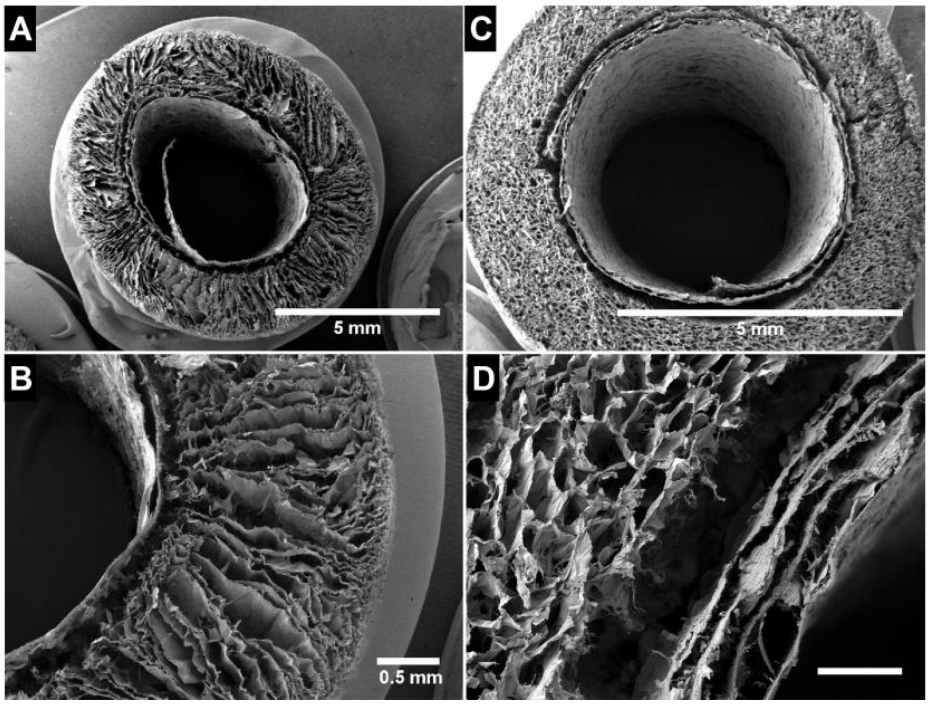

Figure 3.14 Effect of freezing direction on bilayered scaffold microarchitecture

Freezing direction could be controlled to be primarily in the (A, B) vertical direction (parallel to long tubular axis) or (C, D) along the horizontal direction (perpendicular to long tubular axis). The architecture of the bilayered tubular scaffolds is shown with the film lining and porous outer scaffold. Scale bar 200ε m unless otherwise stated.

3.3.3.2 Effect of mandrel material on resulting bilayered scaffold microarchitecture

Utilising the optimal freezing rate (1°C/min) and horizontal freezing, we next sought to assess whether PTFE or stainless steel was the optimal mandrel material as initial results indicated that PTFE mandrels resulted in uneven wall thicknesses. Due to the differences in the thermal conductivity between stainless steel (16 W m^{-1} K^{-1}) and PTFE (0.25 W m^{-1} K^{-1}), it was anticipated that this may have forced ice crystal growth in the circumferential direction although this was not observed (Fig. 3.15 C, D). Macroscopically, it was clear that the PTFE mandrel (Fig. 3.15 A) resulted in separation of the film and outer porous layer. Excellent integration was observed between the layers when a stainless steel mandrel was utilised (Fig. 3.15 B, D, F). While the low coefficient of friction of PTFE allowed easy removal of scaffolds, its low flexural rigidity also often resulted in formation of an eccentric lumen (Fig. 3.15 C) and consequently uneven wall thickness. The optimal mandrel was therefore selected to be stainless steel which facilitated excellent integration of the layers (Fig. 3.15 G) and provided homogenous scaffolds (Fig. 3.15H).

The mean pore size of the final optimal scaffold was found to be 118.4μm ± 22.0μm, significantly larger than the CE100 flat scaffolds produced in Chapter 2 (93.5± 2.9 μm, $p<0.001$), but not significantly different to the initial tubular scaffolds produced in Section 3.1.1 (105.6μm ± 36.0μm, $p>0.05$).Thus, the incorporation of the film layer could be achieved while retaining a good pore architecture which was similar to the single layered scaffolds.

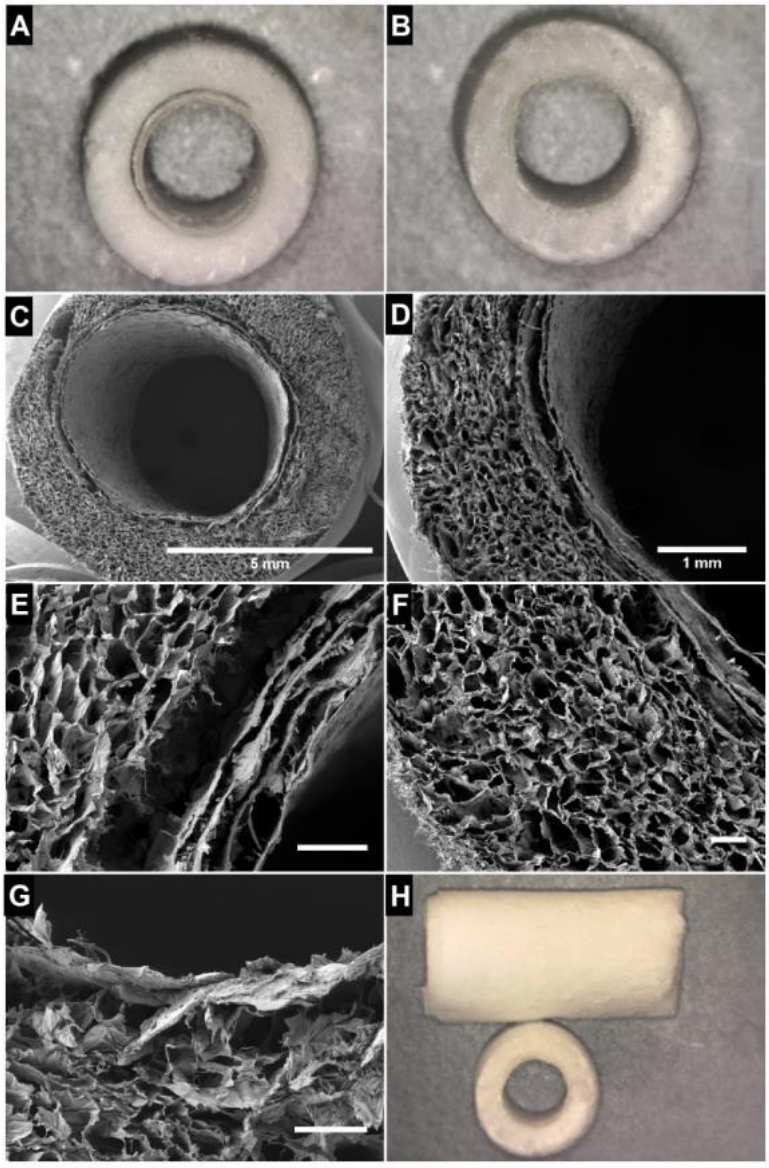

Figure 3.15 Effect of mandrel material on bilayered scaffold microarchitecture

Macroscopic image of bilayered scaffold*s fabricated using horizontal freezing and a PTFE mandrel (A) or a stainless steel mandrel (B). The PTFE mandrel (C, E) has a higher coefficient of thermal expansion than the stainless steel mandrel which resulted in separation of the film and porous layer due to contraction and expansion during the freezedrying cycle. Additionally, the low flexural rigidity of the PTFE mandrel occasionally resulted in an eccentric lumen (C) and consequently a variable wall thickness. The optimal combination of fabrication techniques was to utilise a SS mandrel in the horizontal direction as this produced a* scaffold *with good integration of the layers (D, F, G) and a consistent wall thickness (H). Scale bar 200ε m unless otherwise stated.*

3.3.3.3 Cell seeding, migration, and compaction within tubular scaffolds

Having established the optimal biofabrication methods to create tubular CE100 scaffolds we next seeded hSMCs onto the scaffolds and cultured them for up to 28 days. The static culture rig proved easy to assembly, sterilise, and load the scaffolds onto. Macroscopically the tissue compacted evenly around the mandrel and was easily removed (Fig. 3.16 A). Histologically the vessel walls displayed a uniform thickness and had compacted to a dense organised tissue (Fig. 3.16 B). The initial porous wall thickness had been selected based upon the compaction data observed in Chapter 2 and the wall thickness observed (~500μm) was within the range of normal arteries of this diameter. The method of cell seeding proved to be highly effective as determined with the excellent cell distribution (Fig. 3.16 C) throughout the wall.

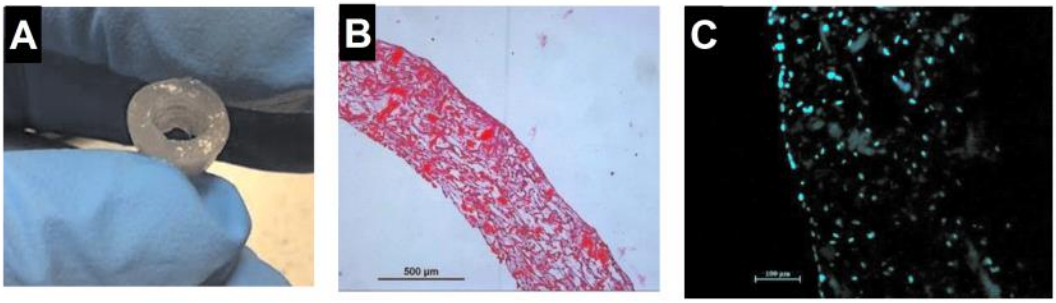

Figure 3.16 Initial cell seeding on tubular scaffolds

Scaffolds compacted over time in culture to produce a dense, homogenous tissue (A) with H&E straining revealing a uniform wall thickness (B) and cell infiltration throughout the wall (C) visualised with blue DAPI fluorescent imaging.

3.4 Discussion

The overall objective of this chapter was to develop bilayered tubular scaffolds suitable for use as a TEVG. Initially we examined methods to modify the optimal collagen-elastin biomaterial developed in Chapter 2 (CE100) into a physiologically relevant tubular architecture using a custom designed mold (Study 1). As arteries are natively composed of multiple layers, we next developed a fabrication method to generate dense CE100 films with controllable properties through crosslinking (Study 2). Combining

these two fabrication techniques allowed the generation of a bilayered tubular scaffold (Study 3). The results of this study has allowed the development of a bilayered scaffold in which the microstructure of the porous outer layer can be tailored by altering the pore direction and size through alterations in freezing rate, direction, and mold materials. Furthermore, we have shown that through crosslinking we can control the film properties including the residual amine content, degradation resistance, mechanical properties, and inflammatory cytokine expression. Taken together, the novel biofabrication methodology developed has led to the development of a biomimetic bilayered scaffold highly suitable for use as a tissue engineered vascular graft.

Tubular porous collagen-elastin scaffolds were successfully fabricated using the custom designed mold (Fig. 3.8). Further control over the pore structure was shown by altering the freezing rate. Controlled freezing (1°C/min) resulted in a homogenous pore structure within the ideal range for the culture of SMCs (105.6μm ± 36.0μm) while flash freezing resulted in significantly smaller pores (16.2μm ± 4.9μm, $p<0.05$). Consequently, controlled freezing was determined to be more suitable for the intended application. The custom mold allowed the fabrication of tubular scaffolds of varying diameters and at lengths of up to 65mm. The process proved to be highly repeatable and the tubular scaffolds were easily removed from the mandrels. Utilising this mold we next sought to develop a suitable luminal lining in order to create bilayered tubular scaffolds.

Dense films were successfully fabricated and crosslinking was examined to allow control over both the biological and mechanical properties of the films independently of the architecture or density. Initially, the degree of crosslinking was determined by analysing the residual amine content for each treatment type (Fig. 3.10). The chemical crosslinkers, EDAC and glutaraldehyde, resulted in the highest crosslink densities with a 1.64-fold and 2.99-fold increase versus the Non-XL controls respectively. This increased crosslink density resulted in these groups also displayed the highest resistant to enzymatic degradation, losing 10.1% and 9% of their

mass respectively (Fig. 3.11). However, while the susceptibility of collagen to enzymatic degradation via collagenases is primarily determined by the type and density of crosslinks formed, consideration must also be shown to the levels of denaturation and the accessibility to cleavage sites (Charulatha and Rajaram, 2003; Zeeman, 1998). This complex relationship can be seen in the DHT crosslinked films which had a similar crosslinking density to the control, yet which were far more resistant to enzymatic degradation. Conversely, riboflavin/UV crosslinking were found to have a 1.23-fold higher crosslink density than the controls, yet displayed less enzymatic degradation resistance than the controls. It is known that DHT and UV-based crosslinking methods result in a portion of the proteins to undergo denaturation simultaneous to the formation of crosslinks, with many researchers seeking to create the optimal balance between crosslink density while minimising the denaturation levels (Gorham et al., 1992; Haugh et al., 2009). It is therefore hypothesized that riboflavin/UV crosslinking results in high levels of denaturation due to the effects of the prolonged exposure to UV (Nishad Fathima et al., 2007; Sionkowska et al., 2005; Weadock et al., 1996). It is suggested that by utilising a higher irradiance level and shorter time the denaturation levels may be minimised and the resistance to enzymatic degradation may increase (Stylianou et al., 2014). Consequently, the crosslinking treatments with suitable crosslinking density and degradation resistance were deemed to be DHT, EDAC, and glutaraldehyde.

The mechanical properties of the CE100 films could also be tailored using crosslinking (Fig. 3.12). Crosslinking was found to cause large changes in the stiffness of the films with tensile moduli up to 67.7-fold higher observed versus the non-crosslinked controls (Fig. 3.12 A, B). The stress-strain curves for the films were primarily non-linear for the non-xl, DHT, riboflavin/UV, and mTGase crosslinking treatments (Fig. 3.12 A). Films crosslinked with the chemical crosslinker EDAC and glutaraldehyde displayed a more linear stress-stress response and stiffness was markedly increased with tensile moduli 23.5-fold and 67.7-fold higher respectively ($p<0.05$ vs non-xl controls). The ability to tailor the stiffness of the films independently of the microarchitecture or composition is a powerful tool in biofabrication as it

allows the ability to tune biomaterials to match native tissue properties and to control cell response. The tensile stiffness of human and porcine coronary arteries has previously been reported to be approximately 2 MPa and so riboflavin/UV, DHT and mTGase crosslinking resulted in films with stiffness values within the same order of magnitude (Koullias et al., 2005; Loree et al., 1994; Sheridan et al., 2012). The UTS of the collagen-elastin films was also significantly affected by crosslinking (1-way ANOVA, $p<0.05$) (Fig. 3.12 D). Riboflavin/UV crosslinking resulted in a 4-2-fold increase ($p<0.05$) in UTS versus the non-xl controls, while all other crosslinking treatments resulted in non-significant increases ranging from 1-6 fold to 3.2 fold ($p>0.05$). The UTS of human and porcine coronary arteries has previously been reported to be approximately 2 MPa and so all crosslinking methods examined produce films which closely match native vessel strength (Holzapfel et al., 2005; Sheridan et al., 2012; Vorp et al., 2003).

An important aspect of biomaterial design for vascular applications is the ability of the biomaterial to withstand *in vivo* strains (5% to 15%) without failure (Lin et al., 2008; van Andel et al., 2003). The strain to failure of the tensile tested films was significantly decreased by all crosslinking methods ($p<0.05$) versus non-crosslinked films, with the exception of mTGase ($p>0.05$) (Fig. 3.12 C). Glutaraldehyde and EDAC crosslinking treatments resulted in low failure strains (< 8%) and the failure was observed to be a brittle failure rather than the ductile failure usually observed with biological materials. However, it has been shown that the mechanical properties of EDAC crosslinked collagen scaffolds alters over time when cultured with cells and also when simply stored in aqueous environments at 37°C without cells (Grover et al., 2012). Consequent determination of the mechanical properties of EDAC crosslinked films which were stored in PBS for 7 days at 37°C revealed that it ameliorated the brittle failure initially observed, with failure strains improving to 21.57% ±1.98% (data not shown). It is suggested that this change is due to the formation of ester bonds during EDAC crosslinking which were subsequently hydrolysed (Everaerts et al., 2008). Thus, in order to utilise EDAC crosslinking for tissues which will be subjected

to high strains it is suggested that pre-storage or pre-culture for a minimum of 7 days is recommended.

The host-macrophage response to ECM materials is a complex process not fully understood but is known to be partially dictated by the specific proteins/biomolecules present, sterilisation technique, residual DNA material, degradation products/rate, and crosslinking treatment. To this end, we have examined the effect of crosslinking on primary human macrophage expression of the pro-inflammatory cytokine TNFα as a marker for the M1 macrophage phenotype (Fig. 3.13). Crosslinking significantly affected ($p<0.001$) the TNFα expression at day 1 ($p<0.05$), with riboflavin/UV crosslinking resulting in a significant increase in the release of TNFα ($p<0.05$) while EDAC crosslinking resulted in the decrease in expression. By day 3 the same trend was observed although the result was non-significant. Thus, we can conclude that riboflavin/UV crosslinking results in increased inflammatory cytokine expression from macrophages while EDAC crosslinking masks some of the negative immunogenic response. The release of pro-inflammatory cytokines has previously been reported to be reduced by EDAC crosslinking which corroborates well with our results (McDade et al., 2013). Crosslinking with riboflavin/UV is an emerging technique within the field of tissue engineering (Tirella et al., 2012) and we believe this is the first study to examine the immune response to this method. It has been suggested that crosslinking density affects protein immunogenicity by shielding or modifying major antigenic sites (Lynn et al., 2004; Yahyouche et al., 2011). Comparing the crosslinking density and TNFα expression we found that no relationship at day 1 ($r=0.34$) but by day 3 there exists a strong correlation between crosslinking density and TNFα expression ($r=0.88$). These results add to the growing body of literature which suggests that the potential immunogenic response is not dictated solely by crosslinking density or immunogenic site masking (Brown et al., 2012). Taken together, EDAC crosslinking produced the most desirable result while DHT treatment was relatively unaltered compared to the controls. Consequently, EDAC and DHT crosslinking were selected for further analysis in Chapter 5.

Utilising the optimal biofabrication methods for the tubular porous scaffolds and dense films, we subsequently developed a physiologically relevant bilayered tubular architecture. Initial results suggested that the freezing dynamics were altered with the addition of the film layer and so optimisation of this process focused on first altering the freezing direction to maintain an isotropic architecture (Fig. 3.14). Utilising a PTFE mandrel in combination with vertical freezing resulted in a primarily radial pore architecture (Fig. 3.14 A, B) as the PTFE's low coefficient of thermal conductivity (0.25 W m-1 K-1) forces the thermal gradient to result in ice crystal growth from the abluminal side towards the lumen side, thus generating a radial architecture (Ma et al., 2010). The presence of the films coating the mandrel exacerbates this issue as the dense film has a lower thermal conductivity than water (0.53 W m-1 K-1 vs 0.6 W m-1 K-1) (Bhattacharya and Mahajan, 2003). By altering the orientation of the mold to the horizontal direction it allowed the formation of a more homogenous pore structure (Fig. 3.14 C, D). Issues with eccentric lumens and poor integration of the film and porous layer became apparent with the use of the PTFE mandrel and were hypothesised to have occurred due to low mandrel flexural rigidity and expansion/contraction during the freezedrying cycle respectively (Fig. 3.15 A, C, E). The optimal scaffolds were fabricated using a horizontally aligned mold, with a film coated stainless steel mandrel, and freezedried at a controlled freezing rate (1°C/min). The final scaffolds (Fig. 3.15 B, D, F-H) displayed good layer integration, uniform wall thickness, and an open homogenous pore structure. The mean pore size was found to be larger (118.4μm ± 22.0μm , $p<0.001$) than the flat scaffolds produced in Chapter 2 (93.5± 2.9 μm), although still within the ideal range for the intended application (Kang et al., 1999; Ross and Tranquillo, 2003). The bilayered design combines the advantages of both the film and the porous scaffolds with the increased mechanical properties of the films, a smooth surface for endothelial monolayer formation and a porous outer layer for smooth muscle cell growth, migration and remodelling. Due to the multi-step fabrication procedure each layer can be differentially modified, thus allowing greater control over the final scaffold properties.

In vitro analysis of the bilayered tubular scaffolds initially focused on validating the method of cell seeding, migration, and compaction on a static culture rig. The static culture rig constrained the scaffolds circumferentially to encourage compaction of the porous layer while maintaining the lumen size. Macroscopically the tissue compacted evenly around the static culture rig to produce a highly desirable dense, compacted tissue (Fig. 3.16 A). The use of contact guidance around mandrels for static culture is well established in the vascular tissue engineering field and has previously been shown to result in superior ECM and cell alignment in the circumferential direction (Barocas et al., 1998; Berglund et al., 2003; Cummings et al., 2003). Histological examination of the scaffolds revealed a uniform wall thickness and the lumen size (5 mm diameter) was maintained throughout the culture period (Fig. 3.16 B). The cell-seeded porous layer compacted effectively around the mandrel and the final wall thickness (~500μm) was within the normal range for small diameter arteries. Attainment of the desired final wall thickness was achieved by utilising the contraction data from Chapter 2 which dictated that an initial wall thickness of 2.5 mm would be compacted to <1000μm after 14 days culture. SMCs were found to have infiltrated through the porous layer effectively and excellent cell distribution was observed (Fig. 3.16C). Previous research utilising acellular collagen luminal supports, similar to the films developed, resulted in a 120-fold increase in ultimate stress and burst pressures up to 600 mmHg (Berglund et al., 2003). Koens et al. (2010) have reported a triple layered collagen/elastin vascular graft which displayed excellent blood compatibility and suitable burst pressures (~400 mmHg) to be utilised as a vascular graft although they did not examine the cellular response or viscoelastic characteristics of the biomaterial. Therefore, the biomimetic bilayered scaffold described represents a promising platform for further examination.

A major limitation of natural polymer vascular grafts is often their inadequate mechanical properties for the challenging haemodynamic system. These limitations range from insufficient strength to deal with the high pressure vascular system, to a compliance mismatch and insufficient suture retention strength (Grassl et al., 2003; L'Heureux et al., 1998; Seliktar et al., 2003a;

Tiwari et al., 2002). We have attempted to address a number of these issues via altering composition, architecture, and crosslinking to strive to match native vessel properties. While we have shown that crosslinking is an effective method to modify the mechanical response of biomaterials, it can also result in an alteration of the material stress-strain behaviour to a purely linear relationship, such as with glutaraldehyde crosslinking. A hallmark of the mechanical response of many native biological tissues is their non-linear stress-strain response where the characteristic J-shaped stress-strain curve allows biological materials to facilitate large extensions for low applied stress (Holzapfel et al., 2005). As the failure point approaches the material gets stiffer and can absorb a large amount of energy, giving rise to the extraordinary toughness of native tissues (Chu et al., 2013; Shahmansouri et al., 2015). Further work on optimising the crosslinking treatments to maintain this non-linear behaviour may be needed. The crosslinking treatments dehydrothermal, riboflavin/ultraviolet and microbial transglutaminase all target at least one unique amino acid residue of collagen (Table. 3.1) and thus theoretically may be combined to enhance their effects. Another interesting biomaterial fabrication strategy to match this non-linear response and/or enable controlled stress transfer are knitted/woven biomaterials, such as woven synthetic polymers combined with biological materials, although this is beyond the scope of this thesis (Heim and Gupta, 2009; Longchamp et al., 2014; Tschoeke et al., 2009; Yeoman et al., 2010).

Table 3.1 Potential target amino acid residues to enable cumulative crosslinking (Adapted from Weadock et al., 1983).

		Reactive residues per alpha chain	
Treatment	Reactive Residues	α 1	α 2
mTGase	Glutamic acid	77	71
	Lysine	32	21
UV	Tyrosine	4	3
	Phenylalanine	12	16
DHT	Aspartic acid	45	47
	Hydroxylysine	10	11

3.5 Conclusion

In this study, we have developed a novel natural polymer bilayered tubular scaffold with highly controllable properties for use as a tissue engineered vascular graft. Porous tubular scaffolds with a suitable microarchitecture were initially developed through controlled freezing (1°C/min) in a custom designed mold (Study 1). Dense collagen-elastin films were next developed, and crosslinking was utilised to modulate the residual amine content, mechanical properties, degradation resistance, and inflammatory cytokine expression from primary human macrophages (Study 2). The optimal crosslinking methods were determined to be DHT and EDAC treatment as they resulted in improved degradation resistance, a suitable range of mechanical properties, and EDAC resulted in a reduced inflammatory response. These two crosslinkers were selected for further examination in Chapter 5. A biomimetic bilayered scaffold was next developed utilising the porous tubular scaffolds and the dense films as a luminal lining (Study 3). Microstructure of the outer porous scaffold section was further optimised by altering the freezing direction and mandrel materials. Following static culture the bilayered scaffold was remodelled into a dense, organised tissue resulting in mechanically robust TEVGs. In summary, this study has resulted in a biomimetic bilayered scaffold which represents a promising platform for further *in vitro* maturation in order to enhance its therapeutic potential and/or application as an *in vitro* testing platform.

Chapter 4: Design and development of a versatile pulsatile bioreactor for culture of small diameter vascular grafts

Note: The work detailed in this chapter was performed as a collaboration with Dr. William S. Sheridan and Dr. Bruce Murphy from Trinity College Dublin.

4.1 Introduction

The *in vitro* generation of functional tissue engineered blood vessels requires a suitable cell-seeded scaffold/construct (Chapters 2 & 3) and the application of appropriate biomechanical and biochemical signals (Niklason et al., 1999; Tschoeke et al., 2009). The appropriate biomechanical signals can be generated by simulating the dynamic physiological environment of native vessels through the use of bioreactor technology (Galie and Stegemann, 2011; Schutte et al., 2010).

Over 20 years ago, pioneering research by Weinberg and Bell (1986) and L'Heureux et al. (1993) demonstrated the possibility of generating tubular vascular models composed of collagen, smooth muscle cells, endothelial cells and fibroblasts in a complex trilayered structure. While encouraging, both of these model systems displayed limited mechanical integrity, inadequate tissue organisation and a lack of vasoactivity. The primary cause of the problems with these early tissue engineered vascular grafts can be attributed to a lack of biomechanical stimuli during *in vitro* maturation of the tissue (Kanda and Matsuda, 1994; Seliktar et al., 2003a). Further research in this area has shown that bioreactor conditioning of cell seeded scaffolds can lead to a contractile smooth muscle cell phenotype and improved cell alignment (Qu et al., 2007; Schutte et al., 2010), increased extracellular matrix deposition (Hahn et al., 2007), a confluent aligned endothelium (Imberti et al., 2002), and mechanical properties closer matching native tissue (Galie and Stegemann, 2011; Niklason et al., 1999; Tschoeke et al., 2009).

However, whilst it is clear that dynamic mechanical stimulation can affect tissue maturation, the optimal method of imparting the complex native biomechanical environment to 3D TEVGs *in vitro* has yet to be elucidated.
Bioreactors are a promising enabling technology which can be utilised to aid in the maturation of tissue engineered vascular grafts. Due to their very specific set of requirements the majority of vascular graft bioreactors are custom built, although recently a small number of commercial systems have

become available, such as Instron's LumeGen. The optimal bioreactor for vascular graft tissue engineering should be capable of recreating the complex cardiovascular biomechanical environment for 3D constructs/vessels *in vitro*. Additionally, the bioreactor should be constructed from non-cytotoxic materials which can be easily sterilised via autoclaving or ethanol sterilisation. Moreover, precise control over the flow dynamics and cyclical strain experienced by mounted constructs is necessary in order to accurately emulate both pathophysiological and physiological conditions. The bioreactor must also be highly adjustable and accommodate varying construct diameters and lengths.

A fundamental aspect of bioreactor design is to determine the design requirements and take a top-down approach to design whereby initial design should focus on the overall bioreactor configuration before progressing to design of individual sections of the bioreactor. To this end we have first detailed the design inputs for the configuration/layout, chamber design, and strain monitoring system. In addition the overall design requirements for the bioreactor were identified:

- The ability to manipulate cyclical strain, pulse rate and shear stress.
- Allow the culture of 3 or more constructs at one time.
- Easily sterilisable and non-cytotoxic.
- Easy assembly in a sterile environment.
- Ability to accommodate a large variety of construct diameters and lengths.
- Simple endothelial cell seeding.
- Easy monitoring of constructs during culture.

4.1.1 Objectives

The overall objective of this study was thus to develop a bioreactor system which was capable of recreating the complex cardiovascular biomechanical environment for culturing vascular constructs *in vitro*. The specific aims/design inputs of the study were to develop a system which could apply physiologically relevant: 1) cyclical strain, 2) shear stress/rate and 3) hydrodynamic pressure, while 4) being constructed from non-cytotoxic materials, and 5) retaining a flexible chamber design which permits the mounting of constructs of varying dimensions and facilitates endothelial cell seeding. In line with these design inputs, the specific aims of this study were:

- 1) Design, develop, and fabricate a versatile bioreactor with consideration for the optimally determined layout/configuration, chamber design, and ability to control culture conditions over a wide physiological range.

- 2) Validation of the bioreactor through assessment of the component cytotoxicity, determination of the flow dynamics and development of a cyclic strain measurement system.

4.2 Materials and Methods

4.2.1 Bioreactor Design

4.2.1.1 Configuration/Layout

The primary design consideration for the bioreactor configuration was to create a pulsatile flow bioreactor capable of extended culture of small diameter vascular grafts. To achieve this, a peristaltic pump was utilised to pump cell culture medium from a reservoir via highly compliant silicone tubing though a 3D vascular construct culture chamber before being returned to the same reservoir in a closed loop system. The system was required to fit

inside a standard cell culture incubator and to be maintained at an environment of 5% CO2 and 37°C.

A key requirement of this custom built pulsatile flow bioreactor was the capability to simultaneously culture multiple constructs using the same system. The two methods identified to achieve this requirement are summarised in Fig. 4.1, below. The use of a single channel peristaltic flow loop to drive 3-4 culture chambers (Fig. 4.1A) was initially investigated as the majority of peristaltic pumps are single channel output. The single channel output then splits into multiple channels to apply the cyclical strain and pressure waveforms to the vascular constructs mounted in the culture chambers. The alternative configuration consisted of a multichannel peristaltic pump with independent flow loops for each culture chamber (Fig. 4.1B).

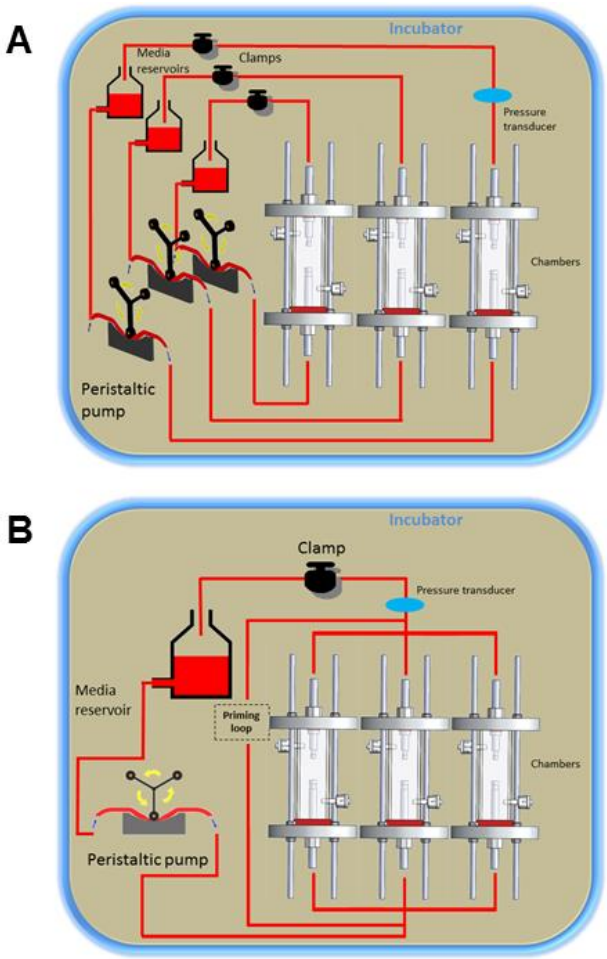

Figure 4.1 Bioreactor Configuration Variants

(A) Single channel closed loop configuration with a common medium reservoir and single channel peristaltic pump. (B) Multi-loop configuration with separate medium reservoirs driven by a multi-channel peristaltic pump.

Platinum cured silicone tubing (I.D 6.4mm, Fisher Scientific, Ireland) was used to connect all components in the system. It displays enhanced biocompatibility versus alternative curing methods such as peroxide. Additionally, silicone exhibits high gas permeability to oxygen and carbon dioxide. The tubing attaches to the culture chamber via a tight interference fit on to a stainless steel tube while all other connections are via tubing connectors.

Each configuration was designed to incorporate a tubing pinch clamp downstream of the culture chamber (Fig. 4.1 A & B). By controlling the degree of occlusion by the pinch clamp it subsequently allowed control over the loop pressure magnitude and the resulting cyclical strain amplitude. A pressure transducer (further detailed in section 4.2.1.3) was connected to the system to measure the pressure while the degree of cyclical strain was determined via video analysis (further detailed in section 4.2.2.3)

4.2.1.2 Chamber design

The culture chamber for the pulsatile bioreactor was designed to house 3D tubular TEVGs which could be subjected to the pulsatile flow and pressure produced by the system. A number of key requirements/design inputs were identified, namely:

- Capability to house 3D tubular vascular constructs of varying length and internal diameter while also being easy to assemble.
- Ability to mount both high strength decellularized vascular constructs and delicate porous scaffolds.
- Non-cytotoxic material construction which also possesses good optical clarity for accurate non-invasive imaging.
- Leak proof construction while also enabling media exchange/sampling and efficient gas exchange.
- Highly flexible design which can be utilised for endothelialisation of vascular constructs on a roller platform at low revolutions to achieve a uniform distribution of cells.

- ¶ Ability to accommodate a silicone sleeve in order to impart only cyclical strain to the overlying vascular constructs.

4.2.1.3 Culture conditions

The culture conditions for the bioreactor system are controlled by the pump pulse frequency, tubing size, reservoir height, and degree of pinch clamp occlusion. During operation the pulse frequency and pressure (through the pinch clamp) can be easily modified without stopping the system, while tubing size and reservoir height are fixed once bioreactor culture begins operation. Consequently, examination of the pulse frequency and pressure allows an accurate assessment of the potential culture conditions the bioreactor can support without modification to the layout.

Pulse frequency

The pulse frequency was controlled via the multichannel peristaltic pump (FH100M, Thermo Scientific). In our current application the pump is utilised to control the flow, pulse frequency and, in combination with suitable tubing and bioreactor layout, also allows control of the pulse waveform. The three roller heads which contact the silicone tubing are offset at 120^{o} apart and thus each revolution of the pump head results in 3 pulses in the system. For calibration and validation the pump was utilised at a speed of 20 rpm which corresponds to 60 beats/min and simulates the frequency of the average human heart rate (~60 beats/min=1 Hz). The system is capable of operating between 6bpm and 600bpm which comprehensively covers the range which the native cardiovascular system operates in (40 bpm-200 bpm).

Pressure

Hydrodynamic pressure in the system is monitored via a digital manometer (Digitron 2082P7, Instrument Technology Ltd, Ireland) which is attached downstream of the bioreactor culture chamber. A 3 way luer stopcock is utilised to connect the manometer to the system and is bled to remove any trapped air. The manometer can also perform a logging function to determine the pressure profile over time. The manometer is capable of accurately measuring pressure in the range of 0-1500mmHg (±0.15%). Pressure in the

system is primarily regulated via a pinch valve attached to the silicone tubing downstream of the culture chamber. As the pinch valve is closed it creates a restriction in the tubing thus increasing the pressure upstream to the valve. The mean pressure level in the system can also be altered by raising the media reservoir to create an increased pressure head height although this is limited to within the incubator dimensions.

4.2.2 Analysis of bioreactor cytotoxicity, flow dynamics and cyclic strain

4.2.2.1 Cytotoxicity of bioreactor components

Cytotoxicity testing was performed on all bioreactor components to ensure that the materials used in the construction of the bioreactor could withstand a wide variety of chemicals and sterilisation techniques without leaching of potentially cytotoxic chemicals into the system. The cytotoxicity testing was performed according to ISO 10993-5 Biological evaluation of medical devices – Part 5: Tests for in vitro cytotoxicity. Each material used in the construction of the bioreactor was individually sterilised by ethanol soaking or autoclaving in order to determine the most efficient sterilisation method for that material. Following identification of the ideal sterilisation method for each material, the entire bioreactor system was set up and additional cytotoxicity testing was performed. These tests were performed as extraction tests on all materials which came into contact with tissue culture medium during normal bioreactor operation. All materials were submerged in growth supplemented rat mesenchymal stem cell tissue culture medium (85% DMEM, 10% FBS, 2% Pen/Strep, 1% Glutamax, 1% L-glutamine, 1% Non-essential amino acids) for 24 hours at 37^{o}C with a ratio of surface area to media volume of 6cm^{2}/ml. The following materials were testing:

- Polycarbonate Chamber
- 316L Stainless Steel Holder
- Polycarbonate Plates
- Silicone Seal
- Silicone Tubing

- Fully assembled bioreactor system
- Polyvinyl chloride (positive control)
- Polystyrene (negative control, tissue culture plastic)

Tissue culture plastic (polystyrene) served as the negative control as this is known to be a non-cytotoxic material upon which cells will readily attach and proliferate. Polyvinyl chloride is known to be a cytotoxic material and so this material was chosen as the positive control. The bioreactor system components were first autoclaved, followed by assembly and flushing the system with ethanol and phosphate buffered saline to ensure sterility was achieved.

Metabolic activity

In order to assess cytotoxicity of the materials tested, we performed a MTT assay to measure cell metabolic activity. Metabolic activity of the cells when subjected to extraction media was quantified via an MTT Cell Growth Assay (Millipore ™, Ireland). MTT [3-(4,5-Dimethylthiazol-2-yl)-2,5-diphenyltetrazolium bromide] is a tetrazolium salt which can be solubilised to produce a yellow solution. Dehydrogenase enzymes present within the mitochondria of cells can cleave the tetrazolium ring in MTT to form insoluble formazan which exhibits a purple colour. This reduction of MTT can thus be correlated to the metabolic activity of the cells and can be quantified via spectrophotometry. Reduction of MTT only occurs in metabolically active cells and thus the level of reduction of the salt can be used as a measure of cell viability and cytotoxicity.

The protocol employed is as per the manufacturer's instructions. Briefly, rat mesenchymal stem cells (MSC) were seeded at a density of 4×10^3 per well in a 96-well plate format and cultured for 24 hours using 100µl of supplemented growth media to allow the cells to attach to the plate. Following this initial 24 hour culture the media was replaced with the relevant material extraction test medium and cultured for a further 24 hours. Reduction of the MTT reagent was initiated by adding 10µl of the solution to each well with 90µl of culture medium and incubating for an additional four

hours. As the insoluble purple formazan product settles to the bottom of the well the overlying medium was removed and the formazan crystals were solubilised by adding 100µl of dimethylsulfoxide (DMSO) to each well and thoroughly mixed via pipetting. The samples were prepared in triplicate and the absorbance was measured at 570 nm with a reference wavelength at 480 nm using a spectrophotometer (Wallac Victor2™ 1420 multilabel counter, Perkin Elmer Life Sciences, Waltham, MA, USA). Sample absorbance was then compared to untreated samples which served as 100% metabolic activity control.

Cell number (dsDNA)

In order to assess the quantity of cells remaining following exposure to conditioned media we performed a double stranded DNA assay using an Invitrogen Quant-iT™ PicoGreen dsDNA kit (Biosciences, Dublin, Ireland). Rat mesenchymal stem cells (MSC) were seeded at a density of 2×10^4 per well in a 6-well plate format and cultured for 24 hours using supplemented growth media to allow the cells to attach to the plate. Following this initial 24 hour culture the media was replaced with the relevant extraction test medium and cultured for a further 24 hours. For analysis each well was washed once in sterile phosphate buffered saline and the cells were lysed using 1 mL of 0.2M carbonate buffer with 1% Triton X-100 followed by three freeze-thaw cycles. Cell number was then quantified as per Chapter 2. Sample fluorescence was compared to a standard curve to determine dsDNA quantity and all samples were normalised to untreated samples.

4.2.2.2 Assessment of bioreactor flow dynamics

The bioreactor system has been designed to match the key features of arterial flow, namely; the flow rate, Reynolds number, shear rate, and shear stress. This allows the added functionality of simulating the forces experienced by the endothelium. In order to study the dynamic flow characteristics of the system a number of simplifications are necessary.

- The vascular constructs are assumed to be straight, rigid tubes with a smooth luminal surface and a non-porous wall.

- The flow is assumed to be steady state and entrance effect are neglected are they are deemed to be negligible.

The flow dynamics of the system were studied using supplemented DMEM and multiple flow loops were tested to ensure that similar conditions were experienced in all chambers. The flow rate in the system was primarily controlled by altering the tubing size and/or increasing the pump speed.

Nature of the flow

For the purpose of vascular tissue engineering the optimal flow profile would be of a laminar nature whereas turbulent flow is characteristically found in in areas where atherosclerotic lesions are present or at bifurcations. In order to determine whether the flow was of a laminar or turbulent nature inside the vascular constructs it was necessary to calculate the Reynolds number (Re). Reynolds number is a dimensionless number which quantifies the relationship between inertial and viscous components in a flow system and can be used to estimate whether the flow was of a laminar or turbulent nature via the following formula:

$$Re = \frac{d \cdot \rho \cdot \bar{v}}{\eta}$$

Where d is the internal construct diameter (0.5cm), ρ is the fluid density (1.05g/cm^3), η is the fluid viscosity which is approximately 1 centipoise (1 mPa.s) at 37°C for supplemented tissue culture medium, and $\bar{v}$ is the mean velocity which can be calculated from the experimentally determined flow rate Q (60mls/min) by equation 1, below

$$\bar{v} = \frac{Q}{\pi \cdot r^2}$$

Mean wall shear stress/rate

The levels of shear stress applied on the wall of the vascular constructs by the flow of media through the bioreactor can be determined mathematically. Variations in wall shear stress are known to be important factors in endothelial cell mechanobiology where the shear stress affects cell morphology, alignment, proliferation, and alters gene expression. The mean wall shear stress, τ_{wall} can be calculated using the Hagen-Poiseuille

equation, below, where the requirements of laminar flow of a Newtonian fluid in a rigid tube have been assumed.

$$\tau_{z,z} = \frac{\dot{\gamma}_{z,z}}{\mu}$$

Where r is the internal radius (0.25cm).

For a Newtonian fluid the wall shear stress can then be related to shear rate by the equation, $\tau = \mu \dot{\gamma}$

4.2.2.3 Cyclic strain measurement system

Vascular cell morphology and function is partially dictated by the mechanosensation of the haemodynamic forces, which manifest as shear stress and cyclic strain within the vascular wall. Consequently, cyclical strain is an important biomechanical force to examine when developing tissue engineered vascular grafts. Bioreactor systems which focus on applying physiologically relevant hoop strains (circumferential) are referred to as medial layer simulators. In order to measure the cyclical strain waveform experienced by the mounted vascular constructs a non-invasive videoextensometer tracking system was developed, in collaboration with Mr. Nicholas Hitchins. As the tubing was constricted by the pinch valve there was an increase in the amplitude of the cyclical strain experienced by the mounted specimens (Fig. 4.2A). The cyclical straining of the vascular construct due to the pulsatile flow (Fig. 4.2B) was captured as a video by a USB microscope (Dino-lite, The Netherlands). Once the cyclical strain measurement system was run it required a reference length for calibration, in this case we utilised the 6mm diameter stainless steel tube (Fig. 4.2C). The video frames were automatically thresholded followed by image analysis to determine the changes in construct strain at three points along the vessel (Fig. 4.2D). A custom MATLAB® (MathWorks Inc, MA, USA) script was written to automate the process of cyclical strain measurement and to increase accuracy. Additionally, a corresponding graphical user interface was designed for ease of use. The vascular construct strain was determined across all video frames and the real-time output was graphed as percentage strain over time.

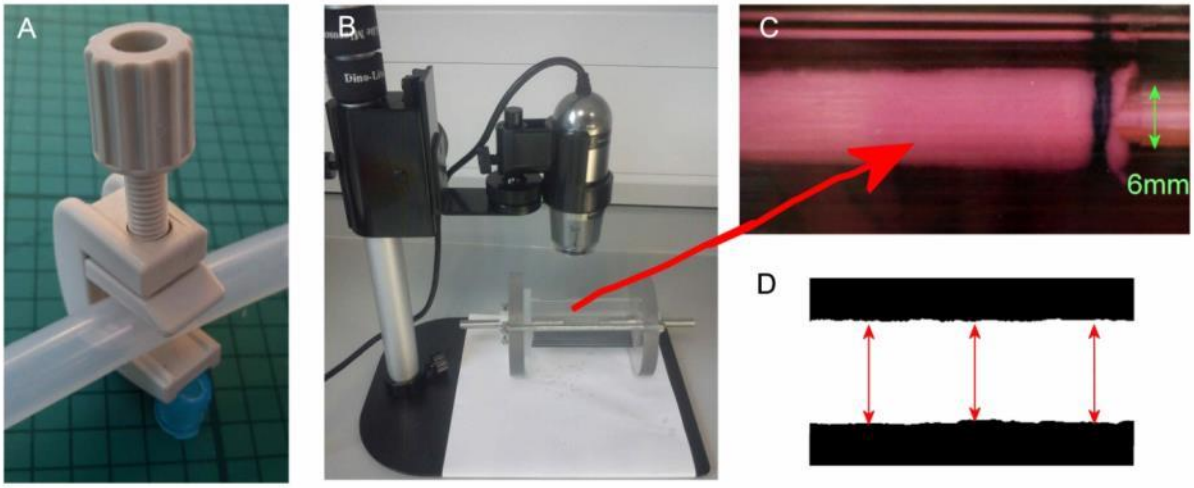

Figure 4.2 Cyclical strain measurement system

(A) A pinch clamp constricts the tubing downstream of the bioreactor chamber. (B) A USB microscope captures video capture of pulsing vascular constructs (C) The captured video was then processed via a custom designed MATLAB® *script and measurements of vascular construct diameter are taken at three points along each frame of the video (D) with the percentage strain then graphed in real time.*

4.3 Results

4.3.1 Bioreactor Design

4.3.1.1 Configuration/Layout

Based upon the design inputs detailed in 4.2.1.1 the configuration was modified until all inputs had been satisfied. Overall bioreactor layout was dictated primarily by the choice of peristaltic pump, with the relative merits of single channel versus multi-channel pumps examined. It was found that utilising a single channel peristaltic pump and subsequently splitting the flow into multiple culture chambers would result in an undesirable drop in the pressure waveform. The single channel closed loop configuration presented many additional challenges for setup as all chambers had to be prepared simultaneously and priming had to be performed on the entire system rather than on an individual flow loop. In the event that multiple time points were to be utilised during bioreactor culture the subsequent flow and pressure waveforms would change drastically in the remaining chambers due to the closed system design. Thus, we opted for a multichannel peristaltic pump

(Fig. 4.3) in order to obtain a system which could easily achieve aseptic operation, minimises contamination risk, and allows the easy assembly and priming of multiple loops.

Figure 4.3 Multi-channel Peristaltic Roller Pump

A multi-channel pump (FH100M, Fisher Scientific) provides pulsatile flow along four large bore tubing channels simultaneously which reduces contamination risk between samples and aids reproducibility.

The use of a multichannel pump also allows the isolation of each vascular construct as well as allowing the operator the ability to culture multiple time point vascular constructs simultaneously under the same conditions. Additionally, the use of multiple cassettes to drive separate flow circuits allows the ability to independently alter the pressure and flow characteristics for each vascular construct chamber. For example, by altering the degree of pinch valve occlusion and/or the use of altered tubing size could be used to alter the pressure profile of a single vascular construct chamber. As each flow loop has a separate pinch valve it is possible to change the pressure in each of the four loops while running off the same pump.

The bioreactor design was successfully constructed with the multichannel peristaltic pump layout presenting many advantages over the single channel pump in terms of assembly simplicity and maintaining sterility of the system (Fig. 4.4). The system was tested beyond normal physiological pressure (>200 mmHg) with all seals functioning correctly and preventing any leaking of medium and maintaining the sterility of the system. The two 0.2μm filters connected to the medium reservoir and culture chamber on each flow loop enabled adequate gas exchange.

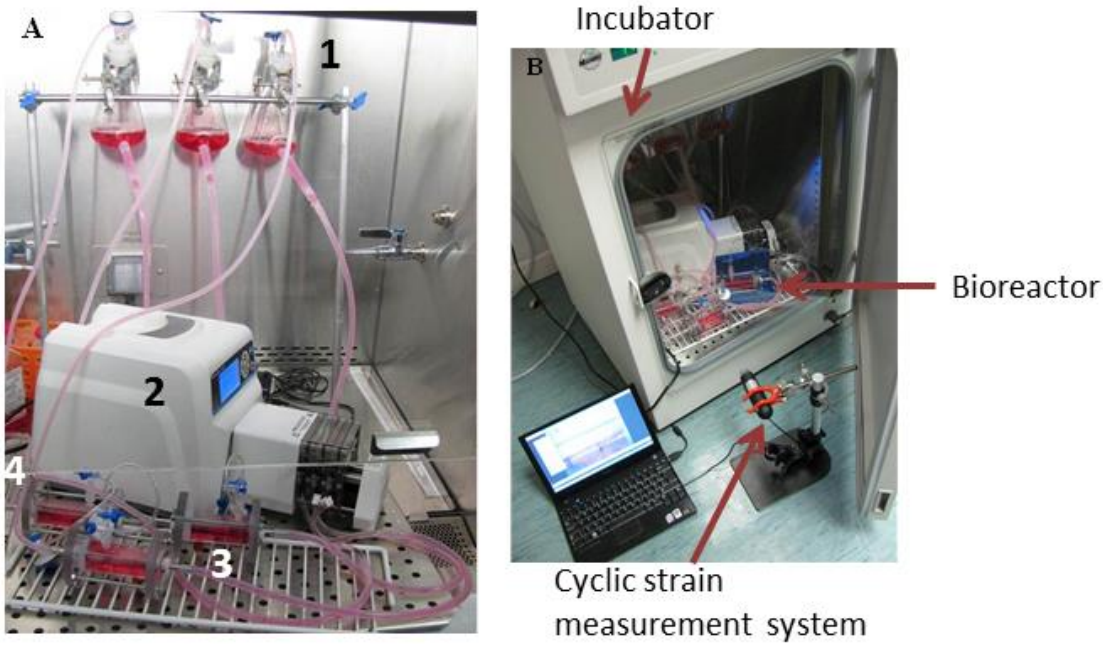

Figure 4.4 Assembled bioreactor system

(A) Entire assembled bioreactor in hood, with (1) media reservoir, (2) peristaltic pump, (3) culture chambers, (4) pinch valves. (B) Bioreactor contained within incubator with cyclical strain measurement system visible outside incubator.

4.3.1.2 Chamber design

A number of design iterations were performed until all the design criteria had been satisfied. A schematic of the final chamber design is shown in Fig. 4.5, below.

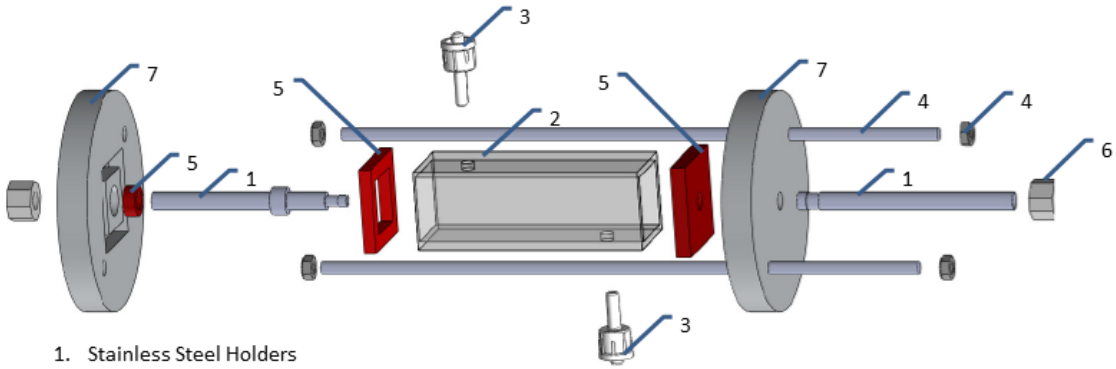

Figure 4.5 Exploded Chamber Design

Individual chamber components shown in an exploded view. Vessels are mounted on to the stainless steel holders (1), maintained in the polycarbonate chamber (2), with luer connectors (3) for media exchange and filter attachment. Threaded bolts and nuts (4) are utilised to guide and maintain compression between the silicone seals (5) and polycarbonate plates (7), with set screw nuts (6) maintaining the desired compression level.

A square polycarbonate tube was utilised to construct the main chamber. Polycarbonate was chosen as it provides excellent optical clarity and the square profile allows undistorted viewing of mounted vascular constructs and allows accurate non-invasive imaging during operation. The method of non-invasive imaging of the vascular constructs is discussed further in Section 4.2.2. Additionally, as the chamber houses the vascular constructs and culture medium it was necessary for the chosen material to be non-cytotoxic and exhibit excellent resistance to chemical attack by both acids and bases, all of which polycarbonate satisfy. Two connectors (female luer locks) are mounted within the chamber walls to allow the connection of a 0.2 micron filter for gas exchange and for medium exchange/sampling. Two custom molded silicone gaskets are compressed between the square culture chamber and two outer circular polycarbonate plates. Compression was

maintained via threaded nuts and bolts which run between the two plates, which ensured a leak proof system.

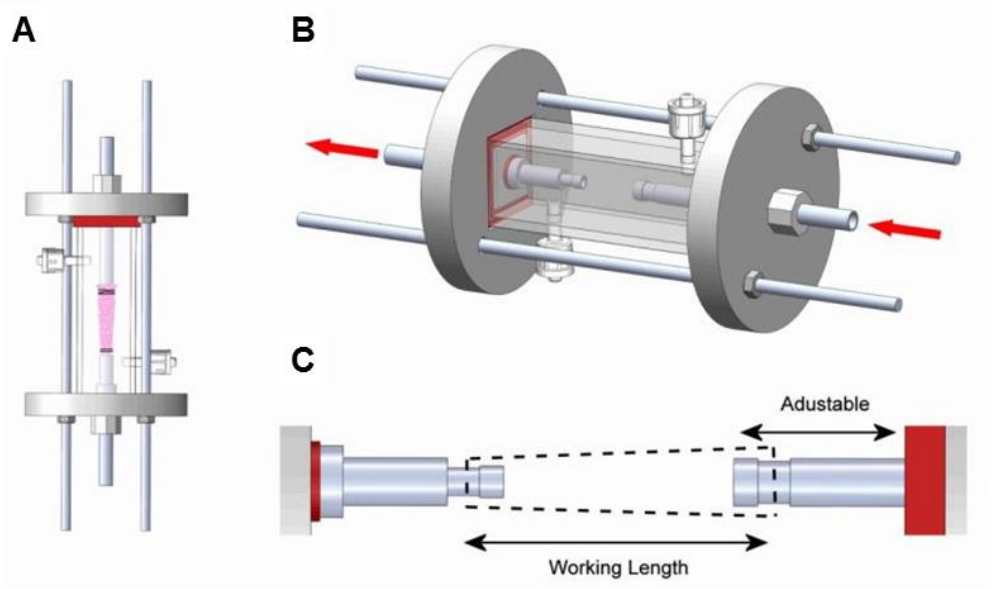

Figure 4.6 Chamber Design

(A) Fully assembled chamber shown with vascular construct sutured on the custom stainless steel holders. (B) Isometric view of the assembled culture chamber showing the direction of medium transfer through the system. (C) The stainless steel holders were designed in a number of sizes in order to accommodate different vascular construct sizes. The ability to adjust the working length was also incorporated into the design with one of the holders having an adjustable length. Additionally, the adjustable holder length can be utilised for applying axial strain.

The stainless steel vascular construct holders are machined to have a ridge over which the vascular constructs can be sutured and maintained. Additionally, the vascular constructs may be secured with biocompatible O-rings such as Viton®. Both sutures and O-rings allowed the ability to securely attach the vascular constructs to the holders without causing damage to the vascular construct. The ability to alter the working length to accommodate different length vascular constructs was achieved by designing one of the specimen holders to have an adjustable length. The adjustable length holder was accomplished by threading the holder though the outer polycarbonate plate followed by threading through the molded silicone gasket which seals the holder in place and prevents any leaks. The distance the specimen holder was threaded through the silicone gasket can be modified which

consequently changes the working length between the two holders. The fixed length specimen holder was similar in design to the adjustable length holder although it contains a flange which seals the holder against the polycarbonate plate with a silicone O-ring. Set screws secure the specimen holder positions against the polycarbonate plates. Multiple sized vascular construct holders were manufactured to enable varying diameter constructs to be utilised within the chamber including the option to mount tapered constructs.

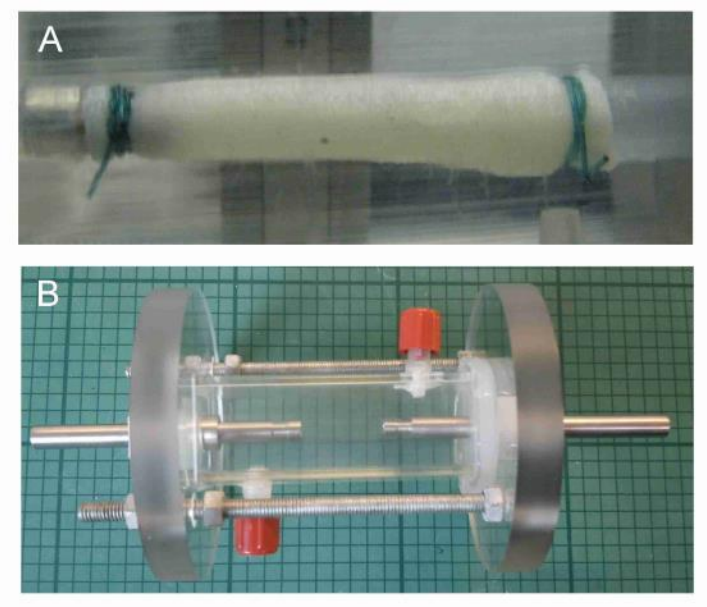

Figure 4.7 Assembled culture chamber

(A) Suture attachment of a decellularized porcine coronary artery which was used as a model artery during calibration and validation of the bioreactor system. The tapered construct shows the versatility of the design to accommodate custom sized constructs. (B) Fully assembled chamber with two luer lock connectors visible (red caps) for connection of gas exchange filters and for media exchange/sampling.

A leak proof chamber for the culture of vascular constructs was successfully designed and constructed (Fig. 4.6). The working length could be successfully altered to accommodate various vascular construct lengths and the holders could be interchanged to accommodate various diameter constructs including tapered geometries. Decellularized porcine carotid arteries were used as model arteries and were successfully sutured to the stainless steel construct holders with minimal handling and the connection proved leak proof under pressure (Fig. 4.7A). The system proved leak proof

during extended culture periods of up to 14 days and sterility was maintained.

The chamber was designed in a modular fashion whereby the chamber could be utilised for efficient endothelialisation of mounted constructs which satisfied one of the key requirements. Endothelial seeding of vascular grafts generally occurs following a number of weeks culturing within a bioreactor in order to mature the medial layer of the construct. Therefore, the chamber design we have developed has the advantage of the ability to seed endothelial cells within the same chamber with the vascular construct still mounted. This was partially achieved by designing the construct chamber to be easily isolated from the bioreactor system. Due to the circular outer end plates the whole chamber can then to be utilised on a roller platform. An endothelial cell suspension can then be injected within the vascular construct lumen and the entire chamber can be rotated at low speed to achieve a uniform distribution of cells on the lumen surface.

4.3.2 Analysis of bioreactor cytotoxicity, flow dynamics and culture conditions

4.3.2.1 Cytotoxicity of bioreactor components

Extraction tests for cytotoxicity were performed on all materials utilised in the construction of the bioreactor. The results of the extraction tests on MSC metabolic activity and cell number after 24 hours is shown in Fig. 4.8 and Fig. 4.9, below. All materials utilised in the construction of the bioreactor passed the cytotoxicity tests as determined by no significant reductions in metabolic activity or cell proliferation after 24 hours versus the negative control, polystyrene ($p>0.05$). Two-way ANOVA indicated that both sterilisation/disinfection method and material had an overall significant effect on cell proliferation and metabolic activity. Two disinfection/sterilisation methods were examined, namely; autoclaving and ethanol disinfection. Utilising ethanol disinfection resulted in stable metabolic activity and proliferation across all materials tested in comparison to the negative control, polystyrene, and significantly higher than the positive control, PVC ($p<0.001$). Autoclave sterilisation also resulted in stable cell proliferation and metabolic

activity, with all groups significantly higher than the positive control PVC ($p<0.001$). Interestingly, the autoclaved polycarbonate chamber exhibited significantly higher metabolic activity than the negative control, polystyrene ($p<0.05$). These results indicate that both sterilisation/disinfection methods were suitable and all materials displayed good cytocompatibility. Consequently, the fully assembled bioreactor system was subjected to a full assembly and sterilised with each of the methods and extraction tests further confirmed the cytocompatibility of the bioreactor system. The efficacy of the sterilisation/disinfection methods was then confirmed by further culturing until day 3 where no bacterial or fungal infections were observed. Additionally, mycoplasma tests were also performed and results remained negative.

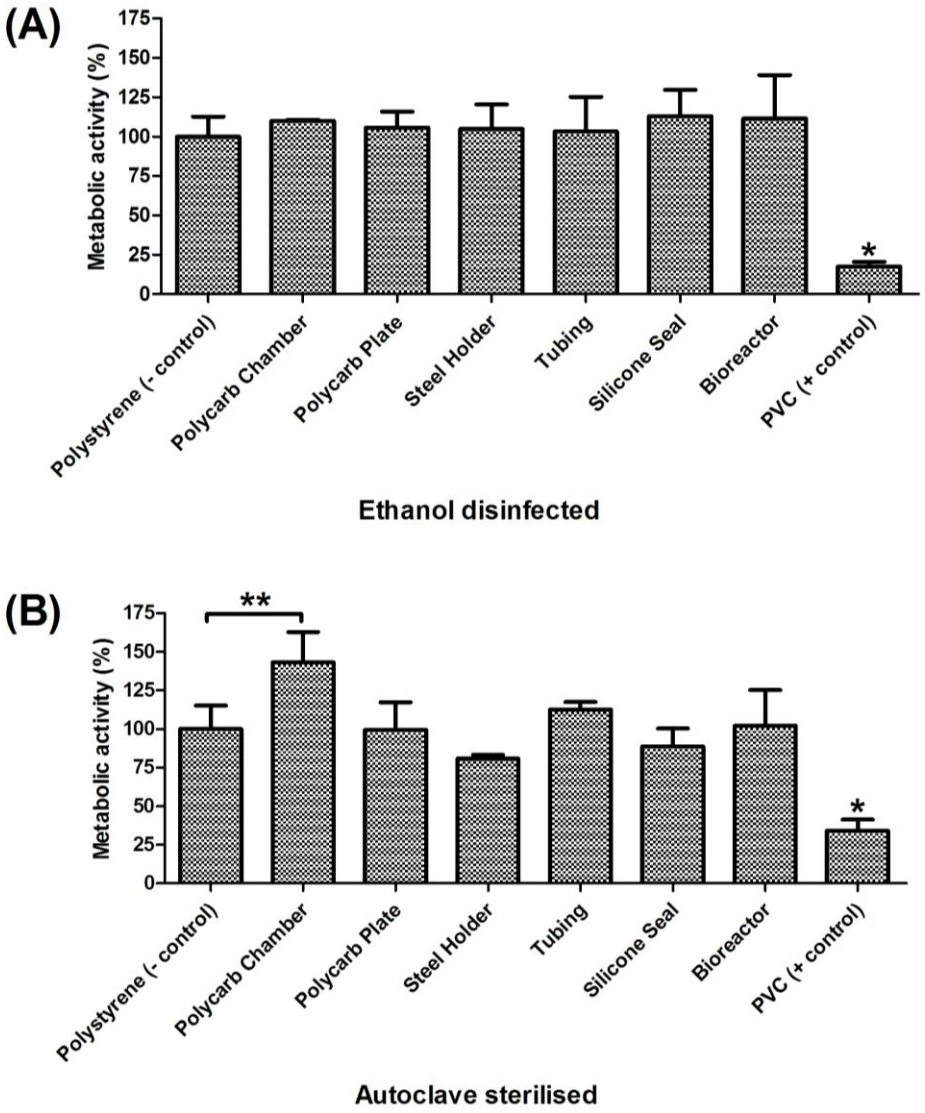

Figure 4.8 Cytotoxicity: The effect of material and sterilisation/disinfection method on the metabolic activity of rat MSCs.

The effect of sterilisation/disinfection method and the bioreactor materials utilised on the metabolic activity of rat MSCs as determined by MTT assays. No significant change ($p>0.05$) in metabolic activity versus the negative control was found when utilising ethanol disinfection (A). Autoclave sterilisation (B) resulted in higher metabolic activity ($p<0.05$ for the polycarbonate chamber versus the negative control but all other bioreactor materials were unaltered ($p>0.05$). All materials displayed significantly higher metabolic activity ($p<0.05$) than the positive control (PVC) when ethanol disinfected or autoclaved. All results are normalised to the negative control, polystyrene, which is expressed as 100% metabolic activity, $*p < 0.05$ vs all other groups, $**p<0.05$ vs indicated interactions.

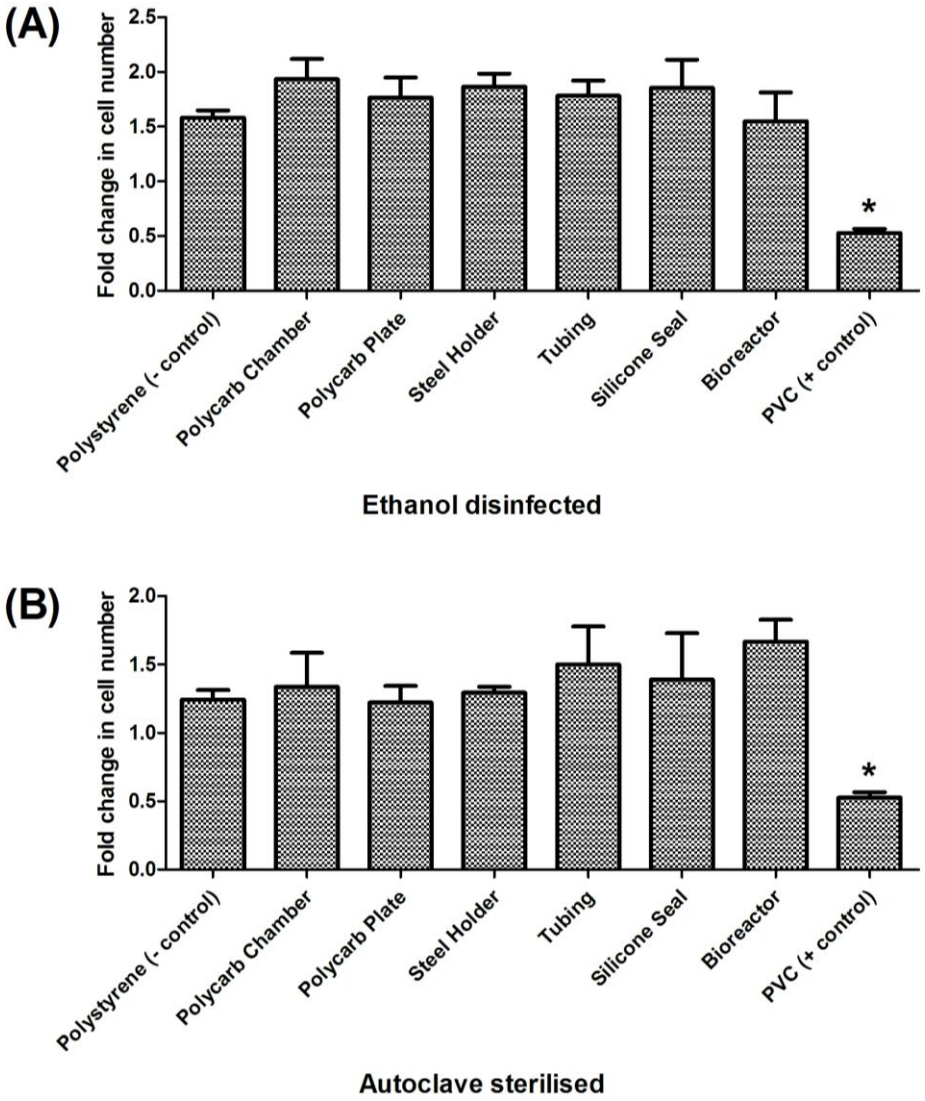

Figure 4.9 Cytotoxicity: The effect of material and sterilisation method on proliferation of rat MSCs.

*The graphs show the effect of sterilisation method and the materials utilised for bioreactor construction on the cell number of rat MSCs as determined by Quant-i TÊ PicoGreen dsDNA assays. No signif versus the negative control utilising either ethanol disinfection (A) or autoclave sterilisation (B) was observed (p>0.05) with the exception of the bioreactor conditioned group which exhibited a significant increase in cell number versus the autoclaved polystyrene control (p<0.05). All materials sterilised by autoclaving displayed significantly higher metabolic activity than the positive control (P<0.05), while no significant change versus the positive control was observed when utilising ethanol sterilisation (p>0.05). *p < 0.05 vs all other groups; **p < 0.05 vs polystyrene*

4.3.2.2 Assessment of bioreactor flow dynamics

At a flow rate of 60mls/min and 60bpm the Reynolds number was calculated to be 160 (Table 4.1). This indicates that the flow was laminar as it is below

the generally accepted threshold of <2100 for fully developed laminar flow. The shear rate within the system was found to be 82 s^{-1} which corresponds to a shear stress of 0.82 dyne/cm^2. As the flow rate can be altered via altering the pulse rate and tubing diameters it is possible to alter the Reynolds number, shear rate and shear stress dynamics of the system. For example, by increasing the pulse rate to 90bpm the flow rate increases to 90mls/min which corresponds to a Reynolds number of 240, a mean shear rate of 122 s^{-1} and mean shear stress of 1.22 dyne/cm^2. As the shear rate and shear stress are both based upon the mean flow rate the maximum and minimum values also vary significantly due to the pulsatile nature of the flow. The bioreactor system produced an average pressure of 50 mm Hg with a systole/diastole amplitude of 30 mm at a reservoir height of 60 cm and 6.4mm diameter tubing. It was possible to further alter the pressure waveform via the pinch valve, altering the reservoir height, and by altering the tubing size.

Table 4.1 Flow dynamics of bioreactor system at varied flow rates

Flow Rate	Pulse Rate	Reynolds number	Shear rate	Shear Stress
60 mls/min	60 bpm	160 (laminar)	82 s^{-1}	0.82 dyne/cm^2
90 mls/min	90 bpm	240 (laminar)	122 s^{-1}	1.22 dyne/cm^2
120 mls/min	120 bpm	320 (laminar)	164 s^{-1}	1.64 dyne/cm^2

4.3.2.3 Cyclical strain measurement system

The video extensometer system proved to be very accurate in the measurement of the applied cyclical strain. The pinch valve could be altered to change the constriction on the tubing which consequently changed the amplitude of the cyclical strain profile to which the construct was being subjected. The system proved to be highly adjustable with cyclical strain ranges of between 1%-20% possible, although at higher strains the pressure exceeded normal physiological values (>200 mmHg). The basal pressure in the system caused the diastolic strain of the construct while the pulsatile pressure waveform generated the systolic strain (Fig. 4.10).

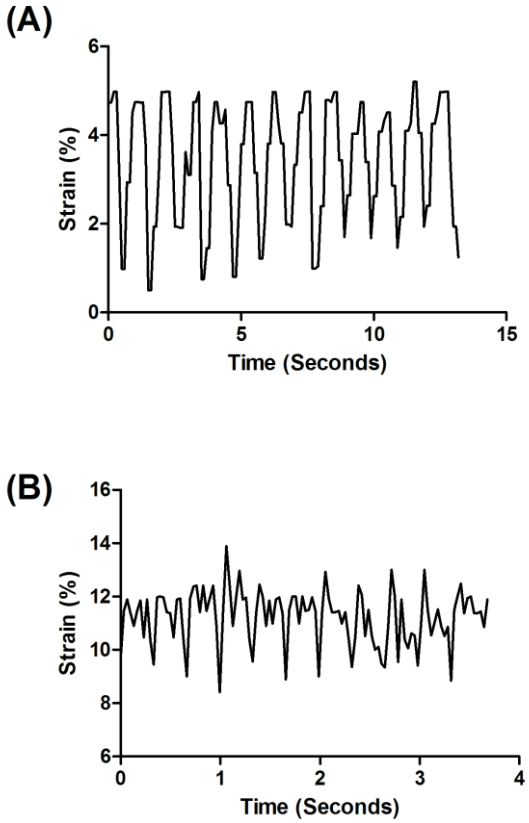

Figure 4.10 Cyclic strain measurement system: Variable bioreactor mean strain, strain amplitude, and beats per minute

The cyclical strain measurement system was used to alter the strain waveform in real time to the desired strain levels. The mean strain, strain amplitude, and beats per minute (BPM) could independently altered by changing the basal pressure, pressure amplitude, and pump rpm respectively. Example graphs showing strains of 3.4% ±1.4% at 60bpm (A), and 11.2% ±1.0% at 180bpm.

4.4 Discussion

The overall goal of this study was to design, build, and validate a novel pulsatile flow bioreactor for the culture of tubular cardiovascular constructs *in vitro*. The study has led to the successful development of a novel bioreactor which is capable of applying the complex cardiovascular biomechanical environment to four independent constructs in a parallel circuit layout. This system described is capable of applying the biomechanical environment experienced by both the medial layer and the endothelium to mounted tubular constructs *in vitro*. The flexible chamber design permits the mounting of constructs of varying dimensions, while we have shown the system to be non-cytotoxic and easy to assemble. The system is capable of applying

physiological relevant levels of pulsatile pressure, cyclical strain, and wall shear rate/stress, and is thus suitable for the *in vitro* maturation of tissue engineered blood vessels/constructs.

The chamber design used in this study included modifications from the design of Lee and Wang (2011) while also applying design elements from Seliktat et al. (2000). It permitted the ability to easily alter the working length and diameter of the holders to accommodate constructs of varying dimensions. The design addresses many of the issues commonly encountered with bioreactor chambers in this field due to the easy assembly process, leak proof design, and ability to be detached from the system for endothelial cell seeding without removing the construct (Avci-Adali et al., 2013). The pulsatile flow of fluid through the bioreactor chamber imparts a cyclical strain on the mounted constructs due to the pressure pulse of the system. While shear stress and strain can be examined via flow dynamics analysis another critical biomechanical force involved in regulating endothelial cell and smooth muscle cell phenotype is cyclical strain. In order to accurately determine the levels of cyclical strain which was being imparted to the mounted constructs, we developed a custom video capture and analysis system in conjunction with Mr. Nicholas Hitchins, a Design Engineer in our lab. A distinct advantage of the cyclical strain measurement system is that the measurement is non-invasive and can be performed while the bioreactor is operating without compromising sterility. This allows the tracking of the cyclical strains experienced by the constructs over the culture period and can be utilised to estimate the Young's modulus of the construct in a non-destructive manner as per Couet and Mantovani (2012). As the system is capable of on-line measurement of a constructs Youngs modulus it could form part of an adaptive flow regime where culture conditions, such as beats per minute, could be automatically controlled in order to maximise the rate at which graft maturation occurs.

One of the primary aims of this study was to develop a bioreactor capable of applying physiological levels of cyclical strain, shear stress and pressure. In the system described, in order to be able to apply both cyclical distension

and physiological flow dynamics the system was designed to distend the mounted construct via the pulsatile pressure waveform travelling through the system. Additionally, this system is capable of applying the cyclical distension indirectly to the construct via distension of a compliant silicone tube over which the construct is mounted, similar to Huang and Niklason (2011). Medial layer simulating bioreactors, such the systems described by Seliktar et al. (2000), and Isenberg and Tranquillo (2003), focus on applying tensile hoop stress and strain which are the primary biomechanical forces experienced by the smooth muscle cells which reside in the medial layer. These medial layer simulators generally apply the cyclical distension required for hoop stress and strain via inflating compliant tubes hydraulically or pneumatically. Medial layer simulators have been shown to lead to improved extracellular matrix deposition, improved cell alignment, and mechanical properties closer matching native tissue (Niklason et al., 1999; Schutte et al., 2010). Endothelial layer bioreactors often neglect tensile hoop stress and strain and focus on applying appropriate shear stress and shear rates While the application of shear stress in these endothelium simulators can be utilised to form a confluent organised endothelium (Imberti et al., 2002), it is the combination of factors which has arguably produced the most promising results (Galie and Stegemann, 2011; Tschoeke et al., 2009). Consequently, the bioreactor described herein has been designed to have the capability to act as a simulating bioreactor for the endothelium, medial layer, or a more physiological relevant combination.

The results of the extraction tests for cytotoxicity indicate that all materials utilised in the construction of the bioreactor were biocompatible and did not elicit a cytotoxic response as determined by no significant reductions in metabolic activity and cell number after 24 hours versus the negative control, polystyrene ($p>0.05$). Additionally, the effect of two sterilisation methods, ethanol soaking and autoclaving, was examined to determine whether it effected the cytotoxicity of the materials utilised in the bioreactors construction. It was found that both ethanol and autoclave sterilisation maintained cell metabolic activity and cell number at the same level as the negative control, polystyrene ($p>0.05$). Increased metabolic activity was

observed in the polycarbonate chamber that was autoclaved versus the negative control ($p<0.05$). It is hypothesised that this may be due to the leaching of Bisphenol-A from the polycarbonate. Bisphenol-A is a monomer used in the production of polycarbonate and has been shown to act as an esterogenic substance which can affect cell proliferation and metabolic activity (Krishnan et al., 1993). However, the polycarbonate plate did not show the same effect although this may be due to the differences in manufacturing as two separate suppliers were utilised for these polycarbonate pieces. Overall, our results indicate that the bioreactor can be sterilised via ethanol soaking or autoclaving with no adverse effects to the inherent cytocompatibility of the materials from which the bioreactor is constructed.

Having determined that the bioreactor could be utilised for the culture of cell seeded constructs and not elicit a cytotoxic response, we next sought to determine the flow dynamics of the system. The bioreactor system was found to be capable of generating intraluminal fluid flow of a laminar nature while applying a shear rate and shear stress within physiological ranges. The Reynolds number for the flow was found to be approximately 160 at 60bpm within the system with this rising to 240 at 90 bpm which indicates that the flow is fully laminar. In human coronary, mesenteric and femoral arteries the Reynolds number ranges from 100-1000 and so the system falls within this physiological range (Caro et al., 1978; Vennemann et al., 2007). Turbulent flow would be undesirable in our bioreactor system as it can lead to very high local shear stresses and may closer match the flow characteristics of a stenosed vessel due to atherosclerosis. Wall shear rate was found to be range between 82 s^{-1} and 122 s^{-1} for 60bpm and 90 bpm respectively. The mean carotid artery shear rate is between 340-475s^{-1} (Samijo et al., 1998) although it ranges from 60-775s^{-1} (Stokholm et al., 2000) due to the pulsatile nature of the flow and so the shear rates in our system tend towards the lower end of this range. However, the mean wall shear rate in our bioreactor system closely matched that of the superficial femoral artery (130s^{-1}) and brachial artery (194s^{-1}) (Wu et al., 2004). Mean wall shear stress ranged from 0.82-1.22 dyne/cm^2 for 60-90bpm respectively. The viscosity of blood

ranges from 3.5cP to 10cP depending on flow conditions and vessel geometries while the viscosity of cell culture medium is approximately 1cP. The lower viscosity medium results in the physiological shear rate of 122 s^{-1} at 90 bpm translating to a low physiological shear stress of 1.22 dyne/cm^2. Mean carotid artery shear stress has been reported to be approximately 10 dyne/cm^2 (Samijo et al., 1998) and so the shear stresses generated by the bioreactor are considered to be low wall shear stresses. Low wall shear stresses are known to be a contributor to atherosclerotic plaque formation via altered endothelial function and phenotype (Malek et al., 1999; Reneman et al., 2006). However, low wall shear stresses (0-4 dyne/cm^2) have also been shown to increase endothelial cell proliferation via a phenotype switch from the normally quiescent atheroprotective phenotype to an atherogenic phenotype (Kaushal et al., 2001; Levesque et al., 1990). Additionally, low wall shear stress has been shown to be an effective method to generate endothelialised tissue engineered vascular grafts due to the increased proliferative nature of the cells followed by an increase in the wall shear stress in order to switch the cells back to a quiescent phenotype (Inoguchi et al., 2007; Kaushal et al., 2001; Ott and Ballermann, 1995). It can be concluded from the flow dynamics analysis that the bioreactor system can be used to apply physiological shear rates and shear stresses to endothelial cells seeded on to the luminal aspect of cultured constructs.

While the bioreactor system is highly adaptable and multiple culture parameters can be adjusted, it is subject to a number of limitations. Although the amplitude of the pressure within the system can be modified via the pinch valves the base pressure cannot be controlled to the same degree. The base pressure is primarily generated due to the pressure head formed by the media reservoirs. By positioning the reservoirs at the highest point of the incubator a base pressure of 50 mm Hg is achievable. In order to obtain a base pressure of 100 mm Hg it would be necessary to arrange the media reservoirs at an additional height of 68 cm. This may be achieved by positioning the media reservoirs in a separate incubator mounted above the culture chamber incubator to gain the additional basal pressure. The pulse amplitude of 30 mm Hg is comparable to the normal physiological pulse

amplitude of 40 mm Hg and can be further altered. A potential disadvantage to the combination endothelium and medial layer biomechanical simulator is that each of the factors is intrinsically linked to the other. For example, if the system was set up to apply 5% radial distension to the cultured construct then the pulsatile pressure of the system must be altered to achieve this. Additionally, the flow rate is directly linked to the pump speed and so to increase or decrease the flow rate the beats per minute must be altered. While this is an inherent limitation present in this design we sought to overcome this limitation by allowing the user the ability to alter the flow rate via the use of altered tubing sizes at the pump and reservoir.

4.5 Conclusion

In this study, we have successfully designed, built, and validated a novel pulsatile flow bioreactor which is capable of applying the complex cardiovascular biomechanical environment to four independent tubular constructs in a parallel circuit layout. The system can be utilised to apply physiological stresses and strains to cell-seeded vascular constructs in order to provide a suitable environment for tissue maturation with the appropriate biomechanical cues. Additionally, the bioreactor system could be utilised to evaluate the performance of medical devices in a physiologically relevant environment. The conclusions from this study can be summarised as follows:

- A bioreactor system has been developed which is capable of recreating the complex cardiovascular biomechanical environment in 3D.
- The novel bioreactor design was shown to incorporate cytocompatible materials, was easy to assemble and could maintain sterility for extended culture periods.
- The novel chamber design permits the ability to alter the working length and diameter to accommodate constructs of varying dimensions.

- The chamber design also allows the ability to remove the chamber and utilise it for rotational endothelial cell seeding on a roller platform without removing the construct.
- The ability to apply physiologically relevant cyclical strain, shear stress and hydrodynamic pressure to mounted constructs.

Chapter 5: Maturation of collagen-elastin based TEVGs: The effect of scaffold architecture, crosslinking, and dynamic conditioning

5.1 Introduction

Maturation of a tissue engineered construct, such as a TEVG, generally refers to the remodelling, compaction, and potential enhancement of the tissue biological and structural properties (Rabkin et al., 2002). ECM-based scaffolds provide structural and mechanical integrity to the developing tissue and should actively support cell adhesion, migration, and normal function (Nishimura et al., 2003). Furthermore, the ECM scaffold should be biodegradable to enable cell-mediated remodelling of the matrix in response to biochemical or biophysical signals. The continuous connection between intracellular cytoskeletal proteins (e.g. filamentous actin) with the surrounding ECM matrix is achieved through transmembrane integrin receptors (Katsumi et al., 2004). Therefore, this facilitates cellular sensing and response to external mechanical stimulation applied to the ECM scaffold. This process is termed mechanotransduction, where mechanical signals are converted to biochemical responses, and is thus intimately associated with the biomaterial from which the scaffold is fabricated (Wang et al., 2009).

So far this thesis has demonstrated the ability to fabricate biomimetic TEVGs which could be crosslinked to alter their degradation rate and also their mechanical properties (Chapters 2/3). Crosslinking is known to affect cell-mediated scaffold degradation and thus affects the rate of remodelling (Yahyouche et al., 2011). Furthermore, the degree of crosslinking has been shown to have drastic effects on scaffold remodelling *in vivo* (Kemp et al., 1995). Positive cell-mediated remodelling occurs when the rate of cell ECM formation is equal to or greater than the rate of ECM degradation (Harley et al., 2004; Lu et al., 2011). This process is particularly pertinent for acellular TEVGs, with must remain stable during the additional time it takes for cells to effectively migrate into and remodel the graft (Huynh et al., 1999). Thus, the influence of the acellular film layer in the TEVGs described in Chapter 3 must be ascertained to determine whether it possesses the required stability to resist proteolytic degradation during culture and remain mechanically robust. Furthermore, the effect of crosslinking on the cell-mediated remodelling of

the porous layer is intimately associated with the resistance of the scaffold to proteolytic degradation.

While the matrix effects on TEVG maturation primarily stem from the physiochemical properties of the biomaterial used, mechanotransduction may also stem from an externally applied force which is transferred through the scaffold matrix to the attached cells (Yang et al., 2002). Dynamic application of force is most often achieved through the use of bioreactors with the primary aims being to condition cells to withstand physiological mechanical conditions and also inducing the cells to remodel the ECM and form functional tissue (Bulick et al., 2009). Bioreactors, such as that described in Chapter 4, have become increasingly complex, and many can exert multiple stimuli simultaneously such as fluid flow, cyclic straining, and complex pressure profiles. Dynamic conditioning of TEVGs has previously been shown to vastly increase ECM production and remodelling (Iwasaki et al., 2008; Syedain et al., 2011a), while also altering cell proliferation (Solan et al., 2003; Yazdani et al., 2009), migration (Sheridan et al., 2014b), and phenotype (Jeong et al., 2005; Stegemann and Nerem, 2003). Bioreactor conditioning exhibits great potential for cardiovascular tissue engineering and it was therefore hypothesised that application of dynamic conditioning would accelerate the rate of tissue maturation of the novel TEVGs described in this thesis.

5.1.1 Objectives

The overall objective of this chapter was to examine the optimal approach to enhance the *in vitro* maturation of collagen-elastin scaffolds to form TEVGs. To achieve this, alterations in construct architecture, crosslinking, and dynamic conditioning on the subsequent bioengineered vessel properties were investigated. The specific aims of this chapter were:

- 1) Examine the effect of construct architecture (single versus bilayered) and crosslinking (DHT versus EDAC) on the maturation of the constructs after 21 days static culture.

- 2) Examine the effect of dynamic conditioning at foetal pulse rates (120bpm) and strain rates (5%±1) within a custom designed bioreactor on the maturation of the constructs after 21 days culture.

5.2 Materials and Methods

5.2.1 Effect of construct architecture and crosslinking on TEVG maturation

In Chapter 3 we demonstrated the ability to create both single layered and bilayered tubular scaffolds suitable for use TEVGs. Modulation of the properties of these TEVGs had been previously examined via crosslinking, with dehydrothermal (DHT) and carbodiimide-based crosslinking (EDAC) deemed to present individual merit for future investigation. Consequently, we next sought to examine the effect of overall TEVG architecture (single layer versus bilayered) and the effect of crosslinking (DHT versus EDAC) on the maturation of the constructs when cultured for up to 21 days.

5.2.1.1 Fabrication of TEVGs and static culture

Both single and bilayered TEVGs were fabricated as per Chapter 3 to be utilising for long term maturation studies. Briefly, a co-suspension of collagen and elastin was blended at a protein ratio of 1:1 in 0.05M acetic acid, with a final protein concentration of 1% w/v. CE100 films were prepared by controlled dehydration of the CE100 suspension on a PTFE substrate before being formed around the tubular mandrel of the mold and re-dried. The CE100 suspension was then pipetted into the remaining cavity in the custom designed mold described in Section 3.2.1, and freeze-dried horizontally to -40^{o}C using a stainless steel mandrel to create bilayered TEVGS. Single layered TEVGs were fabricated utilising the same method with the omission of the film layer. Crosslinking of the constructs was examined by treatment with DHT or EDAC treatment as both treatments were deemed to have merit (Chapter 3). Human smooth muscle cells (hSMCs) were purchased from ATCC (CRL-1999) and cultured using the recommended complete growth media and subculturing procedures as per Chapter 2. Constructs were

mounted on the static constrainment rig (Chapter 3) and seeded at a density of $1.5x10^6$ cells per 10mm construct length. Constructs were cultured for up to 21 days with media changes every 3 days.

5.2.1.2. Assessment of the bioengineered vessel biomechanical properties

The mechanical characterisation of bioengineered vessels and traditional vascular prosthetics primarily focuses on functional tests. Consequently, we analysed the vessel burst pressure, compliance, and suture retention strengths as a measure of vessel strength, elasticity, and suitability for surgical anastomosis respectively.

Assessment of the bioengineered vessel burst pressure

Burst pressure testing was performed using a custom designed device developed according to ISO/ANSI 7198:1998: Cardiovascular Implants – Tubular Vascular Prostheses. Bioengineered vessels, of length 30mm, were removed from culture and hydrated for 1 hour in PBS at 37°C. Vessels were then secured over barbed tubing connectors, secured with sutures, and subjected to a longitudinal strain of 10% to mimic *in vivo* conditions. Vessels were pressurised with PBS until failure at an infusion rate of 40ml/min using a syringe pump (NE-1600, New Era Pump Systems, Farmingdale, NY). Pressure readings were measured with a digital manometer (Digitron 2082P7, Instrument Technology Ltd, Ireland) with a range of 0-1500 mmHg (±0.15%). Burst pressure was defined as the maximum pressure before failure with values reported in mmHg (Note: 100 mmHg = 13.33 kPa).

Assessment of the bioengineered vessel circumferential compliance

Vessel compliance is defined as the ratio change in volume for the vessel for a given pressure change (Eqn. 1). To determine the circumferential compliance of the bioengineered vessels they were sutured over barbed tubing connectors and connected to a closed loop system where pressure could be accurately modified (±2 mm Hg) through control over the pressure head with a syringe pump (NE-1600, New Era Pump Systems, Farmingdale,

NY). Video tracking of vessel diameter was recorded via a USB video microscope (AM7013MT, Dino-Lite, The Netherlands). Image analysis was performed in ImageJ (US National Institutes of Health) by splitting the time stamped video into separate frames, thresholding the images to provide suitable contrast at the vessel edges, and measuring the external diameter at three points along the vessel for each frame. The compliance was determined at static pressure points between 20 mmHg and 40 mmHg and compliance was calculated using the following equation:

$$\text{Compliance} = \frac{D_{40} - D_{20}}{D_{20}} \times \frac{1}{P_{40} - P_{20}} \quad (1)$$

Where:

P_o is the lower pressure value, in mmHg

P_i is the higher pressure value, in mmHg

And r_i is the internal radius which can be calculated from the external diameter measurement (D_o) and vessel wall thickness (t) as follows:

$$r_i = \frac{D_o}{2} - t$$

Assessment of the bioengineered vessel suture retention strength

Suture retention strength was assessed using a tensile testing machine (Z050, Zwick/Roell, Ulm, Germany) and a 4-0 polypropylene suture with a taper point needle (Prolene, Ethicon GmbH, Norderstedt, Germany). The suture was inserted through one wall of the bioengineered vessel at a distance of 2mm from the vessel edge. A 5N load cell was used to measure the force during suture pull out at a crosshead speed of 50mm/min. Suture retention strength was defined as the maximum force experienced during suture pull out and results were recorded in grams-force.

5.2.1.3. Assessment of the bioengineered vessel biological properties

After 21 days in culture, the remodelled bioengineered vessels were washed in PBS and ring shaped sections were cut for analysis of the cell density (DNA quantification) and proportion of collagen in the vessel wall (hydroxyproline quantification).

Assessment of the bioengineered vessel cell density

Ring shaped sections were excised from a minimum of 4 separate vessels per experimental repeat (n=3) for analysis (12 samples per group total). Samples were washed in PBS, weighed, and placed in tubes containing 1mL of lysis buffer (0.2 M carbonate buffer + 1% Triton X). Three freeze-thaw cycles to -80°C were performed to ensure lysis of all cells. DNA content was then quantified using a Quant-iT™ PicoGreen dsDNA kit, as per Section 2.2.4. Results are presented per wet weight of tissue and normalised to the single layer collagen construct (Coll DHT).

Assessment of the bioengineered vessel collagen content.

Assessment of the relative proportion of collagen in the vessels walls was achieved through quantification of the hydroxyproline content of the tissue. Hydroxyproline is an amino acid present primarily in collagen and so may be utilised as a biochemical assay for collagen content (Ignat'eva et al., 2007). Tissue samples were washed in PBS followed by two washed in distilled water before freeze-drying to prepare dry samples for assaying. Collagen was hydrolysed using collagenase from Clostridium histolyticum (C7926 Sigma Blend Type F, Sigma-Aldrich, Dublin, Ireland). Free hydroxyproline was then oxidised through the addition of 0.2 M chloramine-T solution (Sigma-Aldrich, Dublin, Ireland). Finally a colorimetric product was formed by the addition of Ehrlich's reagent (dimethylaminobenzaldehyde in acidified n-proanol). Quantification of the chromophore was performed at 550nm using a spectrophotometer (Wallac Victor2™ 1420 multilabel counter, Perkin Elmer Life Sciences, Waltham, MA, USA) (Reddy and Enwemeka, 1996). A standard curve was prepared using trans-4-hydroxy-Lproline (Sigma-Aldrich, Dublin, Ireland) and conversion to collagen content was determined with a hydroxyproline-to-collagen ratio of 1:7.69 (Ignat'eva et al., 2007).

5.2.1.4. Assessment of the bioengineered vessel morphology

Assessment of the bioengineered vessel structure and collagen orientation

The remodelling of the bioengineered vessel structure was examined via histology. Vessels were formalin fixed, embedded in paraffin and serially sectioned at 8μm transversely, as per Section 2.2.2. General tissue

morphology was examined via haematoxylin and eosin staining which stains nuclei blue/purple and ECM pink. Collagen density and orientation was determined via picrosirius red staining in combination with circularly polarized light (Lattouf et al., 2014; Whittaker et al., 1994). Briefly, picrosirius red was utilised to specifically stain collagen (collagens I and III) to determine the collagen density in the tissue. The orientation of the collagen was then analysed under circularly polarized light of the picrosirius red stained sections, with collagen fibres orientated parallel to the section plane exhibiting enhanced birefringence (Syedain et al., 2011a). The density of the collagen may also be determined via the intensity of the birefringence.

Immunohistochemical assessment of bioengineered vessel structure

The relative expression and location of SMC/vascular specific proteins was determined via immunohistochemistry. Formalin fixed samples were embedded in paraffin and serially sectioned at 8μm. Non-specific binding was blocked by 1% BSA (Bovine Serum Albumin) and cells were permeabilised with 0.1% triton X-100. Antigen retrieval for detection of αSMA and calponin was performed enzymatically with Proteinase K for 15 minutes at 37°. Heat-induced antigen retrieval was utilised for col III by incubating samples for 15 minutes in a 700 W microwave in 0.01M citrate buffer (pH 6) (Koch et al., 2012). Sections were then incubated overnight at 4°C with the following primary antibodies in blocking buffer: Rabbit Anti-smooth muscle actin (anti-αSMA, 1:90 dilution; Sigma-Aldrich, Dublin, Ireland), rabbit Anti-calponin (anti-CNN1, 1:90 dilution; Sigma-Aldrich, Dublin, Ireland), and rabbit anti-collagen III (Anti-COL3A1, 1:80 dilution; Sigma-Aldrich, Dublin, Ireland). Secondary antibody labelling was performed for 1 hour at room temperature with Alexa fluor® 594 goat anti-rabbit IgG (1:800 dilution; Molecular Probes, Leiden, The Netherlands). Samples were mounted with FluoroShield™ with DAPI to counterstain cell nuclei (Sigma-Aldrich, Dublin, Ireland). Negative controls were performed by omitting incubation with primary antibodies. Sections were viewed on an epi-fluorescent microscope (Nikon Eclipse 90i, Nikon, Japan) and digital images were recorded at 10x magnification using the attached control unit connected to a PC and imaging software (Nikon DS

Camera control unit, Nikon, Japan with NIS Elements Basic Research V3.06, Nikon Instruments Europe, The Netherland).

5.2.2 Effect of dynamic conditioning on TEVG maturation

5.2.2.1. Bilayered TEVG fabrication

Having determined the optimal architecture and crosslinking treatment (5.2.1), the TEVG with the most promising characteristics was selected for dynamic conditioning in a custom designed bioreactor (Chapter 4), with the optimal construct being the bilayered CE100 group which was EDAC crosslinked. SMCs were seeded as per sections 5.2.1.1 and the vessel was cultured for 7 days in static conditions prior to the application 14 days of dynamic conditioning.

5.2.2.2 Dynamic conditioning in a custom designed bioreactor

Dynamic biophysical stimulation was applied within the custom-designed bioreactor (Fig. 5.1) which has the capability to generate foetal, physiological, or pathological dynamic mechanical stimulation.

Bilayered CE100 constructs (EDAC crosslinked) were mounted over an underlying silicone support sleeve in order to apply precise cyclical strain across the construct (Niklason et al., 1999; Seliktar et al., 2000) and to minimise the compounding factors involved in the dynamic stimulation of vessels directly in bioreactors e.g. increased fluid permeability, altered pressure to maintain desired strains. Recapitulation of foetal vessel culture conditions was achieved through application of a pulse rate of 120bpm with a mean cyclical strain of 5% and an amplitude of 1% for a period of up to 21 days in order to further enhance the bioengineered vessels promising characteristics. Foetal pulse rates (120bpm) have been shown to result in superior ECM production and higher burst pressures than normal adult pulse rates (Solan et al., 2003). In addition the straining regime was determined to be optimal to enhance cell proliferation while minimising apoptosis (Colombo et al., 2013).

Figure 5.1 Mounting of constructs within the custom designed culture chamber

The bilayered CE100 (EDAC) TEVGs were pre-cultured for 7 days statically prior to mounting within the bioreactor culture chamber. Dynamic stimulation of 5% mean strain (±1%) was applied at a foetal pulse rate (120bpm) for a period of 14 days.

Statistical analysis

Statistical analysis was conducted using one-way or two-way ANOVA followed by Holm-Sidak post hoc test for pairwise comparisons using Sigmaplot Version 11.2 (Systat Software Inc., USA). A P-value of 0.05 or less was considered statistically significant ($p \leq 0.05$).

5.3 Results

5.3.1 Effect of construct architecture and crosslinking on bioengineered vessel maturation

5.3.1.1 Effect of construct architecture and crosslinking on bioengineered vessel biomechanical properties

Biomechanical testing was used to determine the effect of construct architecture (single v bilayer) and crosslinking (DHT v EDAC) on the resulting vessel properties after 21 days static culture (Fig. 5.2). Burst pressure (Fig. 5.2A) was significantly increased in the bilayered CE100 constructs versus the single layered CE100 constructs (1.54-fold, $p<0.05$). EDAC crosslinking further increased the burst pressure by 2.94-fold versus DHT crosslinking in the bilayered constructs (87.5 ± 14.5 mmHg v 29.83 ± 5.0 mmHg, $p<0.05$). Single layer constructs failed below the required pressures for circumferential compliance testing (Fig. 5.2B). Circumferential compliance (Fig. 5.2B) was reduced by 3.45-fold with EDAC crosslinking (0.125 ± 0.02 %/mmHg), to a value closer to native internal thoracic artery (0.115 ± 0.039 %/mmHg) (Konig et al., 2010). Suture retention strength (Fig.5.2C) was increased 4.84-fold ($p<0.05$) in the bilayered CE100 constructs versus the single layer CE100 constructs, and increased a further 27% by EDAC crosslinking ($p<0.05$). The results indicate that the incorporation of the film layer in the bilayered constructs results in significantly improved suture retention strength, burst pressure, and compliance. Crosslinking with EDAC further improved all these properties.

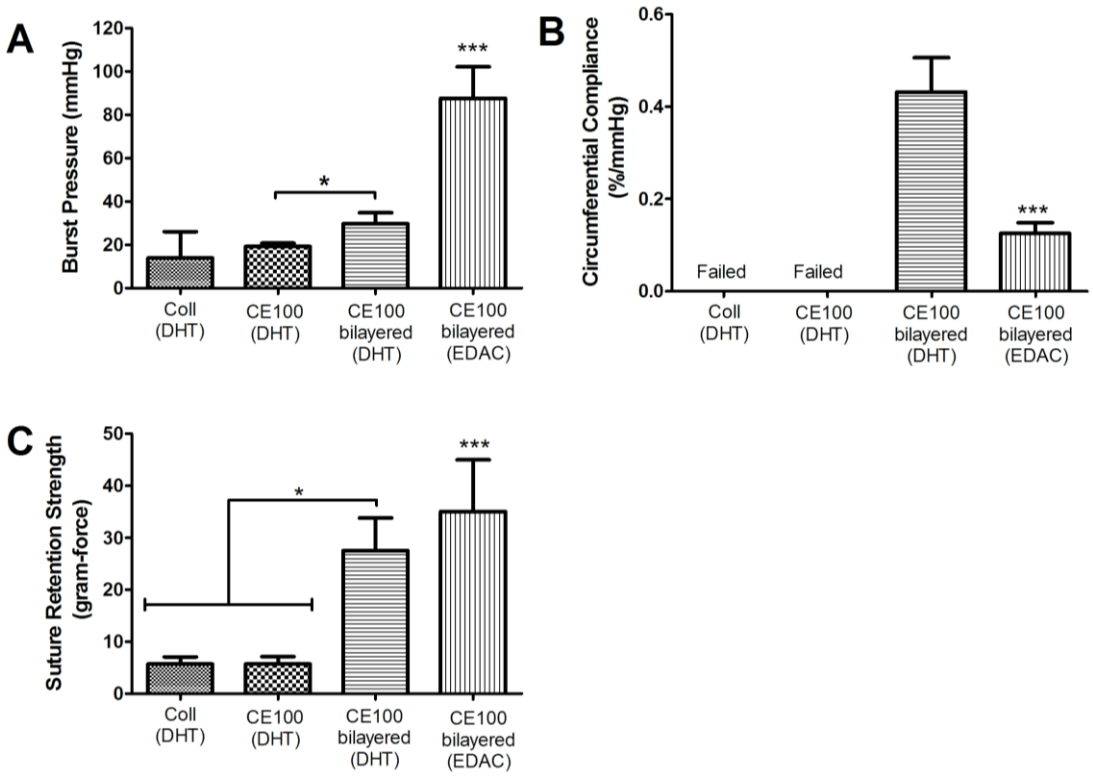

Figure 5.2 Effect of construct architecture and crosslinking on bioengineered vessel biomechanical properties

The vessel burst pressure (A), circumferential compliance (B), and suture retention strength (C) were all significantly affected by the incorporation of the film layer (bilayered groups) and also by crosslinking with EDAC ($p<0.05$). Burst pressure was significantly increased in the bilayered CE100 constructs versus the single layer CE100 construct, while increased suture retention strength was also found with the incorporation of the film layer. Further increases to the burst pressure and suture retention strength was found with EDAC crosslinked constructs, while this treatment also reduced the circumferential compliance to a value closer to native tissue.
(*) denotes $p<0.05$ versus indicated group or (***) versus all other groups.

5.3.1.2 Effect of construct architecture and crosslinking on TEVG biological & morphological properties

Having determined the effect of construct architecture and crosslinking on the biomechanical properties of the bioengineered vessels we next sought to determine their effect on the cellular response and remodelling of the vessels. Cell density (Fig. 5.3A) was similar between the Coll and CE100

single layered constructs while collagen content (Fig. 5.3B) was significantly reduced in the CE100 constructs due to elastin constituting 50% of the starting protein concentration ($p<0.05$). No change in cell density was found between the DHT and EDAC crosslinked bilayered constructs, while collagen content also remained similar ($p>0.05$). A significant reduction in cell density was found between the single layered constructs versus the bilayered constructs, although this was determined to be primarily due to the acellular film layer contributing towards the bilayered construct's weight as the assay was determined per weight of tissue.

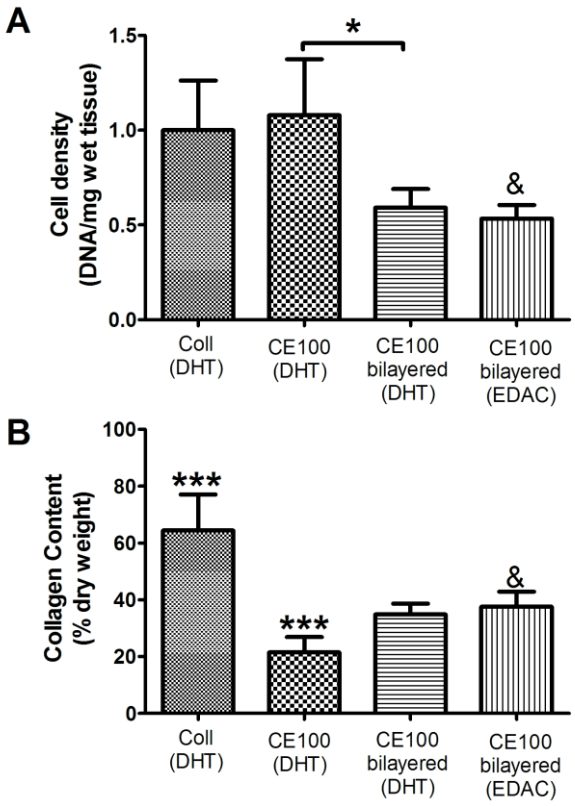

Figure 5.3 Effect of construct architecture and crosslinking on bioengineered vessel biological properties

Cell density (A) and collagen content (B) were significantly altered by construct architecture ($p<0.05$), although this was determined to be due to the acellular film incorporation. No significant change was found between DHT versus EDAC crosslinked bilayered constructs.(*) indicates $p<0.05$ as indicated, (&) indicates $p<0.05$ versus Coll and CE100. (***) denotes $p<0.05$ versus all other groups.

The morphology and tissue organisation of the constructs after 21 days culture was determined via haematoxylin and eosin staining for general tissue structure (Fig. 5.4 A,B,D,E,G,H,J,K) and polarized light of picrosirius red strained sections to determine collagen organisation (Fig. 5.4 C,F,I,L). The single layer Coll and CE100 constructs displayed similar morphology histologically (Fig. 5.4 A,B,D,E) while the static compaction resulted in moderate circumferential alignment of the collagen in the vessel walls (Fig 5.4 C, F). Similar wall thickness was observed for the single layered constructs with a mean of approximately 450μm (Coll: 411 ± 65 μm, CE100: 488 ± 58μm) (Fig.5.5).

The bilayered CE100 constructs crosslinked with DHT displayed a similar morphology to the single layered CE100 constructs, with the 2-ply film lining visible on the luminal side contributing towards the increased wall thickness (696 ± 97 μm, $p<0.05$) versus the single layered CE100 constructs (488 ± 58μm). The high density of collagen in the film layer is clearly visible under polarized light of the picrosirius red stained samples (Fig. 5.4 I). Crosslinking the bilayered constructs with EDAC resulted in a further increase in wall thickness (890 ± 308μm), although this was non-significant versus the DHT crosslinked bilayered construct ($p>0.05$). The EDAC crosslinked constructs resisted cell mediated contraction of the porous outer wall and thus produced a more variable wall thickness in comparison to the DHT crosslinked groups; however tissue stability was greatly increased.

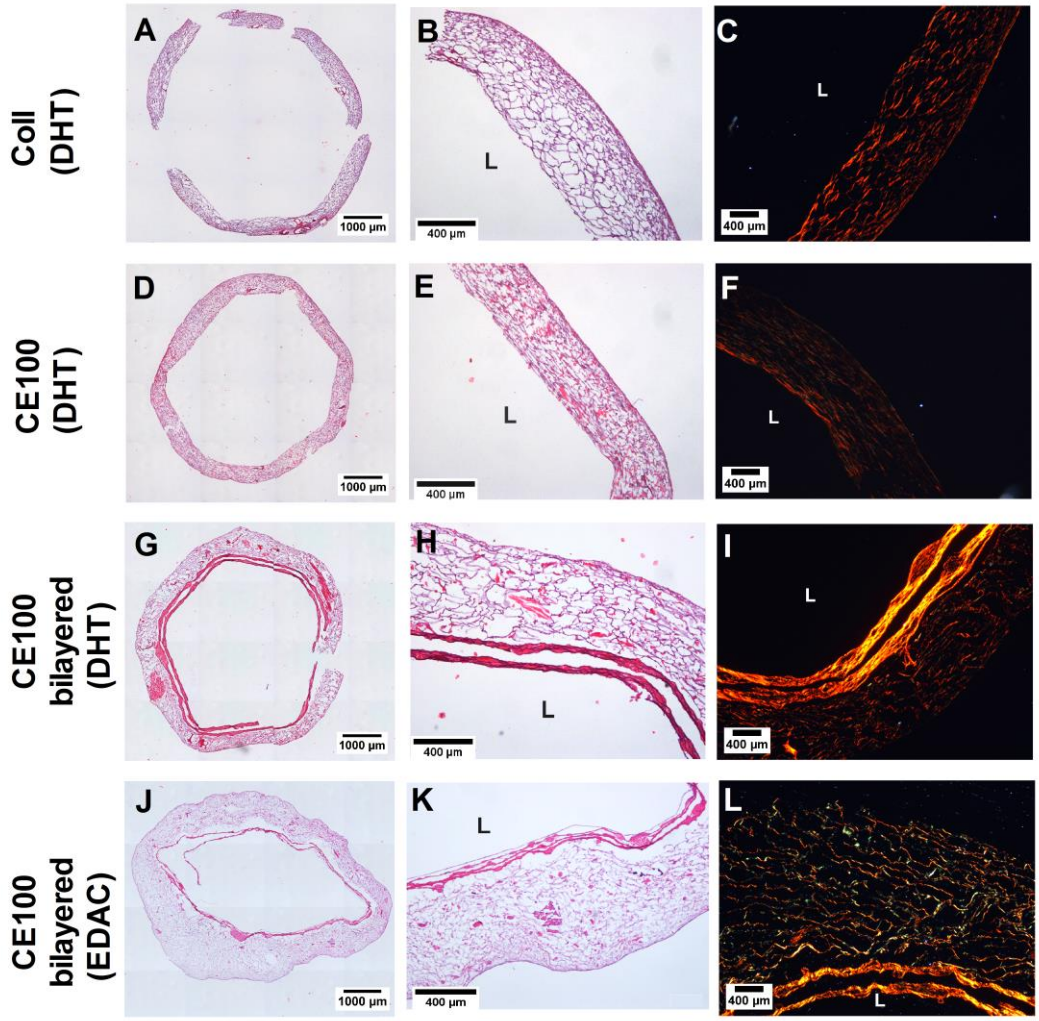

Figure 5.4 Effect of construct architecture and crosslinking on bioengineered vessel morphology and collagen organisation

Haematoxylin and eosin stained sections reveal the degree of wall compaction and general tissue structure following 21 days static culture. Tissue and cell density was found to be highest at the abluminal side of the bioengineered vessels, consistent with the seeding location. Polarized light of picrosirius red stained sections reveals the organisation of collagen in the bioengineered vessels. Compacted and aligned collagen displays long wavelengths (red to yellow) while thinner fibres and less alignment results in shorter wavelengths (yellow to green). Histological artefacts are visible with the walls of A and G rupturing during processing, while partial delamination occurred in J. Vessel lumen is indicated with a L.

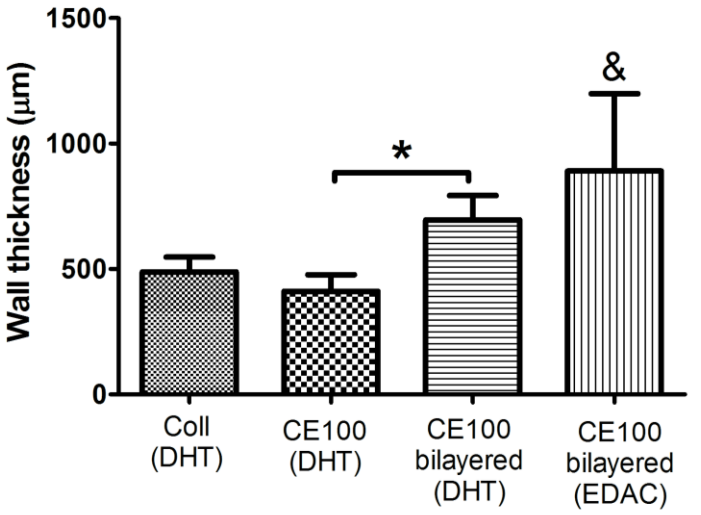

Figure 5.5 Effect of construct architecture and crosslinking on bioengineered vessel wall thickness

Similar wall thickness was observed with the single layered constructs (Coll and CE100) while the incorporation of a film lining significantly increased the wall thickness in the CE100 bilayered (DHT) group ($p<0.05$). EDAC crosslinked bilayered constructs resulted in the highest wall thickness. (*) indicates $p<0.05$ as indicated, (&) indicates $p<0.05$ versus Coll and CE100.

Immunofluorescent imaging was utilised to determine the relative expression and distribution of vascular specific proteins by the seeded SMCs (Fig. 5.6). The early stage SMC marker, αSMA, and the key fibrillar protein, collagen III, were expressed at expressed in all groups at a similar level. Calponin expression was primarily observed on the abluminal side of the vessel wall with the distribution limited to a wall depth of approximately 100µm.

In summary, the optimal TEVG for further examination was determined to be the bilayered CE100 scaffolds crosslinked with EDAC based upon the enhanced biomechanical properties, maintenance of suitable biological properties, and enhanced remodelling potential due to the maintained tissue stability.

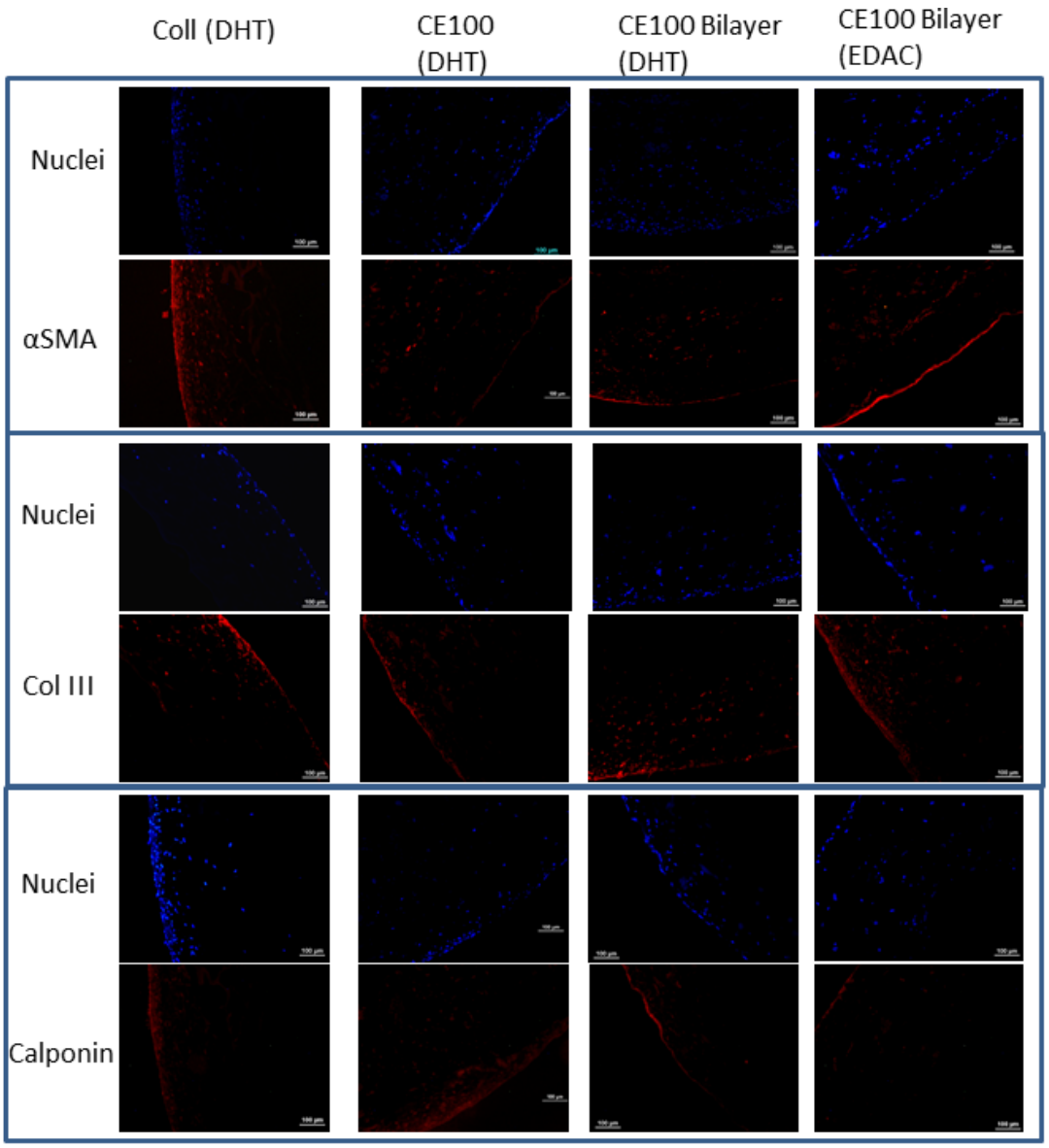

Figure 5.6 Effect of construct architecture and crosslinking on vascular protein expression by SMCs

Immunofluorescent staining (red) for ŭSMA, Calponin, and collagen III with the associated cell nuclei stained using DAPI (blue). Expression of ŭSMA, calponin, and Coll III was primarily located on the abluminal surface of the cultured vessels, with no apparent differences observed between groups. Scale bar = 100ε m.

5.3.2 Effect of dynamic conditioning on bioengineered vessel maturation

5.3.2.1 Effect of dynamic conditioning on bioengineered vessel biomechanical properties

Having determined the effects of construct architecture and crosslinking on the resulting vessel properties, we concluded that the bilayered CE100 constructs crosslinked with EDAC were optimal for further examination. This conclusion was based upon the improved biomechanical properties (burst pressure, compliance, and suture retention strength), maintenance of cell viability during long term culture, and suitable remodelled architecture histologically. We next sought to determine the effect of dynamic conditioning within the custom designed bioreactor on the maturation of the bilayered CE100 TEVGs, crosslinked with EDAC.

Biomechanical testing (Fig. 5.7) was used to determine the effect of dynamic bioreactor conditioning on the resulting vessel properties after 21 days culture (7 static + 14 dynamic). Burst pressure (Fig. 5.7 A) increased by 35.6% ($p<0.05$) in the dynamically conditioned bioengineered vessels (111.7 ± 13.3mmHg) versus the static controls (82.2 ± 16.7 mmHg). Furthermore, dynamic conditioning also resulted in a 24.2% decrease in circumferential compliance (0.105 ± 0.015 %/mmHg) (Fig. 5.7 B) versus the static controls (0.138 ± 0.016 %/mmHg), with an inverse relationship between compliance and burst pressure often found in tissue engineered vascular grafts. Interestingly, suture retention strength (Fig. 5.7.C) remained unchanged due to dynamic conditioning. However, having previously shown that the vessel suture retention strength is primarily conferred by the film lining (Section 5.3.1), we can infer that the acellular layer remains intact and maintains its structural integrity following dynamic conditioning.

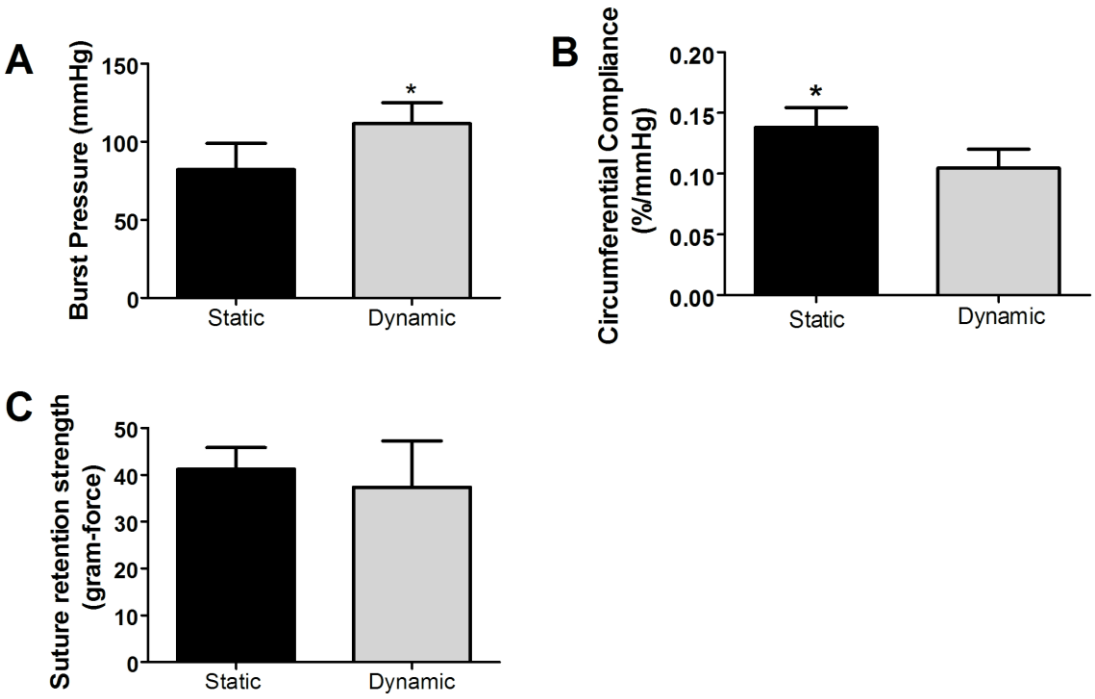

Figure 5.7 Effect of dynamic conditioning on bioengineered vessel biomechanical properties

Dynamic conditioning increased the vessel burst pressure (A) while also resulting in a decrease in the circumferential compliance (B). Suture retention strength was found to be maintained at a similar level between the static and dynamic conditioning. (*) denotes p<0.05 versus indicated group

5.3.2.2 Effect of dynamic conditioning on bioengineered vessel biological & morphological properties

Cell density (Fig. 5.8A) was increased by 1.57-fold ($p<0.05$) following dynamic conditioning. However, the proportion of collagen in the vessel wall decreased from 52.4 ± 7.0% of the dry tissue weight in the statically cultured vessels to 34.8 ± 11.7% in the dynamically conditioned vessels ($p<0.05$). The reduced collagen content in the vessel wall may be due to the increased production of non-collagenous proteins/GAGs (e.g. Elastin) following dynamic conditioning, or increased matrix metalloproteinase (MMP) production which is known to increase following dynamic conditioning (Seliktar et al., 2001).

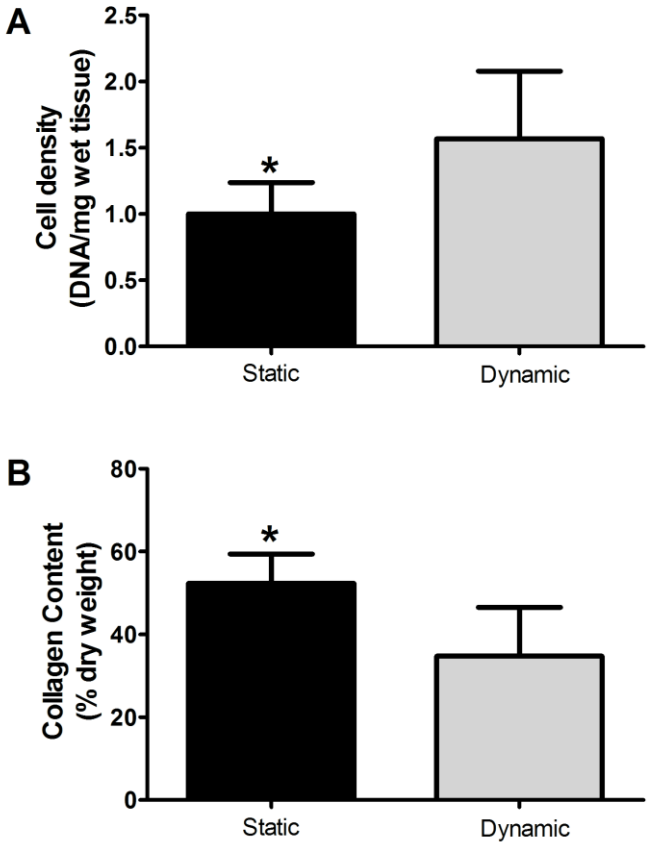

Figure 5.8 Effect of dynamic conditioning on bioengineered vessel biological properties.

Cell density (A) was significantly increased due to dynamic conditioning ($p<0.05$). Overall collagen content was significantly reduced in the dynamically conditioned group ($p<0.05$). (*) indicates $p<0.05$ as indicated

Histological examination of the morphology of the tissue following 21 days culture revealed increased tissue density due to dynamic conditioning (Fig 5.9 B, D) versus the static controls (Fig. 5.9 A, C). The film integrity was maintained during static and dynamic conditioning, and overall vessel integrity was excellent, Picrosirius red stained sections demonstrate the enhanced tissue density and significant circumferential alignment of collagen due to dynamic conditioning (Fig. 5.9 F, H) versus the static controls (Fig. 5.9 E, G). Furthermore, vessel wall thickness was found to decrease by 17% ($p<0.05$) due to dynamic conditioning (Fig. 5.10). A mean wall thickness of 812 ± 179μm under static conditions was reduced to 673 ± 123μm following dynamic conditioning ($p<0.05$).

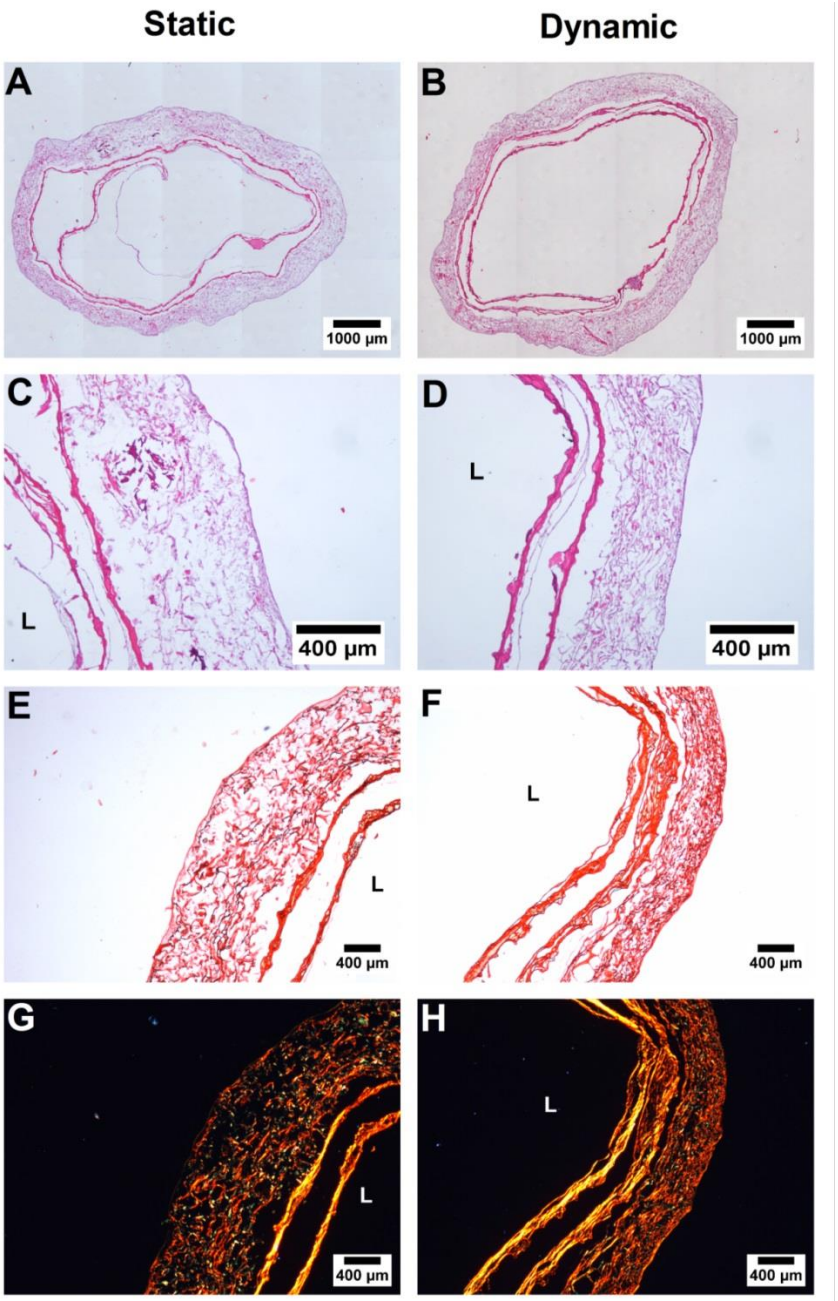

Figure 5.9 Effect of dynamic conditioning on bioengineered vessel morphology and collagen organisation

The EDAC crosslinked bilayered scaffolds were examined under static and dynamic culture conditions after 21 days culture. Dynamic culture (7 days static + 14 dynamic) resulted in an increase in apparent tissue density (B, D) versus the static controls (A, C). This increased density and improved circumferential collagen organisation was further confirmed with picrosirius red staining (E, F) and under polarized light (G, H). Histological artefacts are visible with the film layer exhibiting partial delamination due to the histology processing steps. Vessel lumen is indicated with a L.

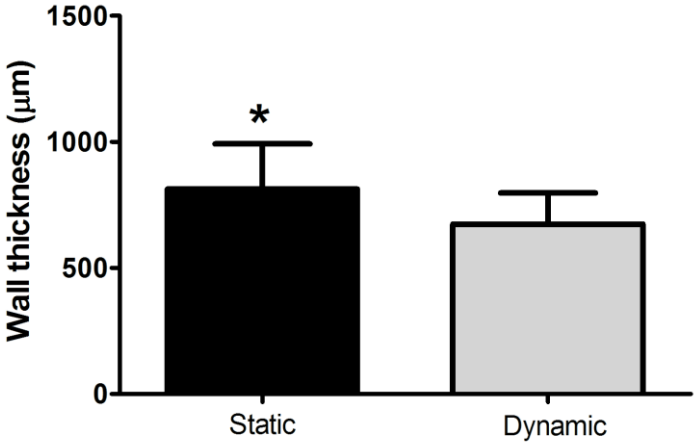

Figure 5.10 Effect of dynamic conditioning on bioengineered vessel wall thickness

Dynamic conditioning resulted in a significant reduction in the mean wall thickness ($p<0.05$) versus static culture conditions after 21 days culture. (*) indicates $p<0.05$.

Immunofluorescent imaging was utilised to determine the relative expression and distribution of vascular specific proteins by the seeded SMCs (Fig. 5.11). The early stage SMC marker, αSMA, was expressed at increased vessel wall depth in the dynamically conditioned vessels which is consistent with the enhanced cell migration observed. Calponin expression was primarily observed on the abluminal side of the vessel wall with the distribution limited to a wall depth of approximately 100µm. Collagen III, a key fibrillar protein in vasculature, was produced by SMCs under both static and dynamic conditioning, although enhanced expression depth was observed in the dynamic groups.

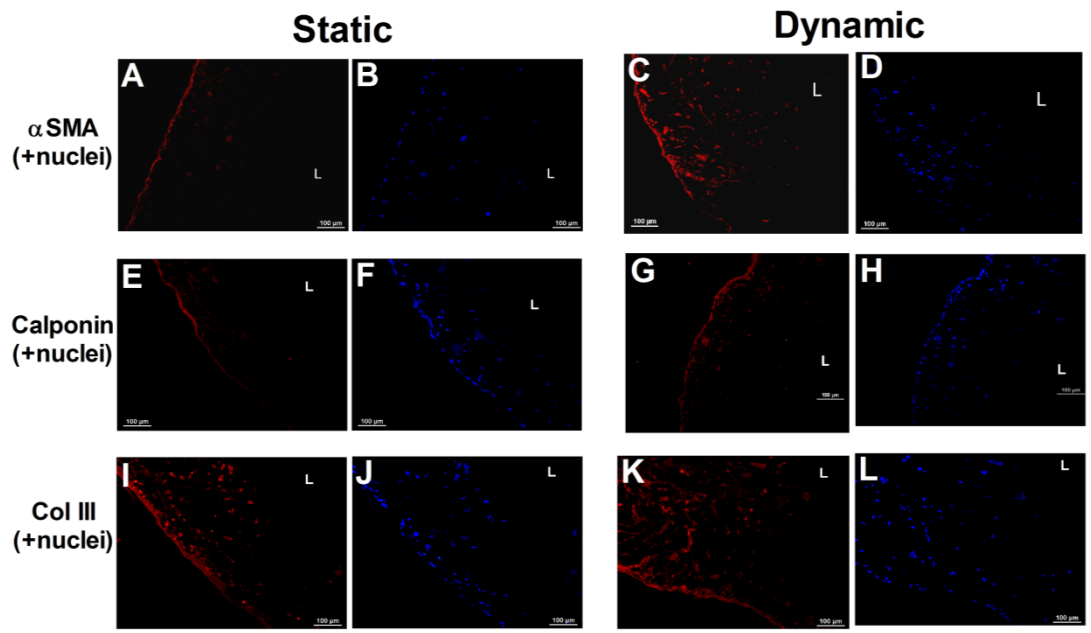

Figure 5.11 Effect of dynamic conditioning on spatial distribution of vascular protein expression by SMCs

Immunofluorescent staining (red) for ŭSMA (A, C), calponin (E, G), and collagen III (I, K) with the associated cell nuclei stained using DAPI (blue). Expression of ŭSMA, calponin, and Coll II was primarily located on the abluminal surface of the statically cultured vessels, while the improved cell migration observed with dynamic conditioning increases the depth of expression of the proteins of interest. Scale bar = 100ε m.Vessel lumen is indicated with a L.

5.4 Discussion

The overall goal of this chapter was to examine methods to enhance the maturation of collagen-elastin constructs to form bioengineered blood vessels. To this end, the specific goals of this chapter were to investigate the effects of construct architecture (single v bilayered), crosslinking (DHT v EDAC), and dynamic conditioning on the subsequent bioengineered vessel properties after 21 days culture. The results demonstrate that bilayered constructs result in enhanced biomechanical properties (burst pressure, compliance, and suture retention) versus the single layer constructs while maintaining suitable biological properties (cell density and collagen content). The vessel biomechanical properties were shown to be further enhanced through crosslinking with the carbodiimide crosslinker EDAC, while biological properties (cell density, collagen content) remained relatively unchanged. Vessel morphological analysis revealed that EDAC crosslinking resulted in increased resistance to cell-mediated vessel wall contraction, leading to thicker walls. However, the application of dynamic conditioning resulted in an apparent increase in vessel wall density, improved cell density, and improved collagen circumferential alignment, which translated to a significant increase in burst pressure and a compliance closer matching native vessels. Additionally, these bioengineered vessels displayed cell-mediated synthesis of the vascular proteins αSMA, calponin, and collagen III within the vessel wall, with enhanced cell migration observed in the dynamically conditioned vessels. Therefore, the optimal strategy established in this study for the maturation of the described natural polymer (Collagen-elastin) TEVGs consists of a bilayered tubular architecture, crosslinked with EDAC, and dynamically conditioned in a bioreactor to produce a novel bioengineered blood vessel.

Structural-functional relationships exist for many organs and tissue engineered products, including vascular grafts (Badylak et al., 2009; Butler et al., 2000). We have previously shown the capability to alter the architecture of our constructs (Chapter 3) through the developed biofabrication techniques and thus we have subsequently assessed the effect this has on

the functional TEVG properties following 21 days culture. The incorporation of a dense film layer resulted in vastly improved biomechanical properties including a 4.84-fold increase in suture retention strength ($p<0.05$) and a 1.54-fold increase in burst pressure ($p<0.05$) versus the single layer constructs (Fig. 5.1). Morphologically, the dense film layer resulted in an increase in overall wall thickness (Fig. 5.4) although similar levels of compaction were observed on the outer porous layer (Fig. 5.3). The film is easily discernable in the polarized light imaging of the picrosirius red stained sections, where the high intensity and colour of the birefringence indicates the very high collagen density and partial circumferential alignment. This alignment in the films is hypothesised to occur due to the method in which the film is fabricated, whereby the protein suspension is dehydrated to effectively form a 2D structure and thus limits the collagen organisation to two potential axes rather than three (Moritani et al., 1971).

While reinforcement of natural polymer vascular grafts has been primarily achieved though incorporation of synthetic polymers (Koch et al., 2010; McClure et al., 2012; Tschoeke et al., 2008) there has also been reports of multi-layered vascular grafts based solely on natural polymers, including the incorporation of acellular support sleeves from collagen (Berglund et al., 2003) and elastin (Koens et al., 2015, 2010). One study has shown the ability to create acellular vascular grafts from collagen and elastin (elastin-like protein polymer) polymer films, with the very high density walls resulting in impressive mechanical properties (Kumar et al., 2013). However, when implanted into a rat aortic interposition model for 2 weeks, no cell infiltration was observed due to the grafts non-porous microstructure leading to questions regarding long term graft stability *in vivo* due to a lack of remodelling. Consequently, the approach detailed in this study exhibits a number of advantages due to the ability to independently alter each of the layers, including modification of the composition, crosslinking type and microstructure suitable for cell infiltration. We have also shown the ability to significantly alter the biomechanical properties of these natural polymer based TEVGs solely through non-cytotoxic crosslinking techniques.

Crosslinking allows the modification of biomaterial mechanical properties and degradation rate independently of the structure/architecture (Chapter 3) (Mason et al., 2013). Consequently, it is a powerful tool to further tailor the properties of TEVGs, such as those described in this thesis. While the base bilayered CE100 constructs were crosslinked with DHT, the application of EDAC crosslinking resulted in a further 2.94-fold increase in burst pressure ($p<0.05$) and a 27% increase in suture retention strength ($p<0.05$) (Fig. 5.1). Additionally, the compliance (0.125 ± 0.02 %/mmHg), was reduced to a value similar to that found in native internal mammary arteries (0.115 ± 0.039 %/mmHg) (Konig et al., 2010). Remodelling of the construct was also altered through crosslinking, with the EDAC crosslinked vessels displaying an increased resistance to cell-mediated contraction of the outer porous layer of the construct wall (Fig. 5.3). This led to an increase in the mean wall thickness ($p<0.05$) (Fig. 5.4). Consequently, this also impacted the density of the tissue, with the EDAC crosslinked group retaining a more open architecture versus the DHT crosslinked group which may aid in further cell migration throughout the walls (Haugh et al., 2011). Both crosslinking methods also supported the attachment and migration of cells and did not elicit any negative cellular response, with a similar cell density (Fig. 5.2) observed between both crosslinking treatments, with similar results previously reported (Hafemann et al., 2001; Haugh et al., 2011, 2009). Therefore, the optimal crosslinking method for the natural polymer TEVGs developed here was determined to be EDAC treatment.

The increased resistance to cell-mediated contraction after EDAC crosslinking may also be explained in part by changes in the local stiffness, with a 4.54-fold increase in tensile modulus found for the outer porous layer with EDAC versus DHT crosslinking (results not shown). Indeed, it is well established that local scaffold stiffness can play a critical role in the biological response of cells, as a scaffold can be considered analogous to the natural extracellular matrix produced by cells by providing structural support, adhesion sites, facilitating movement, regulating cell behaviour, and assisting cell-to-cell recognition. Substrate stiffness has been shown to have a direct influence on cell migration, development, proliferation and shape (Discher et

al., 2005). It has previously been shown that SMC are sensitive to substrate stiffness changes and specify their phenotype commitment partially based on this, with increased SMC marker expression on high stiffness substrates (35-135kPa) versus low stiffness substrates (1-25kPa) (Park et al., 2011; Sazonova et al., 2011). Additionally, myogenic differentiation of MSCs has also be shown to be dependent on substrate viscoelastic properties, with high creep substrates showing enhanced SMC differentiation (Cameron et al., 2014). Thus, it is clear that further investigation would be necessary to elucidate the specific response of EDAC and DHT crosslinking on SMC phenotype and/or myogenic differentiation.

The ability of dynamic conditioning, applied through a custom designed bioreactor (Chapter 4), to aid in the maturation of the TEVGs was then investigated. Recapitulation of foetal vessel culture conditions was achieved through application of a pulse rate of 120bpm (Couet et al., 2011) with a mean cyclical strain of 5% and an amplitude of 1% . Natively, human aortic SMCs generally experience a mean cyclical strain of 10%; however, this physiological strain regime results in significantly reduced cell proliferation (Kona et al., 2009) and increased production of matrix metalloproteinase 2 (MMP2), which may be involved in vessel remodelling or result in loss of structural integrity of the graft due to excessive proteolytic activity (Seliktar et al., 2003, 2001). Low mean circumferential strain (5%) is known to result in higher proliferation than 10% mean strain, while also inducing ECM production/remodelling (Solan et al., 2003). Additionally, low cyclic strain amplitude (1%) is known to decrease apoptosis versus higher strain amplitudes (3%) (Colombo et al., 2013). This is consistent with our results where increased cell density (Fig. 5.8) was observed in the dynamically conditioned vessels which were subjected to cyclical strain of 5% and an amplitude of 1%. However, decreased collagen content was found in the dynamically conditioned vessels which may indicate increased levels of MMP2 production. Despite the decreased collagen content a significant increase in burst pressure was observed with dynamic conditioning (Fig. 5.7), coupled with a decrease in compliance. This would suggest that significant remodelling of the bioengineered vessel is occurring due to the

mechanical conditioning, which was confirmed via histological analysis (Fig. 5.9) where significantly increased vessel wall density and enhanced collagen circumferential organisation were observed. Finally, dynamic conditioning resulted in improved cell migration (Fig. 5.10) and the expression of αSMA, calponin, and collagen III was observed in the vessel walls.

Despite almost 30 year having passed from the first attempt at fabricating a tissue engineered vascular graft (Weinberg and Bell, 1986), their remains no vessel which satisfies the numerous biological and biomechanical requirements to serve as a long term replacement vessel. Due to the challenging haemodynamic environment, a replacement vessel must possess high strength (burst pressure) while also maintaining elasticity (compliance) and the ability to be anastomosed easily with the native vasculature (suture retention strength). Traditionally, the field has focused on achieving suitable burst pressures and suture retention strength, with compliance and biological suitability a secondary concern. The bioengineered vessel described in this chapter has been shown to possess suitable compliance and suture retention strength, while possessing excellent biological characteristics due to the protein composition, 3D architecture, and ability to be actively remodelled. We believe it represents an ideal *in vitro* platform for examining vascular cell interaction, disease progression, pharmacological toxicity, or cardiovascular medical devices testing, in addition to having potential therapeutic as a vascular graft.

5.5 Conclusion

The optimal approach to enhance the *in vitro* maturation of the CE100 TEVGs was examined with alterations in construct architecture, crosslinking, and dynamic conditioning in the custom designed bioreactor. Bilayered TEVGs resulted in enhanced biomechanical properties (burst pressure, compliance, and suture retention) versus the single layered TEVGs while maintaining suitable biological properties (cell density and collagen content). The results of this study also demonstrated that TEVG biomechanical properties could be further improved with EDAC crosslinking. Furthermore, the application of foetal-like dynamic mechanical conditions resulted in significant remodelling of the TEVGs, with an apparent increase in vessel wall density, improved cell density, and improved collagen circumferential alignment, which translated to a significant increase in burst pressure and a compliance closer matching native vessels. These tissue engineered vascular grafts displayed cell-mediated synthesis of the vascular proteins αSMA, calponin, and collagen III within the vessel wall, with enhanced cell migration observed in the dynamically conditioned vessels.

Chapter 6: Discussion

6.1 Overview

Tissue engineering, in its currently recognised form, first came about in the early 1980's through the work of Prof. Ioannas Yannas (MIT) and Dr. John Burke, (Massachusetts General Hospital) for the generation of artificial skin (Vacanti, 2006; Yannas and Burke, 1980). Just a few short years passed before pioneering research by Weinberg and Bell (Weinberg and Bell, 1986) and L'Heureux (L'Heureux et al., 1993) demonstrated the possibility of generating tubular vascular models composed of smooth muscle cells, endothelial cells and fibroblasts embedded within a collagen gel. Almost 30 years have passed since Weinberg and Bells tubular model and while the field has advanced significantly towards the generation of TEVGs suitable for implantation, full scale clinical translation remains an aspirational goal.

While blood vessels may superficially seem to be a comparatively simple tissue to bioengineer, the extremely challenging mechanical conditions coupled with the multifaceted biological requirements, has resulted in limited clinical success. The propensity of the field to focus on a single characteristic, burst pressure, has undoubtedly resulted in many TEVGs with suitable strength yet often at the expense of elasticity and biological characteristics. Consequently, this thesis focused on the latter two aspects,

with a specific focus on creating collagen-elastin composite scaffolds which mimic native vessel composition and anatomical structure.

Due to the many shortcoming of utilising synthetic polymers for vascular graft construction we consequently opted to develop a natural polymer based TEVG. Although it is clear that a TEVG must have sufficient strength to withstand the arterial environment and be non-thrombogenic, it is also imperative that the vessel displays a suitable compliance, be vasoactive, and facilitate active remodelling in order for the vessel to be fully functional (Nerem, 2000; Yao et al., 2005). In Chapter 2 we sought to improve the viscoelastic properties of collagen-based scaffolds through the incorporation of elastin. The results corroborated this hypothesis as elastin addition resulted in a higher degree of cyclical strain recovery and improved creep resistance which may aid in providing compliance closer to native vessels and resisting aneurysm formation *in vivo*. Additionally, the gene expression and proliferation data suggested that the presence of elastin resulted in a more contractile-like SMC phenotype, in the absence of any exogenous stimulation. This biomaterial platform was deemed to possess great potential for cardiovascular tissue engineering and was amenable to multiple fabrication methods to generate a physiologically relevant architecture.

This biomimetic biomaterial was subsequently developed into a novel bilayered tubular architecture (Chapter 3) with a porous outer layer suitable for smooth muscle cell seeding, analogous to the native artery medial layer, while the inner dense film layer was designed to increase the overall graft mechanical properties while also presenting a suitable surface to support a confluent endothelium. Optimisation of the fabrication process allowed the generation of an outer layer with a homogenous pore structure and high porosity, ideally suited to enable very efficient diffusion of cell nutrients and waste products while facilitating cell attachment and migration in an in vivo-like 3D environment. The properties of the dense luminal lining were controllable via crosslinking which enabled the modification of the mechanical properties, degradation resistance, and inflammatory profile. This

bilayered tubular scaffold was ultimately considered highly suitable for use as the basis for a TEVG.

Dynamic biophysical stimulation is an important aspect in the development of a functional tissue engineered vascular graft (Schutte et al., 2010) which has been shown to aid in the development of TEVGs in numerous different ways including improved strength (Tschoeke et al., 2009), improved cell alignment, increased ECM deposition (Hahn et al., 2007), and inducing normal physiological cell phenotype (Qu et al., 2007). Chapter 4 of this thesis outlined the development of a novel pulsatile flow bioreactor system capable of recreating the complex haemodynamic environment in vitro. The system was capable of applying physiological fluid shear stresses, cyclical strain and pulsatile pressure to mounted TEVGs. The flexible design allowed the mounting of variable diameter scaffolds/TEVGs and was designed to be utilised to examine the effect of mechanical stimulation on the *in vitro* maturation of the bilayered tubular collagen-elastin TEVGs.

In the final chapter (Chapter 5) we examined the effect of scaffold architecture, crosslinking, and dynamic conditioning in the custom pulsatile bioreactor from Chapter 4 on the maturation of the TEVGs. Bilayered TEVGs were found to display significantly enhanced mechanical properties versus single layered TEVGs due to the incorporation of the dense film layer. The scaffolds could be crosslinked prior to cell seeding, thus reducing the risk of cytotoxicity which is present when crosslinking cell-embedded hydrogels. Crosslinking with EDAC was shown to further improve the mechanical properties of the grafts and also resist degradation during culture, an issue often present with fibrin based TEVGs (Cholewinski et al., 2009). The optimal TEVGs were dynamic conditioned in the custom designed bioreactor which resulted in higher cell density, improved collagen circumferential alignment, and consequently, enhanced mechanical properties. The following sections will summarise the key findings and implications from each individual chapter and review the possible future directions which have arisen from this research.

6.2 Chapter 2: Effect of elastin incorporation on the microstructure, mechanical properties, and biological response of collagen scaffolds for cardiovascular tissue engineering

A major challenge in cardiovascular tissue engineering is the design and fabrication of biomaterials with suitable biological instructive cues to guide cell behaviour, while additionally supporting the challenging haemodynamic mechanical environment once implanted *in vivo* (Annabi et al., 2013; Quint et al., 2011). Our approach to this has been to utilise insoluble elastin in combination with collagen as the basis of a biomimetic scaffold for cardiovascular tissue engineering. Elastin is an ideal protein to examine as a composite with collagen due to its important mechanical and biological role *in vivo*. Consequently, a series of elastin containing scaffolds were developed with collagen as the base structure. The overall goal of this chapter was to assess the effect of elastin on collagen scaffold microstructure, mechanical properties, and subsequently the response to seeded smooth muscle cells (SMC) *in vitro.*

Morphologically it was shown that elastin was homogenously distributed at higher concentration (CE100, a 1:1 ratio of collagen to elastin), with the elastin fibres primarily encapsulated in the collagen struts. The bulk addition of the protein caused a predictable decrease in scaffold porosity, although it was still comparatively excellent with a minimum of 98.8%, far above the minimum required for effective tissue repair/regeneration (~90%). The pore architecture remained unchanged although some deviations in mean pore size were observed; however the mean pore size results were within the idealised range for effective cell migration, proliferation(Lee et al., 2008) and ECM production (Ross and Tranquillo, 2003) while facilitating sufficient nutrient exchange for SMCs/MSCs.

One of the key finding of this study was that the incorporation of elastin significantly improved the viscoelastic characteristics of the biomaterial. The results suggest that elastin confers a vastly improved resistance to creep,

which supports the importance of elastin as a load bearing cardiovascular protein which store elastic-strain energy. Indeed, multiple reports of tissue engineered vascular grafts with an absence of elastin in their structure have exhibited graft dilation via creep *in vivo* (L'Heureux et al., 2007; Niklason et al., 2001). Although elastin did result in a decrease in the scaffold stiffness, this was to be expected due to elastin natively displaying a stiffness (~0.5MPa) an order of magnitude lower than collagen (~5MPa) (Nowatzki and Tirrell, 2004). Interestingly, following cell-mediated contraction of the scaffold it was determined via cellular solids modelling that the scaffold modulus closely matched native heart tissue at ~33kPa while also being within the range found for native human tunica media moduli, reported to range between 1.3kPa for coronary arteries (Holzapfel et al., 2005) and 190kPa for carotid arteries (Khamdaeng et al., 2012).

Smooth muscle cells (SMCs) display extraordinary plasticity and it is known that they alter their phenotype partly in response to local environmental changes (Rensen et al., 2007). To this end we examined the proliferation and maturation of SMCs seeded on the CE100 composite scaffolds. Elastin addition was found to result in the modulation of the SMC phenotype towards a contractile state which was determined via reduced proliferation and significantly enhanced expression of early (α-SMA), mid (calponin), and late stage (SM-MHC) contractile proteins. Conversely, collagen-only scaffold induced a more synthetic phenotype. While elastin has been implicated in altering SMC/MSC towards a contractile phenotype in 2D (Gong and Niklason, 2008; Park et al., 2004), we believe this is the first conclusive evidence of this effect in 3D. This effect is hypothesised to occur through direct signalling between elastin and SMC with evidence suggesting G-protein coupled receptors, the 67-kDa elastin binding protein, and a variety of integrins (Bax et al., 2009; Lee et al., 2014). Ultimately, the application of this CE100 biomaterial would involve replicating native vasculature structure/architecture, sustained *in vitro* maturation, and mimicking native dynamic stimulation to create a bioengineered blood vessel. This was the focus of the subsequent studies shown in Chapters 3-5.

6.3 Chapter 3: The development of bilayered tubular collagen-elastin scaffolds for vascular tissue engineering

In Chapter 2, CE100 composite scaffolds were shown to emulate many of the desirable characteristics for cardiovascular tissue engineering and represented a promising biomaterial platform for further investigation. Consequently, we sought to utilise this biomimetic biomaterial to create a tissue engineered vascular graft (TEVG) which would mimic not just the native vasculature protein microenvironment but also structure, and be composed of a multi-layered lamellar tubular structure. The overall goal of this chapter was thus to develop a biomimetic scaffold with a physiologically relevant bilayered tubular architecture suitable for vascular tissue engineering.

Natural polymer fabrication techniques have traditionally lagged behind those used with synthetic polymers due to the risk of denaturing the proteins under challenging conditions, such as high temperature. The hierarchically structuring of natural polymers, like collagen, has thus only recently received attention in the field and may be achieved by altering the protein concentration between the layers to leverage the effect of density on the overall mechanical properties (Caliari et al., 2011; Kumar et al., 2013). To this end, dense CE100 films were developed for use as an acellular dense luminal layer on the TEVGs.

Importantly, this study demonstrated the capability to modulate the properties of these films through a number of physical, chemical, and enzymatic crosslinking techniques including DHT, mTGase, riboflavin/UV, EDAC, and glutaraldehyde. These crosslinking treatments were shown to alter the film residual amine content, mechanical properties, degradation resistance, and inflammatory cytokine expression from human macrophages. The optimal crosslinking methods were determined to be DHT and EDAC treatments as they resulted in improved degradation resistance and enhanced mechanical properties over a suitable range. Interestingly, EDAC crosslinking was found to result in an improved immunogenic response with reduced inflammatory

cytokine expression (TNFα) from primary macrophages. Ultimately, both DHT and EDAC crosslinking displayed properties which merited inclusion in future studies on the *in vitro* maturation of the TEVGs (Chapter 5).

Utilising the CE100 films developed above, this study subsequently developed a biomimetic bilayered TEVG with a porous tubular outer scaffold and a dense film luminal lining. Initial results showed the ability to create single layered porous TEVGs using freezedrying in a custom designed mold. The optimal fabrication process allowed the capability to create tubular TEVGs of lengths of up 65mm, with varying diameters, and the ability to further tailor the pore size using controlled freezing (~100μm) or rapid flash freezing (~15μm). Utilising the optimal biofabrication methods for the tubular porous scaffolds and dense films, we subsequently incorporated these two methods to create more a more physiologically relevant bilayered TEVG. Initial results suggested that the freezing dynamics were altered with the addition of the film layer and so optimisation of this process focused on altering the mold freezing direction and mandrel thermal conductivity to control the direction of ice crystal growth and consequently control the final TEVG microarchitecture. The bilayered design combines the advantages of both the film and the porous scaffolds with the increased mechanical properties of the films, a smooth surface for future endothelial monolayer formation, and a porous outer layer for smooth muscle cell growth, migration and remodelling. Due to the multi-step fabrication procedure each layer can be differentially modified, including altered compositions and crosslinking, thus allowing greater control over the final properties to generate a biomimetic TEVG.

Following the development of the bilayered TEVG, an initial *in vitro* study demonstrated the ability of SMCs to attach, migrate, and compact the porous scaffold wall during culture. Overall, the novel bilayered TEVGs were deemed to represent a promising platform for further *in vitro* maturation in order to enhance its therapeutic potential or application as an *in vitro* testing platform.

6.4 Chapter 4: Design, develop, and validate a versatile pulsatile bioreactor for culture of small diameter vascular grafts

In the first two results chapters of the thesis we demonstrated the ability to generate a suitable collagen-elastin biomaterial (Chapter 2) with anatomically relevant architecture (Chapter 3) and controllable properties for vascular tissue engineering. However, the *in vitro* generation of a functional TEVG requires not just a suitable cell-seeded scaffold/construct but also the application of appropriate biomechanical and biochemical signals (Niklason et al., 1999; Tschoeke et al., 2009). The appropriate biomechanical signals can be generated by simulating the dynamic physiological environment of native vessels through the use of bioreactor technology (Galie and Stegemann, 2011; Schutte et al., 2010). Consequently, the aim of this chapter was to design, develop, and validate a bioreactor system which was capable of recreating the complex cardiovascular biomechanical environment for culturing TEVGs *in vitro*.

The overall bioreactor system designed consists of a multi-channel peristaltic pump with four independent flow loops which pumps cell culture medium from an elevated reservoir via highly compliant silicone tubing though a 3D TEVG culture chamber before being returned to the same reservoir in a closed loop system. This layout facilitates the independent setup and priming of each individual loop, minimises contamination risk, and allows the ability to alter culture conditions and timepoints between individual flow loops.

A novel chamber was developed for the mounting of TEVGs for subsequent dynamic stimulation. The chamber design included modifications from the design of Lee and Wang (Lee and Wang, 2011) while also applying design elements from Seliktar (Seliktar et al., 2000). The flexible chamber design permits the mounting of TEVGs of varying length and internal diameter in conjunction to being easy to assemble. The design addresses many of the issues commonly encountered with bioreactor chambers in the field due to the easy assembly process, leak proof design, and ability to be detached from the system for endothelial cell seeding without removing the TEVG

(Avci-Adali et al., 2013). Cytotoxicity analysis of the individual bioreactor components and the fully assembled system revealed that the system was biocompatible and suitable for culturing cell-seeded TEVGs.

One of the primary requirements of the bioreactor was to ensure capability of applying physiological levels of cyclical strain, shear stress and pressure. The bioreactor system was found to be capable of generating intraluminal fluid flow of a laminar nature with a Reynolds number of between 160-320 at pulse rates between 60bpm-120bpm, which is within the physiological range (100-1000) of coronary, mesenteric and femoral arteries (Caro, 2012; Vennemann et al., 2007). It is capable of applying a shear rate (82 s^{-1} -164 s^{-1} at 60-120bpm respectively) closely matching the superficial femoral artery (130s^{-1}) and brachial artery (194s^{-1}) (Wu et al., 2004) and shear stress (0.82-1.64 dyne/cm^2) within the physiological ranges for these vessels (Kornet et al., 2000; Mitchell et al., 2004). Pressure waveforms of 50-80mmHg can be generated in the system, although this can be increased to >100mmHg by positioning the media reservoirs in a separate incubator mounted above the culture chamber incubator to gain the additional basal pressure. Cyclic strain can be applied directly to the TEVGs via the pulsatile fluid pressure or may be applied to TEVGs mounted over a compliant silicone tube to isolate the effects of strain on the maturation of the TEVGs. Measurement of the applied cyclic strain was achieved via a non-invasive video capture and analysis system which may be utilised to estimate the Young's modulus of the TEVG in a non-destructive manner (Couet and Mantovani, 2012).

Overall, the bioreactor system can be utilised to apply physiological stresses and strains to cell-seeded vascular grafts. In order to provide the optimal environment for tissue maturation, the application of dynamic mechanical stimulation within the bioreactor was the subject of investigation in Chapter 5.

6.5 Chapter 5: Maturation of collagen-elastin based TEVGs: The effect of scaffold architecture, crosslinking, and dynamic conditioning

The ideal approach to enhance the *in vitro* maturation of the CE100 TEVGs was examined by first assessing the effect of TEVG architecture (single v bilayered) and the two optimal crosslinking treatments from Chapter 3 (DHT and EDAC) on remodelling and functional characteristics of the vascular grafts after 21 days static culture. The optimal TEVG from this analysis was then selected for dynamic conditioning in the custom designed bioreactor.

Having previously developed both single layered and bilayered TEVGs, the stability of the acellular film layer after long term culture remained unknown. Bilayered TEVGs were found to result in enhanced biomechanical properties (burst pressure, compliance, and suture retention) versus the single layer TEVGs, with suture retention strength alone increased almost 5-fold. This was due to the very high collagen density in the film layer, which was clearly demonstrated via histology. While overall cell density was reduced, this was to be expected as the cell density was assayed per weight of dry tissue, with the acellular film layer contributing negatively towards this. Morphologically, the graft wall was contracted from the initial value of 2mm to approximately 500μm by the seeded SMCs.

The biomechanical properties of the bilayered TEVGs were further improved with EDAC crosslinking, with burst pressure increased almost 3-fold versus DHT crosslinking. Interestingly, EDAC crosslinking also significantly reduced the compliance by almost 3.5-fold and reaching a value (0.125 ± 0.02 %/mmHg) close to that of the internal thoracic artery (0.115 ± 0.039 %/mmHg), a commonly used autologous graft for coronary artery bypass grafting (Konig et al., 2010). Immunofluorescent imaging demonstrated the expression of αSMA, calponin, and Collagen III in all groups, although it was primarily located on the abluminal surface of the cultured TEVGs. SMCs/MSCs have previously been shown to display increased contractile marker expression on stiffer substrates (Park et al., 2011; Sazonova et al.,

2011), and thus it was hypothesised that EDAC crosslinking may have resulted in increased expression of these vascular specific proteins due to the increased stiffness. However, no apparent different was observed between the DHT and EDAC crosslinked groups, although quantification of the expression levels via western blotting would be necessary to confirm this.

Having determined that the bilayered TEVGs crosslinked with EDAC possessed the most potential, we subsequently selected this TEVG to investigate the effect of dynamic conditioning in the bioreactor on the maturation and remodelling of the grafts. Recapitulation of foetal vessel culture conditions was achieved through application of a pulse rate of 120bpm (Couet et al., 2011) with a mean cyclical strain of 5% and an amplitude of 1%. Dynamic conditioning resulted in increased cell density but decreased collagen content which may indicate partial degradation due to increased levels of MMP production. Despite the reduced collagen content, burst pressure was significantly increased while compliance was further improved. This would suggest that significant remodelling of the TEVG is occurring due to the mechanical conditioning, which further supports the hypothesis that increased MMP activity is occurring. While MMP production is necessary for graft remodelling, this may warrant future investigation to balance the effects of matrix remodelling and potential degradation. Nevertheless, dynamic stimulation was found to cause an apparent increase in vessel wall density, and enhanced collagen circumferential organisation. Additionally, these bioengineered vessels displayed cell-mediated synthesis of the vascular proteins αSMA, calponin, and collagen III within the graft walls, with enhanced cell migration observed in the dynamically conditioned TEVGs.

6.6 Future work

¶ This thesis focused in part on the potential of the CE100 biomaterial (Chapter 2) for cardiovascular applications, but future studies on the application of this biomaterial to other tissues where elastin is present in high proportions are merited, including: elastic cartilage, lung, heart valves, tendon, and skin tissue engineering. Furthermore, the technology presented in Chapter 3 could be adapted for other applications. To this end, we have used the same technique to prepare bilayered nerve conduits which have subsequently shown success in repairing damaged nerves *in vivo*. Consequently, we believe that the ability to create complex tubular architectures utilising natural proteins could be successfully applied to tissues other tissues such as airway (trachea, oesophagus), urinary and gastrointestinal tissues.

¶ While the compliance and suture retention strength of the bilayered TEVGs can be deemed sufficient, the burst pressure is below the minimum requirement for *in vivo* implantation. Numerous approaches could be utilised to improve this property, including increasing the number of film layers within the TEVGs, seeding a co-culture of fibroblasts and SMCs to enhance the formation of ECM, or extending the culture period in the bioreactor. Importantly, while the biomaterial described has been shown to induce a more-contractile phenotype, it may be beneficial to add in mitogenic factors such as PDGF-BB during the early stage culture period to induce a synthetic SMC phenotype to enhance cell proliferation and to improve ECM synthesis (Gong and Niklason, 2008).

¶ While we have demonstrated the ability to generate bilayered TEVGs which can be adaptable remodelled by SMCs, the idealised graft would require endothelialisation to further mimic native vessels and to ensure a non-thrombogenic response if implanted *in vivo.* Preliminary work has already been carried out to seed human umbilical vein endothelial cells on the luminal surface of these vessels, with the film layer supporting excellent cell attachment.

¶ While endothelialisation provides a non-thrombogenic interface for blood contacting vascular grafts, it also requires a fully confluent cell monolayer which may be disrupted during implantation or due to the challenging haemodynamic conditions. Consequently, the inherent thrombogenicity of the luminal layer is of great importance. To this end we are currently examining the inherent thrombogenicity of a number of proteins to act as a suitable basement membrane including collagen IV, laminin, and elastin. A custom microfluidic chip is being employed to gain a real-time measurement of the platelet response of whole human blood to each of the proteins both with and without a coating of endothelial cells.

6.7 Thesis conclusions

This study has shown that elastin addition to porous collagen scaffolds can play a major role in altering its biological and mechanical response. The addition of elastin was found to result in improved viscoelastic properties which indicates the biomaterial may possess sufficient recoil to be utilised for long-term cyclical distension for cardiovascular tissue engineering. Additionally, the presence of elastin resulted in a more contractile-like SMC phenotype which is necessary for vasoactivity and inhibition of intimal hyperplasia *in vivo*. This biomimetic biomaterial is amenable to multiple fabrication methods and represents a versatile biomaterial platform which is capable of being applied for numerous tissues including skin, elastic cartilage, lung tissue engineering, or as a cardiac patch for cell delivery.

Utilising the optimal biomaterial formulation, we subsequently developed a biomimetic tubular scaffold with a bilayered architecture and highly controllable properties for use as a tissue engineered vascular graft (TEVG). In order to hierarchically structure the scaffold, dense Coll-Eln films were developed with crosslinking utilised to modulate the residual amine content, mechanical properties, degradation resistance, and inflammatory cytokine expression from human macrophages. A biomimetic bilayered construct was subsequently developed with a porous tubular outer layer and a dense film

luminal lining using a custom mold. The microstructure of the outer porous scaffold section was further optimised by altering the freezing direction and mandrel materials. Initial *in vitro* results revealed the biomimetic TEVGs represented a promising platform for further *in vitro* maturation in order to enhance the therapeutic potential or application as an *in vitro* testing platform.

A novel pulsatile flow bioreactor was successfully designed, built, and validated which was capable of applying the complex cardiovascular biomechanical environment to four independent tubular TEVGs in a parallel circuit layout. The flexible chamber design permitted the mounting of TEVGs of varying dimensions, while we have shown the system to be non-cytotoxic and easy to assemble. The system can be utilised to apply physiological stresses and strains to cell-seeded vascular grafts in order to provide a suitable environment for tissue maturation with the appropriate biomechanical cues. Additionally, the bioreactor system could be utilised to evaluate the performance of medical devices in a physiologically relevant environment.

The optimal approach to enhance the *in vitro* maturation of the CE100 TEVGs was examined with alterations in TEVG architecture, crosslinking, and dynamic conditioning in the custom designed bioreactor. Bilayered TEVGs resulted in enhanced biomechanical properties (burst pressure, compliance, and suture retention) versus the single layer TEVGs, while maintaining suitable biological properties (cell density and collagen content). Biomechanical properties were further improved with EDAC crosslinking while TEVG remodelling through dynamic bioreactor conditioning resulted in an apparent increase in vessel wall density, improved cell density, and improved collagen circumferential alignment, which translated to a significant increase in burst pressure and a compliance closer matching native vessels. Additionally, these bioengineered vascular grafts displayed cell-mediated synthesis of the vascular proteins αSMA, calponin, and collagen III within the vessel wall, with enhanced cell migration observed in the dynamically conditioned TEVGs.

Bibliography

Aggarwal, S., Pittenger, M.F., 2005. Human mesenchymal stem cells modulate allogeneic immune cell responses. Blood 105, 1815–22.

Allaire, E., Bruneval, P., Mandet, C., Becquemin, J.-P., Michel, J.-B., 1997. The immunogenicity of the extracellular matrix in arterial xenografts. Surgery 122, 73–81.

Allen, R.A., Wu, W., Yao, M., Dutta, D., Duan, X., Bachman, T.N., Champion, H.C., Stolz, D.B., Robertson, A.M., Kim, K., Isenberg, J.S., Wang, Y., 2014. Nerve regeneration and elastin formation within poly(glycerol sebacate)-based synthetic arterial grafts one-year post-implantation in a rat model. Biomaterials 35, 165–73.

Al-Munajjed, A.A., O'Brien, F.J., 2009. Influence of a novel calcium-phosphate coating on the mechanical properties of highly porous collagen scaffolds for bone repair. J. Mech. Behav. Biomed. Mater. 2, 138–46.

Ang, G.C., 2005. History of skin transplantation. Clin. Dermatol. 23, 320–4.

Anidjar, S., Salzmann, J.L., Gentric, D., Lagneau, P., Camilleri, J.P., Michel, J.B., 1990. Elastase-induced experimental aneurysms in rats. Circulation 82, 973–81.

Annabi, N., Tsang, K., Mithieux, S.M., Nikkhah, M., Ameri, A., Khademhosseini, A., Weiss, A.S., 2013. Highly Elastic Micropatterned Hydrogel for Engineering Functional Cardiac Tissue. Adv. Funct. Mater. 23.

Arrigoni, C., Camozzi, D., Imberti, B., Mantero, S., Remuzzi, A., 2006. The effect of sodium ascorbate on the mechanical properties of hyaluronan-based vascular constructs. Biomaterials 27, 623–30.

Asahara, T., 1997. Isolation of Putative Progenitor Endothelial Cells for Angiogenesis. Science (80-.). 275, 964–966.

Athanasiou, K.A., Niederauer, G.G., Agrawal, C.M., 1996. Sterilization, toxicity, biocompatibility and clinical applications of polylactic acid/polyglycolic acid copolymers. Biomaterials 17, 93–102.

Avci-Adali, M., Kobba, J., Neumann, B., Lescan, M., Perle, N., Wilhelm, N., Wiedmaier, H., Schlensak, C., Wendel, H.P., 2013. Application of a rotating bioreactor consisting of low-cost and ready-to-use medical disposables for in vitro evaluation of the endothelialization efficiency of small-caliber vascular prostheses. J. Biomed. Mater. Res. B. Appl. Biomater. 101, 1061–8.

Badylak, S.F., Freytes, D.O., Gilbert, T.W., 2009. Extracellular matrix as a biological scaffold material: Structure and function. Acta Biomater. 5, 1–13.

Barocas, V.H., Girton, T.S., Tranquillo, R.T., 1998. Engineered alignment in media equivalents: magnetic prealignment and mandrel compaction. J. Biomech. Eng. 120, 660–6.

Bax, D. V, Rodgers, U.R., Bilek, M.M.M., Weiss, A.S., 2009. Cell adhesion to tropoelastin is mediated via the C-terminal GRKRK motif and integrin alphaVbeta3. J. Biol. Chem. 284, 28616–23.

Beamish, J.A., He, P., Kottke-Marchant, K., Marchant, R.E., 2010. Molecular regulation of contractile smooth muscle cell phenotype: implications for vascular tissue engineering. Tissue Eng. Part B. Rev. 16, 467–91.

Berardinelli, L., 2006. Grafts and graft materials as vascular substitutes for haemodialysis access construction. Eur. J. Vasc. Endovasc. Surg. 32, 203–11.

Berglund, J.D., Mohseni, M.M., Nerem, R.M., Sambanis, A., 2003. A biological hybrid model for collagen-based tissue engineered vascular constructs. Biomaterials 24, 1241–54.

Berglund, J.D., Nerem, R.M., Sambanis, A., 2005. Viscoelastic testing methodologies for tissue engineered blood vessels. J. Biomech. Eng. 127, 1176–84.

Berry, M.F., Engler, A.J., Woo, Y.J., Pirolli, T.J., Bish, L.T., Jayasankar, V., Morine, K.J., Gardner, T.J., Discher, D.E., Sweeney, H.L., 2006. Mesenchymal stem cell injection after myocardial infarction improves myocardial compliance. Am. J. Physiol. Heart Circ. Physiol. 290, H2196–203.

Bhana, B., Iyer, R.K., Chen, W.L.K., Zhao, R., Sider, K.L., Likhitpanichkul, M., Simmons, C.A., Radisic, M., 2010. Influence of substrate stiffness on the phenotype of heart cells. Biotechnol. Bioeng. 105, 1148–60.

Bhattacharya, A., Mahajan, R.L., 2003. Temperature dependence of thermal conductivity of biological tissues. Physiol. Meas. 24, 769–83.

Boland, E.D., Matthews, J.A., Pawlowski, K.J., Simpson, D.G., Wnek, G.E., Bowlin, G.L., 2004. Electrospinning collagen and elastin: preliminary vascular tissue engineering. Front. Biosci. 9, 1422–32.

Bouten, C.V.C., Dankers, P.Y.W., Driessen-Mol, A., Pedron, S., Brizard, A.M.A., Baaijens, F.P.T., 2011. Substrates for cardiovascular tissue engineering. Adv. Drug Deliv. Rev. 63, 221–41.

Brems, J., Castaneda, M., Garvin, P.J., 1986. A five-year experience with the bovine heterograft for vascular access. Arch. Surg. 121, 941–4.

Broekelmann, T.J., Ciliberto, C.H., Shifren, A., Mecham, R.P., 2008. Modification and functional inactivation of the tropoelastin carboxy-terminal domain in cross-linked elastin. Matrix Biol. 27, 631–9.

Brown, B.N., Londono, R., Tottey, S., Zhang, L., Kukla, K.A., Wolf, M.T., Daly, K.A., Reing, J.E., Badylak, S.F., 2012. Macrophage phenotype as a predictor of constructive remodeling following the implantation of biologically derived surgical mesh materials. Acta Biomater. 8, 978–87.

Bulick, A.S., Muñoz-Pinto, D.J., Qu, X., Mani, M., Cristancho, D., Urban, M., Hahn, M.S., 2009. Impact of endothelial cells and mechanical conditioning on smooth muscle cell extracellular matrix production and differentiation. Tissue Eng. Part A 15, 815–25.

Burrows, M.C., Zamarion, V.M., Filippin-Monteiro, F.B., Schuck, D.C., Toma, H.E., Campa, A., Garcia, C.R.S., Catalani, L.H., 2012. Hybrid scaffolds built from PET and collagen as a model for vascular graft architecture. Macromol. Biosci. 12, 1660–70.

Butler, D.L., Goldstein, S.A., Guilak, F., 2000. Functional Tissue Engineering: The Role of Biomechanics. J. Biomech. Eng. 122, 570.

Buttafoco, L., Engbers-Buijtenhuijs, P., Poot, A.A., Dijkstra, P.J., Daamen, W.F., van Kuppevelt, T.H., Vermes, I., Feijen, J., 2006a. First steps towards tissue engineering of small-diameter blood vessels: preparation of flat scaffolds of collagen and elastin by means of freeze drying. J. Biomed. Mater. Res. B. Appl. Biomater. 77, 357–68.

Buttafoco, L., Kolkman, N.G., Engbers-Buijtenhuijs, P., Poot, a a, Dijkstra, P.J., Vermes, I., Feijen, J., 2006b. Electrospinning of collagen and elastin for tissue engineering applications. Biomaterials 27, 724–34.

Caliari, S.R., Harley, B.A.C., 2014. Collagen-GAG Scaffold Biophysical Properties Bias MSC Lineage Choice in the Presence of Mixed Soluble Signals. Tissue Eng. Part A.

Caliari, S.R., Ramirez, M. a, Harley, B. a C., 2011. The development of collagen-GAG scaffold-membrane composites for tendon tissue engineering. Biomaterials 32, 8990–8.

Cameron, A.R., Frith, J.E., Gomez, G.A., Yap, A.S., Cooper-White, J.J., 2014. The effect of time-dependent deformation of viscoelastic hydrogels on myogenic induction and Rac1 activity in mesenchymal stem cells. Biomaterials 35, 1857–68.

Cao, Y., Mitchell, G., Messina, A., Price, L., Thompson, E., Penington, A., Morrison, W., O'Connor, A., Stevens, G., Cooper-White, J., 2006. The influence of architecture on degradation and tissue ingrowth into three-dimensional poly(lactic-co-glycolic acid) scaffolds in vitro and in vivo. Biomaterials 27, 2854–64.

Caro, C.G., 2012. The Mechanics of the Circulation, 2nd Editio. ed. Cambridge University Press.

Caro, C.G., Pedley, T.J., Schroter, R.C., 1978. Seed WA The Mechanics of the Circulation.

Cartmell, S.H., Dobson, J., Verschueren, S.B., El Haj, A.J., 2002. Development of magnetic particle techniques for long-term culture of bone cells with intermittent mechanical activation. IEEE Trans. Nanobioscience 1, 92–7.

Centre for Disease Control, 2013. National Vital Statistics Report: Heart Disease Facts & Statistics.

Charulatha, V., Rajaram, A., 1997. Crosslinking density and resorption of dimethyl suberimidate-treated collagen. J. Biomed. Mater. Res. 36, 478–86.

Charulatha, V., Rajaram, A., 2003. Influence of different crosslinking treatments on the physical properties of collagen membranes. Biomaterials 24, 759–67.

Chau, D.Y.S., Collighan, R.J., Verderio, E.A.M., Addy, V.L., Griffin, M., 2005. The cellular response to transglutaminase-cross-linked collagen. Biomaterials 26, 6518–29.

Chemla, E.S., Morsy, M., 2009. Randomized clinical trial comparing decellularized bovine ureter with expanded polytetrafluoroethylene for vascular access. Br. J. Surg. 96, 34–9.

Chen, R.-N., Ho, H.-O., Sheu, M.-T., 2005. Characterization of collagen matrices crosslinked using microbial transglutaminase. Biomaterials 26, 4229–35.

Cholewinski, E., Dietrich, M., Flanagan, T.C., Schmitz-Rode, T., Jockenhoevel, S., 2009. Tranexamic acid--an alternative to aprotinin in fibrin-based cardiovascular tissue engineering. Tissue Eng. Part A 15, 3645–53.

Chu, B., Gaillard, E., Mongrain, R., Reiter, S., Tardif, J.-C., 2013. Characterization of fracture toughness exhaustion in pig aorta. J. Mech. Behav. Biomed. Mater. 17, 126–36.

Cizek, S.M., Bedri, S., Talusan, P., Silva, N., Lee, H., Stone, J.R.,. Risk factors for atherosclerosis and the development of preatherosclerotic intimal hyperplasia. Cardiovasc. Pathol. 16, 344–50.

Colombo, A., Guha, S., Mackle, J.N., Cahill, P.A., Lally, C., 2013. Cyclic strain amplitude dictates the growth response of vascular smooth muscle cells in vitro: role in in-stent restenosis and inhibition with a sirolimus drug-eluting stent. Biomech. Model. Mechanobiol. 12, 671–83.

Conklin, B.S., Richter, E.R., Kreutziger, K.L., Zhong, D.-S., Chen, C., 2002. Development and evaluation of a novel decellularized vascular xenograft. Med. Eng. Phys. 24, 173–183.

Conklin, B.S., Surowiec, S.M., Lin, P.H., Chen, C., 2000. A simple physiologic pulsatile perfusion system for the study of intact vascular tissue. Med. Eng. Phys. 22, 441–9.

Connell, P.S., Han, R.I., Grande-Allen, K.J., 2012. Differentiating the aging of the mitral valve from human and canine myxomatous degeneration. J. Vet. Cardiol. 14, 31–45.

Corson, M.A., James, N.L., Latta, S.E., Nerem, R.M., Berk, B.C., Harrison, D.G., 1996. Phosphorylation of endothelial nitric oxide synthase in response to fluid shear stress. Circ. Res. 79, 984–91.

Couet, F., Mantovani, D., 2012. A new bioreactor adapts to materials state and builds a growth model for vascular tissue engineering. Artif. Organs 36, 438–45.

Couet, F., Meghezi, S., Mantovani, D., 2011. Fetal development, mechanobiology and optimal control processes can improve vascular

tissue regeneration in bioreactors: An integrative review. Med. Eng. Phys. 1–10.

Crapo, P.M., Gilbert, T.W., Badylak, S.F., 2011. An overview of tissue and whole organ decellularization processes. Biomaterials 32, 3233–43.

Crapo, P.M., Wang, Y., 2010. Physiologic compliance in engineered small-diameter arterial constructs based on an elastomeric substrate. Biomaterials 31, 1626–35.

Csiszar, K., 2001. Lysyl oxidases: a novel multifunctional amine oxidase family. Prog. Nucleic Acid Res. Mol. Biol. 70, 1–32.

Cummings, C.L., Gawlitta, D., Nerem, R.M., Stegemann, J.P., 2003. Properties of engineered vascular constructs made from collagen , fibrin , and collagen – fibrin mixtures.

Daamen, W.F., Nillesen, S.T.M., Hafmans, T., Veerkamp, J.H., van Luyn, M.J. a, van Kuppevelt, T.H., 2005. Tissue response of defined collagen-elastin scaffolds in young and adult rats with special attention to calcification. Biomaterials 26, 81–92.

Daamen, W.F., Nillesen, S.T.M., Wismans, R.G., Reinhardt, D.P., Hafmans, T., Veerkamp, J.H., van Kuppevelt, T.H., 2008. A biomaterial composed of collagen and solubilized elastin enhances angiogenesis and elastic fiber formation without calcification. Tissue Eng. Part A 14, 349–60.

Dahl, S.L.M., Kypson, A.P., Lawson, J.H., Blum, J.L., Strader, J.T., Li, Y., Manson, R.J., Tente, W.E., DiBernardo, L., Hensley, M.T., Carter, R., Williams, T.P., Prichard, H.L., Dey, M.S., Begelman, K.G., Niklason, L.E., 2011. Readily available tissue-engineered vascular grafts. Sci. Transl. Med. 3, 68ra9.

Dantzer, E., Braye, F.M., 2001. Reconstructive surgery using an artificial dermis (Integra): results with 39 grafts. Br. J. Plast. Surg. 54, 659–64.

Davidson, J.M., LuValle, P. a, Zoia, O., Quaglino, D., Giro, M., 1997. Ascorbate differentially regulates elastin and collagen biosynthesis in vascular smooth muscle cells and skin fibroblasts by pretranslational mechanisms. J. Biol. Chem. 272, 345–52.

Davies, P.F., 2009. Hemodynamic shear stress and the endothelium in cardiovascular pathophysiology. Nat. Clin. Pract. Cardiovasc. Med. 6, 16–26.

De Mel, A., Jell, G., Stevens, M.M., Seifalian, A.M., 2008. Biofunctionalization of biomaterials for accelerated in situ endothelialization: a review. Biomacromolecules 9, 2969–79.

De Torre, I.G., Wolf, F., Santos, M., Rongen, L., Alonso, M., Jockenhoevel, S., Rodríguez-Cabello, J.C., Mela, P., 2015. Elastin-like recombinamer-covered stents: Towards a fully biocompatible and non-thrombogenic device for cardiovascular diseases. Acta Biomater. 12, 146–55.

De Valence, S., Tille, J.-C., Mugnai, D., Mrowczynski, W., Gurny, R., Möller, M., Walpoth, B.H., 2012. Long term performance of polycaprolactone

vascular grafts in a rat abdominal aorta replacement model. Biomaterials 33, 38–47.

Deutsch, M., Meinhart, J., Fischlein, T., Preiss, P., Zilla, P., 1999. Clinical autologous in vitro endothelialization of infrainguinal ePTFE grafts in 100 patients: A 9-year experience. Surgery 126, 847–855.

Dimitrievska, S., Cai, C., Weyers, A., Balestrini, J.L., Lin, T., Sundaram, S., Hatachi, G., Spiegel, D.A., Kyriakides, T.R., Miao, J., Li, G., Niklason, L.E., Linhardt, R.J., 2015. Click-coated, heparinized, decellularized vascular grafts. Acta Biomater. 13, 177–87.

Discher, D.E., Janmey, P., Wang, Y.-L., 2005. Tissue cells feel and respond to the stiffness of their substrate. Science 310, 1139–43.

Duffy, G.P., McFadden, T.M., Byrne, E.M., Gill, S.-L., Farrell, E., O'Brien, F.J., 2011. Towards in vitro vascularisation of collagen-GAG scaffolds. Eur. Cell. Mater. 21, 15–30.

Dunphy, S.E., Bratt, J.A.J., Akram, K.M., Forsyth, N.R., El Haj, A.J., 2014. Hydrogels for lung tissue engineering: Biomechanical properties of thin collagen-elastin constructs. J. Mech. Behav. Biomed. Mater. 38, 251–9.

Dye, W.W., Gleason, R.L., Wilson, E., Humphrey, J.D., 2007. Altered biomechanical properties of carotid arteries in two mouse models of muscular dystrophy. J. Appl. Physiol. 103, 664–72.

Elbjeirami, W.M., Yonter, E.O., Starcher, B.C., West, J.L., 2003. Enhancing mechanical properties of tissue-engineered constructs via lysyl oxidase crosslinking activity. J. Biomed. Mater. Res. A 66, 513–21.

Engbers-Buijtenhuijs, P., Buttafoco, L., Poot, A. a, Dijkstra, P.J., de Vos, R. a I., Sterk, L.M.T., Geelkerken, R.H., Vermes, I., Feijen, J., 2006. Biological characterisation of vascular grafts cultured in a bioreactor. Biomaterials 27, 2390–7.

Engler, A.J., Sen, S., Sweeney, H.L., Discher, D.E., 2006. Matrix elasticity directs stem cell lineage specification. Cell 126, 677–89.

Enomoto, S., Sumi, M., Kajimoto, K., Nakazawa, Y., Takahashi, R., Takabayashi, C., Asakura, T., Sata, M., 2010. Long-term patency of small-diameter vascular graft made from fibroin, a silk-based biodegradable material. J. Vasc. Surg. 51, 155–64.

Everaerts, F., Torrianni, M., Hendriks, M., Feijen, J., 2008. Biomechanical properties of carbodiimide crosslinked collagen: influence of the formation of ester crosslinks. J. Biomed. Mater. Res. A 85, 547–55.

Flanagan, T.C., Cornelissen, C., Koch, S., Tschoeke, B., Sachweh, J.S., Schmitz-Rode, T., Jockenhoevel, S., 2007. The in vitro development of autologous fibrin-based tissue-engineered heart valves through optimised dynamic conditioning. Biomaterials 28, 3388–97.

Fratzl, P., Weinkamer, R., 2007. Nature's hierarchical materials. Prog. Mater. Sci. 52, 1263–1334.

Galie, P.A., Stegemann, J.P., 2011. Simultaneous application of interstitial flow and cyclic mechanical strain to a three-dimensional cell-seeded hydrogel. Tissue Eng. Part C. Methods 17, 527–36.

Gao, J., Crapo, P., Nerem, R., Wang, Y., 2008. Co-expression of elastin and collagen leads to highly compliant engineered blood vessels. J. Biomed. Mater. Res. A 85, 1120–8.

Garcia, Y., Wilkins, B., Collighan, R.J., Griffin, M., Pandit, A., 2008. Towards development of a dermal rudiment for enhanced wound healing response. Biomaterials 29, 857–68.

Gershon, B., Cohn, D., Marom, G., 1992. Compliance and ultimate strength of composite arterial prostheses. Biomaterials 13, 38–43.

Girton, T.S., Oegema, T.R., Grassl, E.D., Isenberg, B.C., Tranquillo, R.T., 2000. Mechanisms of stiffening and strengthening in media-equivalents fabricated using glycation. J. Biomech. Eng. 122, 216–23.

Gleeson, J.P., O'Brien, F.J., 2011. Composite scaffolds for orthopaedic regenerative medicine. In: Attaf, B. (Ed.), Advances in Composite Materials for Medicine and Nanotechnology. InTech, Rijecka, Croatia, pp. 34–52.

Golomb, G., Schoen, F.J., Smith, M.S., Linden, J., Dixon, M., Levy, R.J., 1987. The role of glutaraldehyde-induced cross-links in calcification of bovine pericardium used in cardiac valve bioprostheses. Am. J. Pathol. 127, 122–30.

Gong, Z., Niklason, L.E., 2008. Small-diameter human vessel wall engineered from bone marrow-derived mesenchymal stem cells (hMSCs). FASEB J. 22, 1635–48.

Gong, Z., Niklason, L.E., 2011. Use of human mesenchymal stem cells as alternative source of smooth muscle cells in vessel engineering. Methods Mol. Biol. 698, 279–94.

Gorham, S.D., Light, N.D., Diamond, A.M., Willins, M.J., Bailey, A.J., Wess, T.J., Leslie, N.J., 1992. Effect of chemical modifications on the susceptibility of collagen to proteolysis. II. Dehydrothermal crosslinking. Int. J. Biol. Macromol. 14, 129–138.

Gough, J.E., Scotchford, C.A., Downes, S., 2002. Cytotoxicity of glutaraldehyde crosslinked collagen/poly(vinyl alcohol) films is by the mechanism of apoptosis. J. Biomed. Mater. Res. 61, 121–30.

Grassl, E.D., Oegema, T.R., Tranquillo, R.T., 2003. A fibrin-based arterial media equivalent. J. Biomed. Mater. Res. A 66, 550–61.

Grouf, J.L., Throm, A.M., Balestrini, J.L., Bush, K.A., Billiar, K.L., 2007. Differential effects of EGF and TGF-beta1 on fibroblast activity in fibrin-based tissue equivalents. Tissue Eng. 13, 799–807.

Grover, C.N., Cameron, R.E., Best, S.M., 2012. Investigating the morphological, mechanical and degradation properties of scaffolds comprising collagen, gelatin and elastin for use in soft tissue engineering. J. Mech. Behav. Biomed. Mater. 10, 62–74.

Guidoin, R., Domurado, D., Couture, J., Dubé, S., Marois, M., Roy, P.E., Sigot, M.F., Martin, L., 1989. Chemically processed bovine heterografts of the second generation as arterial substitutes: a comparative evaluation of three commercial prostheses. J. Cardiovasc. Surg. (Torino). 30, 202–9.

Guillotin, B., Guillemot, F., 2011. Cell patterning technologies for organotypic tissue fabrication. Trends Biotechnol. 29, 183–90.

Gwyther, T.A., Hu, J.Z., Christakis, A.G., Skorinko, J.K., Shaw, S.M., Billiar, K.L., Rolle, M.W., 2011. Engineered vascular tissue fabricated from aggregated smooth muscle cells. Cells. Tissues. Organs 194, 13–24.

Hafemann, B., Ghofrani, K., Gattner, H.G., Stieve, H., Pallua, N., 2001. Cross-linking by 1-ethyl-3- (3-dimethylaminopropyl)-carbodiimide (EDC) of a collagen/elastin membrane meant to be used as a dermal substitute: effects on physical, biochemical and biological features in vitro. J. Mater. Sci. Mater. Med. 12, 437–46.

Hahn, M.S., McHale, M.K., Wang, E., Schmedlen, R.H., West, J.L., 2007. Physiologic pulsatile flow bioreactor conditioning of poly(ethylene glycol)-based tissue engineered vascular grafts. Ann. Biomed. Eng. 35, 190–200.

Halpern, V.J., Nackman, G.B., Gandhi, R.H., Irizarry, E., Scholes, J. V, Ramey, W.G., Tilson, M.D., 1994. The elastase infusion model of experimental aortic aneurysms: synchrony of induction of endogenous proteinases with matrix destruction and inflammatory cell response. J. Vasc. Surg. 20, 51–60.

Han, J., Lazarovici, P., Pomerantz, C., Chen, X., Wei, Y., Lelkes, P.I., 2011. Co-electrospun blends of PLGA, gelatin, and elastin as potential nonthrombogenic scaffolds for vascular tissue engineering. Biomacromolecules 12, 399–408.

Harley, B. a, Hastings, A.Z., Yannas, I. V, Sannino, A., 2006. Fabricating tubular scaffolds with a radial pore size gradient by a spinning technique. Biomaterials 27, 866–74.

Harley, B.A., Leung, J.H., Silva, E.C.C.M., Gibson, L.J., 2007. Mechanical characterization of collagen-glycosaminoglycan scaffolds. Acta Biomater. 3, 463–474.

Harley, B.A., Spilker, M.H., Wu, J.W., Asano, K., Hsu, H.-P., Spector, M., Yannas, I. V, 2004. Optimal degradation rate for collagen chambers used for regeneration of peripheral nerves over long gaps. Cells. Tissues. Organs 176, 153–65.

Haugh, M.G., Jaasma, M.J., O'Brien, F.J., 2009. The effect of dehydrothermal treatment on the mechanical and structural properties of collagen-GAG scaffolds. J. Biomed. Mater. Res. A 89, 363–9.

Haugh, M.G., Murphy, C.M., McKiernan, R.C., Altenbuchner, C., O'Brien, F.J., 2011. Crosslinking and mechanical properties significantly influence cell attachment, proliferation, and migration within collagen glycosaminoglycan scaffolds. Tissue Eng. Part A 17, 1201–8.

Haugh, M.G., Murphy, C.M., O'Brien, F.J., 2010. Novel freeze-drying methods to produce a range of collagen-glycosaminoglycan scaffolds with tailored mean pore sizes. Tissue Eng. Part C. Methods 16, 887–94.

He, H., Matsuda, T., 2002. Arterial replacement with compliant hierarchic hybrid vascular graft: biomechanical adaptation and failure. Tissue Eng. 8, 213–24.

Heim, F., Gupta, B.S., 2009. Textile Heart Valve Prosthesis: The Effect of Fabric Construction Parameters on Long-term Durability. Text. Res. J. 79, 1001–1013.

Hey, K.B., Lachs, C.M., Raxworthy, M.J., Wood, E.J., 1990. Crosslinked fibrous collagen for use as a dermal implant: control of the cytotoxic effects of glutaraldehyde and dimethylsuberimidate. Biotechnol. Appl. Biochem. 12, 85–93.

Heydarkhan-Hagvall, S., Schenke-Layland, K., Dhanasopon, A.P., Rofail, F., Smith, H., Wu, B.M., Shemin, R., Beygui, R.E., MacLellan, W.R., 2008. Three-dimensional electrospun ECM-based hybrid scaffolds for cardiovascular tissue engineering. Biomaterials 29, 2907–14.

Hirai, J., Kanda, K., Oka, T., Matsuda, T., 1994. Highly oriented, tubular hybrid vascular tissue for a low pressure circulatory system. ASAIO J. 40, M383–8.

Hoerstrup, S.P., Zünd, G., Sodian, R., Schnell, a M., Grünenfelder, J., Turina, M.I., 2001. Tissue engineering of small caliber vascular grafts. Eur. J. Cardiothorac. Surg. 20, 164–9.

Hoffmann, U., Kwait, D.C., Handwerker, J., Chan, R., Lamuraglia, G., Brady, T.J., 2003. Vascular calcification in ex vivo carotid specimens: precision and accuracy of measurements with multi-detector row CT. Radiology 229, 375–81.

Holzapfel, G.A., Gasser, T.C., Ogden, R.W., 2000. A New Constitutive Framework for Arterial Wall Mechanics and a Comparative Study of Material Models. J. Elast. Phys. Sci. solids 61, 1–48.

Holzapfel, G.A., Sommer, G., Gasser, C.T., Regitnig, P., 2005. Determination of layer-specific mechanical properties of human coronary arteries with nonatherosclerotic intimal thickening and related constitutive modeling. Am. J. Physiol. Heart Circ. Physiol. 289, H2048–58.

Huang, A.H., Niklason, L.E., 2011. Engineering biological-based vascular grafts using a pulsatile bioreactor. J. Vis. Exp.

Humphrey, J.D., 2013. Cardiovascular Solid Mechanics: Cells, Tissues, and Organs. Springer Science & Business Media.

Humphrey, J.D., Eberth, J.F., Dye, W.W., Gleason, R.L., 2009. Fundamental role of axial stress in compensatory adaptations by arteries. J. Biomech. 42, 1–8.

Huynh, T., Abraham, G., Murray, J., Brockbank, K., Hagen, P.O., Sullivan, S., 1999. Remodeling of an acellular collagen graft into a physiologically responsive neovessel. Nat. Biotechnol. 17, 1083–6.

Huynh, T.N., Tranquillo, R.T., 2010. Fusion of concentrically layered tubular tissue constructs increases burst strength. Ann. Biomed. Eng. 38, 2226–36.

Ibusuki, S., Halbesma, G.J., Randolph, M.A., Redmond, R.W., Kochevar, I.E., Gill, T.J., 2007. Photochemically cross-linked collagen gels as three-dimensional scaffolds for tissue engineering. Tissue Eng. 13, 1995–2001.

Ignat'eva, N.Y., Danilov, N.A., Averkiev, S. V., Obrezkova, M. V., Lunin, V. V., Sobol', E.N., 2007. Determination of hydroxyproline in tissues and the evaluation of the collagen content of the tissues. J. Anal. Chem. 62, 51–57.

Imberti, B., Seliktar, D., Nerem, R.M., Remuzzi, A., 2002. The response of endothelial cells to fluid shear stress using a co-culture model of the arterial wall. Endothelium 9, 11–23.

Inoguchi, H., Tanaka, T., Maehara, Y., Matsuda, T., 2007. The effect of gradually graded shear stress on the morphological integrity of a huvec-seeded compliant small-diameter vascular graft. Biomaterials 28, 486–95.

Isenberg, B.C., Tranquillo, R.T., 2003. Long-Term Cyclic Distention Enhances the Mechanical Properties of Collagen-Based Media-Equivalents. Ann. Biomed. Eng. 31, 937–949.

Isenberg, B.C., Williams, C., Tranquillo, R.T., 2006. Small-diameter artificial arteries engineered in vitro. Circ. Res. 98, 25–35.

Iwasaki, K., Kojima, K., Kodama, S., Paz, A.C., Chambers, M., Umezu, M., Vacanti, C. a, 2008. Bioengineered three-layered robust and elastic artery using hemodynamically-equivalent pulsatile bioreactor. Circulation 118, S52–7.

Jeong, S.I., Kwon, J.H., Lim, J.I., Cho, S.-W., Jung, Y., Sung, W.J., Kim, S.H., Kim, Y.H., Lee, Y.M., Kim, B.-S., Choi, C.Y., Kim, S.-J., 2005. Mechano-active tissue engineering of vascular smooth muscle using pulsatile perfusion bioreactors and elastic PLCL scaffolds. Biomaterials 26, 1405–11.

Jockenhoevel, S., 2001. Fibrin gel – advantages of a new scaffold in cardiovascular tissue engineering. Eur. J. Cardio-Thoracic Surg. 19, 424–430.

Jockenhoevel, S., Chalabi, K., Sachweh, J.S., Groesdonk, H. V, Demircan, L., Grossmann, M., Zund, G., Messmer, B.J., 2001. Tissue engineering: complete autologous valve conduit--a new moulding technique. Thorac. Cardiovasc. Surg. 49, 287–90.

Johnson, T.R., Tomaszewski, J.E., Carpenter, J.P., 2000. Cellular repopulation of human vein allograft bypass grafts. J. Vasc. Surg. 31, 994–1002.

Jorge-Herrero, E., Fernández, P., Turnay, J., Olmo, N., Calero, P., García, R., Freile, I., Castillo-Olivares, J.., 1999. Influence of different chemical cross-linking treatments on the properties of bovine pericardium and collagen. Biomaterials 20, 539–545.

Jun, H.-W., West, J.L., 2005. Endothelialization of microporous YIGSR/PEG-modified polyurethaneurea. Tissue Eng. 11, 1133–40.

Kakisis, J.D., Liapis, C.D., Breuer, C., Sumpio, B.E., 2005. Artificial blood vessel: the Holy Grail of peripheral vascular surgery. J. Vasc. Surg. Off. Publ. Soc. Vasc. Surg. [and] Int. Soc. Cardiovasc. Surgery, North Am. Chapter 41, 349–54.

Kanda, K., Matsuda, T., 1994. In vitro reconstruction of hybrid arterial media with molecular and cellular orientations. Cell Transplant. 3, 537–45.

Kang, H.W., Tabata, Y., Ikada, Y., 1999. Fabrication of porous gelatin scaffolds for tissue engineering. Biomaterials 20, 1339–44.

Kappetein, A.P., Feldman, T.E., Mack, M.J., Morice, M.-C., Holmes, D.R., Ståhle, E., Dawkins, K.D., Mohr, F.W., Serruys, P.W., Colombo, A., 2011. Comparison of coronary bypass surgery with drug-eluting stenting for the treatment of left main and/or three-vessel disease: 3-year follow-up of the SYNTAX trial. Eur. Heart J. 32, 2125–34.

Karageorgiou, V., Kaplan, D., 2005. Porosity of 3D biomaterial scaffolds and osteogenesis. Biomaterials 26, 5474–5491.

Karnik, S.K., Brooke, B.S., Bayes-Genis, A., Sorensen, L., Wythe, J.D., Schwartz, R.S., Keating, M.T., Li, D.Y., 2003. A critical role for elastin signaling in vascular morphogenesis and disease. Development 130, 411–23.

Karnik, S.K., Wythe, J.D., Sorensen, L., Brooke, B.S., Urness, L.D., Li, D.Y., 2003. Elastin induces myofibrillogenesis via a specific domain, VGVAPG. Matrix Biol. 22, 409–425.

Katsumi, A., Orr, A.W., Tzima, E., Schwartz, M.A., 2004. Integrins in mechanotransduction. J. Biol. Chem. 279, 12001–4.

Kaushal, S., Amiel, G.E., Guleserian, K.J., Shapira, O.M., Perry, T., Sutherland, F.W., Rabkin, E., Moran, A.M., Schoen, F.J., Atala, A., Soker, S., Bischoff, J., Mayer, J.E., 2001. Functional small-diameter neovessels created using endothelial progenitor cells expanded ex vivo. Nat. Med. 7, 1035–40.

Kelm, J.M., Lorber, V., Snedeker, J.G., Schmidt, D., Broggini-Tenzer, A., Weisstanner, M., Odermatt, B., Mol, A., Zünd, G., Hoerstrup, S.P., 2010. A novel concept for scaffold-free vessel tissue engineering: self-assembly of microtissue building blocks. J. Biotechnol. 148, 46–55.

Kemp, P.D., Cavallaro, J.F., Hastings, D.N., 1995. Effects of carbodiimide crosslinking and load environment on the remodeling of collagen scaffolds. Tissue Eng. 1, 71–9.

Khamdaeng, T., Luo, J., Vappou, J., Terdtoon, P., Konofagou, E.E., 2012. Arterial stiffness identification of the human carotid artery using the stress-strain relationship in vivo. Ultrasonics 52, 402–11.

Kim, B.S., Nikolovski, J., Bonadio, J., Mooney, D.J., 1999a. Cyclic mechanical strain regulates the development of engineered smooth muscle tissue. Nat. Biotechnol. 17, 979–83.

Kim, B.S., Nikolovski, J., Bonadio, J., Smiley, E., Mooney, D.J., 1999b. Engineered smooth muscle tissues: regulating cell phenotype with the scaffold. Exp. Cell Res. 251, 318–28.

Kim, D.H., Yoo, K.H., Choi, K.S., Choi, J., Choi, S.-Y., Yang, S.-E., Yang, Y.-S., Im, H.J., Kim, K.H., Jung, H.L., Sung, K.W., Koo, H.H., 2005. Gene expression profile of cytokine and growth factor during differentiation of bone marrow-derived mesenchymal stem cell. Cytokine 31, 119–26.

Kobayashi, N., Yasu, T., Ueba, H., Sata, M., Hashimoto, S., Kuroki, M., Saito, M., Kawakami, M., 2004. Mechanical stress promotes the expression of smooth muscle-like properties in marrow stromal cells. Exp. Hematol. 32, 1238–45.

Koch, S., Flanagan, T.C., Sachweh, J.S., Tanios, F., Schnoering, H., Deichmann, T., Ellä, V., Kellomäki, M., Gronloh, N., Gries, T., Tolba, R., Schmitz-Rode, T., Jockenhoevel, S., 2010. Fibrin-polylactide-based tissue-engineered vascular graft in the arterial circulation. Biomaterials 31, 4731–9.

Koch, S., Stappenbeck, N., Cornelissen, C.G., Flanagan, T.C., Mela, P., Sachweh, J., Hermanns-Sachweh, B., Jockenhoevel, S., 2012. Tissue engineering: selecting the optimal fixative for immunohistochemistry. Tissue Eng. Part C. Methods 18, 976–83.

Koens, M.J.W., Faraj, K. a, Wismans, R.G., van der Vliet, J. a, Krasznai, a G., Cuijpers, V.M.J.I., Jansen, J. a, Daamen, W.F., van Kuppevelt, T.H., 2010. Controlled fabrication of triple layered and molecularly defined collagen/elastin vascular grafts resembling the native blood vessel. Acta Biomater. 6, 4666–74.

Koens, M.J.W., Krasznai, A.G., Hanssen, A.E.J., Hendriks, T., Praster, R., Daamen, W.F., van der Vliet, J.A., van Kuppevelt, T.H., 2015. Vascular replacement using a layered elastin-collagen vascular graft in a porcine model: one week patency versus one month occlusion. Organogenesis 11, 105–21.

Koh, C.J., Atala, A., 2004. Tissue engineering, stem cells, and cloning: opportunities for regenerative medicine. J. Am. Soc. Nephrol. 15, 1113–25.

Kona, S., Chellamuthu, P., Xu, H., Hills, S.R., Nguyen, K.T., 2009. Effects of cyclic strain and growth factors on vascular smooth muscle cell responses. Open Biomed. Eng. J. 3, 28–38.

Konig, G., McAllister, T.N., Dusserre, N., Garrido, S. a, Iyican, C., Marini, A., Fiorillo, A., Avila, H., Wystrychowski, W., Zagalski, K., Maruszewski, M., Jones, A.L., Cierpka, L., de la Fuente, L.M., L'Heureux, N., 2009.

Mechanical properties of completely autologous human tissue engineered blood vessels compared to human saphenous vein and mammary artery. Biomaterials 30, 1542–50.

Konig, G., Mcallister, T.N., Ph, D., Dusserre, N., Garrido, S.A., Iyican, C., Marini, A., Fiorillo, A., Avila, H., Zagalski, K., Maruszewski, M., 2010. and mammary artery 30, 1542–1550.

Kornet, L., Hoeks, A.P., Lambregts, J., Reneman, R.S., 2000. Mean wall shear stress in the femoral arterial bifurcation is low and independent of age at rest. J. Vasc. Res. 37, 112–22.

Kothapalli, C.R., Ramamurthi, A., 2009a. Biomimetic regeneration of elastin matrices using hyaluronan and copper ion cues. Tissue Eng. Part A 15, 103–13.

Kothapalli, C.R., Ramamurthi, A., 2009b. Lysyl oxidase enhances elastin synthesis and matrix formation by vascular smooth muscle cells. J. Tissue Eng. Regen. Med. 3, 655–61.

Koullias, G., Modak, R., Tranquilli, M., Korkolis, D.P., Barash, P., Elefteriades, J.A., 2005. Mechanical deterioration underlies malignant behavior of aneurysmal human ascending aorta. J. Thorac. Cardiovasc. Surg. 130, 677–83.

Krishnan, A. V, Stathis, P., Permuth, S.F., Tokes, L., Feldman, D., 1993. Bisphenol-A: an estrogenic substance is released from polycarbonate flasks during autoclaving. Endocrinology 132, 2279–86.

Kumar, V., Abbas, A.K., Aster, J.C., 2014. Robbins and Cotran Pathologic Basis of Disease. Elsevier/Saunders.

Kumar, V.A., Caves, J.M., Haller, C.A., Dai, E., Liu, L., Grainger, S., Chaikof, E.L., 2013. Acellular vascular grafts generated from collagen and elastin analogs. Acta Biomater. 9, 8067–74.

Kundu, B., Rajkhowa, R., Kundu, S.C., Wang, X., 2013. Silk fibroin biomaterials for tissue regenerations. Adv. Drug Deliv. Rev. 65, 457–70.

Kural, M.H., Cai, M., Tang, D., Gwyther, T., Zheng, J., Billiar, K.L., 2012. Planar biaxial characterization of diseased human coronary and carotid arteries for computational modeling. J. Biomech. 45, 790–8.

Kurane, A., Simionescu, D.T., Vyavahare, N.R., 2007. In vivo cellular repopulation of tubular elastin scaffolds mediated by basic fibroblast growth factor. Biomaterials 28, 2830–8.

L'Heureux, N., Germain, L., Labbé, R., Auger, F.A., 1993. In vitro construction of a human blood vessel from cultured vascular cells: A morphologic study. J. Vasc. Surg. 17, 499–509.

L'Heureux, N., McAllister, T.N., 2010. Preparation And Use Of Cell-Synthesized Threads.

L'Heureux, N., McAllister, T.N., de la Fuente, L.M., 2007. Tissue-engineered blood vessel for adult arterial revascularization. N. Engl. J. Med. 357, 1451–3.

L'Heureux, N., Pâquet, S., Labbé, R., Germain, L., Auger, F.A., 1998. A completely biological tissue-engineered human blood vessel. FASEB J. 12, 47–56.

L'Heureux, N., Stoclet, J.C., Auger, F.A., Lagaud, G.J., Germain, L., Andriantsitohaina, R., 2001. A human tissue-engineered vascular media: a new model for pharmacological studies of contractile responses. FASEB J. 15, 515–24.

Lammers, G., Tjabringa, G.S., Schalkwijk, J., Daamen, W.F., van Kuppevelt, T.H., 2009. A molecularly defined array based on native fibrillar collagen for the assessment of skin tissue engineering biomaterials. Biomaterials 30, 6213–20.

Langer, R., Vacanti, J., 1993. Tissue engineering. Science (80-.). 260, 920–926.

Lattouf, R., Younes, R., Lutomski, D., Naaman, N., Godeau, G., Senni, K., Changotade, S., 2014. Picrosirius red staining: a useful tool to appraise collagen networks in normal and pathological tissues. J. Histochem. Cytochem. 62, 751–8.

Leach, J.B., Wolinsky, J.B., Stone, P.J., Wong, J.Y., 2005. Crosslinked alpha-elastin biomaterials: towards a processable elastin mimetic scaffold. Acta Biomater. 1, 155–64.

Lee, K.-W., Stolz, D.B., Wang, Y., 2011. Substantial expression of mature elastin in arterial constructs. Proc. Natl. Acad. Sci. U. S. A. 108, 2705–10.

Lee, K.-W., Wang, Y., 2011. Elastomeric PGS scaffolds in arterial tissue engineering. J. Vis. Exp.

Lee, M., Wu, B.M., Dunn, J.C.Y., 2008. Effect of scaffold architecture and pore size on smooth muscle cell growth. J. Biomed. Mater. Res. A 87, 1010–6.

Lee, P., Bax, D. V, Bilek, M.M.M., Weiss, A.S., 2014. A novel cell adhesion region in tropoelastin mediates attachment to integrin αVβ5. J. Biol. Chem. 289, 1467–77.

Lendlein, A., Schmidt, A.M., Langer, R., 2001. AB-polymer networks based on oligo(epsilon-caprolactone) segments showing shape-memory properties. Proc. Natl. Acad. Sci. U. S. A. 98, 842–7.

Levesque, M.J., Nerem, R.M., Sprague, E.A., 1990. Vascular endothelial cell proliferation in culture and the influence of flow. Biomaterials 11, 702–7.

Li, D.Y., Brooke, B., Davis, E.C., Mecham, R.P., Sorensen, L.K., Boak, B.B., Eichwald, E., Keating, M.T., 1998a. Elastin is an essential determinant of arterial morphogenesis. Nature 393, 276–80.

Li, D.Y., Faury, G., Taylor, D.G., Davis, E.C., Boyle, W.A., Mecham, R.P., Stenzel, P., Boak, B., Keating, M.T., 1998b. Novel arterial pathology in mice and humans hemizygous for elastin. J. Clin. Invest. 102, 1783–7.

Li, S., Henry, J.J.D., 2011. Nonthrombogenic approaches to cardiovascular bioengineering. Annu. Rev. Biomed. Eng. 13, 451–75.

Libby, P., Ridker, P.M., Hansson, G.K., 2011. Progress and challenges in translating the biology of atherosclerosis. Nature 473, 317–25.

Lim, D.W., Nettles, D.L., Setton, L.A., Chilkoti, A., 2008. In situ cross-linking of elastin-like polypeptide block copolymers for tissue repair. Biomacromolecules 9, 222–30.

Lin, A.P., Bennett, E., Wisk, L.E., Gharib, M., Fraser, S.E., Wen, H., 2008. Circumferential strain in the wall of the common carotid artery: comparing displacement-encoded and cine MRI in volunteers. Magn. Reson. Med. 60, 8–13.

Lin, S., Sandig, M., Mequanint, K., 2011. Three-dimensional topography of synthetic scaffolds induces elastin synthesis by human coronary artery smooth muscle cells. Tissue Eng. Part A 17, 1561–71.

Long, J.L., Tranquillo, R.T., 2003. Elastic fiber production in cardiovascular tissue-equivalents. Matrix Biol. 22, 339–50.

Longchamp, A., Alonso, F., Dubuis, C., Allagnat, F., Berard, X., Meda, P., Saucy, F., Corpataux, J.-M., Déglise, S., Haefliger, J.-A., 2014. The use of external mesh reinforcement to reduce intimal hyperplasia and preserve the structure of human saphenous veins. Biomaterials 35, 2588–99.

Loree, H.M., Grodzinsky, A.J., Park, S.Y., Gibson, L.J., Lee, R.T., 1994. Static circumferential tangential modulus of human atherosclerotic tissue. J. Biomech. 27, 195–204.

Lovett, M.L., Cannizzaro, C.M., Vunjak-Novakovic, G., Kaplan, D.L., 2008. Gel spinning of silk tubes for tissue engineering. Biomaterials 29, 4650–7.

Lozito, T.P., Kuo, C.K., Taboas, J.M., Tuan, R.S., 2009. Human mesenchymal stem cells express vascular cell phenotypes upon interaction with endothelial cell matrix. J. Cell. Biochem. 107, 714–22.

Lu, P., Takai, K., Weaver, V.M., Werb, Z., 2011. Extracellular matrix degradation and remodeling in development and disease. Cold Spring Harb. Perspect. Biol. 3.

Lüscher, T.F., 1990. Endothelium-derived vasoactive factors and regulation of vascular tone in human blood vessels. Lung 168, 27–34.

Lynn, A.K., Yannas, I. V, Bonfield, W., 2004. Antigenicity and immunogenicity of collagen. J. Biomed. Mater. Res. B. Appl. Biomater. 71, 343–54.

Ma, H., Hu, J., Ma, P.X., 2010. Polymer scaffolds for small-diameter vascular tissue engineering. Adv. Funct. Mater. 20, 2833–2841.

Makris, E.A., Responte, D.J., Paschos, N.K., Hu, J.C., Athanasiou, K.A., 2014. Developing functional musculoskeletal tissues through hypoxia and lysyl oxidase-induced collagen cross-linking. Proc. Natl. Acad. Sci. U. S. A. 111, E4832–41.

Malek, A.M., Alper, S.L., Izumo, S., 1999. Hemodynamic shear stress and its role in atherosclerosis. JAMA 282, 2035–42.

Marelli, B., Alessandrino, A., Farè, S., Freddi, G., Mantovani, D., Tanzi, M.C., 2010. Compliant electrospun silk fibroin tubes for small vessel bypass grafting. Acta Biomater. 6, 4019–26.

Marga, F., Jakab, K., Khatiwala, C., Shepherd, B., Dorfman, S., Hubbard, B., Colbert, S., Gabor, F., 2012. Toward engineering functional organ modules by additive manufacturing. Biofabrication 4, 022001.

Martino, M.M., Mochizuki, M., Rothenfluh, D.A., Rempel, S.A., Hubbell, J.A., Barker, T.H., 2009. Controlling integrin specificity and stem cell differentiation in 2D and 3D environments through regulation of fibronectin domain stability. Biomaterials 30, 1089–97.

Mason, B.N., Starchenko, A., Williams, R.M., Bonassar, L.J., Reinhart-King, C.A., 2013. Tuning three-dimensional collagen matrix stiffness independently of collagen concentration modulates endothelial cell behavior. Acta Biomater. 9, 4635–44.

Matsumura, G., Isayama, N., Matsuda, S., Taki, K., Sakamoto, Y., Ikada, Y., Yamazaki, K., 2013. Long-term results of cell-free biodegradable scaffolds for in situ tissue engineering of pulmonary artery in a canine model. Biomaterials 34, 6422–8.

Mattsson, E.J., Kohler, T.R., Vergel, S.M., Clowes, A.W., 1997. Increased blood flow induces regression of intimal hyperplasia. Arterioscler. Thromb. Vasc. Biol. 17, 2245–9.

McClure, M.J., Simpson, D.G., Bowlin, G.L., 2012. Tri-layered vascular grafts composed of polycaprolactone, elastin, collagen, and silk: Optimization of graft properties. J. Mech. Behav. Biomed. Mater. 10, 48–61.

McDade, J.K., Brennan-Pierce, E.P., Ariganello, M.B., Labow, R.S., Michael Lee, J., 2013. Interactions of U937 macrophage-like cells with decellularized pericardial matrix materials: influence of crosslinking treatment. Acta Biomater. 9, 7191–9.

McKee, J.A., Banik, S.S.R., Boyer, M.J., Hamad, N.M., Lawson, J.H., Niklason, L.E., Counter, C.M., 2003. Human arteries engineered in vitro. EMBO Rep. 4, 633–8.

Meinhart, J.G., Schense, J.C., Schima, H., Gorlitzer, M., Hubbell, J.A., Deutsch, M., Zilla, P., 2005. Enhanced endothelial cell retention on shear-stressed synthetic vascular grafts precoated with RGD-cross-linked fibrin. Tissue Eng. 11, 887–95.

Mi, S., Khutoryanskiy, V. V, Jones, R.R., Zhu, X., Hamley, I.W., Connon, C.J., 2011. Photochemical cross-linking of plastically compressed collagen gel produces an optimal scaffold for corneal tissue engineering. J. Biomed. Mater. Res. A 99, 1–8.

Mikos, A.G., Sarakinos, G., Lyman, M.D., Ingber, D.E., Vacanti, J.P., Langer, R., 1993. Prevascularization of porous biodegradable polymers. Biotechnol. Bioeng. 42, 716–23.

Miles, C.A., Bailey, A.J., 2001. Thermally labile domains in the collagen molecule. Micron 32, 325–32.

Mitchell, G.F., Parise, H., Vita, J.A., Larson, M.G., Warner, E., Keaney, J.F., Keyes, M.J., Levy, D., Vasan, R.S., Benjamin, E.J., 2004. Local shear stress and brachial artery flow-mediated dilation: the Framingham Heart Study. Hypertension 44, 134–9.

Mithieux, S.M., Rasko, J.E.J., Weiss, A.S., 2004. Synthetic elastin hydrogels derived from massive elastic assemblies of self-organized human protein monomers. Biomaterials 25, 4921–7.

Mochizuki, S., Brassart, B., Hinek, A., 2002. Signaling pathways transduced through the elastin receptor facilitate proliferation of arterial smooth muscle cells. J. Biol. Chem. 277, 44854–63.

Mohr, F.W., Morice, M.-C., Kappetein, A.P., Feldman, T.E., Ståhle, E., Colombo, A., Mack, M.J., Holmes, D.R., Morel, M., Van Dyck, N., Houle, V.M., Dawkins, K.D., Serruys, P.W., 2013. Coronary artery bypass graft surgery versus percutaneous coronary intervention in patients with three-vessel disease and left main coronary disease: 5-year follow-up of the randomised, clinical SYNTAX trial. Lancet 381, 629–38.

Moore, J.E., Bürki, E., Suciu, A., Zhao, S., Burnier, M., Brunner, H.R., Meister, J.J., 1994. A device for subjecting vascular endothelial cells to both fluid shear stress and circumferential cyclic stretch. Ann. Biomed. Eng. 22, 416–22.

Moritani, M., Hayashi, N., Utsuo, A., Kawai, H., 1971. Light-Scattering Patterns from Collagen Films in Relation to the Texture of a Random Assembly of Anisotropic Rods in Three Dimensions. Polym. J. 2, 74–87.

Mozaffarian, D., Benjamin, E.J., Go, A.S., Arnett, D.K., Blaha, M.J., Cushman, M., de Ferranti, S., Després, J.-P., Fullerton, H.J., Howard, V.J., Huffman, M.D., Judd, S.E., Kissela, B.M., Lackland, D.T.,, et al., 2014. Heart Disease and Stroke Statistics-2015 Update: A Report From the American Heart Association. Circulation 131, e29–322.

Murphy, C.M., Haugh, M.G., O'Brien, F.J., 2010. The effect of mean pore size on cell attachment, proliferation and migration in collagen-glycosaminoglycan scaffolds for bone tissue engineering. Biomaterials 31, 461–466.

Nackman, G.B., Fillinger, M.F., Shafritz, R., Wei, T., Graham, A.M., 1998. Flow modulates endothelial regulation of smooth muscle cell proliferation: A new model. Surgery 124, 353–361.

Nakayama, K.H., Hou, L., Huang, N.F., 2014. Role of extracellular matrix signaling cues in modulating cell fate commitment for cardiovascular tissue engineering. Adv. Healthc. Mater. 3, 628–41.

Nerem, R.M., 2000. Tissue engineering a blood vessel substitute: the role of biomechanics. Yonsei Med. J. 41, 735–9.

Niklason, L.E., Abbott, W., Gao, J., Klagges, B., Hirschi, K.K., Ulubayram, K., Conroy, N., Jones, R., Vasanawala, a, Sanzgiri, S., Langer, R., 2001. Morphologic and mechanical characteristics of engineered bovine arteries. J. Vasc. Surg. Off. Publ. Soc. Vasc. Surg. [and] Int. Soc. Cardiovasc. Surgery, North Am. Chapter 33, 628–38.

Niklason, L.E., Gao, J., Abbott, W.M., Hirschi, K.K., Houser, S., Marini, R., Langer, R., 1999. Functional arteries grown in vitro. Science 284, 489–93.

Nishad Fathima, N., Suresh, R., Raghava Rao, J., Unni Nair, B., 2007. Effect of UV irradiation on the physicochemical properties of collagen stabilized using aldehydes. J. Appl. Polym. Sci. 104, 3642–3648.

Nishimura, I., Garrell, R.L., Hedrick, M., Iida, K., Osher, S., Wu, B., 2003. Precursor tissue analogs as a tissue-engineering strategy. Tissue Eng. 9 Suppl 1, S77–89.

Norotte, C., Marga, F.S., Niklason, L.E., Forgacs, G., 2009. Scaffold-free vascular tissue engineering using bioprinting. Biomaterials 30, 5910–5917.

Nowatzki, P.J., Tirrell, D.A., 2004. Physical properties of artificial extracellular matrix protein films prepared by isocyanate crosslinking. Biomaterials 25, 1261–7.

O'Brien, F.J., Harley, B.A., Yannas, I. V, Gibson, L., 2004. Influence of freezing rate on pore structure in freeze-dried collagen-GAG scaffolds. Biomaterials 25, 1077–86.

O'Brien, F.J., Harley, B.A., Yannas, I. V, Gibson, L.J., 2005. The effect of pore size on cell adhesion in collagen-GAG scaffolds. Biomaterials 26, 433–441.

O'Connell, M.K., Murthy, S., Phan, S., Xu, C., Buchanan, J., Spilker, R., Dalman, R.L., Zarins, C.K., Denk, W., Taylor, C.A., 2008. The three-dimensional micro- and nanostructure of the aortic medial lamellar unit measured using 3D confocal and electron microscopy imaging. Matrix Biol. 27, 171–81.

O'Flaherty, M., Buchan, I., Capewell, S., 2013. Contributions of treatment and lifestyle to declining CVD mortality: why have CVD mortality rates declined so much since the 1960s? Heart 99, 159–62.

Oh, S.H., Park, I.K., Kim, J.M., Lee, J.H., 2007. In vitro and in vivo characteristics of PCL scaffolds with pore size gradient fabricated by a centrifugation method. Biomaterials 28, 1664–71.

Olde Damink, L.H., Dijkstra, P.J., van Luyn, M.J., van Wachem, P.B., Nieuwenhuis, P., Feijen, J., 1996. Cross-linking of dermal sheep collagen using a water-soluble carbodiimide. Biomaterials 17, 765–73.

Ott, M.J., Ballermann, B.J., 1995. Shear stress-conditioned, endothelial cell-seeded vascular grafts: improved cell adherence in response to in vitro shear stress. Surgery 117, 334–9.

Pahlavan, P.S., Niroomand, F., 2006. Coronary artery aneurysm: A review. Clin. Cardiol. 29, 439–443.

Park, J.S., Chu, J.S., Tsou, A.D., Diop, R., Tang, Z., Wang, A., Li, S., 2011. The effect of matrix stiffness on the differentiation of mesenchymal stem cells in response to TGF-β. Biomaterials 32, 3921–30.

Park, J.S., Chu, J.S.F., Cheng, C., Chen, F., Chen, D., Li, S., 2004. Differential effects of equiaxial and uniaxial strain on mesenchymal stem cells. Biotechnol. Bioeng. 88, 359–68.

Pashneh-Tala, S., MacNeil, S., Claeyssens, F., 2015. The Tissue-Engineered Vascular Graft-Past, Present, and Future. Tissue Eng. Part B. Rev.

Passerini, A.G., Polacek, D.C., Shi, C., Francesco, N.M., Manduchi, E., Grant, G.R., Pritchard, W.F., Powell, S., Chang, G.Y., Stoeckert, C.J., Davies, P.F., 2004. Coexisting proinflammatory and antioxidative endothelial transcription profiles in a disturbed flow region of the adult porcine aorta. Proc. Natl. Acad. Sci. U. S. A. 101, 2482–7.

Patel, A., Fine, B., Sandig, M., Mequanint, K., 2006. Elastin biosynthesis: The missing link in tissue-engineered blood vessels. Cardiovasc. Res. 71, 40–9.

Peck, M., Dusserre, N., McAllister, T.N., L'Heureux, N., 2011. Tissue engineering by self-assembly. Mater. Today 14, 218–224.

Peichev, M., Naiyer, A.J., Pereira, D., Zhu, Z., Lane, W.J., Williams, M., Oz, M.C., Hicklin, D.J., Witte, L., Moore, M.A., Rafii, S., 2000. Expression of VEGFR-2 and AC133 by circulating human CD34(+) cells identifies a population of functional endothelial precursors. Blood 95, 952–8.

Powell, H.M., Boyce, S.T., 2006. EDC cross-linking improves skin substitute strength and stability. Biomaterials 27, 5821–7.

Pugsley, M.K., Tabrizchi, R., 2000. The vascular system. J. Pharmacol. Toxicol. Methods 44, 333–340.

Qu, M.-J., Liu, B., Wang, H.-Q., Yan, Z.-Q., Shen, B.-R., Jiang, Z.-L., 2007. Frequency-dependent phenotype modulation of vascular smooth muscle cells under cyclic mechanical strain. J. Vasc. Res. 44, 345–53.

Quint, C., Arief, M., Muto, A., Dardik, A., Niklason, L.E., 2012. Allogeneic human tissue-engineered blood vessel. J. Vasc. Surg. 55, 790–8.

Quint, C., Kondo, Y., Manson, R.J., Lawson, J.H., Dardik, A., Niklason, L.E., 2011. Decellularized tissue-engineered blood vessel as an arterial conduit. Proc. Natl. Acad. Sci. U. S. A. 108, 9214–9.

Rabkin, E., Hoerstrup, S.P., Aikawa, M., Mayer, J.E., Schoen, F.J., 2002. Evolution of cell phenotype and extracellular matrix in tissue-engineered heart valves during in-vitro maturation and in-vivo remodeling. J. Heart Valve Dis. 11, 308–14; discussion 314.

Ratcliffe, A., 2000. Tissue engineering of vascular grafts. Matrix Biol. 19, 353–357.

Reddy, G.K., Enwemeka, C.S., 1996. A simplified method for the analysis of hydroxyproline in biological tissues. Clin. Biochem. 29, 225–9.

Reneman, R.S., Arts, T., Hoeks, A.P.G., 2006. Wall shear stress--an important determinant of endothelial cell function and structure--in the arterial system in vivo. Discrepancies with theory. J. Vasc. Res. 43, 251–69.

Rensen, S.S.M., Doevendans, P.A.F.M., van Eys, G.J.J.M., 2007. Regulation and characteristics of vascular smooth muscle cell phenotypic diversity. Netherlands Hear. J. 15, 100–108.

Rezwan, K., Chen, Q.Z., Blaker, J.J., Boccaccini, A.R., 2006. Biodegradable and bioactive porous polymer/inorganic composite scaffolds for bone tissue engineering. Biomaterials 27, 3413–31.

Roche, E.T., Hastings, C.L., Lewin, S.A., Shvartsman, D.E., Brudno, Y., Vasilyev, N. V, O'Brien, F.J., Walsh, C.J., Duffy, G.P., Mooney, D.J., 2014. Comparison of biomaterial delivery vehicles for improving acute retention of stem cells in the infarcted heart. Biomaterials 35, 6850–8.

Rosenman, J.E., Kempczinski, R.F., Pearce, W.H., Silberstein, E.B., 1985. Kinetics of endothelial cell seeding. J. Vasc. Surg. 2, 778–784.

Ross, J.J., Tranquillo, R.T., 2003. ECM gene expression correlates with in vitro tissue growth and development in fibrin gel remodeled by neonatal smooth muscle cells. Matrix Biol. 22, 477–90.

Rotmans, J.I., Heyligers, J.M.M., Verhagen, H.J.M., Velema, E., Nagtegaal, M.M., de Kleijn, D.P. V, de Groot, F.G., Stroes, E.S.G., Pasterkamp, G., 2005. In vivo cell seeding with anti-CD34 antibodies successfully accelerates endothelialization but stimulates intimal hyperplasia in porcine arteriovenous expanded polytetrafluoroethylene grafts. Circulation 112, 12–8.

Ryan, A.J., Gleeson, J.P., Matsiko, A., Thompson, E.M., O'Brien, F.J., 2014. Effect of different hydroxyapatite incorporation methods on the structural and biological properties of porous collagen scaffolds for bone repair. J. Anat.

Salacinski, H.J., Goldner, S., Giudiceandrea, A., Hamilton, G., Seifalian, A.M., Edwards, A., Carson, R.J., 2001a. The mechanical behavior of vascular grafts: a review. J. Biomater. Appl. 15, 241–78.

Salacinski, H.J., Punshon, G., Krijgsman, B., Hamilton, G., Seifalian, A.M., 2001b. A hybrid compliant vascular graft seeded with microvascular endothelial cells extracted from human omentum. Artif. Organs 25, 974–82.

Samijo, S.K., Willigers, J.M., Barkhuysen, R., Kitslaar, P.J., Reneman, R.S., Brands, P.J., Hoeks, A.P., 1998. Wall shear stress in the human common carotid artery as function of age and gender. Cardiovasc. Res. 39, 515–22.

Sarkar, S., Schmitz-Rixen, T., Hamilton, G., Seifalian, A.M., 2007. Achieving the ideal properties for vascular bypass grafts using a tissue engineered approach: a review. Med. Biol. Eng. Comput. 45, 327–36.

Sazonova, O. V, Lee, K.L., Isenberg, B.C., Rich, C.B., Nugent, M.A., Wong, J.Y., 2011. Cell-cell interactions mediate the response of vascular smooth muscle cells to substrate stiffness. Biophys. J. 101, 622–30.

Schutte, S.C., Chen, Z., Brockbank, K.G.M., Nerem, R.M., 2010. Cyclic strain improves strength and function of a collagen-based tissue-engineered vascular media. Tissue Eng. Part A 16, 3149–57.

Seifalian, A.M., Tiwari, A., Hamilton, G., Salacinski, H.J., 2002. Improving the Clinical Patency of Prosthetic Vascular and Coronary Bypass Grafts: The Role of Seeding and Tissue Engineering. Artif. Organs 26, 307–320.

Seifu, D.G., Purnama, A., Mequanint, K., Mantovani, D., 2013. Small-diameter vascular tissue engineering. Nat. Rev. Cardiol. 10, 410–21.

Seliktar, D., Black, R.A., Vito, R.P., Nerem, R.M., 2000. Dynamic mechanical conditioning of collagen-gel blood vessel constructs induces remodeling in vitro. Ann. Biomed. Eng. 28, 351–62.

Seliktar, D., Nerem, R.M., Galis, Z.S., 2001. The role of matrix metalloproteinase-2 in the remodeling of cell-seeded vascular constructs subjected to cyclic strain. Ann. Biomed. Eng. 29, 923–34.

Seliktar, D., Nerem, R.M., Galis, Z.S., 2003a. Mechanical strain-stimulated remodeling of tissue-engineered blood vessel constructs. Tissue Eng. 9, 657–66.

Seliktar, D., Nerem, R.M., Galis, Z.S., 2003b. Mechanical strain-stimulated remodeling of tissue-engineered blood vessel constructs. Tissue Eng. 9, 657–66.

Sell, S.A., McClure, M.J., Barnes, C.P., Knapp, D.C., Walpoth, B.H., Simpson, D.G., Bowlin, G.L., 2006. Electrospun polydioxanone-elastin blends: potential for bioresorbable vascular grafts. Biomed. Mater. 1, 72–80.

Shahmansouri, N., Cartier, R., Mongrain, R., 2015. Characterization of the toughness and elastic properties of fresh and cryopreserved arteries. J. Biomech. 48, 2205–9.

Shapiro, S.D., Endicott, S.K., Province, M.A., Pierce, J.A., Campbell, E.J., 1991. Marked longevity of human lung parenchymal elastic fibers deduced from prevalence of D-aspartate and nuclear weapons-related radiocarbon. J. Clin. Invest. 87, 1828–34.

Sheridan, W.S., Duffy, G.P., Murphy, B.P., 2012. Mechanical characterization of a customized decellularized scaffold for vascular tissue engineering. J. Mech. Behav. Biomed. Mater. 8, 58–70.

Sheridan, W.S., Grant, O.B., Duffy, G.P., Murphy, B.P., 2014a. The application of a thermoresponsive chitosan/β-GP gel to enhance cell repopulation of decellularized vascular scaffolds. J. Biomed. Mater. Res. B. Appl. Biomater. 102, 1700–10.

Sheridan, W.S., Ryan, A.J., Duffy, G.P., O'Brien, F.J., Murphy, B.P., 2014b. An experimental investigation of the effect of mechanical and biochemical stimuli on cell migration within a decellularized vascular construct. Ann. Biomed. Eng. 42, 2029–38.

Shi, Q., Rafii, S., Wu, M.H., Wijelath, E.S., Yu, C., Ishida, A., Fujita, Y., Kothari, S., Mohle, R., Sauvage, L.R., Moore, M.A., Storb, R.F., Hammond, W.P., 1998. Evidence for circulating bone marrow-derived endothelial cells. Blood 92, 362–7.

Shimizu, K., Ito, A., Arinobe, M., Murase, Y., Iwata, Y., Narita, Y., Kagami, H., Ueda, M., Honda, H., 2007. Effective cell-seeding technique using magnetite nanoparticles and magnetic force onto decellularized blood vessels for vascular tissue engineering. J. Biosci. Bioeng. 103, 472–8.

Shindo, S., Takagi, A., Whittemore, A.D., 1987. Improved patency of collagen-impregnated grafts after in vitro autogenous endothelial cell seeding. J. Vasc. Surg. 6, 325–332.

Shinoka, T., Shum-Tim, D., Ma, P.X., Tanel, R.E., Isogai, N., Langer, R., Vacanti, J.P., Mayer, J.E., 1998. Creation of viable pulmonary artery autografts through tissue engineering. J. Thorac. Cardiovasc. Surg. 115, 536–45; discussion 545–6.

Shoulders, M.D., Raines, R.T., 2009. Collagen structure and stability. Annu. Rev. Biochem. 78, 929–58.

Simionescu, D.T., Lu, Q., Song, Y., Lee, J.S., Rosenbalm, T.N., Kelley, C., Vyavahare, N.R., 2006. Biocompatibility and remodeling potential of pure arterial elastin and collagen scaffolds. Biomaterials 27, 702–13.

Singer, V.L., Jones, L.J., Yue, S.T., Haugland, R.P., 1997. Characterization of PicoGreen reagent and development of a fluorescence-based solution assay for double-stranded DNA quantitation. Anal. Biochem. 249, 228–38.

Singh, V., Misra, A., Parthasarathy, R., Ye, Q., Spencer, P., 2015. Viscoelastic properties of collagen-adhesive composites under water-saturated and dry conditions. J. Biomed. Mater. Res. A 103, 646–57.

Sionkowska, A., Wisniewski, M., Skopinska, J., Vicini, S., Marsano, E., 2005. The influence of UV irradiation on the mechanical properties of chitosan/poly(vinyl pyrrolidone) blends. Polym. Degrad. Stab. 88, 261–267.

Solan, A., Dahl, S.L.M., Niklason, L.E., 2009. Effects of mechanical stretch on collagen and cross-linking in engineered blood vessels. Cell Transplant. 18, 915.

Solan, A., Mitchell, S., Moses, M., Niklason, L., 2003. Effect of pulse rate on collagen deposition in the tissue-engineered blood vessel. Tissue Eng. 9, 579–86.

Spofford, C.M., Chilian, W.M., 2003. Mechanotransduction via the elastin-laminin receptor (ELR) in resistance arteries. J. Biomech. 36, 645–52.

Spronck, B., Megens, R.T.A., Reesink, K.D., Delhaas, T., 2014. Three-dimensional vascular smooth muscle orientation as quantitatively assessed by multiphoton microscopy: mouse carotid arteries do show a helix. Conf. Proc. ... Annu. Int. Conf. IEEE Eng. Med. Biol. Soc. IEEE Eng. Med. Biol. Soc. Annu. Conf. 2014, 202–5.

Stegemann, J.P., Nerem, R.M., 2003. Phenotype modulation in vascular tissue engineering using biochemical and mechanical stimulation. Ann. Biomed. Eng. 31, 391–402.

Stella, J.A., D'Amore, A., Wagner, W.R., Sacks, M.S., 2010. On the biomechanical function of scaffolds for engineering load-bearing soft tissues. Acta Biomater. 6, 2365–81.

Stitzel, J., Liu, J., Lee, S.J., Komura, M., Berry, J., Soker, S., Lim, G., Van Dyke, M., Czerw, R., Yoo, J.J., Atala, A., 2006. Controlled fabrication of a biological vascular substitute. Biomaterials 27, 1088–94.

Stokholm, R., Oyre, S., Ringgaard, S., Flaagoy, H., Paaske, W.P., Pedersen, E.M., 2000. Determination of wall shear rate in the human carotid artery by magnetic resonance techniques. Eur. J. Vasc. Endovasc. Surg. 20, 427–33.

Stylianou, A., Yova, D., Alexandratou, E., 2014. Investigation of the influence of UV irradiation on collagen thin films by AFM imaging. Mater. Sci. Eng. C. Mater. Biol. Appl. 45, 455–68.

Swartz, D.D., Russell, J. a, Andreadis, S.T., 2005. Engineering of fibrin-based functional and implantable small-diameter blood vessels. Am. J. Physiol. Heart Circ. Physiol. 288, H1451–60.

Syed, M., Lesch, M., 1997. Coronary artery aneurysm: A review. Prog. Cardiovasc. Dis. 40, 77–84.

Syedain, Z.H., Meier, L. a, Bjork, J.W., Lee, A., Tranquillo, R.T., 2011a. Implantable arterial grafts from human fibroblasts and fibrin using a multi-graft pulsed flow-stretch bioreactor with noninvasive strength monitoring. Biomaterials 32, 714–22.

Syedain, Z.H., Meier, L.A., Bjork, J.W., Lee, A., Tranquillo, R.T., 2011b. Implantable arterial grafts from human fibroblasts and fibrin using a multi-graft pulsed flow-stretch bioreactor with noninvasive strength monitoring. Biomaterials 32, 714–22.

Tai, N.R., Salacinski, H.J., Edwards, A., Hamilton, G., Seifalian, A.M., 2000. Compliance properties of conduits used in vascular reconstruction. Br. J. Surg. 87, 1516–24.

Taite, L.J., Yang, P., Jun, H.-W., West, J.L., 2008. Nitric oxide-releasing polyurethane-PEG copolymer containing the YIGSR peptide promotes endothelialization with decreased platelet adhesion. J. Biomed. Mater. Res. B. Appl. Biomater. 84, 108–16.

Tarbell, J.M., Shi, Z.-D., Dunn, J., Jo, H., 2014. Fluid Mechanics, Arterial Disease, and Gene Expression. Annu. Rev. Fluid Mech. 46, 591–614.

Taylor, R., 1990. Interpretation of the Correlation Coefficient: A Basic Review. J. Diagnostic Med. Sonogr. 6, 35–39.

Tedder, M.E., Liao, J., Weed, B., Stabler, C., Zhang, H., Simionescu, A., Simionescu, D.T., 2009. Stabilized collagen scaffolds for heart valve tissue engineering. Tissue Eng. Part A 15, 1257–68.

Thomas, a, 2003. Advances in vascular tissue engineering. Cardiovasc. Pathol. 12, 271–276.

Thorpe, S.D., Buckley, C.T., Vinardell, T., O'Brien, F.J., Campbell, V.A., Kelly, D.J., 2010. The response of bone marrow-derived mesenchymal

stem cells to dynamic compression following TGF-beta3 induced chondrogenic differentiation. Ann. Biomed. Eng. 38, 2896–909.

Tierney, E.G., McSorley, K., Hastings, C.L., Cryan, S.-A., O'Brien, T., Murphy, M.J., Barry, F.P., O'Brien, F.J., Duffy, G.P., 2013. High levels of ephrinB2 over-expression increases the osteogenic differentiation of human mesenchymal stem cells and promotes enhanced cell mediated mineralisation in a polyethyleneimine-ephrinB2 gene-activated matrix. J. Control. Release 165, 173–82.

Tillman, B.W., Yazdani, S.K., Lee, S.J., Geary, R.L., Atala, A., Yoo, J.J., 2009. The in vivo stability of electrospun polycaprolactone-collagen scaffolds in vascular reconstruction. Biomaterials 30, 583–8.

Tirella, A., Liberto, T., Ahluwalia, A., 2012. Riboflavin and collagen: New crosslinking methods to tailor the stiffness of hydrogels. Mater. Lett. 74, 58–61.

Tiwari, A., Salacinski, H.J., Punshon, G., Hamilton, G., Seifalian, A.M., 2002. Development of a hybrid cardiovascular graft using a tissue engineering approach. FASEB J. 16, 791–6.

Tsai, M.-C., Chen, L., Zhou, J., Tang, Z., Hsu, T.-F., Wang, Y., Shih, Y.-T., Peng, H.-H., Wang, N., Guan, Y., Chien, S., Chiu, J.-J., 2009. Shear stress induces synthetic-to-contractile phenotypic modulation in smooth muscle cells via peroxisome proliferator-activated receptor alpha/delta activations by prostacyclin released by sheared endothelial cells. Circ. Res. 105, 471–80.

Tschoeke, B., Flanagan, T.C., Cornelissen, A., Koch, S., Roehl, A., Sriharwoko, M., Sachweh, J.S., Gries, T., Schmitz-Rode, T., Jockenhoevel, S., 2008. Development of a composite degradable/nondegradable tissue-engineered vascular graft. Artif. Organs 32, 800–9.

Tschoeke, B., Flanagan, T.C., Koch, S., Harwoko, M.S., Deichmann, T., Ellå, V., Sachweh, J.S., Kellomåki, M., Gries, T., Schmitz-Rode, T., Jockenhoevel, S., 2009. Tissue-engineered small-caliber vascular graft based on a novel biodegradable composite fibrin-polylactide scaffold. Tissue Eng. Part A 15, 1909–18.

Urbán, Z., Riazi, S., Seidl, T.L., Katahira, J., Smoot, L.B., Chitayat, D., Boyd, C.D., Hinek, A., 2002. Connection between elastin haploinsufficiency and increased cell proliferation in patients with supravalvular aortic stenosis and Williams-Beuren syndrome. Am. J. Hum. Genet. 71, 30–44.

Vacanti, C.A., 2006. History of tissue engineering and a glimpse into its future. Tissue Eng. 12, 1137–42.

Van Andel, C.J., Pistecky, P. V, Borst, C., 2003. Mechanical properties of porcine and human arteries: implications for coronary anastomotic connectors. Ann. Thorac. Surg. 76, 58–64; discussion 64–5.

VanderWerf, B.A., Rattazzi, L.C., Katzman, H.A., Schild, A.F., 1975. Three year experience with bovine graft arteriovenous (A-V) fistulas in 100 patients. Trans. Am. Soc. Artif. Intern. Organs 21, 296–9.

Veit, G., Kobbe, B., Keene, D.R., Paulsson, M., Koch, M., Wagener, R., 2006. Collagen XXVIII, a novel von Willebrand factor A domain-containing protein with many imperfections in the collagenous domain. J. Biol. Chem. 281, 3494–504.

Vennemann, P., Lindken, R., Westerweel, J., 2007. In vivo whole-field blood velocity measurement techniques. Exp. Fluids 42, 495–511.

Vorp, D.A., Schiro, B.J., Ehrlich, M.P., Juvonen, T.S., Ergin, M.A., Griffith, B.P., 2003. Effect of aneurysm on the tensile strength and biomechanical behavior of the ascending thoracic aorta. Ann. Thorac. Surg. 75, 1210–4.

Wagenseil, J.E., Mecham, R.P., 2007. New insights into elastic fiber assembly. Birth Defects Res. C. Embryo Today 81, 229–40.

Wang, N., Tytell, J.D., Ingber, D.E., 2009. Mechanotransduction at a distance: mechanically coupling the extracellular matrix with the nucleus. Nat. Rev. Mol. Cell Biol. 10, 75–82.

Wang, Y., Ameer, G.A., Sheppard, B.J., Langer, R., 2002. A tough biodegradable elastomer. Nat. Biotechnol. 20, 602–6.

Waterhouse, A., Wise, S.G., Ng, M.K.C., Weiss, A.S., 2011. Elastin as a Nonthrombogenic Biomaterial. Tissue Eng. Part B Rev. 17, 93–99.

Weadock, K., Olson, R.M., Silver, F.H., 1983. Evaluation of collagen crosslinking techniques. Biomater. Med. Devices. Artif. Organs 11, 293–318.

Weadock, K.S., Miller, E.J., Keuffel, E.L., Dunn, M.G., 1996. Effect of physical crosslinking methods on collagen-fiber durability in proteolytic solutions. J. Biomed. Mater. Res. 32, 221–6.

Weinberg, C., Bell, E., 1986. A blood vessel model constructed from collagen and cultured vascular cells. Science (80-.). 231, 397–400.

Weinberg, C.., Bell, E., 1986. A blood vessel model constructed from collagen and cultured vascular cells. Science 231, 397–400.

Whittaker, P., Kloner, R.A., Boughner, D.R., Pickering, J.G., 1994. Quantitative assessment of myocardial collagen with picrosirius red staining and circularly polarized light. Basic Res. Cardiol. 89, 397–410.

Williams, D.F., 2008. On the mechanisms of biocompatibility. Biomaterials 29, 2941–53.

Wingate, K., Bonani, W., Tan, Y., Bryant, S.J., Tan, W., 2012. Compressive elasticity of three-dimensional nanofiber matrix directs mesenchymal stem cell differentiation to vascular cells with endothelial or smooth muscle cell markers. Acta Biomater. 8, 1440–9.

Wise, S.G., Byrom, M.J., Waterhouse, A., Bannon, P.G., Weiss, A.S., Ng, M.K.C., 2011. A multilayered synthetic human elastin/polycaprolactone

hybrid vascular graft with tailored mechanical properties. Acta Biomater. 7, 295–303.

World Health Organisation, 2012. Cardiovascular diseases (CVDs). World Health Organization.

Wu, S.P., Ringgaard, S., Oyre, S., Hansen, M.S., Rasmus, S., Pedersen, E.M., 2004. Wall shear rates differ between the normal carotid, femoral, and brachial arteries: an in vivo MRI study. J. Magn. Reson. Imaging 19, 188–93.

Wu, W., Allen, R.A., Wang, Y., 2012. Fast-degrading elastomer enables rapid remodeling of a cell-free synthetic graft into a neoartery. Nat. Med. 18, 1148–53.

Wystrychowski, W., McAllister, T.N., Zagalski, K., Dusserre, N., Cierpka, L., L'Heureux, N., 2014. First human use of an allogeneic tissue-engineered vascular graft for hemodialysis access. J. Vasc. Surg. 60, 1353–7.

Yahyouche, a, Zhidao, X., Czernuszka, J.T., Clover, a J.P., 2011. Macrophage-mediated degradation of crosslinked collagen scaffolds. Acta Biomater. 7, 278–86.

Yamamoto, M., Yamamoto, K., Noumura, T., 1993. Type I collagen promotes modulation of cultured rabbit arterial smooth muscle cells from a contractile to a synthetic phenotype. Exp. Cell Res. 204, 121–9.

Yang, B., Zhang, Y., Zhou, L., Sun, Z., Zheng, J., Chen, Y., Dai, Y., 2010. Development of a porcine bladder acellular matrix with well-preserved extracellular bioactive factors for tissue engineering. Tissue Eng. Part C. Methods 16, 1201–11.

Yang, Q., Zhong, Y., Ritchey, M., Loustalot, F., Hong, Y., Merritt, R., Bowman, B.A., 2015. Predicted 10-year risk of developing cardiovascular disease at the state level in the U.S. Am. J. Prev. Med. 48, 58–69.

Yang, Y., Magnay, J.L., Cooling, L., El Haj, A.J., 2002. Development of a "mechano-active" scaffold for tissue engineering. Biomaterials 23, 2119–2126.

Yannas, I. V, Burke, J.F., 1980. Design of an artificial skin. I. Basic design principles. J. Biomed. Mater. Res. 14, 65–81.

Yao, L.A.N., Swartz, D.D., Gugino, S.F., Russell, J.A., Andreadis, S.T., 2005. Fibrin-Based Tissue-Engineered Blood Vessels : Differential Strength and Vascular Reactivity 11.

Yao, Y., Wang, J., Cui, Y., Xu, R., Wang, Z., Zhang, J., Wang, K., Li, Y., Zhao, Q., Kong, D., 2014. Effect of sustained heparin release from PCL/chitosan hybrid small-diameter vascular grafts on anti-thrombogenic property and endothelialization. Acta Biomater. 10, 2739–49.

Yazdani, S.K., Watts, B., Machingal, M., Jarajapu, Y.P.R., Van Dyke, M.E., Christ, G.J., 2009. Smooth muscle cell seeding of decellularized scaffolds: the importance of bioreactor preconditioning to development

of a more native architecture for tissue-engineered blood vessels. Tissue Eng. Part A 15, 827–40.

Yeoman, M.S., Reddy, D., Bowles, H.C., Bezuidenhout, D., Zilla, P., Franz, T., 2010. A constitutive model for the warp-weft coupled non-linear behavior of knitted biomedical textiles. Biomaterials 31, 8484–93.

Yoshida, T., Owens, G.K., 2005. Molecular determinants of vascular smooth muscle cell diversity. Circ. Res. 96, 280–91.

Zeeman, R., 1998. Cross-linking of collagen-based materials.

Zeltinger, J., Sherwood, J.K., Graham, D.A., Müeller, R., Griffith, L.G., 2001. Effect of pore size and void fraction on cellular adhesion, proliferation, and matrix deposition. Tissue Eng. 7, 557–572.

Zhang, F., Tsai, S., Kato, K., Yamanouchi, D., Wang, C., Rafii, S., Liu, B., Kent, K.C., 2009. Transforming growth factor-beta promotes recruitment of bone marrow cells and bone marrow-derived mesenchymal stem cells through stimulation of MCP-1 production in vascular smooth muscle cells. J. Biol. Chem. 284, 17564–74.

Zhang, L., Ao, Q., Wang, A., Lu, G., Kong, L., Gong, Y., Zhao, N., Zhang, X., 2006. A sandwich tubular scaffold derived from chitosan for blood vessel tissue engineering. J. Biomed. Mater. Res. A 77, 277–84.

Zhang, X., Baughman, C.B., Kaplan, D.L., 2008. In vitro evaluation of electrospun silk fibroin scaffolds for vascular cell growth. Biomaterials 29, 2217–27.

Zhang, Z., Wang, Z., Liu, S., Kodama, M., 2004. Pore size, tissue ingrowth, and endothelialization of small-diameter microporous polyurethane vascular prostheses. Biomaterials 25, 177–187.

Zhao, Q., Zhang, J., Song, L., Ji, Q., Yao, Y., Cui, Y., Shen, J., Wang, P.G., Kong, D., 2013. Polysaccharide-based biomaterials with on-demand nitric oxide releasing property regulated by enzyme catalysis. Biomaterials 34, 8450–8.

Zhao, S., Suciu, A., Ziegler, T., Moore, J.E., Bürki, E., Meister, J.J., Brunner, H.R., 1995. Synergistic effects of fluid shear stress and cyclic circumferential stretch on vascular endothelial cell morphology and cytoskeleton. Arterioscler. Thromb. Vasc. Biol. 15, 1781–6.

Zheng, W., Wang, Z., Song, L., Zhao, Q., Zhang, J., Li, D., Wang, S., Han, J., Zheng, X.-L., Yang, Z., Kong, D., 2012. Endothelialization and patency of RGD-functionalized vascular grafts in a rabbit carotid artery model. Biomaterials 33, 2880–91.

Zhu, C., Fan, D., Duan, Z., Xue, W., Shang, L., Chen, F., Luo, Y., 2009. Initial investigation of novel human-like collagen/chitosan scaffold for vascular tissue engineering. J. Biomed. Mater. Res. A 89, 829–40.